# The dynamics of cosmological scenarios inspired by quantum gravity

Mulryne, David James

# The dynamics of cosmological scenarios inspired by quantum gravity

David James Mulryne

Thesis submitted for the degree of
Doctor of Philosophy (PhD)
of the University of London

Queen Mary, University of London

September 2006

# Abstract

In this thesis we study the dynamics of cosmological scenarios inspired by quantum gravity.

Part I investigates novel features of the semi-classical regime of homogeneous and isotropic loop quantum cosmology. Dynamics in this regime becomes modified by non-perturbative quantum effects, subject to a number of ambiguities. For a flat universe the quantum effects accelerate a scalar field along its self-interaction potential during a period of super-inflation. We study how this behaviour can in principle set the initial conditions for subsequent slow-roll inflation. We also calculate a first approximation for the spectrum of perturbations produced during the super-inflationary phase. For the positively-curved case we investigate how a bounce from a contracting to an expanding phase can occur, and show that this can lead to oscillations of the universe. During the oscillations the inflaton field can roll monotonically up its potential. Once the potential energy becomes sufficiently large, however, the cycles end and inflation commences. For a constant potential the oscillations occur about a centre fixed point allowing the construction of 'new emergent universe' scenarios where the universe is past-eternally an Einstein static universe, but subsequently evolves into inflation.

Part II considers positively-curved braneworld models in which the dynamical equations become modified in such a way as to permit a bounce. It is conjectured that models of this type can exhibit similar behaviour to the positively-curved LQC scenario. General conditions for this behaviour are determined in braneworld settings and we investigate an explicit example – the baneworld of Shtanov and Sanhi – in detail.

# Declaration

I hereby declare that the work presented in this thesis is my own, unless otherwise stated, and resulted from collaborations with Martin Bojowald, Geogre Ellis, James Lidsey, Nelson Nunes, Parampreet Singh and Reza Tavakol. Some of the content of chapters 3-7 and chapter 9 has been published in the articles:

**D. J. Mulryne** & N. J. Nunes, *Constraints on a scale invariant power spectrum from superinflation in LQC*, to appear in Phys. Rev. D.

J. E. Lidsey & **D. J. Mulryne**, *A graceful entrance to braneworld inflation*, 2006, Phys. Rev., D73, 083508 (11 pages).

**D. J. Mulryne**, R. Tavakol, J. E. Lidsey & G. F. R. Ellis, *An emergent universe from a loop*, 2005, Phys. Rev., D71, 123512 (11 pages).

**D. J. Mulryne**, N. J. Nunes, R. Tavakol & J. E. Lidsey, *Inflationary cosmology and oscillating universes in loop quantum cosmology*, 2005, Int. J. Mod. Phys., A20, 2347-2357.

J. E. Lidsey, **D. J. Mulryne**, N. J. Nunes & R. Tavakol, *Oscillatory universes in loop quantum cosmology and initial conditions for inflation*, 2004, Phys. Rev., D70, 063521 (6 pages).

M. Bojowald, J. E. Lidsey, **D. J. Mulryne**, P. Singh & R. Tavakol, *Inflationary cosmology and quantization ambiguities in semi-classical loop quantum gravity*, 2004, Phys. Rev., D70, 043530 (15 pages).

David Mulryne

13 September 2006

# Acknowledgements

First, I wish to thank my supervisors Jim Lidsey and Reza Tavakol for their tireless help and guidance. Not only have they provided me with a continuous supply of research ideas, but have also been a constant source of inspiration. I am particularly indebted to them for their insightful comments and strong, but hugely constructive, criticism of this thesis. This final product of my last three years' work would have been a shadow of its present form without them.

I thank also my other collaborators, with whom it has been a pleasure and privilege to work: Martin Bojowald, George Ellis, Nelson Nunes and Parampreet Singh. In particular, I thank Nelson, a friend as well as collaborator, for sparing so much of his own valuable time to discuss cosmology (and so much more) and instruct me in the art of numerical work.

My family have always been a constant source of encouragement to me. I am especially grateful to my parents for their love and support (monetary and emotional!). I thank my father for his knowledgeable advice and invaluable efforts in proof reading, and my mother for the unlimited, unquestioning support only a mother can provide. Thanks also to Phil and Christine; Mark, Caroline, Josh and Daniel; and to Ruth and Pete.

I am blessed to have many friends (too many to name!) who seem to find it bearable to spend time with me. Without them I would not have survived the last three years. Thanks to you all, and particularly to Anne, Bob, Charles, Chris, David, James, Simon and Rose for your friendship. And thanks to my fellow cosmology and relativity PhD students Carlos, Ed, John, Kotub and Will for reminding me that I was not suffering alone!

Finally, I'd like to thank Jackie. There is no space to illustrate all the reasons why, so let me simply dedicate this thesis to her.

# Contents

# List of Figures

# Chapter 1

# Background and Motivation

As our understanding of fundamental theories of physics continues to advance, this in turn helps us to understand phenomena which may have occurred in the extreme conditions of the very early universe. In particular, theories of high energy particle physics and of quantum gravity continue to inspire new scenarios of the early universe, which aim to resolve shortcomings in our understanding of the universe's evolution. It is also hoped that by studying these scenarios one may open a window into possible observational consequences of the theories which inspire them.

This thesis develops novel scenarios, inspired by quantum gravity, which aim to address questions regarding the earliest stages of the universe's existence. In this chapter, we present some useful background to cosmology and particularly to the very early universe and the inflationary scenario. This is not intended as a comprehensive review, for which the reader can turn to the numerous excellent standard texts (see for example Peacock, 1999; Liddle and Lyth, 2000; Dodelson, 2003, and references therein).

## 1.1 The standard model of cosmology

Due to modern high precision observations and a well developed theoretical framework in which to interpret them, the last few years have seen the emergence of what has come to be known as the 'standard model' of cosmology. Observations include those of the cosmic microwave background (CMB) (most recently by the Wilkinson Microwave Anisotropy Probe (WMAP), Spergel *et al*, 2003, 2006), the distant supernovae (Riess *et al*, 1998; Perlmutter *et al*, 1999), large scale structure (see for example Tegmark *et al*, 2004) and the luminosity of galactic clusters (White *et al*, 1993). When combined with constraints from the hot big bang model of the universe and particularly from primordial nucleosynthesis (Smith *et al*, 1993; Walker *et al*, 1991), these observations have constrained the 'cosmological parameters' with unprecedented accuracy. In particular, it

appears that the geometry of our universe can be well described, on the largest scales, by a flat Friedmann-Robertson-Walker (FRW) metric. Moreover, the universe's dynamics appear to be accurately described by the field equations of general relativity (GR) for such a metric when the matter content of the universe consists of three major components. These are baryonic matter, which accounts for approximately 4% of the total, an unknown form of non-baryonic matter called cold dark matter (23%), and another unknown component called 'dark energy' (73%) which acts to accelerate the universe's expansion. Finally, the observations (particularly those of the CMB) also reveal that the origin of structure in the universe is consistent with small primordial perturbations with a near scale-invariant power spectrum (see section 1.4).

With regard to the very early universe, the cornerstone of our current understanding has become the theory of cosmological inflation. Inflation arises when the expansion of the universe accelerates (see, in particular, Starobinsky (1980); Guth (1981); Albrecht and Steinhardt (1982); Hawking and Moss (1982); Linde (1982, 1983) and for reviews Lyth and Riotto (1999); Lidsey *et al* (1997); Liddle and Lyth (2000)). Inflation was initially introduced to solve a number of problems with the hot big bang model, including the horizon problem, the flatness problem, the homogeneity problem, and the relic problem (see Kolb and Turner, 1990, for a detailed discussion of these problems). Much more importantly, however, it was soon realised that inflation also provides a mechanism for generating the correct form of primordial perturbations needed to seed cosmic structure. It is this facet of the scenario which has consolidated inflation's position as a central tenet of the standard model of cosmology.

Let us now develop the quantitative framework for discussing the evolution of the universe, and the inflationary scenario.

## 1.2 Relativistic cosmology

Modelling the universe using the homogeneous and isotropic FRW metric agrees well with observations, and forms the basis for the study of relativistic cosmology. The FRW metric can be written as

$$\begin{aligned} ds^2 &= g_{\mu\nu}dx^\mu dx^\nu \\ &= c^2dt^2 - a^2(t)\left[\frac{dr^2}{1-kr^2} + r^2\left(d\theta^2 + \sin^2(\theta)d\phi^2\right)\right], \end{aligned} \tag{1.1}$$

where $k = \{0, -1, 1\}$ for flat, negatively-curved, or positively-curved spatial sections, respectively.

The evolution of such a universe can be connected to its matter content via a theory

of gravitation. In particular, the usual assumption is that below Planck scale energies the correct theory is General Relativity (GR). The Einstein field equations of GR are derived by varying the action

$$S = -\frac{c^4}{16\pi G}\int dx^4\sqrt{-g}R + \int dx^4\sqrt{-g}\mathcal{L}_m \tag{1.2}$$

with respect to the metric $g_{\mu\nu}$, where $\mathcal{L}_m$ represents the Lagrangian density of the matter fields. The resulting equations are given by

$$G_{\mu\nu} \equiv R_{\mu\nu} - \frac{1}{2}Rg_{\mu\nu} = \frac{8\pi G}{c^4}T_{\mu\nu} \ , \tag{1.3}$$

where $G$ is the gravitational constant and $c$ is the speed of light. $G_{\mu\nu}$ is called the Einstein tensor, and $R_{\mu\nu}$ and $R = R^{\mu}_{\mu}$ are the Ricci tensor and scalar respectively[1]. $T_{\mu\nu}$ is the stress-energy tensor, which arises from the variation of the matter Lagrangian thus

$$T_{\mu\nu} = \frac{2}{\sqrt{-g}}\frac{\delta(\sqrt{-g}\mathcal{L}_m)}{\delta g^{\mu\nu}} \ . \tag{1.4}$$

For a perfect fluid, the stress-energy tensor takes the form

$$T^{\mu\nu} = \left(\rho + \frac{p}{c^2}\right)u^{\mu}u^{\nu} - pg^{\mu\nu} \ , \tag{1.5}$$

where $\rho$ is the energy density, $p$ the pressure and $u^{\mu}$ the four-velocity of the matter. Assuming that the matter content of the universe corresponds to one or more non-interacting perfect fluids co-moving with the expansion of the universe, the field equations become the Friedmann equation

$$H^2 \equiv \left(\frac{\dot{a}}{a}\right)^2 = \frac{8\pi G}{3}\sum_i \rho_i - \frac{k}{a^2} \tag{1.6}$$

and the Raychaudhuri equation

$$\dot{H} = -4\pi G\sum_i (\rho_i + p_i) + \frac{k}{a^2} \ , \tag{1.7}$$

and these lead to the conservation equation for each fluid

$$\dot{\rho}_i = -3H\left(\rho_i + p_i\right) \ . \tag{1.8}$$

The energy density and pressure of a fluid are related through the equation of state defined by

$$w_i = \frac{p_i}{\rho_i} \ . \tag{1.9}$$

[1]For completeness we recall that $R_{\mu\nu} = R^{\rho}_{\mu\rho\nu}$, where $R^{\eta}_{\mu\rho\nu} = \left(\partial_{\rho}\Gamma^{\eta}_{\mu\nu} + \Gamma^{\epsilon}_{\nu\mu}\Gamma^{\eta}_{\epsilon\rho}\right) - \left(\partial_{\nu}\Gamma^{\eta}_{\mu\rho} + \Gamma^{\epsilon}_{\rho\mu}\Gamma^{\eta}_{\epsilon\nu}\right)$ is the Riemann tensor, and $\Gamma^{\mu}_{\nu\rho} = \frac{1}{2}g^{\mu\eta}\left(\partial_{\nu}g_{\eta\rho} + \partial_{\rho}g_{\eta\nu} - \partial_{\eta}g_{\nu\rho}\right)$ are the Christoffel symbols.

Solving Eq. (1.8) with a constant equation of state gives $\rho_i \propto a^{-3(1+w_i)}$. For the standard matter sources of non-relativistic and relativistic matter, $w = 0$ and $w = 1/3$ respectively. An important point to note is that within this model any matter sources with $w > -1/3$ lead to a curvature singularity as $a \to 0$, which implies a singular origin for our universe.

The inflationary scenario describes a universe which is undergoing accelerated expansion. Eqs. (1.6) and (1.7), coupled with the expression

$$\frac{\ddot{a}}{a} = \dot{H} + H^2 \tag{1.10}$$

imply that in order for acceleration to occur we require the condition

$$\sum_i p_i < -\frac{1}{3}\sum_i \rho_i \tag{1.11}$$

to be met, which is not possible with standard matter sources alone. This condition is equivalent to a violation of the strong energy condition, which for a FRW cosmology is equivalent to the conditions $\rho + p > 0$ and $\rho + 3p > 0$. The simplest way to realise acceleration is to introduce a matter source with stress-energy tensor $T_{\mu\nu} = \Lambda g_{\mu\nu}$, where $\Lambda$ is known as the cosmological constant. From a particle physics point of view this is interpreted as the vacuum energy of spacetime, since it is invariant under Poincare transformations. The vacuum energy describes a matter source with equation of state $w = -1$, and can clearly give rise to acceleration if it accounts for a sufficient fraction of the universe's density.

In order to develop a realistic inflationary scenario, however, a constant vacuum energy is not particularly useful, since a universe sourced by a such a term would be eternally inflating. On the other hand, one can also imagine a universe in which the vacuum energy changes, allowing an exit from the inflationary phase. This could occur either through a rapid change associated with a phase transition, or through a more gradual relaxation of the vacuum energy. One realisation of this latter possibility, the chaotic inflationary scenario (Linde, 1983), has become the favoured standard model of early universe inflation. This scenario utilises the dynamics of one or more scalar fields to generate an effective vacuum energy, which slowly decays. In its simplest form, chaotic inflation employs a single scalar field known as the 'inflaton'. Scalar fields are common in theories of particle physics, and although the identity of the inflaton (if indeed this is the correct mechanism for inflation) is at present unknown, there are many possible candidates such as Higgs bosons associated with grand unified theories.

We now proceed to review the single field inflationary scenario and its associated dynamics. This thesis often considers novel scalar field dynamics, so our discussion of the standard, classical dynamics will serve to put this new work into its proper context.

For convenience, in what follows units are chosen such that $\hbar = c = 1$, with the Planck length and mass defined by $m_{\rm Pl} = \ell_{\rm Pl}^{-1} = G^{-1/2}$.

## 1.3 Scalar field dynamics and chaotic inflation

The matter Lagrangian density for a scalar field $\phi$, self-interacting through a potential $V(\phi)$, is given by

$$\mathcal{L}_\phi = \left(\frac{1}{2}\partial_\mu\phi\partial^\mu\phi - V(\phi)\right) \ , \tag{1.12}$$

which gives rise to the stress-energy tensor

$$T_{\mu\nu} = \partial_\mu\phi\partial_\nu\phi - g_{\mu\nu}\left(\frac{1}{2}\partial_\sigma\phi\partial^\sigma\phi - V(\phi)\right) \ . \tag{1.13}$$

The field equations (Eq. (1.3)) then become the Friedmann equation

$$H^2 = \frac{8\pi\ell_{\rm Pl}^2}{3}\left(\frac{\dot\phi^2}{2} + V(\phi)\right) - \frac{k}{a^2} \ , \tag{1.14}$$

and the Raychaudhuri equation

$$\dot H = -4\pi\ell_{\rm Pl}^2\dot\phi^2 + \frac{k}{a^2} \ . \tag{1.15}$$

Combining Eqs. (1.14) and (1.15) leads to the scalar field equation

$$\ddot\phi + 3H\dot\phi + V' = 0 \ , \tag{1.16}$$

where a prime represents a derivative with respect to the field.

Comparing these expressions to those for a perfect fluid (Eqs. (1.6)-(1.8)), the density and pressure of the scalar field can be identified as

$$\rho = \frac{\dot\phi^2}{2} + V \ , \quad p = \frac{\dot\phi^2}{2} - V \ , \tag{1.17}$$

respectively. Eq. (1.11) then implies that acceleration occurs if the condition

$$\dot\phi^2 < V(\phi) \tag{1.18}$$

is satisfied.

An interesting limiting case occurs when $\dot\phi^2 \ll V(\phi)$, referred to as the slow-roll limit. In order for this state to be maintained, the condition $|\ddot\phi| \ll H|\dot\phi|$ must also be satisfied. Eq. (1.16) then gives

$$V' \approx -3H\dot\phi \ , \tag{1.19}$$

implying that the driving term, provided by the gradient of the potential, is balanced by the frictional term $3H\dot\phi$ during the cosmic expansion. This causes the field to evolve

slowly down its self-interaction potential. Moreover, the Hubble parameter is almost constant during a slow-roll phase and is given by

$$H^2 \approx \frac{8\pi\ell_{\rm Pl}^2}{3}V \ . \tag{1.20}$$

The universe therefore undergoes a close to de Sitter (exponential) accelerated expansion. Importantly, this state can be shown to be a dynamical attractor (Salopek and Bond, 1990; Liddle, 1994), so generic initial conditions will evolve into this state if the field is situated on a region of the potential which satisfies the conditions required for slow-roll. Eqs. (1.18)-(1.20) together imply that the slow-roll parameter (Liddle and Lyth, 1992, 1993)

$$\epsilon = \frac{m_{Pl}^2}{16\pi}\left(\frac{V'}{V}\right)^2 \tag{1.21}$$

must be much less than unity. Furthermore, derivatives of this parameter must also be small for this condition to be maintained, and these derivatives lead to further slow-roll parameters. The first of these is given by

$$\eta = \frac{m_{Pl}^2}{8\pi}\left(\frac{V''}{V}\right) \ . \tag{1.22}$$

The minimal conditions required for a prolonged period of slow-roll are therefore that $\epsilon \ll 1$ and $|\eta| \ll 1$.

Inflation ends when $\epsilon \approx 1$, and it is typical to assume that the inflaton is initially displaced away from this point and rolls slowly towards it. Most commonly, one assumes that the field is initially displaced from a minimum of its potential, assumed to occur at $V = 0$, and rolls towards this minimum where slow-roll will clearly come to an end. The amount of expansion the universe undergoes during inflation is measured in terms of the number of e-foldings, where during one e-folding the size of the universe grows by a factor of $e$. The total number of e-foldings which occur during inflation can be calculated using the formula

$$N = \ln\frac{a_{\rm end}}{a_{\rm initial}} = \int_{t_{\rm initial}}^{t_{\rm end}} H dt \approx 8\pi\ell_{\rm Pl}^2 \int_{\phi_{\rm end}}^{\phi_{\rm initial}} \frac{V}{V'} d\phi \ , \tag{1.23}$$

where we have used Eqs. (1.19) and (1.20). $\phi_{\rm end}$ can be calculated from the condition $\epsilon = 1$.

Once the field reaches the minimum of its potential it starts to oscillate. At this point the inflaton's couplings to other matter fields become important. The field's energy then decays into other particles through these couplings. This process is known as reheating, and allows the hot big bang to be recovered. In order to solve the problems with the hot big bang model, roughly 60 e-folds of inflation must occur, although the precise amount

depends on a number of uncertainties, and particularly on the reheating temperature of the universe. Indeed, the number of e-folds can be as low as 30 for a reheating temperature at the electroweak energy scale.

## 1.4 The power spectrum from inflation

Inflation offers an explanation for the origin of cosmic structure. As inflation proceeds the universe becomes progressively more homogeneous, but at the same time the inflaton field undergoes quantum mechanical fluctuations. These quantum fluctuations are stretched by the universe's rapid growth, and can become classical. Moreover, it is also possible to show that the perturbations created in this way can have a suitable form to explain the origin of cosmic structure. The most severe observational restrictions on the form of primordial perturbations come from observations of the CMB. If primordial perturbations originate from slow-roll inflation, therefore, CMB observations place strong constraints on the form of the inflationary potential. In this section, we review the calculation of the spectrum of perturbations from slow-roll inflation, in order to understand these constraints. This calculation also has particular importance for this thesis since in chapter 7 we calculate a first approximation to the spectrum of perturbations produced by a non-standard inflationary phase, and in that chapter we follow as closely as possible the methodology presented here. For a full account of cosmological perturbation theory, and the calculation of the inflationary spectrum, the reader is referred to the review by Mukhanov *et al* (1992).

Before beginning our calculation, we introduce an important length scale for cosmology. This is the Hubble length, given by

$$\text{Hubble length} \equiv H^{-1} \ . \tag{1.24}$$

We will often refer to this length scale and the associated co-moving Hubble length $1/aH$ in this thesis. In an abuse of terminology, however, the Hubble length is often referred to as the cosmological horizon or simply the horizon, and we continue that practice here. Although it is neither an event horizon nor a particle horizon, the Hubble length is related to both, and gives an estimate of the scale beyond which causal processes cannot operate.

Inflation causes the comoving Hubble length to shrink. The beauty of inflation is that a quantum fluctuation on a particular comoving length scale which is initially well inside the horizon naturally becomes a fluctuation outside the horizon as inflation proceeds. In other words, the physical length of the fluctuation is stretched by inflation, until it exceeds the physical horizon scale. Thus, a very small quantum fluctuation is stretched to very large scales where it can be assumed to be classical.

Let us now proceed to consider the quantitative calculation of the inflationary spectrum. The calculation begins by perturbing the background spacetime and the scalar field. This assumes that the scalar field is given by

$$\phi = \phi_0(t) + \delta\phi(t, x) \ , \tag{1.25}$$

and the perturbed metric by

$$ds^2 = a^2(\tau)\left((1+2\varphi)d\tau^2 - (1-2\varphi)\delta_{ij}dx^i dx^j\right) \ , \tag{1.26}$$

where $\varphi$ is a perturbation to the metric and $d\tau \equiv adt$ denotes conformal time. Here we are considering only the perturbed flat FRW metric and we have picked a particular gauge called the longitudinal gauge. Moreover, we have considered only scalar perturbations.

For comparison with observations a useful quantity is the curvature perturbation on comoving hypersurfaces, which in the longitudinal gauge is given by (Liddle and Lyth, 2000)

$$\mathcal{R} = -\varphi - \frac{H}{\dot{\phi}}\delta\phi \ . \tag{1.27}$$

This quantity is useful because under very general circumstances it is time-independent on length scales larger than the horizon size (see for example Lyth *et al*, 2005). At this point it is also useful to define the Mukhanov variable (Mukhanov, 1985, 1988)

$$u \equiv a\left(\delta\phi + \frac{\dot{\phi}}{H}\varphi\right) \ , \tag{1.28}$$

and also the variable

$$z \equiv \frac{a\dot{\phi}}{H} \ . \tag{1.29}$$

We note that

$$u = -z\mathcal{R} \ . \tag{1.30}$$

These expressions are useful because it can be shown using the perturbed metric and scalar field, together with the action (1.2) and the Lagrangian density (1.12), that the full action for linear perturbations is given by

$$\begin{aligned} S &= \int d^4x\mathcal{L} \\ &= \frac{1}{2}\int d\tau d^3\mathbf{x}\left(u_\tau^2 - \delta^{ij}\partial_i u\partial_j u + \frac{z_{\tau\tau}}{z}u^2\right) \ , \end{aligned} \tag{1.31}$$

where a subscript $\tau$ denotes partial differentiation with respect to conformal time. This action is formally equivalent to the action for a scalar field in Minkowski space in the

presence of a time-dependent potential, and can be quantised in a similar manner to such a field.

The momentum canonically conjugate to $u$ is given by

$$\pi(\tau, \mathbf{x}) = \frac{\partial \mathcal{L}}{\partial u_\tau} = u_\tau(\tau, \mathbf{x}) \ . \tag{1.32}$$

The theory is then quantised by promoting $u$ and $\pi$ to operators $\hat{u}$ and $\hat{\pi}$ which satisfy the usual commutation relations. $\hat{u}$ can be Fourier decomposed to give

$$\hat{u}(\tau, \mathbf{x}) = \int \frac{d^3\mathbf{k}}{(2\pi)^{3/2}} \left[ w_k(\tau)\hat{a}_\mathbf{k} e^{i\mathbf{k}.\mathbf{x}} + w_k^*(\tau)\hat{a}_\mathbf{k}^\dagger e^{-i\mathbf{k}.\mathbf{x}} \right] \ , \tag{1.33}$$

where $w_k$ are mode functions which satisfy an equation derived by varying Eq. (1.31) with respect to $u$ and using Eq. (1.33). This is the Mukhanov equation, given by

$$\frac{d^2 w_k}{d\tau^2} + \left(k^2 + m_{\text{eff}}^2\right) w_k = 0 \ , \tag{1.34}$$

where $m_{\text{eff}}^2 = -z_{\tau\tau}/z$.

In order to have a well defined field theory, we must also ensure that $w_k$ are defined such that the creation and annihilation operators, $\hat{a}_\mathbf{k}^\dagger$ and $\hat{a}_\mathbf{k}$, satisfy the usual commutation relations for bosons. These take the form

$$[\hat{a}_\mathbf{k}, \hat{a}_\mathbf{l}] = [\hat{a}_\mathbf{k}^\dagger, \hat{a}_\mathbf{l}^\dagger] = 0 \ , \quad [\hat{a}_\mathbf{k}, \hat{a}_\mathbf{l}^\dagger] = \delta(\mathbf{k} - \mathbf{l}) \ , \tag{1.35}$$

which implies that $w_k$ must satisfy the Wronskian condition

$$w_k^* \frac{dw_k}{d\tau} - w_k \frac{dw_k^*}{d\tau} = -i \, . \tag{1.36}$$

In general, however, this condition does not give rise to a unique choice for $w_k$; instead it allows a set of possible choices corresponding to a set of different Fock representations. In the cosmological context a unique choice is normally determined by considering a limit in which the time-dependence of the scale factor can be neglected, and hence where the physics ought to reduce to that of Minkowski space. In this limit, $w_k$ is normalised to select only the advanced solution. Once the initial condition is selected and the Wronskian condition met, a vacuum state is defined which is annihilated by all $\hat{a}_\mathbf{k}$, such that $\hat{a}_\mathbf{k}|0\rangle = 0$.

Considering the Fourier decomposition of the curvature perturbation

$$\mathcal{R} = \int \frac{d^3\mathbf{k}}{(2\pi)^{3/2}} \mathcal{R}_\mathbf{k} e^{i\mathbf{k}.\mathbf{x}} \ , \tag{1.37}$$

the power spectrum of curvature fluctuations is defined by the vacuum expectation value such that

$$\langle \mathcal{R}_\mathbf{k} \mathcal{R}_\mathbf{l}^* \rangle = \frac{2\pi^2}{k^3} P_\mathcal{R} \delta^{(3)}(\mathbf{k} - \mathbf{l}) \ . \tag{1.38}$$

Using Eqs. (1.30) and (1.33) we find

$$\langle \mathcal{R}_{\mathbf{k}} \mathcal{R}_{\mathbf{l}}^{*} \rangle = \left| \frac{w_k}{z} \right|^2 \delta^{(3)}(\mathbf{k} - \mathbf{l}) \ , \tag{1.39}$$

and hence that the power spectrum is given by

$$\mathcal{P}_{\mathcal{R}} = \frac{k^3}{2\pi^2} \left| \frac{w_k}{z} \right|^2 \ . \tag{1.40}$$

### 1.4.1 Power-law inflation

In order to calculate the power spectrum of the primordial perturbations, we must solve Eq. (1.34). When the universe is sourced by a scalar field with a general self-interaction potential this is not always possible analytically. For the case of an exponential potential, however, an exact solution exists in which the universe evolves according to a power-law. In this case $a \propto t^p$, with $p$ a constant, and Eq. (1.34) also admits an exact solution (Stewart and Lyth, 1993). Assuming the field evolves on its potential such that $\phi$ is increasing, the form of the potential which gives rise to the power-law behaviour is (Lucchin and Matarrese, 1985a,b)

$$V(\phi) \propto \exp\left( -\sqrt{\frac{16\pi}{p}} \frac{\ell_{\rm Pl}^2}{} \phi \right) \ . \tag{1.41}$$

Changing to conformal time, we have $a \propto (-\tau)^{p/(1-p)}$ and $aH \propto \phi_\tau \propto (-\tau)^{-1}$. It is clear that $\tau$ is negative and increases as inflation proceeds, with $\tau = 0$ corresponding to the infinite future. For this potential we note that the slow-roll parameters are constants and are given by $\epsilon = \eta/2 = 1/p$. It is also useful to note that $\tau$ can be related to the horizon size using

$$\tau = \int \frac{da}{a^2 H} = -\frac{1}{aH} + \int \frac{da}{pa^2 H} \ , \tag{1.42}$$

which leads to the expression

$$\tau = -\frac{1}{aH} \frac{1}{1-\epsilon} \ . \tag{1.43}$$

Using the time-dependences given above to evaluate $z_{\tau\tau}/z$, Eq. (1.34) becomes

$$\left( \frac{d^2}{d\tau^2} + k^2 - \frac{\left(\nu^2 - \frac{1}{4}\right)}{\tau^2} \right) u_k = 0 \ , \tag{1.44}$$

where $\nu = 3/2 + 1/(p-1)$. This admits the exact solution

$$w_k(\tau) = \frac{\sqrt{\pi}}{2} e^{i(\nu+1/2)\pi/2} (-\tau)^{1/2} H_\nu^{(1)}(-k\tau) \ , \tag{1.45}$$

where $H_\nu^{(1)}$ is a Hankel function of the first kind of order $\nu$. We have normalised the solution to satisfy Eq. (1.36), and fixed the Fock space representation by selecting only the advanced solution in the limit $k \gg aH$ and introducing a phase factor such that in this limit the solution has the form $u_k \to \frac{1}{\sqrt{2k}} e^{-ik\tau}$. This is the plane wave form for flat space, and shows us that in this limit ordinary flat spacetime quantum field theory is recovered. This choice is known as the adiabatic (Bunch-Davis) vacuum.

The solution exhibits the expected behaviour that as inflation progresses and $\tau \to 0$, a given $k$ mode evolves from the limit of being far inside the cosmological horizon to being far outside it where $k \ll aH$. Considering the limit $k \ll aH$, therefore, and expanding the Hankel function to leading order leads to the asymptotic form

$$w_k \to e^{i(\nu-1/2)\pi/2} 2^{\nu-3/2} \frac{\Gamma(\nu)}{\Gamma(3/2)} \frac{(-k\tau)^{-\nu+1/2}}{\sqrt{2k}} \ . \tag{1.46}$$

Using this equation together with Eqs. (1.40) and (1.43) implies that the spectrum for $\mathcal{R}$ is given by

$$P_{\mathcal{R}}^{1/2}(k) = \frac{2^{\nu-5/2}}{\pi} \frac{\Gamma(\nu)}{\Gamma(3/2)} \frac{H}{a\dot{\phi}} \left( \frac{1}{aH(1-\epsilon)} \right)^{-\nu+1/2} k^{-\nu+3/2} \ . \tag{1.47}$$

The scale-dependence of this power spectrum is $k^{2\nu-3}$, and the spectrum becomes arbitrarily close to the scale-invariant form as $\nu \to 3/2$. This corresponds to $p \to \infty$, and hence to the slow-roll parameters tending to zero. In other words, the spectrum is close to a scale-invariant form in the slow-roll regime. It is usual to parametrise the deviation from scale-invariance in terms of the spectral index, $n$, defined by

$$n - 1 = \frac{d \ln P_{\mathcal{R}}}{d \ln k} \ , \tag{1.48}$$

and given in this case by $n = 1 + 2/(p-1)$. Finally, the spectrum is often written in the form

$$P_{\mathcal{R}}^{1/2}(k) = \left[ 2^{\nu-5/2} \frac{\Gamma(\nu)}{\Gamma(3/2)} (1-\epsilon)^{\nu-1/2} \frac{H^2}{\pi\dot{\phi}} \right]_{k=aH} \ , \tag{1.49}$$

where the right-hand side is evaluated when the wavelength equals the cosmological horizon ($k = aH$).

### 1.4.2 General potentials

It is clear that the method presented in the previous subsection cannot be employed for a general potential, since in that case the background does not evolve in a power-law manner. If we consider slow-roll inflation, however, progress can be made. It can be straight-forwardly shown, to first order in the slow-roll parameters, that

$$\frac{z_{\tau\tau}}{z} = 2a^2H^2 \left( 1 + \frac{5}{2}\epsilon - \frac{3}{2}\eta \right) \ , \tag{1.50}$$

and that to this order $\tau$ is still given by Eq. (1.43). To proceed, each $k$ mode is considered individually, where it is assumed that the slow-roll parameters can be taken as constants while the mode evolves between the limits $k \gg aH$ and $k \ll aH$. We can, therefore, still employ the solution given in Eq. (1.45), but with Eq. (1.50) now implying that $\nu = 3/2 + 3\epsilon - \eta$. The slow-roll parameters are evaluated for a given mode at the point at which $k = aH$. In this case, the spectrum will be scale-dependent with a spectral index given by

$$n = 1 + 2\eta - 6\epsilon \ . \tag{1.51}$$

Furthermore, to leading order in a slow-roll expansion, this approximation leads to an amplitude for the perturbations of the form

$$P_{\mathcal{R}}^{1/2}(k) = \left[\frac{H^2}{2\pi\dot{\phi}}\right]_{k=aH} \ , \tag{1.52}$$

which can be conveniently written in terms of the potential and $\epsilon$ using Eqs. (1.19)-(1.20) as

$$P_{\mathcal{R}}^{1/2}(k) = \left[\sqrt{\frac{8}{3}}\left(\frac{V}{\epsilon}\right)^{1/2}\ell_{\rm Pl}^2\right]_{k=aH} \ . \tag{1.53}$$

It is also important to note that a similar calculation can be performed for tensor perturbations. To keep our discussion to a reasonable length we will not present the details here, but rather simply state the results (see Lidsey *et al*, 1997, for a derivation similar to the one we have presented for scalar perturbations). The tensor power spectrum is given by

$$P_g^{1/2}(k) = \left[\frac{4}{\sqrt{\pi}}H\ell_{\rm Pl}\right]_{k=aH} \ , \tag{1.54}$$

and the spectral index, conventionally defined to be $n_g = d\ln P_g/d\ln k$, is given by $n_g = -2\epsilon$. Comparison between the scalar and tensor spectra reveals that the tensor perturbations are sub-dominant compared with the scalar perturbations when $\epsilon \ll 1$.

## 1.5 A working example: The quadratic potential

All the elements are now in place to consider a concrete model of inflation which allows 60 e-folds of inflation, and agrees with current observations of the CMB. We choose the simplest possible example, that of the quadratic potential given by

$$V(\phi) = \frac{1}{2}m^2\phi^2 \ , \tag{1.55}$$

where $m$ represents the mass of the field. A quadratic potential may also be viewed as a lowest-order Taylor expansion of a more general potential around a turning point. Throughout this thesis we will often use this example in our calculations to illustrate a concrete realisation of the effects we discuss. For this potential, the slow-roll parameters are given by

$$\epsilon = \eta = \frac{m_{Pl}^2}{4\pi\phi^2} \ , \tag{1.56}$$

and become progressively smaller the further the field is from the minimum of the potential.

The largest scales visible on the CMB correspond to comoving scales which exited the cosmological horizon 60 e-foldings before the end of inflation. On these scales observations from the Cosmic Background Explorer (COBE) satellite provide a normalisation for the total density perturbation. Neglecting tensor perturbations, this normalisation in turn implies that the amplitude of $P_{\mathcal{R}}$ should be approximately $5 \times 10^{-5}$ (see Liddle and Lyth, 2000, for details). Moreover, the latest WMAP results (Spergel *et al*, 2006) constrain the spectral index to be $n \approx 0.95 \pm 0.02$. Employing the condition $\epsilon = 1$ we can see that for the quadratic potential inflation ends when

$$\phi_{\rm end} \approx \frac{1}{4}\ell_{\rm Pl}^{-1} \ . \tag{1.57}$$

Using this value together with Eq. (1.23) and setting $N = 60$, one can determine that

$$\phi_{60} \approx 3\ell_{\rm Pl}^{-1} \ , \tag{1.58}$$

in order for 60 e-folds of inflation to occur. This also implies that the field took the value $\phi_{60}$ when the scales corresponding to the largest scales on the CMB exited the horizon. The slow-roll parameters at this epoch are given by

$$\epsilon = \eta \approx 9 \times 10^{-3} \ , \tag{1.59}$$

and hence the spectral index is $n \approx 0.96$, which is within the current observational limits. Furthermore, considering Eq. (1.53) with the COBE normalisation amplitude $5 \times 10^{-5}$, and employing Eqs. (1.55), (1.58) and (1.59), we can determine that the mass of the field must be $m \approx 10^{-6}\ell_{\rm Pl}^{-1}$.

In conclusion, the quadratic potential with $m \approx 10^{-6}\ell_{\rm Pl}^{-1}$ forms a working model of inflation if the field is initially displaced by at least $3\ell_{\rm Pl}^{-1}$ from the minimum of its potential. This initial displacement is of great importance to this thesis, as we shall see.

## 1.6 Motivation for considering fundamental theories

The standard model of cosmology, encompassing early universe inflation and the hot big bang, has been incredibly successful. The model has allowed us to constrain the form and contents of the universe, has provided us with a solution to the problems of the standard hot big bang model, and has given us a plausible explanation for the origin of structure. However, a dramatic consequence which has emerged is that the identity of 96% of the universe's matter content is unknown. It is only indirectly observed through its effects on the universe's dynamics, and its exact nature and origin remains uncertain.

To address the problem of what these forms of matter are, one must turn to fundamental physics. For example, a candidate for the dark matter is the lightest supersymmetric particle. On the other hand, in order to explain the 'dark energy' the usual approach has been to introduce a vacuum energy (cosmological constant) of the required magnitude. Alternative models of dark energy use one or more self-interacting scalar fields, which produce acceleration in a similar way to slow-roll inflation in the early universe. Ultimately, however, a model of the universe, directly derived from fundamental theory, must explain either the magnitude of the vacuum energy, the origin of the scalar fields or provide an alternative source for the present-day acceleration.

In the very early universe other problems are present. The origin of the inflaton field is unknown, and this needs to be identified with a field arising within a fundamental theory. Alternatively another mechanism which provides inflation must be derived from theory. Moreover, within the context of slow-roll inflation, the high energy initial state of the field remains unexplained. The inflaton must begin its evolution displaced from the minimum of its potential and this may be considered unnatural. Furthermore, the problem of initial singularities in cosmological models is still present in inflationary scenarios, and the universe still appears to evolve from a singular origin. It is natural to ask, therefore, whether scenarios based on fundamental physics can address these problems.

Motivated by some of these questions regarding the early universe, this thesis investigates the dynamics of a number of scenarios inspired by two fundamental theories of quantum gravity: Loop Quantum Gravity and String Theory. A number of issues are addressed. Part I considers semi-classical Loop Quantum Cosmology, which is inspired by Loop Quantum Gravity. Chapters 2 and 3 introduce Loop Quantum Cosmology and the semi-classical regime of this theory, and describe how a number of ambiguities arise in this regime. Chapter 4 then investigates how a flat, isotropic and homogeneous semi-classical model can cause a scalar field to accelerate up its self-interaction potential, offering an explanation for the high potential energy state required by inflation. The effect of the ambiguities on this mechanism is then studied in detail. Chapter 5 shows that the semi-classical regime can allow a bounce from a contracting to an expanding phase to

occur. This feature is applied to the positively-curved cosmology to develop a model for the generation of the inflationary initial conditions through oscillations of the universe. Chapter 6 is concerned with a non-singular model for the origin of the universe known as the the emergent universe scenario. It is shown that the semi-classical regime allows a very appealing version of this scenario to be constructed. Chapter 7 considers a further consequence of the semi-classical regime, which is that it forces the universe to undergo a period of inflation independently of the form of the inflationary potential. The chapter addresses the question of whether this phase could replace or supplement standard slow-roll inflation by calculating a first approximation to the spectrum of perturbations that are generated.

Part II of the thesis considers the braneworld scenario which is inspired by string theory. Chapter 8 introduces this scenario and discusses the motivation behind it. Chapter 9 then analyses braneworld models which allow a bounce, and hence oscillations. It investigates whether the initial conditions for inflation can be generated in these models though oscillations, and whether this can be used to develop emergent universe scenarios in the braneworld setting. A concrete example which can realise both these possibilities is then studied in detail. We conclude with a discussion in chapter 10.

# Part I

# LQC

# Chapter 2

# Background

In this first part of the thesis we consider cosmological scenarios inspired by loop quantum gravity (LQG). LQG, or quantum geometry as it is also known, is an attempt to quantise gravity in a background independent and non-perturbative manner. There are a great many reviews of LQG available (see for example Thiemann, 2001; Rovelli, 2004; Thiemann, 2003; Rovelli, 1998; Ashtekar and Lewandowski, 2004; Nicolai and Peeters, 2006). The major achievement of LQG is to successfully implement these two guiding principles (of a non-perturbative treatment and background independence) within a mathematically well defined framework. The theory has also led to a number of interesting predictions and impressive successes. In particular, LQG predicts a discrete spectrum for geometrical operators such as the area and volume operator (Rovelli and Smolin, 1995; Ashtekar and Lewandowski, 1997, 1998; Thiemann, 1998a). It also allows the definition of matter Hamiltonian operators which are free from ultraviolet divergences (Thiemann, 1998b), and provides a derivation of the Bekenstein–Hawking entropy formula (Rovelli, 1996; Ashtekar *et al*, 1998; Krasnov, 1998). Despite many open issues remaining, these advances have led to a sustained interest in the field, a rapidly increasing body of literature (see Corichi and Hauser, 2005, for a recent bibliography), and considerable optimism over the ultimate success of the programme.

Given the increasing maturity of the field, it is natural that there is also an increasing interest in its phenomenological implications. For example, it has been suggested that quantum gravity might modify Lorentz invariance, and this idea can be investigated within the LQG framework (see for example Gambini and Pullin, 1999; Alfaro *et al*, 2002, 2004). The hope with all phenomenological studies is twofold; first that comparison of these studies with experiment or observation may constrain the theory, and secondly that new and interesting behaviour may be uncovered, perhaps even behaviour that resolves existing problems. An example would be the possibility that Lorentz violation may solve the apparent lack of a cut-off in the energy of cosmic rays (Amelino-Camelia

and Piran, 2001). Here we are interested in phenomenological applications within cosmology, and the resolution of cosmological problems.

Since quantum gravitational effects are expected to have important consequences in high energy and high curvature regimes, the early universe provides a natural environment to explore the new features of LQG. Cosmological models are also important from a more fundamental perspective since symmetry reduced models allow issues in the full theory to be addressed within a much simpler environment. In recent years, therefore, considerable interest has focused on applying LQG to homogeneous cosmological models. The field has been pioneered by Martin Bojowald with a string of important papers (see the review papers Ashtekar *et al*, 2003; Bojowald and Morales-Tecotl, 2004; Bojowald, 2004, 2005a,b,c, and references therein). The resulting theory is loop quantum cosmology (LQC). The main attraction of LQC is that it follows closely the quantisation scheme of the (well defined) full theory of LQG. This is not possible for conventional Wheeler-DeWitt quantisation where the full theory is only defined in a formal manner. This means we can be optimistic that the features of the symmetry reduced models are consequences of the structure of the full theory.

This work has led to the resolution of a number of difficulties encountered in Wheeler-DeWitt quantisation of homogeneous models. In particular, at the quantum level the Wheeler-DeWitt equations are replaced with discrete difference equations with a non-singular evolution in both the isotropic and anisotropic cases (Bojowald, 2001a,b,c).

While the quantum difference equations are fascinating developments, it is difficult to connect them to the other theories of the early universe, and in particular to inflationary theory. They also suffer from the interpretational problems inherent in quantum cosmology. In order to overcome these problems a complementary approach has been to incorporate the characteristic effects of the quantum equations into 'effective' equations of motion. In practice this involves defining an effective Hamiltonian which incorporates non-perturbative quantum effects while ignoring the underlying discrete structure. In this 'semi-classical' approach the dynamics is described by ordinary or partial differential equations, rather than quantum operators, but the non-perturbative quantisation effects modify the dynamics. Within this approximation a host of interesting phenomenological effects have been uncovered, including those contained in this thesis. Of particular importance is the removal of the chaotic behaviour close to the singularity in the Bianchi IX model (Bojowald and Date, 2004), the presence of a super-inflationary phase in the isotropic model discovered by Bojowald (2002a), and the presence of a bounce from a contracting to an expanding phase in the positively-curved isotropic model (Singh and Toporensky, 2004; Bojowald *et al*, 2004; Date and Hossain, 2005).

This part of the thesis is concerned with the 'semi-classical' regime of homogeneous

and isotropic LQC. In order to understand semi-classical LQC, we begin by briefly reviewing the key features of LQG. We do not attempt to give a complete summary, but rather focus on the structure of LQG and the operators which are important for the effects seen in the semi-classical regime. We then present an overview of the symmetry reduction process and quantisation procedure which leads to isotropic loop quantum cosmology. Chapter 3 studies the approximation of the semi-classical regime, and focuses on ambiguities in this regime which come both from the full theory, and from the cosmological model. Finally, chapters 4-7 study dynamical phenomena in this regime and determine how ambiguities can affect these phenomena.

## 2.1 The structure of loop quantum gravity

LQG is a canonical quantisation of GR. GR is first put into its canonical form in which the basic variables are the spatial part of the metric $q_{ab}$, and the canonical momenta are the extrinsic curvature $K_{ab}$, where $a = 1, 2, 3$. In canonical form the field equations of GR are replaced by a Hamiltonian formulation, with constraints. There are two constraint equations, the Hamiltonian constraint and the diffeomorphism constraint. The theory is then recast in terms of Ashtekar variables. This reformulation is necessary because the space of spatial metrics or extrinsic curvature tensors (upon which Wheeler-DeWitt quantisation is based) is poorly understood.

In moving to Ashtekar variables, the first step is to represent the spatial geometry not by the spatial metric, but by three orthogonal triad vectors $e^a_i$, such that $e^a_i e^b_i = q^{ab}$, where $i = 1, 2, 3$. Ashtekar variables are then the densitised triad

$$E^a_i = |\mathrm{det} e^b_j|^{-1} e^a_i \ , \tag{2.1}$$

and the Ashtekar connection

$$A^i_a = \Gamma^i_a + \gamma K^i_a \ , \tag{2.2}$$

where $K^i_a = K_{ab} e^b_i$, $\Gamma^i_a = -\epsilon^{ijk} e^b_j \left( \partial_{[a} e^k_{b]} + \frac{1}{2} e^c_k e^l_a \partial_{[c} e^l_{b]} \right)$ is the spin connection and $\gamma = 0.274$ is the Barbero-Immirzi parameter. The Barbero-Immirzi parameter becomes important quantum-mechanically but does not affect the classical theory. Its value given here has been fixed by comparison of LQG black hole entropy predictions with the Bekenstein-Hawking formula (Domagala and Lewandowski, 2004; Meissner, 2004). The introduction of triads means that an $\mathrm{SO}(3)$ gauge freedom has been introduced, associated with the freedom to orientate the triads in space. This leads to a further constraint equation which must be satisfied. This is referred to as the Gauss constraint. We note that the Ashtekar connection and the triad are conjugate to one another

$$\{A^i_a(x), E^b_j(y)\} = 8\pi \ell^2_{\mathrm{Pl}} \gamma \delta^b_a \delta^i_j \delta(x, y) \ , \tag{2.3}$$

where $\{\ ,\ \}$ are Poisson brackets. The next step is to smear the fields in order to obtain a well defined algebra without delta functions. Since LQG is background independent, this cannot be done as an integral over space. Instead the connection is integrated along curves and exponentiated to form holonomies

$$h_c(A) = \mathcal{P} \exp \int_c \tau_i A_a^i \dot{c}^a(t) \mathrm{d}t \ , \tag{2.4}$$

where $\mathcal{P}$ indicates a path ordered exponentiation, $\dot{c}^a$ is the tangent vector to the curve $c$, and $\tau_i$ are the generators of $\mathrm{SU}(2)$. For the fundamental representation of $\mathrm{SU}(2)$, $\tau_j = -i\sigma_j/2$ where $\sigma_j$ are the Pauli matrices. The densitised triads are integrated over 2-dimensional surfaces resulting in fluxes

$$F_S(E) = \int_S \tau^i E_i^a n_a(y) \mathrm{d}^2 y \ , \tag{2.5}$$

where $n_a$ is the unit norm to the surface $S$. The Poisson algebra of the holonomies and the fluxes is well-defined. They are closed under Poisson brackets and the delta function is not involved. Holonomies and fluxes are therefore considered to be the basic variables and the ones promoted to operators by quantisation. A suitable Hilbert space can be formed using the holonomies as creation operators acting on a ground state. The resulting states only depend on connections along the edges used in the holonomies, and these edges can be collected together to form a graph which labels the state. States can then be given by spin networks, which are graphs in which the edges are labelled by irreducible representations of $\mathrm{SU}(2)$, and the vertices by matrices that specify how the holonomies which come together at the vertex are multiplied. An inner product can also be defined on this space such that the spin network states are orthogonal. The details of the Hilbert space and the states defined on it are not important for our purpose here, but what is crucial is how the basic variables, which are promoted to operators, are used to construct more complicated operators.

### 2.1.1 Composite operators and the constraints

With the basic variables in place, more complicated operators can be constructed. This is done by rewriting (or regularising) their classical expressions in terms of the basic variables which are then promoted to operators. Of particular importance are the operators which encode the constraints of the classical theory. Indeed, to complete the theory the constraints must be implemented to create a physical Hilbert space of states which satisfy the quantum constraints. The most important constraint for our cosmological applications is the Hamiltonian constraint, and particularly the matter part of this constraint. A complication immediately arises, however, when rewriting complicated classical expressions such as the Hamiltonian constraint in terms of the basic operators. There are

a number of ways to rewrite these expressions, and this leads to ambiguities in the final operator.

This can be illustrated by the construction of the matter Hamiltonian operator for a scalar field. The reformulation and quantisation of this operator is also the source of the semi-classical effects we investigate in subsequent chapters, so it is important to review the method of its reformulation at this stage.

### 2.1.2 The scalar field Hamiltonian in the full theory

The classical matter Hamiltonian density for a scalar field is given by the expression

$$\mathcal{H}_\phi = \frac{p_\phi^2}{2\sqrt{|\det E^c_j|}} + \frac{E^a_i E^b_i \partial_a\phi\partial_b\phi}{2\sqrt{|\det E^c_j|}} + \sqrt{|\det E^c_j|}\, V(\phi) \tag{2.6}$$

in terms of Ashtekar variables, where $p_\phi$ is the momentum conjugate to the scalar field. We see therefore that the matter Hamiltonian operator contains both the volume

$$\int_{\mathrm{R}} \sqrt{|\det E^a_i|}d^3x = \int_{\mathrm{R}} \sqrt{\left|\frac{1}{3!}\epsilon_{abc}\epsilon^{ijk}E^a_i E^b_j E^c_k\right|}d^3x \ , \tag{2.7}$$

and the inverse of this expression. These expressions must then be rewritten using fluxes and holonomies rather than the triad variable itself. This is important as it is fluxes and holonomies which are promoted to operators and not triads. For the volume operator this rewriting is relatively straightforward and only fluxes are required. It is achieved by dividing the volume into small cells, writing the triad in terms of a flux over infinitesimal surfaces, and changing the integral into a sum carefully defined to reproduce the classical value.

Inverse expressions, however, such as the inverse volume are more complicated. Since fluxes and hence the volume operator have discrete spectra which can include zero, inverse operators are not well defined. It turns out, however, that the classical inverse expressions can be rewritten using holonomies and the Poisson bracket, with no inverse terms appearing explicitly. This was first shown by Thiemann (1998b,c). On quantisation the Poisson bracket is then simply promoted to a commutator.

Let us consider the expression

$$2\pi\ell^2_{\mathrm{Pl}}\gamma\epsilon^{ijk}\epsilon_{abc}\frac{E^b_j E^c_k}{\sqrt{|\mathrm{det}E^a_i|}} = \{A^i_a(x), \int d^3y\sqrt{|\mathrm{det}E^a_i|}\} \ , \tag{2.8}$$

where we have employed the Poisson bracket and integrated over an arbitrary region containing $x$. The LHS of Eq. (2.8) does not involve any inverses and can be quantised in a well-defined manner by rewriting it in terms of holonomies and fluxes and promoting these to operators, whilst simultaneously raising the Poisson bracket to a commutator.

We are now in a position to consider the inverse expressions contained in the matter Hamiltonian, Eq. (2.6). The first of these is the inverse volume $|\det E^a_i|^{-1/2}$ itself. To reformulate this quantity, we must first note that the LHS of Eq. (2.8) is equal to $12\pi\ell^2_{\rm Pl}\gamma e^i_a$. In other words, Eq. (2.8) is the inverse undensitised triad up to a factor. More generally, therefore,

$$e^i_a(x)\,(\det E^a_i)^{(1-m)/2m} = \frac{m}{12\pi\ell^2_{\rm Pl}\gamma}\{A^i_a(x), \mathcal{V}^{1/m}\}\ , \tag{2.9}$$

where we write $\mathcal{V}$ for $\int d^3y\sqrt{|\det E^a_i(y)|}$, and $m$ is an integer. We can now see that:

$$\begin{aligned}\frac{1}{\sqrt{|\det E^a_i|}} &= \frac{\det e^i_a}{\det E^a_i} = \frac{\frac{1}{6}\epsilon^{abc}\epsilon_{ijk}e^i_a e^j_b e^k_c}{\det E^a_i}\\ &= \frac{1}{6}\epsilon^{abc}\epsilon_{ijk}\left(4\pi\ell^2_{\rm Pl}\gamma\right)^{-3}\{A^i_a, \mathcal{V}^{1/3}\}\\ &\times \{A^j_b, \mathcal{V}^{1/3}\}\{A^k_c, \mathcal{V}^{1/3}\}\ ,\end{aligned} \tag{2.10}$$

where we have used Eq. (2.9) with $m = 3$.

There is still some freedom, however. For example, we can multiply by any positive integer power of $\det e^i_a$, such that

$$\begin{aligned}\frac{1}{\sqrt{|\det E^a_i|}} &= \frac{(\det e^i_a)^k}{(\det E^a_i)^{(k+1)/2}}\\ &= \left(\frac{1}{6}\epsilon^{abc}\epsilon_{ijk}\left(\frac{4(2k-1)}{k}\pi\ell^2_{\rm Pl}\gamma\right)^{-3}\{A^i_a, \mathcal{V}^{(2k-1)/3k}\}\right.\\ &\times \left.\{A^j_b, \mathcal{V}^{(2k-1)/3k}\}\{A^k_c, \mathcal{V}^{(2k-1)/3k}\}\right)^k\ ,\end{aligned} \tag{2.11}$$

with an ambiguity parameter $k$ which can take discrete positive integer values. The value $k = 2$ results from multiplying by $\det E^a_i$ and can be argued to be the most natural choice when we keep in mind that $E$, rather than $e$, is the basic geometrical variable underlying loop quantum gravity.

A second ambiguity also appears at this level. This ambiguity appears because we must write the above expressions in terms of holonomies rather than the Ashtekar connection, $A$. This can be done using the following reformulation:

$$\begin{aligned}\{A^i_a, \mathcal{V}^{1/3}\}\Delta x^a &= \frac{1}{j(j+1)(2j+1)}\\ &\times {\rm tr}_j\sum_i\left(\tau_i h_{\Delta x}(A)\{h_{\Delta x}(A)^{-1}, \mathcal{V}^{1/3}\}\right)\ ,\end{aligned} \tag{2.12}$$

where $\Delta x$ is an infinitesimal element of length, and we have used the freedom of taking the trace using any irreducible representation of SU(2) with spin $j$. $j$ is the new ambiguity

parameter, and can in general take any half integer value. The fundamental representation corresponds to $j = \frac{1}{2}$.

The term $E^a_i E^b_i / \sqrt{|\det E^c_j|}$ in Eq. (2.6) must also be rewritten in a similar fashion to the inverse volume term. For isotropic LQC, however, this term is zero since spatial gradients vanish.

In summary, in this subsection we have discussed a great achievement of LQG, which is to allow the definition of inverse operators in a rigorous manner. This allows complicated operators such as the Hamiltonian constraint to be quantised. We have sketched how the matter Hamiltonian is regularised so that it is suitable for quantisation. Of course, the more complicated gravitational part of the Hamiltonian must also be rewritten using similar techniques. We have focused on the matter Hamiltonian, however, since it is responsible for the effects we study in the following chapters. The important lesson of this section is that the process of regularisation is rather complicated and it is therefore not surprising that a number of ambiguities arise, even at the level of the full theory. It is important to mention that there are a number of other ambiguities in complicated operators such as the Hamiltonian constraint, which arise due to factor ordering. Although this also deserves attention, we will not consider this further here as we do not expect such ambiguities to have an effect on the semi-classical approximation that this thesis considers.

## 2.2 Isotropic loop quantum cosmology

The idea behind LQC is to study the effects of the quantisation scheme used in full LQG through symmetric models. An excellent summary of LQC can be found in the review paper of Bojowald (2005c). Symmetry reduction is performed first, and then quantisation proceeds following the steps for the full theory which we outlined above. For this thesis, only the homogeneous and isotropic case is needed, and we therefore outline the procedure to derive this model.

In LQG the structures we described in the previous section are defined on a differentiable manifold $\Sigma$. The symmetry is then introduced through the mapping $S : \Sigma \to \Sigma$, where $S$ is the symmetry group. Although the action of this group introduces a background into the theory, the method for the background independent theory can still be followed. Through careful reference to the full theory, therefore, we can still capture elements unique to the background independent theory in the symmetry reduced models.

Considering the homogeneous and isotropic metric Eq. (1.1), it is clear that the only free component is the scale factor $a$. Therefore, when we come to write the system in terms of triad and connection variables, we should expect one free component for each,

which is what is found. The isotropic connection is given by $A_a^i = \tilde{c}\alpha_I^i\omega_a^I$, where $\tilde{c}$ contains the single gauge invariant degree of freedom and $\omega_a^I$ is a left invariant one-form under a suitable three dimensional translational subgroup of the $G_6$ symmetry group of homogeneity and isotropy (for details of the construction of invariant connections see appendices A and B of Bojowald, 2005c). For $k = 0$ and $k = 1$ (which we consider solely from here on) it is possible to choose the translational subgroup such that the integral curves of its generators are related simply by rotations. It is sufficient, therefore, to consider holonomies along integral curves of one of the symmetry generators. We have that

$$h_I = \exp \int A_a^i X_I^a \tau_i = \cos(\frac{1}{2}\mu c) + 2\alpha_I^i \tau_i \sin(\frac{1}{2}\mu c) \ , \tag{2.13}$$

where $X_I^a$ is the symmetry generator, and we have normalised such that $X_I^a\omega_a^J = \delta_I^J$. Furthermore, $\mu$ depends only on the length of the curve and $c = \tilde{c}/V_0$, where $V_0$ represents the classical volume of the region of space to be quantised (which is assumed to be topologically compact). If we know the holonomy for all $\mu$, we can determine $c$, the only gauge invariant piece of information. The algebra generated by sums of products of matrix elements is the algebra of almost periodic functions of the form

$$f(c) = \sum_\mu f_\mu \exp(i\mu c/2) \ , \tag{2.14}$$

where $f_\mu$ are constants. It is this algebra, together with the fluxes, which must be represented on a Hilbert space. Fluxes need only be constructed for special surfaces. A suitable choice simply allows the flux to be written in terms of a single number, $p$. $p$ is then conjugate to $c$ through the relation

$$\{c, p\} = \frac{8\pi\gamma\ell_{\rm Pl}^2}{3} \ . \tag{2.15}$$

Hence the Poisson algebra, which is to be elevated to a commutation algebra upon quantisation, is given by

$$\{f(c), p\} = \frac{8\pi\ell_{\rm Pl}^2}{6} \sum (i\mu f_\mu) \exp(i\mu c/2) \ . \tag{2.16}$$

This means that upon quantisation, the flux $p$ is represented as a derivative operator

$$\hat{p} = -\frac{8\pi}{3} i\gamma\ell_{\rm Pl}^2 \frac{d}{dc} \ , \tag{2.17}$$

so that the commutation algebra is satisfied. Using the standard bra-ket notation we have $\langle\mu|c\rangle = e^{i\mu c/2}$, and

$$\hat{p}|\mu\rangle = \frac{8\pi}{6}\gamma\ell_{\rm Pl}^2\mu|\mu\rangle \equiv p_\mu|\mu\rangle \ . \tag{2.18}$$

Finally, given the FRW metric (1.1), we can compare our triad and connection components to the standard metric variables, which reveals that $c = \Gamma + \gamma\dot{a} = (k^{1/2} + \gamma\dot{a})$ and $|p| = a^2$.

Having defined our basic variables and their representation as operators in the isotropic case, we are now in a position to construct the composite operators following the steps we described for the full theory in the previous section. Let us consider the Hamiltonian constraint. We note that the choice of variables means that the diffeomorphism and Gauss constraints are already satisfied. The full Hamiltonian constraint can be written in terms of our isotropic variables as

$$\mathcal{H} = -\frac{3}{8\pi\ell_{\rm Pl}^2}(\gamma^{-2}(c-\Gamma)^2 + \Gamma^2)\sqrt{p} + \mathcal{H}_{\rm matter}(p) = 0 \ , \tag{2.19}$$

where $H_{\rm matter}$ is the matter Hamiltonian, which we again take to be the Hamiltonian for a scalar field, Eq. (2.6). In terms of our isotropic components this becomes $\mathcal{H}_\phi = 1/2p^{-3/2}p_\phi^2 + p^{3/2}V$ since the gradient terms are identically zero. The Hamiltonian constraint controls the dynamics of the theory. Indeed, the dynamical effects which are studied in the following chapters are very closely connected with the Hamiltonian constraint and particularly the matter Hamiltonian.

In order to quantise the Hamiltonian constraint in the isotropic case the classical expression (2.19) is rewritten following (as closely as possible) the method by which the analogous expressions in the full theory are rewritten. Let us again consider the matter Hamiltonian in detail. In this case we must reformulate the inverse volume, $p^{-3/2}$. This can be done in an analogous fashion to the reformulations used in the full theory, given in Eqs. (2.11) and (2.12). It can readily be verified that classically

$$p^{-3/2} = \left(\frac{3}{8\pi\gamma\ell_{\rm Pl}^2 l j(j+1)(2j+1)}\sum_{I=1}^{3}{\rm tr}_j\left(\tau_I h_I\{h_I^{-1}, |p|^l\}\right)\right)^{3/(2-2l)} \ , \tag{2.20}$$

where for purely isotropic variables there is no restriction on $l$ except that $0 < l < 1$. However, direct comparison with Eq. (2.11) leads to 'preferred' values of $l$ which are given by $l = l_k = 1 - (2k)^{-1}$. This expression can be quantised by promoting the holonomy and the flux, $p$, to operators, and promoting the Poisson bracket to a commutator. Performing this procedure and operating on a state $u$, the eigenvalues of the inverse volume operator can be determined from the resulting expression:

$$\hat{d}(p)_{j,l}|\mu\rangle = \left(\frac{9}{8\pi\gamma\ell_{\rm Pl}^2 l j(j+1)(2j+1)}\sum_{k=-j}^{j}k|p_{\mu+2k}|^l\right)^{3/(2-2l)}|\mu\rangle \ . \tag{2.21}$$

(For details see Bojowald, 2002b).

An important property of the eigenvalues of the inverse volume operator is that they are bounded from above and do not diverge to infinity as $p_\mu \to 0$. The inverse volume,

therefore, does not diverge even when the volume is zero. Moreover, the eigenvalues can be approximated by a continuous function given by

$$d_{j,l}(p) = d_{j,l}(a) = D_l(q)a^{-3} \ , \tag{2.22}$$

where $q = a^2/a_*^2$, $a_*^2 = \gamma l_{\rm Pl}^2\, j/3$ and

$$D_l(q) = D_{j,l}(a) = \left\{ \frac{3}{2l} q^{1-l} \left[ (l+2)^{-1} \left( (q+1)^{l+2} - |q-1|^{l+2} \right) \right.\right. \\ \left.\left. - \frac{1}{1+l} q \left( (q+1)^{l+1} - \mathrm{sgn}(q-1)|q-1|^{l+1} \right) \right] \right\}^{3/(2-2l)} \ . \tag{2.23}$$

This approximation is arrived at by replacing the summation in Eq. (2.21) with an integral. It therefore requires that the summation is over a sufficiently large number of values and hence gets progressively better with larger values of $j$.

In order to complete the quantisation of the isotropic LQC model, the whole of the Hamiltonian constraint must be rewritten in terms of holonomies and fluxes. In this process inverse reformulations are used in both the gravitational and the matter parts of the Hamiltonian constraint, and hence ambiguities from this process can occur in the gravitational sector as well as in the matter sector. In this thesis we only consider the effects of ambiguities in the matter Hamiltonian. It is important to point out, however, that gravitational ambiguities can also be important. In what follows, we will implicitly assume that the parameter $j_g$, which plays an analogous role in the gravitational sector to that of the parameter $j$, is fixed to have a small value such as $j_g = 1/2$.

Throughout this thesis we will be as quantitative as possible, but we should always be mindful that there are a number of ambiguities (some of which we account for and others, like $j_g$, which we implicitly specify) which could influence our results.

Moving on from this issue of ambiguities, let us briefly summarise the results of applying a suitably quantised isotropic LQC Hamiltonian constraint to the state space of the theory. The result turns out to be a discrete difference equation which evolves a wavefunction representing the state of the universe in discrete steps. The size of discreteness is given by the important quantity

$$a_i = \sqrt{\gamma}\ell_{\rm Pl} \ . \tag{2.24}$$

LQC can therefore be seen to be a fundamentally discrete theory just like LQG. On scales greater than $a_i$, however, the difference equation approximates to the Wheeler-DeWitt equation for an isotropic cosmology. This means that on scales larger than $a_i$ the underlying discreteness of the theory can be ignored. This is the basis of the semi-classical approximation which we will explore in detail in the following chapter.

# Chapter 3

# The semi-classical regime and its ambiguities

In this section we discuss the 'semi-classical' approximation of LQC. The approximation is based on an effective Hamiltonian which is used to derive dynamical equations of motion. We show how this approximation arises, and how the ambiguity parameter $j$ defines the regime over which this approximation leads to dynamics which differ radically from those of the classical isotropic universe. Other ambiguities which exist in this regime are also discussed, and we show how they affect the semi-classical equations of motion. As we have seen, the ambiguity $l$ (as well as $j$) appears at the level of the full theory of LQG and survives the symmetry reduction process. Therefore, $l$ also plays a significant role in the semi-classical approximation. The process of constructing the semi-classical Hamiltonian, however, also allows other ambiguities to enter into the equations, which we also discuss. Finally, an alternative to deriving the evolution equations from the effective Hamiltonian, which was suggested by Hossain (2004), is reviewed and the resulting semi-classical equations derived. It is important to understand the ambiguities of the semi-classical regime in order to establish the robustness of our results, and to determine whether these results favour certain choices for the ambiguities, or whether observational signatures can distinguish between them.

## 3.1 The semi-classical approximation

Let us return to the inverse volume operator. For an isotropic universe the classical expression for the inverse volume is simply given by $p^{-3/2}$ or $a^{-3}$. It is the fact that $a^{-3} \to \infty$ as $a \to 0$ which is primarily responsible for the breakdown of classical dynamics and the presence of a singularity in this model. The same is true for quantisation based on the Wheeler-DeWitt procedure, where the matter Hamiltonian operator diverges in the

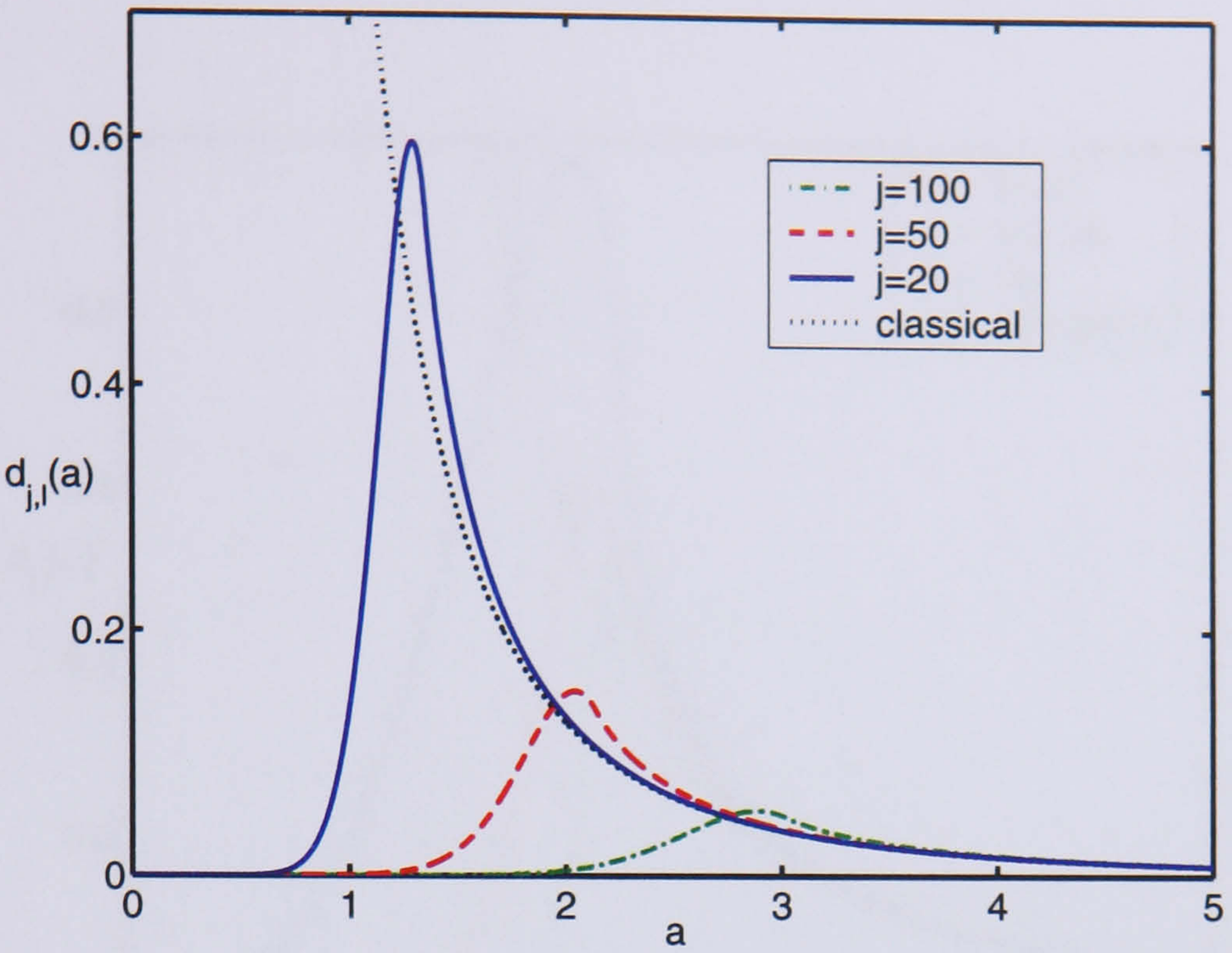


Figure 3.1: The small $a$ behaviour of the inverse volume ($d_{j,l}(a)$) for different values of $j$ and $l = \frac{3}{4}$. The monotonically increasing dotted line corresponds to the classical inverse volume $a^{-3}$. The modified inverse volume peaks close to $a_*$. $j = 20$ corresponds to $a_* = 1.35$, $j = 50$ corresponds to $a_* = 2.14$ and $j = 100$ corresponds to $a_* = 3.02$. The axes are labelled in Planck units.

limit $a \to 0$. We have seen, however, that LQC provides a major insight into this issue and allows a well-defined quantisation of inverse powers of metrical expressions which are not divergent. Indeed, in the previous section, we discussed the bounded nature of the eigenvalues of the inverse volume operator, and gave the continuous approximation, $d_{j,l}(a)$, to its spectrum, which is valid above the scale of discreteness. Let us now study this approximation to the inverse volume in detail. Fig. 3.1 plots the inverse volume (Eq. (2.22)) as a function of $a$ for different values of the parameter $j$. We can clearly see from this figure that the scale $a_*$ determines the size of the scale factor below which the inverse volume is significantly different from its classical form. On the other hand, for $a \gg a_*$, $d_{j,l}(a) \propto a^{-3}$, as we would expect. The size of $a_*$ is determined by the half integer parameter $j$ which is unrestricted by considerations from the full theory (although one can argue that smaller values appear more natural; see the following subsection).

Fig. 3.2. plots the inverse volume as a function of $a$ for different values of the parameter $l$, and Fig. 3.3 plots the function $D_l(q)$ (Eq. (2.23)) for the same values of $l$. We can see that $l$ has the effect of varying the rate at which $d_{j,l}(a)$ tends to zero below $a_*$.

The behaviour of $d_{j,l}(a)$ can therefore be summarised by three key features for all values of $j$ and $l$. First, $d_{j,l}(a)$ approaches the classical behaviour $a^{-3}$ for $a \gg a_*$. Secondly, there is a peak value around $a_*$ where the inverse volume is maximal. Thirdly, for $a \ll a_*$ the inverse volume approaches zero. Furthermore, consideration of Eq. (2.23)

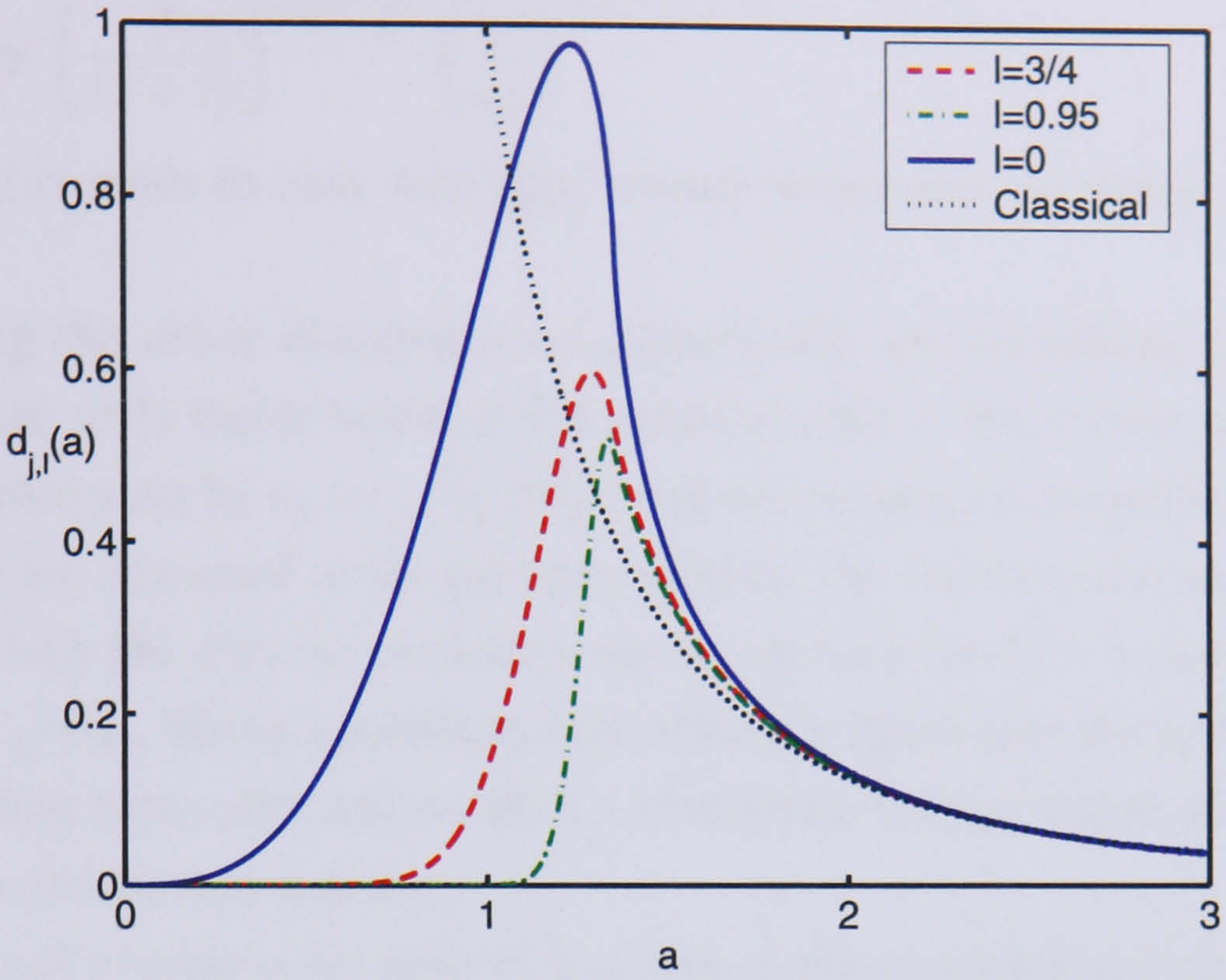


Figure 3.2: The small $a$ behaviour of the inverse volume ($d_{j,l}(a)$) for different values of $l$ and $j = 20$. The monotonically increasing dotted line corresponds to the classical expectation $a^{-3}$. The axes are labelled in Planck units.

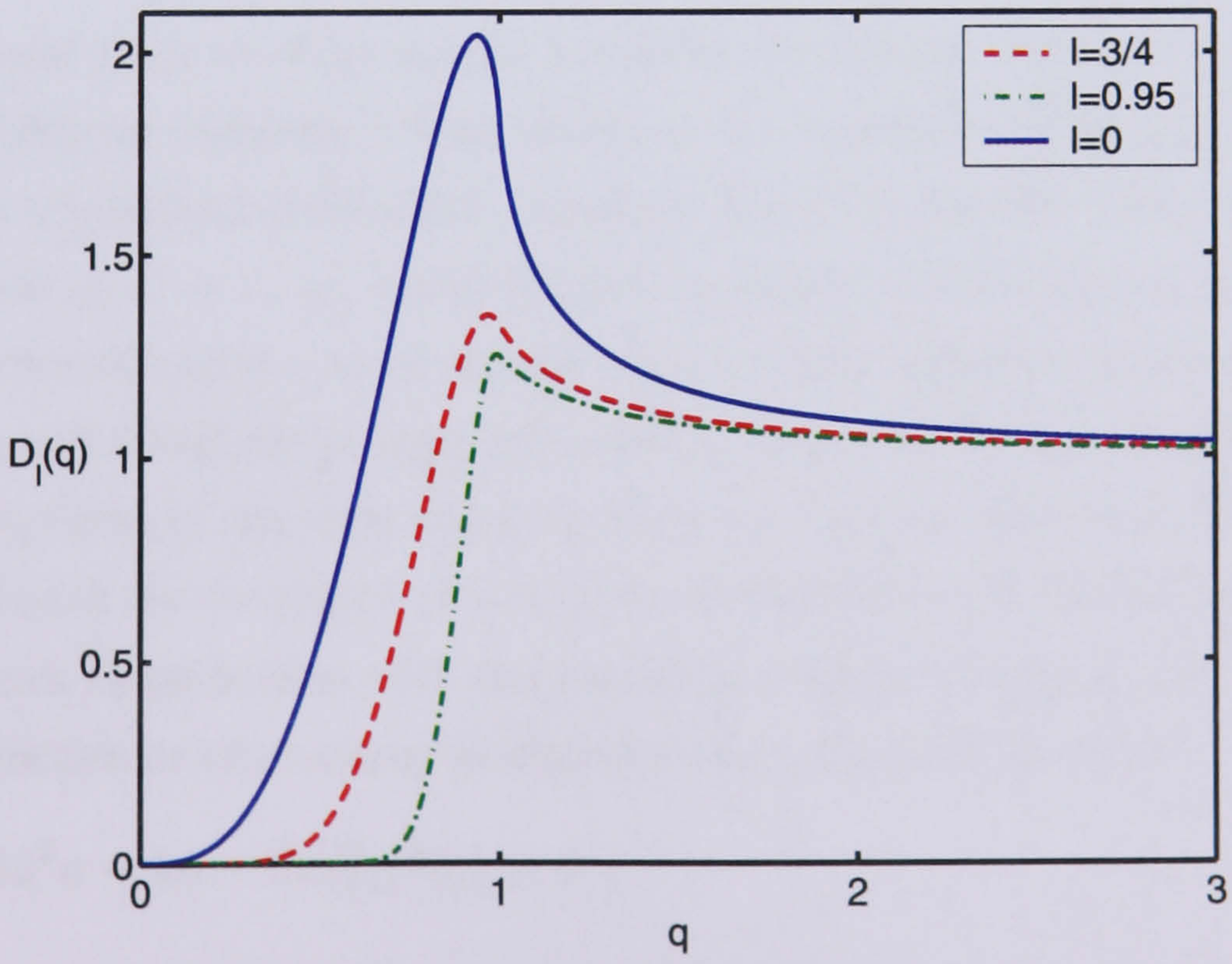


Figure 3.3: The small $q$ behaviour of the function $D_l(q)$ for different values of $l$ and $j = 20$. The axes are labelled in Planck units.

shows that for $a \ll a_*$

$$D_{j,l}(a) \approx \left(\frac{3}{(1+l)}\right)^{3/(2-2l)} \left(\frac{a}{a_*}\right)^{3(2-l)/(1-l)} , \tag{3.1}$$

and hence $d_{j,l}(a)$ tends to zero with approximate power-law behaviour with exponent $3/(1-l)$.

Considering the above discussion we immediately see something very important, which is that the scale factor below which modifications to the inverse volume become important is always set by $a_* = \sqrt{\gamma j/3}\ell_{\rm Pl}$, and hence only by the parameter $j$. On the other hand, as we discussed in the previous chapter, the fundamental scale of discreteness, above which the discrete evolution can be approximated by a continuous one, is given by $a_i \approx \sqrt{\gamma}\ell_{\rm Pl}$. We see, therefore, that when $j$ is larger than three, there is an overlap between these two scales and we have a continuous evolution, but with a significant modification to the inverse volume.

This region of overlap is the basis of the semi-classical approximation and our aim is to understand the effect of this region on the classical dynamics.

Since loop quantum gravity is a canonical quantisation, its dynamics are encoded in a Hamiltonian, which for isotropic LQC is a single constraint equation. This becomes the difference equation for the wave function in the full quantum regime. It is a quantisation of the classical Hamiltonian constraint,

$$\mathcal{H} = -3\dot{a}^2 a - ka + 8\pi\ell_{\rm Pl}^2\mathcal{H}_\phi = 0 , \tag{3.2}$$

which we present once more in metric variables for clarity. After dividing by $a^3$, this yields the Friedmann equation. Now, above $a_i$ the quantum difference equation is approximated by a quantum differential equation (the Wheeler-De Witt equation). If we are in the region $a_i < a < a_*$, however, this continuous differential equation will have the modified inverse volume in its matter sector. When coherent states are considered, their evolution will therefore be approximated by the dynamics generated by the classical Hamiltonian constraint, but with one complication. The complication is of course that we need to account for the region of overlap outlined above. To do this we must replace $a^{-3}$ in the matter Hamiltonian with the modified inverse volume $d_{j,l}(a)$. We therefore arrive at an effective or semi-classcial Hamiltonian constraint given by

$$\mathcal{H} = -3\dot{a}^2 a - ka + 8\pi\ell_{\rm Pl}^2\langle\hat{\mathcal{H}}_\phi\rangle = 0 , \tag{3.3}$$

where

$$\langle\hat{\mathcal{H}}_\phi\rangle = \frac{1}{2}D_{j,l}(a)a^{-3}p_\phi^2 + a^3V(\phi) . \tag{3.4}$$

We note that this effective Hamiltonian has become sensitive to the same quantisation ambiguities as the inverse volume.

Dividing by $a^3$, we find a modified Friedmann equation

$$H^2 = \frac{8\pi l_{\rm Pl}^2}{3}\frac{1}{a^3}\langle\hat{\mathcal{H}}_\phi\rangle - \frac{k}{a^2} \ . \tag{3.5}$$

It is important to remember, however, that from the point of view of the quantisation, the primary object is $\mathcal{H}$, and there is no direct quantisation of the Friedmann equation. Moreover, since the classical constraint $\mathcal{H} = 0$ plays the role of the Hamiltonian for the whole system of gravity and matter, it determines the full dynamics via the Hamiltonian equations of motion. For the scalar field, this results in equations of the form

$$\dot{\phi} = \{\phi, \mathcal{H}\} \quad , \quad \dot{p}_\phi = \{p_\phi, \mathcal{H}\} \ . \tag{3.6}$$

The first of these equations leads to $\dot{\phi} = \partial\mathcal{H}/\partial p_\phi$, and this allows us to show that the scalar field momentum is given by

$$p_\phi = a^3 D_l^{-1}\dot{\phi} \ , \tag{3.7}$$

which is different from the classical value because of the modified Hamiltonian.

We may now derive the 'semi-classical' versions of the Friedmann equation, the Raychaudhuri equation and the scalar field equation. The Friedmann equation follows from substituting Eq. (3.7) into Eq. (3.5) and is given by

$$H^2 = \frac{8\pi l_{\rm Pl}^2}{3}\left(\frac{1}{2}D_{j,l}(a)^{-1}\dot{\phi}^2 + V(\phi)\right) - \frac{k}{a^2} \ . \tag{3.8}$$

The scalar field equation follows from combining both Hamiltonian equations, given in Eq. (3.6), to form a second-order differential equation for $\phi$, which is given by

$$\ddot{\phi} + \left(3 - \frac{d\ln D_{j,l}(a)}{d\ln a}\right)H\dot{\phi} + D_{j,l}V'(\phi) = 0 \ . \tag{3.9}$$

Finally, the Raychaudhuri equation can be obtained via a Poisson bracket of the gravitational degrees of freedom, but more straightforwardly also follows from combining the scalar field equation (3.9) with the Friedmann equation (3.8). The Raychaudhuri equation is given by

$$\dot{H} = -4\pi\ell_{\rm Pl}^2\frac{\dot{\phi}^2}{D_{j,l}(a)}\left(1 - \frac{1}{6}\frac{d\ln D_{j,l}(a)}{d\ln a}\right) + \frac{k}{a^2} \ . \tag{3.10}$$

This derivation of these effective semi-classical equations was originally performed by Bojowald (2002a) (see also Bojowald and Vandersloot, 2003) in order to facilitate phenomenological studies. In what follows we will refer to this set of equations as the HAM scheme, highlighting the fact that the Hamiltonian is the primary dynamical object in their derivation.

The above discussion is not rigorous in the sense that we have only stated that the dynamics of coherent states will be approximated by the semi-classical equations. Considerable work has gone into verifying that this is indeed the case. This has been done in the context of a WKB approximation (Date and Hossain, 2004), by using a path integral approach (Vandersloot, 2005) and by directly applying the difference equations (Bojowald *et al*, 2004; Singh and Vandersloot, 2005). In all cases the appearance of the non-perturbative correction term $D_{j,l}(a)$ is a robust feature of the dynamics.

### 3.1.1 The logarithmic derivative of $D_{j,l}(a)$

From Eqs. (3.8)-(3.10) it is clear that the quantity $d\ln D_{j,l}(a)/d\ln a$ plays an important role in the semi-classical regime. Before progressing with our discussion, therefore, we determine the properties of this quantity which will be useful for the chapters which follow.

The full expression for this quantity is rather long and not particularly illuminating, so we do not give it here. Instead, in Fig 3.4 we plot this expression as a function of $q$ to highlight its form. For convenience we often denote this function as $A(a)$, and we note that

$$A(a) \equiv \frac{d\ln D_{j,l}(a)}{d\ln a} = 2\frac{d\ln D_l(q)}{d\ln q} \ . \tag{3.11}$$

Considering this expression, we see that $A$ plotted as a function of $q$ is identical for all values of $j$, and allows us to simultaneously understand the form of $A$ for all $j$. Considering Fig. 3.4, we can see that the function asymptotes to a constant value as $q \to 0$ ($a \to 0$). Moreover, from Eq. (3.1) we can determine that this value is given by

$$A_{a\to 0} = \frac{3(2-l)}{1-l} \ , \tag{3.12}$$

since $D_{j,l}$ is approximated by $a$ raised to this power. We can also see that $A$ reaches a minimum at $q = 1$ ($a = a_*$), and that this point is a cusp. Using the full expression for $A$, and taking the limit $q \to 1$, it is straightforward to determine that the minimum occurs at the value

$$A_{\min} = \frac{3(l-2)}{2l} \ . \tag{3.13}$$

Finally, we note that for $a > a_*$ the function $A$ rapidly tends to zero.

### 3.1.2 A density bound

From our discussion thus far, it is clear that the semi-classical equations of motion are valid only when $a > a_i$. It is important, however, to ask whether there are any other constraints on their validity.

When considering a completely classical spacetime, within the framework of general relativity, the classical equations of motion cease to be valid when the energy density approaches the Planck scale. This conclusion is usually arrived at by considering the de Broglie wavelength associated with the mass of a small region of spacetime, and the Schwarzschild radius associated with the same region. At the Planck scale the de Broglie wavelength becomes smaller than the Schwarzschild radius. This suggests that at this energy scale quantum black holes could be formed, and full quantum gravity needs to be considered. The concept of classical spacetime and continuous evolution equations therefore breaks down at Planck scale densities. Since the semi-classical regime assumes a continuous spacetime, it is possible to argue that the density must also be bounded by the Planck scale in this regime. Indeed, at the very least, energy densities must be smaller than the Planck scale at $a_*$, where the transition to a fully classical universe occurs.

A complementary way of arguing that there is an additional constraint on the validity of the semi-classical equations is to consider the fundamental length scale $a_i$, and the Hubble length $H^{-1}$. A useful measure of validity then comes from comparing the two, and considering Hubble lengths which are smaller than the fundamental scale to be inconsistent. Using Eq. (2.24), this leads to the consistency condition

$$H^{-1} > \sqrt{\gamma}\ell_{\rm Pl} \ . \tag{3.14}$$

The two points of view are closely related since $H$ is related to the energy density through the Friedmann equation (1.6).

Throughout this thesis we will use Eq. (3.14) to indicate when the semi-classical equations are valid. This proves most convenient since the concept of energy density becomes less well defined in the semi-classical regime. It is clearly not an exact condition, but serves as a useful measure which is sufficiently accurate for our purposes.

## 3.2 Additional ambiguities and quantisation schemes

At this point in our discussion let us consider the possibility of additional ambiguities. Since we are considering the Hamiltonian as a composite object, it is possible to insert arbitrary positive powers of $a^3 d_{j,l}(a)$ into the expression. At the classical level this factor would just be equal to unity. In particular, multiplying the matter Hamiltonian by a power $[a^3 d_{j,l}(a)]^n$ leads to the Friedmann equation,

$$H^2 = \frac{8\pi l_{\rm Pl}^2}{3} D^n \left( \frac{1}{2} D\, a^{-6} p_\phi^2 + V(\phi) \right) \ , \tag{3.15}$$

where $n > 0$ is a new ambiguity parameter. For simplicity, we have considered only the flat ($k = 0$) case. In Eq. (3.15) we have dropped the subscripts $j$ and $l$ when writing

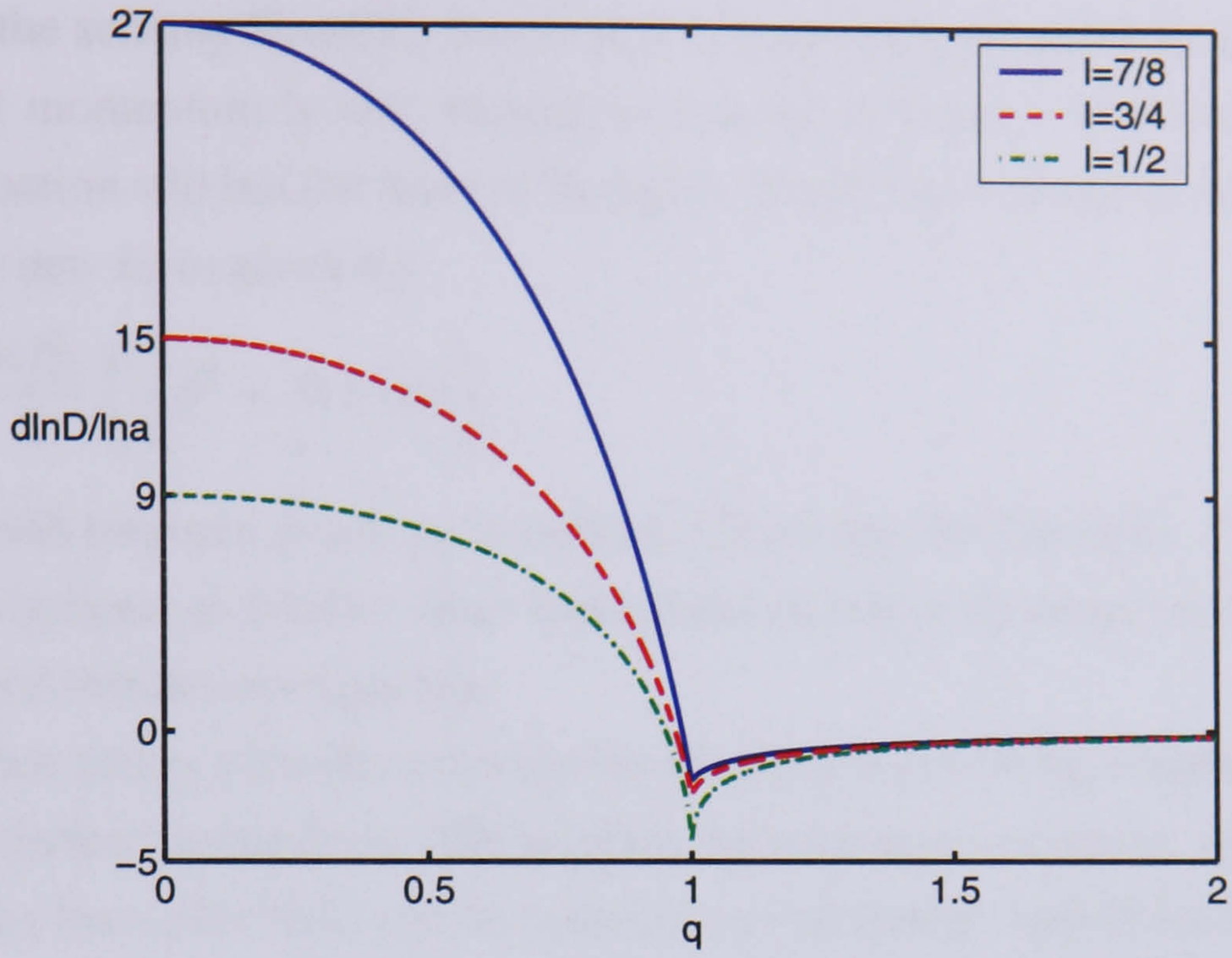


Figure 3.4: The small $q$ behaviour of the function $d \ln D_{j,l}(a)/\ln a$, plotted as a function of $q$ for different values of $l$. The axes are labelled in Planck units.

$D$, and have also not explicitly indicated that it is a function of $a$. For convenience we will continue to do this throughout the rest of the thesis. In the same way as before, we can compute the scalar field's momentum and equation of motion using Eq. (3.6). In this case $\dot{\phi} = a^{-3} D^{1+n} p_\phi$ and thus

$$H^2 = \frac{8\pi l_{\rm Pl}^2}{3} \left( \frac{1}{2} D^{-1-n} \dot{\phi}^2 + D^n V(\phi) \right) \tag{3.16}$$

and

$$\ddot{\phi} + \left( 3 - (1+n) \frac{d\ln D}{d\ln a} \right) H\dot{\phi} + D^{1+2n} V'(\phi) = 0 \ . \tag{3.17}$$

This more general scheme will be called HAM(n) in what follows. For $n = 0$ the equations reduce to those of HAM.

An alternative to the HAM approach has been advocated by Hossain (2004) in which the Hubble parameter is viewed as the primary object in order to derive the effective dynamical field equations. While the Hubble operator still involves the matter Hamiltonian, there is an additional difference in its spectrum which arises due to a quantisation of the $1/a^3$ term in Eq. (3.5). This equation is therefore replaced by

$$\langle \hat{H}^2 \rangle = \frac{8\pi}{3} l_{\rm Pl}^2 \langle \hat{a^{-3}} \rangle \langle \hat{\mathcal{H}}_\phi \rangle \ , \tag{3.18}$$

where again we have considered $k = 0$. The result is a Friedmann equation different in form to that of Eq. (3.8), but identical to that of HAM(1) in terms of $p_\phi$ :

$$H^2 = \frac{8\pi l_{\rm Pl}^2}{3} \left( \frac{1}{2} D^2 a^{-6} p_\phi^2 + D\, V(\phi) \right) \ . \tag{3.19}$$

In contrast to the scheme HAM(1), however, it is implicitly assumed by Hossain (2004) that the scalar momentum is not changed compared to HAM. As a consequence, the scalar field equation still has the form of HAM(0). Moreover, in terms of $\dot{\phi}$ the Friedmann equation has a new form given by

$$H^2 = \frac{8\pi l_{\rm Pl}^2}{3}\left(\frac{1}{2}\dot{\phi}^2 + D\,V(\phi)\right) \ , \tag{3.20}$$

since the relation between $\dot{\phi}$ and $p_\phi$ is different from that for HAM(1). We will refer to this alternative scheme as FRIED, since the dynamical law is obtained from an expression analogous to the Friedmann equation.

The quantum theory provides even further freedom for deriving Friedmann equations and results in further ambiguities. We mention just one other example, which is that the Hamiltonian for the scalar field can be written in a classically equivalent form as

$$\begin{aligned} \mathcal{H}_\phi &= \frac{1}{2}\frac{1}{a^3}\,p_\phi^2 + a^3\,V(\phi) \\ &= \frac{1}{2}\frac{1}{a^{3(n+1)}}\,a^{3n}\,p_\phi^2 + \frac{1}{a^{3m}}\,a^{3(m+1)}\,V(\phi) \ , \end{aligned} \tag{3.21}$$

where $\{n, m\}$ are arbitrary, semi-positive definite constants (for $m = n$ we obtain HAM(n)). The HAM Friedmann equation (3.5) thus becomes

$$H^2 = \frac{8\pi\ell_{\rm Pl}^2}{3}\left(\frac{1}{2}\,D^{-(n+1)}\,\dot{\phi}^2 + D^m\,V(\phi)\right) \ , \tag{3.22}$$

whereas adopting the FRIED quantisation procedure beginning with Eq. (3.18) implies that

$$H^2 = \frac{8\pi\ell_{\rm Pl}^2}{3}\left(\frac{1}{2}\,D^{-n}\,\dot{\phi}^2 + D^{(m+1)}\,V(\phi)\right) . \tag{3.23}$$

In these extended schemes the scalar field equation becomes

$$\ddot{\phi} + \left(3 - (n+1)\frac{d\ln D}{d\ln a}\right) H\dot{\phi} + D^{(m+n+1)}\,V'(\phi) = 0 \, . \tag{3.24}$$

Thus, freedom at the quantum level, as parametrised by non-zero values of $\{m, n\}$, results in effective cosmological field equations that are radically different from the natural (minimal) choice corresponding to $m = n = 0$.

In summary, we have seen that in addition to the ambiguity parameters $j$ and $l$, which are inherited from the full theory, the procedure for deriving the quantised version of the Friedmann equation is not unique: differences arise depending upon whether one quantises the matter Hamiltonian or directly quantises the Friedmann equation by viewing the Hubble parameter as an operator. Finally, there is an additional freedom in writing down the Hamiltonian, and hence the Friedmann equation. This is parametrised by the constants $m$ and $n$.

## 3.3 Comparing ambiguities from the point of view of the full theory of LQG

It is clear that the ambiguities listed in the preceding discussion do not all appear at the same level from a theoretical perspective. The parameters $j$ and $l$ emerge when we quantise the inverse volume and are therefore already present even before the Hamiltonian constraint is applied to the quantum states. They are therefore common to all quantisation schemes. It is important to understand, however, that not all choices for these ambiguities appear equally natural, and that some values of the parameters may be preferred over others. Insight into what values are preferred may be made by comparing the expressions in loop quantum cosmology with the corresponding ones of full loop quantum gravity.

For the parameter $j$, there are virtually no internal restrictions, even when we use the full theory, since the same freedom appears in both cases. Because it corresponds to choosing a non-trivial irreducible representation, one may argue that the most natural value is $j = 1/2$, corresponding to the fundamental representation. This is also the smallest allowed value for $j$. An additional argument is that, from the fundamental perspective, we really choose two representations, one for the gravitational part of the constraint and one for the matter part. For the gravitational part we have implicitly assumed a small value of $j_g$ so that inverse volume effects in the Hamiltonian do not become important. One would therefore regard a choice of $j$ as more natural if the two representations are close to each other, which points toward smaller $j$. But if we are not restricted to this choice, there is no distinction between lower and higher values of $j$, except that huge values (of the order $10^{20}$ or larger) would be excluded by particle physics experiments. In this regard $j$ is the main ambiguity parameter and there is much scope for an input from phenomenological studies in determining a favoured value. In particular, it is interesting to consider whether the cosmological evolution of the early universe favours smaller values of $j$.

Concerning the parameter $l$, the situation is different. This parameter arises because $p^{-3/2}$ is rewritten as a Poisson bracket involving a positive power of $p$. From the point of view of the full theory, $p$ corresponds to the isotropic component of a densitised triad, on which the loop quantisation is based. In section 2.1.2 we saw that without symmetry assumptions, it is more difficult to rewrite the inverse volume in a way which is suitable for quantisation. The extra difficulty means that, even though there is no unique choice, not all values in the range $0 < l < 1$ can be used. Instead of a continuous range, only the discrete sequence, $l_k = 1 - (2k)^{-1}$, $k \in \mathbb{N}$ is allowed. Moreover, $k = 2$, which implies $l_2 = 3/4$, was argued to be the most natural.

The schemes HAM(n) and FRIED can also be distinguished by internal considerations. As explained before, the Hamiltonian is the primary object in a canonical quantisation so FRIED, which puts the emphasis on the Hubble parameter, is more specific. In fact, a corresponding quantisation of the full theory is not possible, while the quantisation steps of HAM are modelled on those of full loop quantum gravity. Among the different possibilities in HAM(n), it is clear that HAM=HAM(0) is most natural since it does not involve the introduction of powers of $a^3 d_{j,l}(a)$.

To summarise, for $j$ there are only weak restrictions from the theoretical side alone, even though small values look more natural. For $l$ there is a discrete set of preferred choices when we compare with the full theory, such that all values lie in the interval $1/2 \leq l < 1$. Theoretical considerations for the dynamical ambiguities strongly prefer the original scheme HAM. The reason that the dynamical ambiguities are more restricted conceptually follows from the different way they emerge. We cannot avoid the ambiguities $\{j, l\}$ since the most direct way to quantise $a^{-3}$ is ruled out by the non-existence of an inverse of $\hat{a}$ in the loop quantisation. We then have to use a more complicated quantisation, obtained by rewriting the classical expression. For the Hamiltonian constraint, on the other hand, the most direct quantisation does work and leads us to HAM. The other choices change this procedure in a similar way to that which introduces the $l$ ambiguity, but these changes are no longer forced upon us. Thus, the most direct procedure which works appears to be the most natural.

In this thesis we will at various times consider different ambiguity parameters. We will always consider the effect of $j$ taking different values, since it is largely unrestricted by theoretical considerations. The other ambiguities we consider will be motivated by how they modify the dynamics of the most natural choice of HAM, corresponding to $l = 3/4$ and $n = m = 0$. In particular, we will be interested in whether or not the conceptual expectations discussed so far are also favoured by phenomenological considerations.

# Chapter 4

# Setting the initial conditions for slow-roll inflation

In this chapter we study our first phenomenological consequence of the semi-classical regime of isotropic LQC. Our focus will be to investigate the ability of the semi-classical evolution equations to establish the appropriate initial conditions for slow-roll inflation, and how this is affected by the various quantisation ambiguities discussed in the preceding chapter. In particular, as well as considering the ambiguity parameters $j$ and $l$, we will study both the HAM and FRIED quantisation schemes. Despite the superior theoretical justification for HAM, both schemes are considered because it turns out that the magnitude of the effect we consider becomes significant only when the energy bound of the semi-classical approximation (Eq. (3.14)) is close to being violated. It is therefore interesting to see whether or not this is sensitive to the quantisation scheme being used and whether the scheme favoured from a theoretical point of view is also favoured from a phenomenological one.

We begin by discussing the question of the initial conditions required for slow-roll inflation. We then investigate qualitatively how the semi-classical equations may help in answering this question, before addressing quantitatively whether or not they do.

## 4.1 The question of initial conditions

In order to form a working model of inflation using a scalar field, we need to specify the scalar field's initial conditions. The fact that slow-roll inflation is a dynamical attractor means that, provided the potential satisfies the slow-roll conditions (i.e. that the slow-roll parameters (1.21)-(1.22) are small), the system is very insensitive to the initial value of $\dot{\phi}$. The initial position of the field on the potential (given by an initial condition for $\phi$) is, however, very important since for a general inflationary potential the slow-roll conditions

are not satisfied everywhere. Indeed, the slow-roll conditions must be broken at some point on the potential in order to provide a natural mechanism to exit inflation. As we discussed in section 1.3, in the standard inflationary scenario it is usual to assume that the inflaton is initially in a state of high potential energy. Inflation then ends when the field rolls far enough down its potential and approaches a minimum where $V = 0$. Moreover, when we considered the concrete example of the quadratic potential in section 1.5, we saw that the field needed to be initially displaced by at least $3\ell_{\rm Pl}^{-1}$ from the minimum. It is clear that a similar displacement is required of any slow-roll model. The question which immediately arises, therefore, is why the inflaton begins in this state of high potential energy.

Answering the question of whether or not this initial state is to be expected requires a full understanding of inflation in the setting of a complete theory of quantum gravity. Our present understanding is clearly deficient, but a number of arguments can be put forward in the context of more specific settings.

The most common argument, originally advanced by Linde (1983) within the context of the chaotic inflationary scenario, is that the universe emerges from a spacetime foam at the Planck scale, where the energy density is of the order $m_{\rm Pl}^4$. The inflaton takes different values in different regions of the universe, and inflation proceeds in those regions where the field has suitable initial values.

On the other hand one can address the initial conditions question via the Wheeler-DeWitt approach to quantum cosmology. Here the square of the wavefunction is interpreted as the probability distribution for initial values of the scalar field in an ensemble of universes. In order to make physical predictions one must impose boundary conditions on the set of solutions, and it turns out that the results depend heavily on what choice is made. The tunnelling boundary condition (Vilenkin, 1984; Linde, 1984) supports the picture of an initially high potential energy. In this approach the probability distribution for initial values of the inflaton field is given by $\mathcal{P}_{\rm T} \propto \exp(-3/[8\pi\ell_{\rm Pl}^2 V(\phi)])$, implying that the universe is more likely to nucleate with the largest possible vacuum energy, $V$. However, this is in contrast to the no-boundary approach of Hartle and Hawking (1983), where the probability is given by $\mathcal{P}_{\rm NB} \propto \exp(+3/[8\pi\ell_{\rm Pl}^2 V(\phi)])$, and is therefore peaked at $V \to 0$. This seems to indicate that the initial conditions will not favour inflation.

In the context of LQC, it has been argued by Bojowald and Vandersloot (2003) that for the case of a constant potential, the wavefunction in LQC most closely resembles the Hartle-Hawking no-boundary wavefunction. More specifically, the difference equation in LQC requires the wavefunction to tend to zero near to the classical singularity (Bojowald, 2001b), and this resembles DeWitt's initial condition (DeWitt, 1967). However, within the context of more general solutions to the Wheeler-DeWitt equation, requiring

the wavefunction to be bounded as $a \to 0$ selects the exponentially increasing WKB mode (Bojowald and Vandersloot (2003)) which corresponds to the no-boundary wavefunction. Following this reasoning, it is possible to argue that within LQC a natural initial condition for the field is the minimum of the potential.

In view of this argument and the general uncertainty over what the initial condition for $\phi$ should be, it is important to investigate physical processes that enable the inflaton field to reach the values required for inflationary expansion. It turns out that the modified equations of semi-classical LQC provide a dynamical mechanism which may allow this to occur.

## 4.2 Setting the initial conditions through semi-classical LQC

Let us first consider the HAM equations (3.8)-(3.10) in a qualitative manner in order to illustrate the scalar field's behaviour in the semi-classical regime. The qualitative behaviour for the FRIED scheme is unchanged. We consider how the behaviour of equations (3.8)-(3.10) changes from that of the standard equations (1.14)-(1.16) for small values of the scale factor. First let us consider the Raychaudhuri equation (3.10). When $a \gg a_*$, $D = 1$ and the important quantity $A \equiv d\ln D/d\ln a$ we discussed in section 3.1.1 is zero. Eqs. (3.8)-(3.10) therefore reduce to the classical equations (1.14)-(1.16). When $a < a_*$, however, $D$ begins to change radically from unity, as was shown in Fig. 3.3. More importantly, $A$ also starts to vary markedly. In Fig. 3.4 we plotted the behaviour of this quantity as a function of $q = a^2/a_*^2$ to demonstrate how it depends on the ambiguity parameter $l$. If $a \ll a_*$, $A$ tends to a constant, which we determined to be $3(2-l)/(1-l)$. In the intermediate region $A$ varies from zero to this limiting value. We can see from Eq. (3.10) that the value $A = 6$ is important. When the universe is expanding with $A > 6$, then $\dot{H} > 0$, and the universe undergoes super-inflationary expansion[1]. This was first shown by Bojowald (2002a) and further studied by Bojowald and Vandersloot (2003). It is interesting to ask whether this phase of inflation, driven not by the potential energy of the inflaton but by quantisation effects, can replace or supplement standard inflation. One aspect of this question is considered further in chapter 7. Here, however, we focus on what effects the regime $a < a_*$ can have for standard inflation. This is interesting irrespective of the role super-inflation might play.

[1] In this chapter we assume that the curvature is negligible, and hence we take $k = 0$. Indeed, even if the curvature is not negligible initially it will rapidly become so if an extended period of accelerated expansion occurs. The case in which the curvature cannot be neglected is considered in the next chapter where we consider positively-curved universes.

Keeping in mind the form of $A$, let us now look at the scalar field equation (3.9). We see that the quantity $(3 - A)H\dot{\phi}$, which classically is the frictional term that allows slow-roll inflation to occur, changes sign when $A > 3$. If we again consider an expanding universe, it is clear that if the evolution begins for $a \ll a_*$, the frictional term will become an anti-frictional one, and the field will be accelerated along its potential. Moreover, the potential term in Eq. (3.9) becomes unimportant compared to this anti-frictional term since it contains a factor of $D$ which tends to zero when $a \ll a_*$. This acceleration effect is therefore very robust. The effect was also first discussed by Bojowald (2002a).

Let us now think qualitatively about what this means for inflation. If we consider the inflaton located initially at the minimum of its potential when the universe is in the regime $a \ll a_*$, we see that the field will be accelerated away from this minimum as the universe expands. As the universe grows larger than $a_*$, however, the anti-friction is replaced again by the standard frictional effect and the field decelerates. The field then reaches its maximal displacement before eventually turning around on the potential and rolling back down. Assuming the potential is of the correct form, and that the field has moved far enough, slow-roll inflation then commences. It is clear, therefore, that if the field is able to move sufficiently far up its potential, the conditions relevant to standard, slow–roll inflation may be realised in a natural way even if the field is initially situated in the minimum of its potential.

This scenario was investigated further by Tsujikawa *et al* (2004) where the emphasis was on determining if the turning around of the field on the potential can leave an observational signature on the CMB. They determined that if the field reaches its point of maximal displacement 60 e-foldings or so before the end of inflation, the perturbations generated during the turning point could lead to observable effects on the largest scales of the CMB.

Leaving observational effects aside, it seems from a conceptual point of view that the set of initial conditions that lead to slow-roll inflation might be significantly widened by the semi-classical dynamics of LQC. A crucial question that must be addressed, however, is whether or not this behaviour is robust under the quantum ambiguities discussed in the previous chapter, and how these ambiguities affect the behaviour. Since the scalar field equation (3.9) has the same functional form for both the HAM and FRIED quantisation schemes and, since $D \ll 3$ for $a \ll a_*$ for all values of $l$ , we expect the universe to enter the anti-frictional epoch for all cases. This would suggest that the qualitative behaviour should be the same. More quantitatively, it is also important to investigate whether the process of setting the initial conditions for inflation violates any of the assumptions which must be satisfied in the semi-classical regime, and in particular the energy bound (Eq. (3.14)).

For a quantitative analysis, therefore, we begin at the onset of the semi–classical regime ($a \approx a_i$), where we can first use the semi-classical equations for both quantisation schemes. We assume that the universe is flat and hence that $k = 0$. We also assume that the inflaton is initially at the minimum of the potential. This position is chosen for the reasons outlined above and also because it is in some sense the antithesis of the initial Planck scale potential energy. It is important to note, however, that the minimum is not the worst case scenario for the initial position of the field in terms of the number of e-folds of inflation that will be generated. To see this we must understand that the sign of the field's velocity at the beginning of the semi-classical regime is important. Consider again the quadratic potential. If the field is initially displaced in the direction of positive values of $\phi$, and if $\mathrm{sgn}(l_{\mathrm{Pl}}^2\dot{\phi}_{\mathrm{init}}) = +1$, the field begins moving up its potential immediately. If, on the other hand, $\mathrm{sgn}(l_{\mathrm{Pl}}^2\dot{\phi}_{\mathrm{init}}) = -1$, the inflaton rapidly falls back through the minimum of its potential before rolling up the other side. Consequently, the worst case scenario would be for the field to be displaced far from the minimum in one direction but begin its evolution moving in the opposite direction. As well as being motivated on other grounds, therefore, starting the field at the minimum allows us to side-step the issue of the initial direction of the field.

In the following subsections, we continue to use the quadratic potential (1.55) as a concrete example of the dynamics. In line with the previous discussion the initial conditions are given by $\{\phi_{\mathrm{init}} = 0, \dot{\phi}_{\mathrm{init}} > 0\}$.

## 4.3 Approximate analytic scheme

### 4.3.1 Transition from semi-classical to classical dynamics

In this section, we develop an approximate analytical approach to estimate the initial conditions for successful inflation in LQC for both the HAM and FRIED quantisation schemes. In both schemes the scalar field equation of motion is given by Eq. (3.9). The approximation separates the rolling of the field to its maximal value $\phi_{\mathrm{max}}$ into two distinct epochs, a semi-classical, anti-frictional phase followed by a classical epoch. The major simplifying assumption we make is to assume the asymptotic form (3.1) of the eigenvalue function, $D$, throughout the semi-classical era. It is also assumed that the transition to classical dynamics occurs instantaneously when $D$ reaches unity and that once this condition has been attained, $D$ remains fixed at unity. In essence we are assuming that the middle section of $D$ which contains the maximum, is unimportant for the dynamics. Ultimately the validity of this approximation will be tested with numerical integration.

The field reaches its point of maximal displacement when its potential energy begins

to dominate its kinetic energy. At this point the universe is considered to be classical (since $D = 1$) and previous investigations indicate that a good estimate for the turning point can be determined from the condition (Madsen and Coles, 1988)

$$\frac{1}{2}\dot{\phi}^2_{\text{max}} \approx V\left(\phi_{\text{max}}\right) \ . \tag{4.1}$$

Although for concreteness we are considering the quadratic potential, the approach we develop is independent of the particular functional form of the inflaton potential, and can be applied in principle to any potential. Moreover, since the inflaton is evolving away from the minimum, it is expected that its kinetic energy will dominate the cosmic dynamics until Eq. (4.1) applies. We therefore view the inflaton as a massless field ($V = 0$) until it reaches its turning point.

From a phenomenological point of view, there are two important constraints that must be satisfied for successful inflation. First, sufficient inflation must occur to solve the horizon problem and this implies that the field must be sufficiently displaced from its minimum when it begins to roll back down. As we have discussed, for the quadratic potential this requires $l_{\text{Pl}}\phi_{\text{max}} \geq 3$, if we assume 60 e-folds are required.

The second constraint concerns the region of parameter space where the semi-classical and classical approximations are valid. In section 3.1.2, we noted that this requires both $a > a_i$ and that the Hubble length be greater than $a_i$ (Eq. (3.14)). Eq. (3.14) is equivalent to the condition that a classical description of the dynamics is only consistent at energy scales below the Planck scale, and a minimal requirement is that it is met at the transition from the semi-classical to the classical regimes. Since the Hubble parameter and the inflaton's kinetic energy are monotonically increasing functions during the semi-classical regime, this leads to an upper bound on the duration of that phase. Moreover, we are neglecting the potential energy, so an estimate for the limit on the field's kinetic energy at the transition epoch follows directly from the Friedmann equation by setting $D = 1$. For both the HAM and FRIED quantisation schemes, this implies that $H_S^2 \approx 4\pi l_{\text{Pl}}^2 \dot{\phi}_S^2/3$ and hence that

$$\left| l_{\text{Pl}}^2 \dot{\phi}_S \right| \leq \left( \frac{3}{4\pi\gamma} \right)^{1/2} \ , \tag{4.2}$$

where a subscript $S$ denotes values of the parameters at the transition time. We refer to the bound (4.2) as the *kinetic bound*.

### 4.3.2 Classical dynamics

To proceed, let us now consider the classical phase. Our aim is to solve the equations for the field's evolution once the transition to classical dynamics has occurred. It proves convenient to consider the Hamilton-Jacobi form of the classical equations (1.14)-(1.16),

which can be derived by considering $H$ as a function of the field. For $V = 0$ the Friedmann and scalar field equations are therefore given by

$$\left(\frac{dH}{d\phi}\right)^2 = 12\pi\ell_{\rm Pl}^2 H^2 \ , \tag{4.3}$$

$$\frac{dH}{d\phi} = -4\pi l_{\rm Pl}^2 \dot{\phi} \ , \tag{4.4}$$

where time derivatives are replaced throughout by derivatives with respect to the scalar field. This form of the equations is useful as the general solution to Eqs. (4.3) and (4.4) is easily seen to be

$$H = H_S \exp\left[-\sqrt{12\pi} l_{\rm Pl}\left(\phi - \phi_S\right)\right] \ . \tag{4.5}$$

Substituting Eqs. (4.4) and (4.5) into Eq. (4.1) implies that the maximal value attained by the field for both the HAM and FRIED schemes is given by

$$\phi_{\rm max} e^{\sqrt{12\pi} l_{\rm Pl}\phi_{\rm max}} \approx \frac{\left|\dot{\phi}_S\right|}{m} e^{\sqrt{12\pi} l_{\rm Pl}\phi_S} \ . \tag{4.6}$$

When the potential is negligible, and the approximate power-law form of $D$ is valid, the scalar field equation (3.9) admits the first integral

$$\dot{\phi} = \dot{\phi}_{\rm init}\left(\frac{a}{a_{\rm init}}\right)^{3/(1-l)} \ , \tag{4.7}$$

where the subscript init denotes initial values at the beginning of the semi-classical regime. Substituting Eq. (4.7) into Eq. (4.6) then implies that

$$\phi_{\rm max} e^{\sqrt{12\pi} l_{\rm Pl}\phi_{\rm max}} \approx \frac{\left|\dot{\phi}_{\rm init}\right|}{m}\left(\frac{a_S}{a_{\rm init}}\right)^{3/(1-l)} e^{\sqrt{12\pi} l_{\rm Pl}\phi_S} \ . \tag{4.8}$$

Since we are assuming that the universe commences its evolution at $a_i$ we have that $a_{\rm init} = a_i$ and that

$$a_i \approx \sqrt{\gamma} l_{\rm Pl}, \qquad \frac{a_i}{a_*} \approx \left(\frac{3}{j}\right)^{1/2} \ . \tag{4.9}$$

It then follows from Eq. (3.1) that

$$\frac{a_S}{a_*} \approx \left(\frac{l+1}{3}\right)^{1/(4-2l)} \ ,$$

$$\frac{a_S}{a_i} \approx \left(\frac{j}{3}\right)^{1/2}\left(\frac{l+1}{3}\right)^{1/(4-2l)} \ . \tag{4.10}$$

Substituting Eq. (4.10) into Eq. (4.7) then yields an estimate for the initial value of the field's kinetic energy in terms of its value at the transition time:

$$\dot{\phi}_{\rm init} = \dot{\phi}_S\left(\frac{3}{j}\right)^{3/(2-2l)}\left(\frac{3}{l+1}\right)^{3/[(4-2l)(1-l)]} \ . \tag{4.11}$$

Imposing the kinetic bound (4.2) then leads to an estimate for an upper limit on the combination of parameters $j|l_{\rm Pl}^2\dot{\phi}_{\rm init}|^{2(1-l)/3}$ in terms of a constant with numerical value determined by the parameters $\gamma$ and $l$:

$$j\left|l_{\rm Pl}^2\dot{\phi}_{\rm init}\right|^{2(1-l)/3} \leq 3\left(\frac{3}{4\pi\gamma}\right)^{(1-l)/3}\left(\frac{3}{1+l}\right)^{1/(2-l)} . \tag{4.12}$$

Using the theoretically favoured value of $l = 3/4$, Eq. (4.12) simplifies to

$$j \leq \frac{4.6}{\left|l_{\rm Pl}^2\dot{\phi}_{\rm init}\right|^{1/6}} \tag{4.13}$$

and to

$$j \leq \frac{5.0}{\left|l_{\rm Pl}^2\dot{\phi}_{\rm init}\right|^{2/3}} \tag{4.14}$$

for $l \ll 1$.

We now require the value of the scalar field at the transition epoch in order to estimate the maximal value of the scalar field from Eq. (4.8) in terms of its initial value. This is determined from the solution to the field equations for each of the quantisation schemes.

### 4.3.3 HAM Quantisation

The solution to the Friedmann equation (3.8), neglecting the potential, is

$$\phi = \phi_{\rm init} + B_l\left[\left(\frac{a}{a_i}\right)^{3(2-l)/(2-2l)} - 1\right] , \tag{4.15}$$

where

$$\begin{aligned} B_l &= \frac{2(1-l)}{3(2-l)}\left(\frac{6}{8\pi l_{\rm Pl}^2}\right)^{1/2} \\ &\quad\times\left(\frac{3}{l+1}\right)^{3/(4-4l)}\left(\frac{a_i}{a_*}\right)^{3(2-l)/(2-2l)} \end{aligned} \tag{4.16}$$

is a constant. Since the expressions for general $l$ are cumbersome, we focus in what follows on the value $l = 3/4$ and the limit $l \ll 1$. We discuss the limit $l \to 1$ in section 3.5.2. Eq. (4.15) simplifies to

$$\phi = \phi_{\rm init} + B\left[\left(\frac{a}{a_i}\right)^{15/2} - 1\right] , \tag{4.17}$$

$$B_{3/4} \equiv \frac{2}{15}\left(\frac{6}{8\pi l_{\rm Pl}^2}\right)^{1/2}\left(\frac{12}{7}\right)^3\left(\frac{a_i}{a_*}\right)^{15/2} \tag{4.18}$$

for $l = 3/4$, and to

$$\phi = \phi_{\rm init} + B_0 \left[ \left( \frac{a}{a_{\rm i}} \right)^3 - 1 \right] \ , \tag{4.19}$$

$$B_0 = 3^{-1/4} \left( \frac{6}{8\pi l_{\rm Pl}^2} \right)^{1/2} \left( \frac{a_{\rm i}}{a_*} \right)^3 \tag{4.20}$$

for $l \ll 1$.

In general, the total shift in the value of the field induced by the anti-frictional effect of the semi-classical phase increases for increasing $j$, since the duration of the super-inflationary dynamics is enhanced for higher values of $j$. Consequently, the condition for the horizon problem to be solved can be expressed as a lower limit on the value of $j$ for given values of $\{l, \dot{\phi}_{\rm init}\}$.

Substituting Eqs. (4.17) and (4.18) into Eq. (4.8) and employing the estimates (4.9) and (4.10) implies that

$$l_{\rm Pl}\phi_{\rm max} e^{\sqrt{12\pi} l_{\rm Pl}\phi_{\rm max}} \approx 140 j^6 \left| l_{\rm Pl}^2 \dot{\phi}_{\rm init} \right| e^{\sqrt{12\pi} l_{\rm Pl}\phi_{\rm init}} \ , \tag{4.21}$$

when $l = 3/4$, where it is assumed that $j$ is sufficiently large for $(a_S/a_i)^{15/2} \gg 1$ (this requires $j \geq \mathcal{O}(3)$). The COBE normalisation constraint on the mass of the inflaton field has also been imposed. The horizon problem is therefore solved ($l_{\rm Pl}\phi_{\rm max} \geq 3$) if

$$\ln \left( j^6 \left| l_{\rm Pl}^2 \dot{\phi}_{\rm init} \right| \right) + \sqrt{12\pi} l_{\rm Pl}\phi_{\rm init} \geq 14.6 \ . \tag{4.22}$$

Eq. (4.22) then implies that

$$j \geq \frac{11}{\left| l_{\rm Pl}^2 \dot{\phi}_{\rm init} \right|^{1/6}} \ , \tag{4.23}$$

for $\phi_{\rm init} = 0$ and comparing the limits (4.23) and (4.13) for the HAM quantisation implies that they are incompatible for this value of $l$. This would seem to indicate that successful inflation within a purely semi-classical description is not possible with these initial conditions.

It is worth addressing briefly the question of how different values of the parameter $l$ would alter this conclusion. Since lowering the value of $l$ leads to super-inflationary expansion that is closer to the exponential limit, it might be expected that the kinetic energy of the inflaton field would grow less rapidly during the semi-classical phase. However, Eq. (4.14) implies that lowering $l$ does not significantly weaken the kinetic bound on $j$. Furthermore, for $l \ll 1$, substituting Eq. (4.19) into Eq. (4.8) implies that the horizon problem is only solved if

$$\ln \left( j^{3/2} \left| l_{\rm Pl}^2 \dot{\phi}_{\rm init} \right| \right) + \sqrt{12\pi} l_{\rm Pl}\phi_{\rm init} \geq 7.2 \ , \tag{4.24}$$

and for $\phi_{\rm init} = 0$, the constraint (4.24) reduces to the condition

$$j \geq \frac{120}{\left|l_{\rm Pl}^2 \dot{\phi}_{\rm init}\right|^{2/3}} \ . \tag{4.25}$$

### 4.3.4 FRIED Quantisation

For the FRIED quantisation scheme, the solution to the Friedmann equation (3.20) in the limit of kinetic energy domination is

$$\phi = \phi_{\rm init} + \left(\frac{3}{4\pi l_{\rm Pl}^2}\right)^{1/2} \ln\left(\frac{a}{a_i}\right) \ , \tag{4.26}$$

and substituting Eq. (4.26) into Eq. (4.8) implies that

$$\phi_{\rm max} e^{\sqrt{12\pi} l_{\rm Pl} \phi_{\rm max}} \approx \frac{\left|\dot{\phi}_{\rm init}\right|}{m} \left(\frac{a_S}{a_i}\right)^{3(2-l)/(1-l)} e^{\sqrt{12\pi} l_{\rm Pl} \phi_{\rm init}} \ . \tag{4.27}$$

The method of estimating when the horizon problem is solved is similar to that employed in the previous subsection for HAM quantisation. Substituting Eqs. (4.9) and (4.10) into Eq. (4.27) and imposing the requirement that $l_{\rm Pl}\phi_{\rm max} \geq 3$ leads to

$$\ln\left(j^{15/2}\left|l_{\rm Pl}^2 \dot{\phi}_{\rm init}\right|\right) + \sqrt{12\pi} l_{\rm Pl} \phi_{\rm init} \geq 17.2 \ , \qquad l = \frac{3}{4} \ , \tag{4.28}$$

$$\ln\left(j^{3}\left|l_{\rm Pl}^2 \dot{\phi}_{\rm init}\right|\right) + \sqrt{12\pi} l_{\rm Pl} \phi_{\rm init} \geq 10.6 \ , \qquad l \ll 1 \ . \tag{4.29}$$

For the case where $\phi_{\rm init} = 0$, this implies that the horizon problem is solved if

$$j \geq \frac{9.9}{\left|l_{\rm Pl}^2 \dot{\phi}_{\rm init}\right|^{2/15}} \ , \qquad l = \frac{3}{4} \ , \tag{4.30}$$

$$j \geq \frac{35}{\left|l_{\rm Pl}^2 \dot{\phi}\right|^{1/3}} \ , \qquad l \ll 1 \ . \tag{4.31}$$

Comparing the limits (4.30) and (4.31) with the corresponding kinetic bounds (4.13) and (4.14) implies that

$$\frac{9.9}{\left|l_{\rm Pl}^2 \dot{\phi}_{\rm init}\right|^{2/15}} \leq j \leq \frac{4.6}{\left|l_{\rm Pl}^2 \dot{\phi}_{\rm init}\right|^{1/6}} \ , \qquad l = \frac{3}{4} \ , \tag{4.32}$$

$$\frac{35}{\left|l_{\rm Pl}^2 \dot{\phi}_{\rm init}\right|^{1/3}} \leq j \leq \frac{5.0}{\left|l_{\rm Pl}^2 \dot{\phi}_{\rm init}\right|^{2/3}} \ , \qquad l \ll 1 \ . \tag{4.33}$$

As a result, the horizon problem can only be solved if $\left|l_{\rm Pl}^2 \dot{\phi}\right| \leq 10^{-9}$ when $l = 3/4$ and if $\left|l_{\rm Pl}^2 \dot{\phi}\right| \leq 3 \times 10^{-3}$ when $l \ll 1$.

## 4.4 Numerical results

The above analytic approach is very useful since it allows us to draw conclusions for wide ranges of initial conditions and parameter choices without the tedious process of integrating the equations numerically. We should, however, bear in mind its limitations. In particular Eq. (4.7) overestimates the value of the field's kinetic energy at the transition since the form of the eigenvalue function, $D$, given in Eq. (3.1), represents its asymptotic form in the limit $a \ll a_*$. Moreover, the estimate for $a_S$, the scale factor at the transition epoch, given in Eq. (4.10), is not precise, since there is no exact definition for this parameter. We must therefore check the accuracy of the analytic results found within this approximation scheme.

In this section, we determine the regions of parameter space that lead to successful inflation in the HAM and FRIED quantisation schemes by numerically integrating the field equations, where the complete expression (2.23) is assumed for the eigenvalue function and the inflaton potential is included. The results are presented in the form of plots of the ambiguity parameter, $j$, against $\dot{\phi}_{\text{init}}$ for a given value of $l$. On each plot a solid line represents the boundary for the horizon problem to be just solved (and consequently for large angular scales on the CMB to correspond to the turning point in the field's dynamics). A dashed line represents the boundary where the kinetic bound is just violated. Shaded areas represent regions for successful inflation. We also generate similar plots using the analytic approximation. This allows us to compare the analytic results with those obtained by numerical integration, and to assess the accuracy of the former.

### 4.4.1 $\{\phi_{\text{init}} = 0, \dot{\phi}_{\text{init}} > 0, l = 3/4\}$

We begin by considering the set of initial conditions $\{\phi_{\text{init}} = 0, \dot{\phi}_{\text{init}} > 0\}$ with $l = 3/4$ in order to compare the exact numerical results with the approximation scheme developed in section 4.3. Fig. 4.1 shows the analytic estimates for HAM quantisation and Fig. 4.2 shows the results for the same system from numerical integration. The corresponding results for FRIED quantisation are shown in Figs. 4.3 and 4.4, respectively. The horizon problem is solved above the solid line and the kinetic constraint is satisfied below the dashed line. Necessary conditions for successful FRIED inflation are $|l_{\text{Pl}}^2 \dot{\phi}_{\text{init}}| \leq 10^{-8}$ and $j \sim 100$.

There is good agreement between the analytic and numerical approaches in both schemes. The analytic approximation typically underestimates the maximum value of the scalar field by about $0.1 l_{\text{Pl}}^{-1}$ when $\phi_{\text{max}} \approx 3 l_{\text{Pl}}^{-1}$ leading to a small error in the total number of e–foldings, $\Delta N \approx 4$. Such an error is comfortably within other uncertainties that change the total number of e-foldings required to solve the horizon problem. In

particular, the reheating temperature has a major effect as discussed in section 1.3.

### 4.4.2 Effects of varying $l$

We now consider how different values of $l$ alter the above conclusions. We have numerically integrated the field equations where $l$ varies in the range $0.01 \leq l \leq 0.95$. In section 4.3.4, it was found that in the case of FRIED quantisation, the region of parameter space for successful inflation is widened for smaller values of $l$. This follows because the power dependences on the initial kinetic energy in Eq. (4.33) differ to a greater degree as $l$ decreases and the intersection of the two constraints in Fig. 4.3 is located at higher values of $\{j, \dot{\phi}_{\rm init}\}$. A lower value of $l$ corresponds to an expansion rate that is closer to the exponential limit and therefore the kinetic energy of the field grows less rapidly. Consequently, the superinflation phase must last longer to ensure the field has sufficient kinetic energy to solve the horizon problem. The full numerical integration supports this generic behaviour. The agreement between the analytic and numerical approaches improves at higher $l$. This can be understood by considering Fig. 3.2 which shows that the regime of the peak (which is neglected in our analytic scheme) widens for small $l$. For smaller $l$ values, the turning point of the field is underestimated by no more than $0.1 l_{\rm Pl}^{-1}$ to $0.2 l_{\rm Pl}^{-1}$ when $\phi_{\rm max} \approx 3 l_{\rm Pl}^{-1}$.

For the HAM quantisation scheme, the kinetic bound and the horizon problem constraint both take the form $j |l_{\rm Pl}^2 \dot{\phi}_{\rm init}|^{2(1-l)/3} \approx C_k$, where $C_k = C_k(l)$ is a numerical constant determined by $l$. In this case, it is the numerical factor $C_k$ which is important and successful inflation requires $C_{\rm kinetic} > C_{\rm horizon}$. The analytic approach for the case of $\phi_{\rm init} = 0$, as summarized in Eqs. (4.14) and (4.25), indicates that reducing $l$ below $l = 3/4$ strengthens the inequality $C_{\rm kinetic} < C_{\rm horizon}$. For $l > 3/4$, numerical integration implies that the difference in the numerical factors is reduced, but not sufficiently for the inequality to be reversed, at least up to $l \approx 0.95$. Hence, the two lines never intersect in Fig. 4.2 and there is no region of parameter space which simultaneously satisfies both bounds. Indeed, for given values of $\{\dot{\phi}_{\rm init}, l\}$, the highest value of $j$ that is just consistent with the kinetic bound typically leads to a turning point in the field's motion at $\phi_{\rm max} \approx 2.4 l_{\rm Pl}^{-1}$. Numerical integration indicates that this holds over a wide range of $l$ and implies that the field must be displaced from its minimum for successful inflation to proceed.

As in FRIED quantisation, the agreement between analytic and numerical results is good, and improves at higher $l$. We conclude, therefore, that varying $l$ does not significantly alter the overall qualitative picture in this scenario.

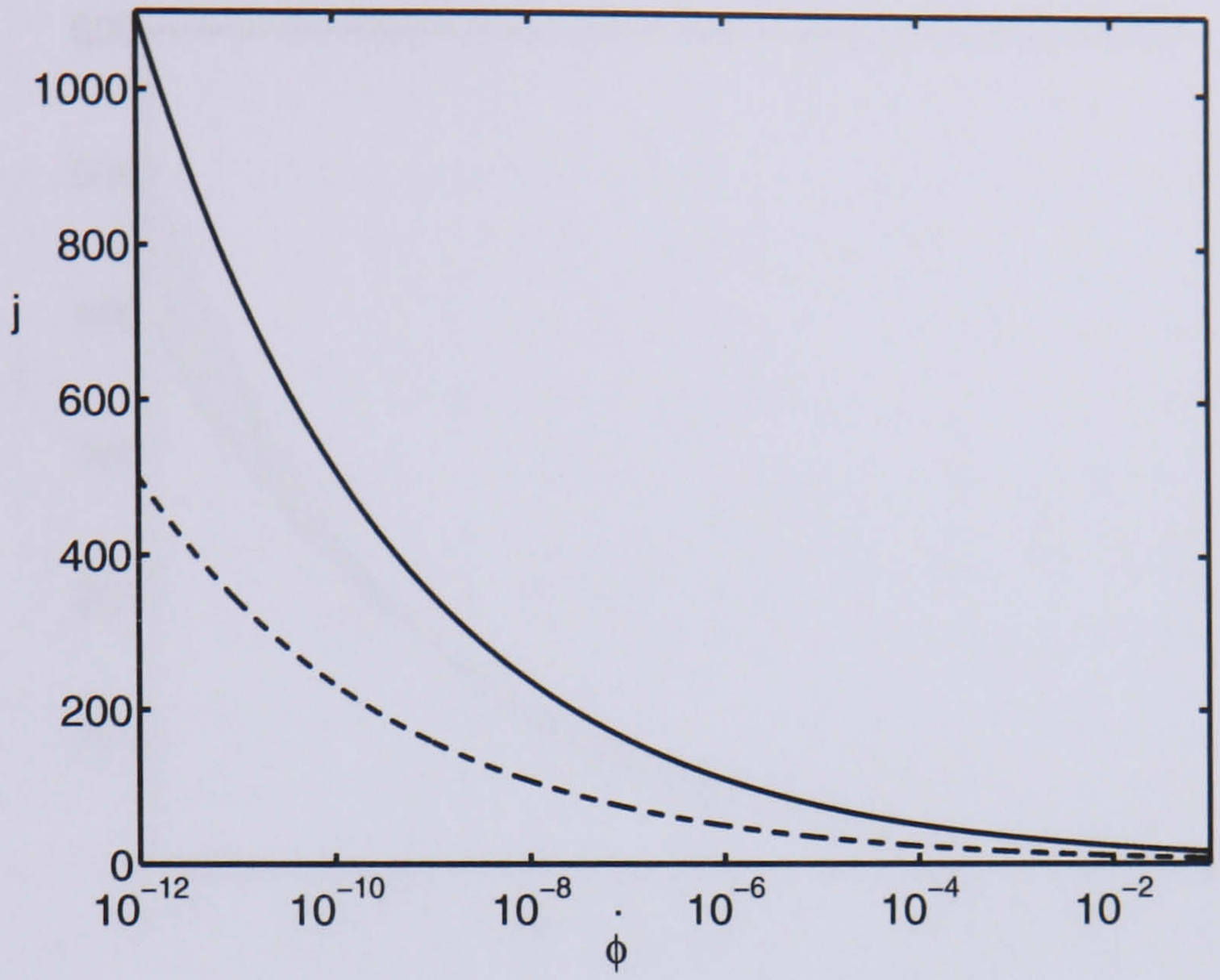


Figure 4.1: Analytic results for HAM quantisation with $l = 3/4$ and initial conditions $\phi_{\text{init}} = 0$ and $\dot{\phi}_{\text{init}} > 0$. The solid line corresponds to the case where the turning point of the inflaton is at $\phi = 3l_{\text{Pl}}$. Sufficient inflation to solve the horizon problem arises in the region above this line. The kinetic bound is satisfied in the region below the dashed line. The two regions do not overlap. The $x$-axes is labelled in Planck units.

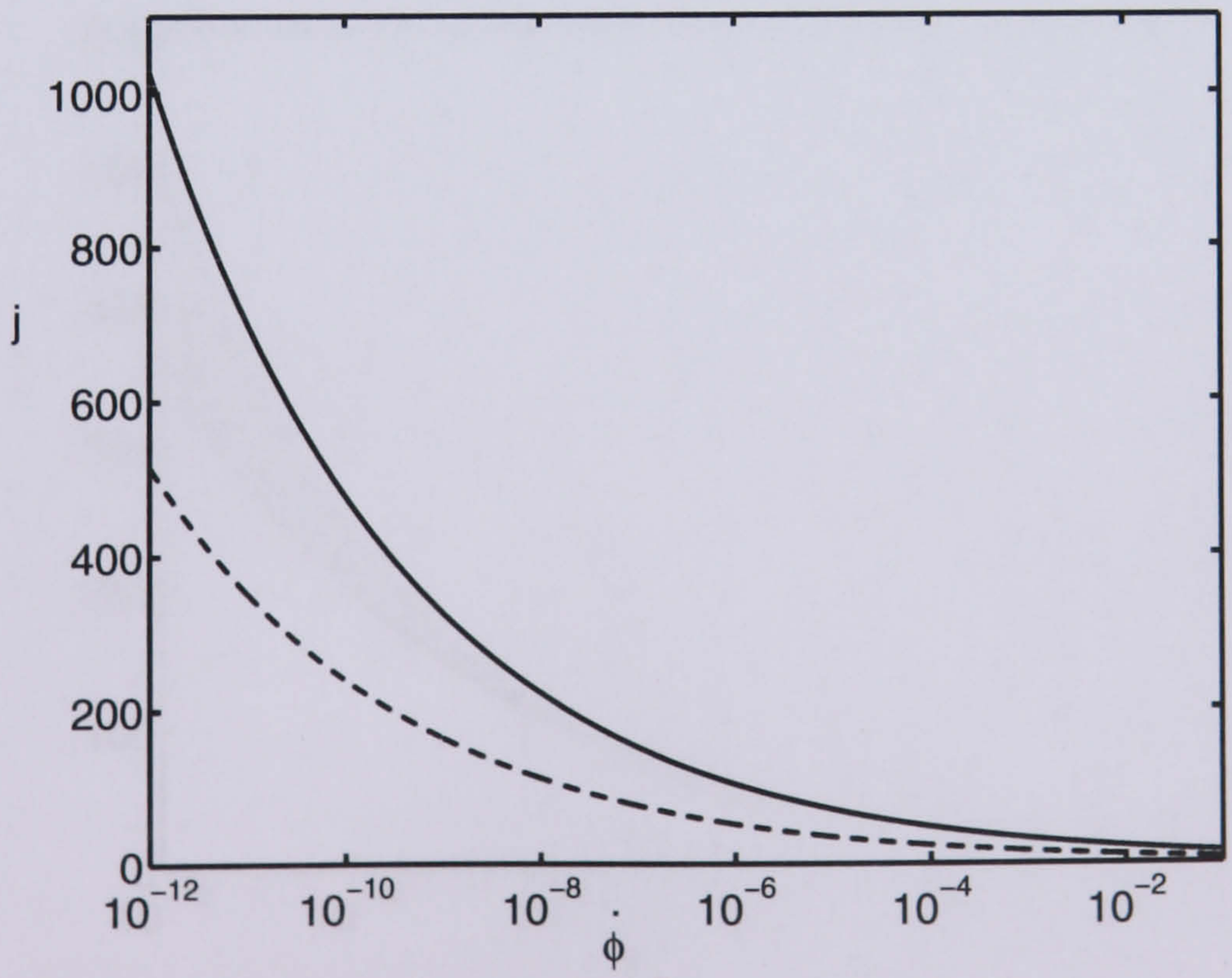


Figure 4.2: Numerical results corresponding to the scheme shown in Fig. 4.1.

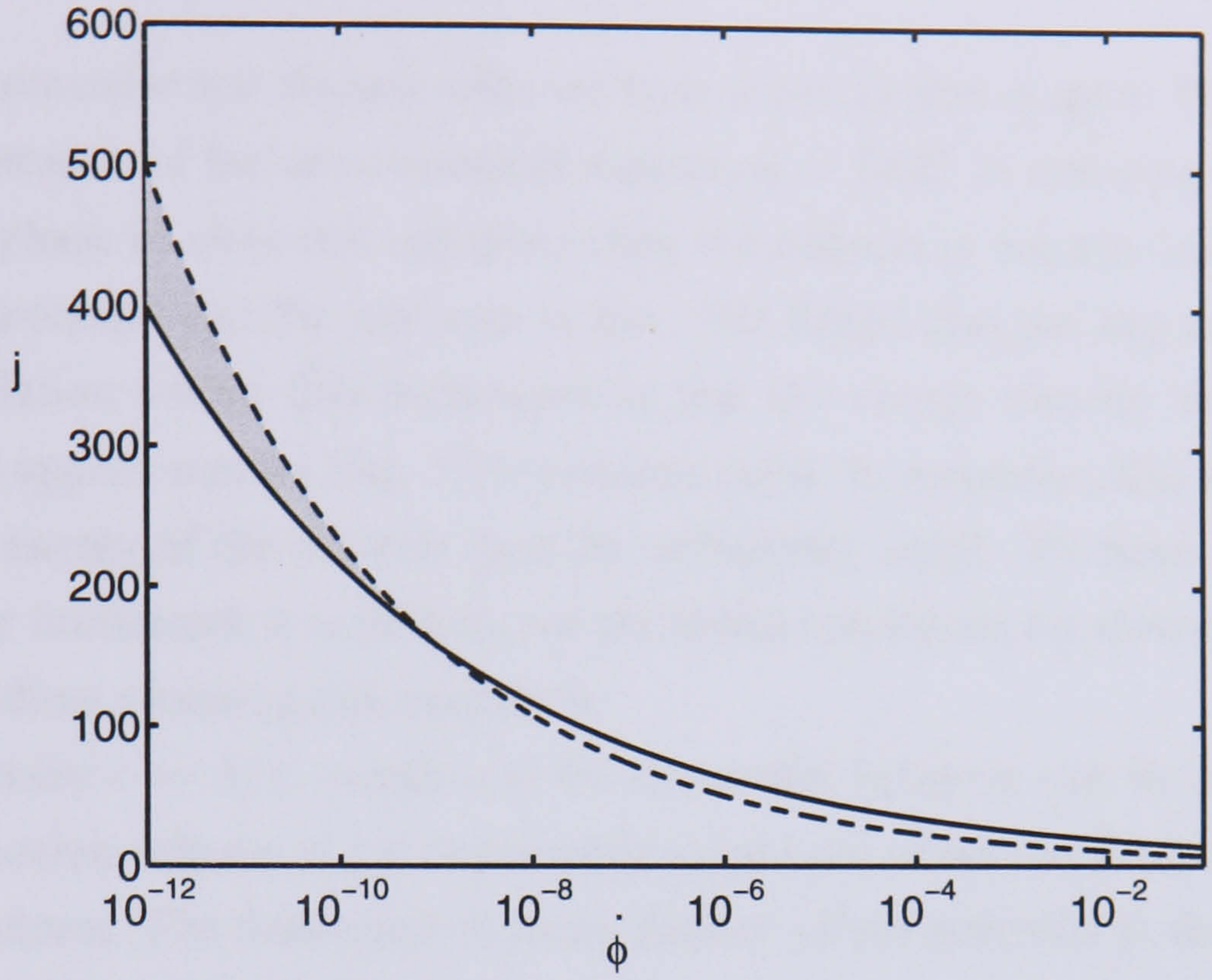


Figure 4.3: Analytic results for FRIED quantisation with $l = 3/4$ and initial conditions $\phi_{\text{init}} = 0$ and $\dot{\phi}_{\text{init}} > 0$. The horizon problem is solved in the region above the solid line and the kinetic bound is satisfied below the dashed line. The shaded area represents the region of parameter space that leads to successful inflation for this set of initial conditions. The $x$-axes is labelled in Planck units.

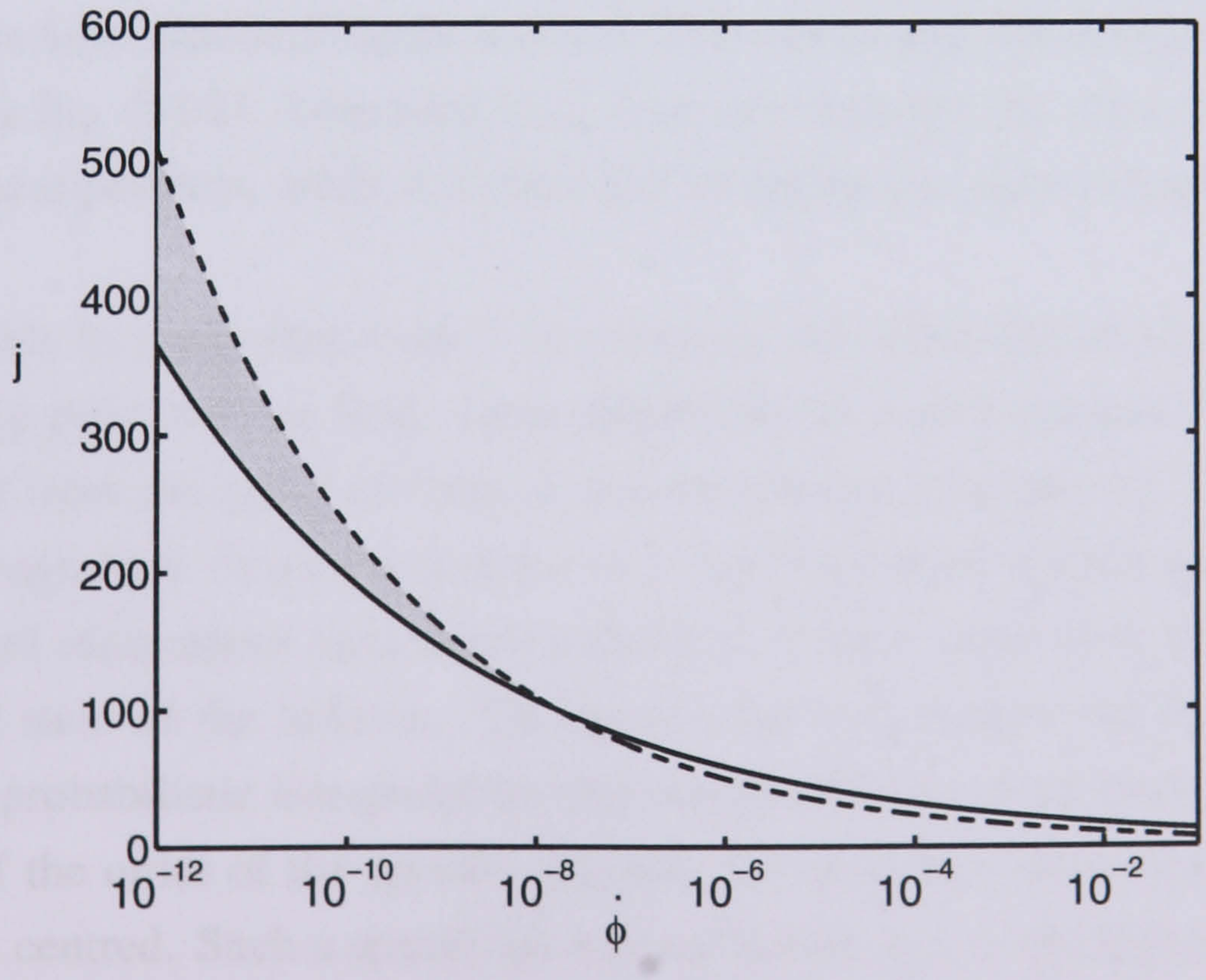


Figure 4.4: Numerical results corresponding to the scheme shown in Fig 4.3.

## 4.5 Discussion

Let us now summarise and discuss what we have learnt in this chapter. We have considered the importance of the semi-classical equations of LQC in realising the conditions that lead to a phase of slow-roll inflation when the inflaton is initially located in a minimum of its potential and the universe is flat. We found that the key requirement for successful inflation within this framework is that the energy density condition of the semi-classical approximation (Eq. 3.14) remains valid. In particular, this implies that the initial kinetic energy of the inflaton must be sufficiently small. We have seen, however, that within our framework it is difficult for the initial conditions for slow-roll inflation to be realised without violating this condition.

For the choice $l = 3/4$, conditions for successful inflation can be achieved in the FRIED quantisation scheme if $j$ is sufficiently large even when the field is located at the potential minimum. The field tends to move further up the potential in the FRIED quantisation than in HAM quantisation. In this sense, FRIED quantisation might be favoured from a phenomenological point of view at the semi-classical level, as it results in a larger region of parameter space for successful inflation (this has already been indicated in Hossain (2004)). This is interesting given that the HAM quantisation scheme is directly based on a Hamiltonian whereas FRIED involves additional multiplication with eigenvalues of the inverse volume operator and is therefore less natural conceptually.

In HAM quantisation, it appears that the field needs to be displaced initially from its minimum if it is to move sufficiently far up the potential without violating the bounds imposed by the semi-classical approximation. This can be seen from the analytic scheme by considering Eq. (4.22). Increasing $\phi_{\rm init}$ from zero reduces the value of $j$ required to solve the horizon problem, while it is clear that changing $\phi_{\rm init}$ does not affect the kinetic bound.

It is possible to argue that even if we consider the minimum of the potential as a natural starting point for the field, some displacement is still natural. This argument was advanced from the point of view of the uncertainty principle by Tsujikawa *et al* (2004). The argument views the inflaton as a localised wave packet with a spread in its position and momentum (and hence velocity). This is equivalent to considering a semi-classical state of the inflaton. The spread can be parametrised by $\Delta\phi$ and $\Delta\dot{\phi}$. In a standard probabilistic interpretation this implies that the most likely values for the inflaton are of the order of the spreads $\Delta\phi$ and $\Delta\dot{\phi}$ away from the value on which the wavepacket is centred. Such a spread has a lower bound due to the minimal uncertainty relation, $|\Delta\phi\Delta p_\phi| \geq 1$. The argument then proceeds by identifying the uncertainty in the momentum with the value of the initial momentum of the semi-classical system, and identifying the field's position in a similar way. This implicitly specifies a value for $\Delta p_\phi$,

and hence a value for $\phi_{\rm init}$, through the uncertainty principle. To see this we note that in the HAM quantisation scheme, the momentum canonically conjugate to the field is given by $p_\phi = a^3 D^{-1}\dot{\phi}$, and so with these identifications, the uncertainty relation gives

$$\left|\phi_{\rm init}\dot{\phi}_{\rm init}\right| \geq a^{-3}D(a_i) \ . \tag{4.34}$$

With $\dot{\phi}_{\rm init}$ fixed we see that $\phi_{\rm init}$ takes a particular value, which can become very large for small values of $j$ and small values of $\dot{\phi}_{\rm init}$.

Making the identification $p_{\phi_{\rm init}} = \Delta p_\phi$, however, assumes that the wave packet is localised about $p_\phi = 0$. Since we are making the assumption that the position variable is localised about $\phi = 0$, it may also seems natural to assume that the momentum is localised about $p_\phi = 0$, but we do not have any a priori reason to expect this. To proceed further, one would have to understand why the universe should emerge from the Planck regime with a particular semi-classical state, which is beyond the scope of our analysis. It is clear that some delocalisation of the field's position is to be expected, but we cannot uniquely determine the value of $\phi_{\rm init}$ even when considering a semi-classical state localised on $\phi_{\rm init} = 0$, with a fixed value for $\dot{\phi}_{\rm init}$. Moreover, the idea of moving the field using a quantum principle is not in the spirit of this investigation, where we have focused on a dynamical mechanism for setting the initial conditions for inflation. We have therefore focused on the value $\phi_{\rm init} = 0$.

It would be wrong to conclude outright, however, that HAM is unable to set the initial conditions for inflation in view of this delocalisation argument and given that only a small initial displacement is necessary to ensure Eqs. (4.23) and (4.13) are simultaneously satisfied. In addition, care should be taken in interpreting the kinetic bound (4.13). Failure to satisfy this bound does not necessarily rule out certain parameter choices or quantisation schemes, but only limits the allowed range where the approximate equations we are using can be employed. Outside this range we would have to employ the full quantum equations. It is possible that in this framework both the HAM and FRIED schemes would become equally viable at a phenomenological level. Indeed, if the kinetic bound (4.13) were to be relaxed slightly, then it would become marginally consistent with the horizon problem constraint (4.23). This also indicates that *if* successful inflation could be realised within this semi-classical framework, the conditions would be such that just enough e-folds of accelerated expansion would arise for the horizon problem to be solved. As a result, the largest scales on the CMB which are astrophysically observable today would correspond to the turning point in the field's dynamics.

Considering values $l < 3/4$ does not alter the qualitative behaviour of the dynamics. In general, for a given initial kinetic energy, this leads to an increase in the lowest value of $j$ consistent with successful inflation in FRIED quantisation, since the semi-classical phase must last longer. Conversely, when $l > 3/4$, successful inflation is possible for

lower initial kinetic energies and lower values of $j$. For HAM quantisation, reducing $l$ makes it harder to satisfy the horizon and kinetic bounds simultaneously. The kinetic energy of the field increases less rapidly for $l \to 0$ and it might therefore be expected that it would be easier to satisfy the kinetic bound. However, in this case the field lacks the kinetic energy needed to reach a sufficiently high value after the semi-classical era. Thus, the phenomenological indications for $l$ are in agreement with the expectations from the full theory which lead to $l \geq 1/2$.

In fact, the results allow us to draw further lessons for the full theory. As discussed in chapter 2, HAM is analogous to the full quantisation procedure whose dynamics is governed by a constraint, while FRIED does not have an analogue in the full theory. From the phenomenological point of view, however, we have seen that FRIED is more robust to ambiguities and for a wide range of parameters allows more than 60 e-folds of inflation to occur. On the other hand, HAM is less robust and does not result in a sufficient number of e-folds. If our kinetic bound could be relaxed a little, however, we have argued that there could be marginal agreement between Eqs. (4.13) and (4.23). This is interesting since it would mean that if the universe attains the initial conditions for slow-roll in this way, the region of parameter space which works would lead to maximal inflaton field values which lie at the borderline for sufficient inflation. This is precisely the situation which could lead to the observable effects studied by Tsujikawa *et al* (2004) and may indicate that observations of loop quantum gravity are within reach.

As for $j$, the bounds we have derived are larger than unity, as expected, but not unreasonably large. Thus, the scenario appears realistic and does not require fine tuning.

In conclusion we have shown that by considering the initial conditions for inflation, set using this anti-frictional mechanism, it is possible to gain insight into which quantisation schemes and values of the ambiguity parameters are favoured by phenomenological considerations. However, the results are clearly sensitive to our assumptions and particularly the chosen initial conditions. On the other hand, the most important and extremely interesting result is that a negligible initial potential energy and an initial kinetic energy many orders of magnitude below the Planck scale can lead to a significant period of slow-roll inflation, even though difficulties arise if we wish this period to last for more than 60 e-folds.

# Chapter 5

# Bouncing universes in LQC and the initial conditions for inflation

In this chapter we consider another aspect of the semi-classical equations of loop quantum cosmology. As we will show, the semi-classical equations permit a collapsing universe to undergo a bounce into an expanding phase. Given the long history of interest in bouncing and cyclic/oscillatory cosmologies, this feature of the semi-classical dynamics is very interesting. It has long been thought that once a collapsing universe approaches the Planck scale, quantum gravitational effects may allow the universe to evolve from collapse into expansion. LQC therefore appears to give a concrete realisation of this hope.

We proceed by briefly discussing the history and recent incarnations of bouncing and cyclic universes in section 5.1, before describing in detail how bounces can occur in the semi-classical approximation of LQC in section 5.2. That the semi-classical equations give rise to a bounce was first realised by Singh and Toporensky (2004) in the context of a positively-curved universe. The mechanism of the bounce and how generically it occurs, however, was not fully understood in this work. The work in this section expands greatly on previous results by identifying precisely the conditions for which a bounce is possible, and, moreover, yields new insight into the mechanism by which the bounce occurs.

Having done this we investigate various bouncing scenarios within LQC. First, we show that a positively-curved oscillatory LQC universe can establish the appropriate initial conditions for subsequent slow-roll inflation in section 5.3. We study the effectiveness of this mechanism when compared with the one described in chapter 4, and its robustness to ambiguities. Finally, the question of whether the bounce which occurs in LQC is able to realise any of the bouncing or cyclic/oscillatory scenarios which have previously been proposed is discussed in section 5.4. We conclude in section 5.5.

Throughout this chapter only the HAM quantisation scheme is considered and we con-

centrate on a particular value of the quantisation parameter $l = 3/4$. We will, however, consider whether the observed effects are to be expected in more general quantisation schemes during the discussion and particularly in the concluding section.

## 5.1 A brief history of cyclic universes

Cyclic/oscillatory universes have a long history in cosmology. A collapsing universe which undergoes a bounce instead of continuing to contract is clearly singularity free. Moreover, if the expanding universe subsequently recollapses, there is no reason why this sequence cannot continue indefinitely. Originally, this observation was one of the main attractions of a cyclic universe since it suggested that initial conditions can in principle be avoided. The big bang which occurred in our universe's past would then be interpreted as simply one in an infinite series of bounces. Closer consideration of such models, however, revealed severe difficulties in their construction. In particular, Tolman (1934) showed, using thermodynamic arguments, that the entropy of the universe would increase from one cycle to the next. This argument in turn implies that the number of bounces into the past must in fact be finite, thereby reintroducing the need for an origin and for initial conditions. While this was a disappointing conclusion, it had an interesting consequence. The generation of entropy with each bounce was shown to imply that the maximal size of the universe would increase with each successive bounce. This could then offer a possible resolution of the flatness and horizon problems of standard, big bang cosmology (see Durrer and Laukenmann, 1996, and references therein). Essentially the argument is that after a very large number of bounces one would expect the universe to be very large and hence to appear to be close to flatness. Moreover, the horizon problem can also be solved since the universe is much older than the length of time to the last big bang event. Hence, regions which would not have had time to come into causal contact with each other since the big bang would have been able to do so during previous cycles.

A central difficulty with these models, however, is that when treated classically within the context of GR, a collapsing universe generically becomes singular and its evolution breaks down before any bounce can occur if it is sourced by matter which satisfies the strong energy condition. Restricting ourselves to positive energy densities, the strong energy condition is equivalent to the condition that the equation of state (1.9) satisfies $w > -1/3$. Within the context of a positively-curved FRW universe, as is discussed in more detail below, violation of this condition during a collapse is sufficient to give a bounce. On the other hand, for a flat universe it is necessary to violate the condition that $w \geq -1$, and even this may not be sufficient. $w < -1$ implies a violation of the weak energy condition, which for an FRW cosmology is simply that $\rho > 0$ and $\rho + p \geq 0$.

All standard forms of matter (dust, radiation and even scalar fields) satisfy the weak energy condition, while dust and radiation also satisfy the strong energy condition. Moreover, during a classical collapse scalar fields generically evolve to satisfy the strong energy condition. We can clearly see, therefore, that within the FRW framework of GR, the generic result of a collapse is that the universe's evolution becomes singular.

Recently M-theory inspired braneworld models have renewed interest in bouncing and oscillatory universes. The most well known models are the ekpyrotic scenario, originally proposed by Khoury *et al* (2001b) (also see Khoury *et al*, 2001a, 2002), and the 'cyclic' universe proposed later by Steinhardt and Turok (2002a,b). The ekpyrotic scenario consists of just a single bounce, while in the 'cyclic universe' the bounces repeat at regular intervals in time. In these scenarios, the universe is assumed to be one of two four-dimensional orbifold planes, or branes, embedded in a higher five-dimensional bulk spacetime (examples of such an embedding are considered in part II). In this scenario the branes can move towards each other, and to an observer situated on one of the branes this is perceived as the universe undergoing a collapse. When the branes collide one dimension of spacetime disappears. The branes are then assumed to immediately rebound from one another, which is interpreted by a brane-bound observer as the universe undergoing a bounce. In the cyclic scenario this process repeats indefinitely. The scenario claims to avoid the singularity problem since only one dimension becomes singular, and moreover the matter content of the universe, which is confined to the brane, has a finite energy density during the collision. Furthermore, the cyclic version of the scenario also circumvents the entropy objections to oscillatory universes, for although the four-dimensional branes move backwards and forwards periodically in the fifth dimension, their size does not contract and expand periodically as an observer on the brane might think. Rather the size of the branes can become larger with each cycle, and this allows the ever increasing entropy to be diluted. A further feature of these scenarios is the possibility that the spectrum of scale-invariant curvature perturbations, required for structure formation and usually assumed to be generated during inflation, can be generated during the collapsing phase, subject to particular matching conditions at the brane collision (Khoury *et al*, 2002; Gratton *et al*, 2004; Tolley *et al*, 2004).

Despite these intriguing aspects of the scenarios, however, problems still remain (see Kallosh *et al*, 2001; Lyth, 2002a,b, for criticisms of the scenarios). For example, there are difficulties in developing a successful treatment of the brane collision, and establishing that the evolution of quantities confined to the brane is non-singular. Progress in these directions continues (see Niz and Turok, 2006; McFadden *et al*, 2005; Turok *et al*, 2004, for recent developments), although the scenarios remain controversial.

Another bouncing model we should mention was investigated by Kanekar *et al* (2001).

In this scenario the universe undergoes a number of cycles before ultimately undergoing inflationary expansion. This model is in the same spirit as the one we propose in this chapter, but is fundamentally different both qualitatively and because it lacks a physical mechanism for inducing bounces, such as the one we now proceed to discuss.

## 5.2 Bouncing cosmologies in semi-classical LQC

Let us now understand qualitatively how bouncing cosmologies can occur in semi-classical LQC. Consider again the semi-classical equations with a scalar field matter source, Eqs. (3.8)-(3.10). In the previous chapter we described how during an expansionary phase the $\dot{\phi}$ term in the scalar field equation (3.9), which classically is a frictional term, changes sign and becomes an anti-frictional one when $A \equiv d\ln D/d\ln a$ passes through three. We now consider this effect for a collapsing universe. For a classical, collapsing FRW universe this term is an anti-frictional one, since $H$ is negative. For the semi-classical regime of LQC, however, once the collapse proceeds to the point at which $A$ passes through three, this term becomes a frictional one. This means that the velocity of the scalar field can start to decrease, and hence so can the kinetic energy of the field. We have to be a little careful in this argument, however, since in the Friedmann equation (3.8), there is a factor of $1/D$ in the kinetic term, and it is not immediately clear whether the effective kinetic energy given by $\rho_{\text{kin}} = \dot{\phi}^2/D$ would also decrease. For the moment, however, let us assume that this effective term does indeed decrease, an assumption which we will confirm later. Considering the Friedmann equation, it is then clear that if there is a negative term on the RHS, for example either a negative potential or the negative term associated with a positively curved universe, there can come a point, as the kinetic term decreases, at which it becomes of equal magnitude to this negative contribution. At this point $H$ goes to zero, and the collapse halts. Assuming that $\dot{H}$ does not also go to zero as $H$ reaches zero, a bounce will then occur. We can easily argue that generically $\dot{H} > 0$ as $H$ reaches zero. During the collapse $\dot{H}$ must be greater than zero since $H$ is tending towards zero from below. Moreover, Eq. (3.10) implies that when the semi-classical effects cause $\dot{\phi}$ to decrease, $\dot{H}$ will become progressively more positive as the collapse proceeds. Then, once $A$ passes through six, $\dot{H}$ must always be positive and Eq. (3.12) tells us that this condition is always met below a particular value of the scale factor when the quantisation parameter $l$ is in the allowed range $0 < l < 1$.

This argument does not rule out circumstances in which $H = 0$ and $\dot{H} = 0$ which would represent equilibrium points of the evolution. This possibility is investigated further in the next chapter. However, we now quote a result, which we will prove in that chapter, which is of importance here. This is that the only types of equilibrium points

which are supported by the semi-classical equations are centre and saddle points. Since simple dynamical theory tells us that generic trajectories never evolve towards equilibrium points of this type (i.e. they are not stable attractor equilibrium points), we need not worry about the possibility that a collapse will end with the universe evolving into a static point. Only an infinitely finely-tuned trajectory can evolve to a saddle equilibrium point, while no trajectory can evolve to a centre point. We conclude, therefore, that if we can show that $H$ goes to zero during a collapse, a re-expansion will necessarily proceed.

In the case of a positively-curved universe, the curvature term in the Friedmann equation grows during a collapse. In this case, therefore, we actually only require the total energy density term $\rho_{\text{eff}} \equiv \dot{\phi}^2/D + V$ to grow less rapidly than the curvature for $H$ to go to zero. Since the curvature term scales as $a^{-2}$, it can be thought of as a negative energy term with equation of state $w = -1/3$. This then allows us to understand why it is that for a positively-curved universe only the strong energy condition need be violated during a collapse for a bounce to occur. For a flat universe, however, the weak energy condition must clearly be violated during a collapse, as the energy density must tend to zero in order for $H$ to go to zero, which would require an energy source with $w < -1$.

It is worth pointing out that $H$ can also go to zero during an expansionary phase and that if this occurs a recollapse will ensue. This is a completely classical effect. In a positively-curved universe the energy density of any matter source which satisfies the strong energy condition ($w > -1/3$) will decrease during an expansion more rapidly than the curvature term, and hence a point of equality will occur. When a negative potential is present, this is again a possibility. Further, we note that since the semi-classical equations of LQC allow a bounce to occur, and the classical equations allow for a recollapse, we should expect oscillatory universes to be a real possibility within LQC.

### 5.2.1 A perfect fluid description

We now add support to the qualitative argument above for how a bounce can occur within LQC. What we really want to know is whether or not a point must necessarily be reached during a collapse in the semi-classical regime at which $H$ will go to zero. Given the connection between this occurring and the violation of certain energy conditions, it proves useful to reformulate the semi-classical equations in the form of the standard classical equations for a universe sourced by a perfect fluid. These consist of the Friedmann equation (1.6), the Raychaudhuri equation (1.7) and the conservation equation (1.8). With the equations in this form the semi-classical corrections can be completely absorbed into definitions of an effective energy density, which we introduced in the previous section, and an effective pressure, allowing us to define an effective equation of state. We arrive

at the Friedmann equation

$$H^2 = \frac{8\pi\ell_{\rm Pl}^2}{3}\rho_{\rm eff} - \frac{k}{a^2} \ , \tag{5.1}$$

the Raychaudhuri equation

$$\dot{H} = -4\pi\ell_{\rm Pl}^2\left(\rho_{\rm eff} + p_{\rm eff}\right) + \frac{k}{a^2} \ , \tag{5.2}$$

and the conservation equation

$$\dot{\rho}_{\rm eff} = -3H\left(\rho_{\rm eff} + p_{\rm eff}\right) \ , \tag{5.3}$$

where

$$\rho_{\rm eff} \equiv \frac{1}{2}\frac{\dot{\phi}^2}{D} + V \ , \tag{5.4}$$

$$p_{\rm eff} \equiv \frac{1}{2}\frac{\dot{\phi}^2}{D}\left(1 - \frac{1}{3}\frac{d\ln D}{d\ln a}\right) - V \tag{5.5}$$

define the effective energy density and pressure of the fluid, respectively. The effective equation of state, $w \equiv p_{\rm eff}/\rho_{\rm eff}$, is then given by

$$w = -1 + \frac{2\dot{\phi}^2}{\dot{\phi}^2 + 2DV}\left(1 - \frac{1}{6}\frac{d\ln D}{d\ln a}\right) \ . \tag{5.6}$$

The LQC corrections to the cosmic dynamics can therefore be conveniently parametrised in terms of the equation of state.

Considering the equations above, an immediate and important result is that when the condition $A > 6$ is satisfied, the fluid represents 'phantom' matter ($w < -1$) that violates the weak energy condition *independently of the form of the potential.* This condition is always met below a particular value of the scale factor, which we label $a_{\rm ph}$. For $l = 3/4$, the numerical solution of $A = 6$ implies that $a_{\rm ph} \approx 0.914 a_*$.

If we consider the classical regime where $D = 1$, and if we further assume that the condition $\dot{\phi}^2 > V$ is met, the scalar field satisfies the strong energy condition. During a classical collapse this condition is generically rapidly satisfied. This is because the classical anti-frictional effect of the scalar field equation will rapidly come to dominate the potential gradient term in the scalar field equation (3.9), except for exceptionally steep potentials, and the field will accelerate. Considering a collapse which begins in the classical regime, we can therefore safely assume that the strong energy condition is initially met. Given this assumption, our earlier result implies that as the collapse proceeds and the universe enters the semi-classical regime, the effective energy density necessarily violates first the strong energy condition and then, when $A > 6$ is met, the weak energy condition. At this point, therefore, the effective energy density of the universe actually

starts to decrease. With this result in mind, we see that during a collapse in a positively-curved universe, the density term in the Friedmann equation is eventually balanced by the growing curvature term, at which point $H$ goes to zero.

In the case of a flat universe, the energy density also starts to decrease during a collapse. Since the curvature term is not present, however, for a bounce to occur the decreasing energy density must instantaneously vanish at a non-zero value of the scale factor. If the scalar field's self-interaction potential is positive-definite then this is obviously not possible. For a negative potential, however, it is, since the positive kinetic energy component can be balanced by the negative potential energy. In order to see whether this does actually occur, let us consider the two components of the effective energy density separately. The kinetic energy term must have greater magnitude than the potential term initially. In order for a bounce to occur, therefore, we require that the magnitude of the positive kinetic term decreases more rapidly than the magnitude of the negative potential term as the scale factor decreases, so that there comes a point at which the magnitudes of the two components are equal and $H$ goes to zero.

Considering a negative-definite potential, there are essentially two possibilities. First, the potential energy can be decreasing which means its magnitude is increasing, and this corresponds to the field moving along its potential to progressively more negative values. In this case, since the total energy must decrease once $A$ passes through six, the magnitude of the kinetic term must decrease and hence a bounce will occur in this case. The second possibility is that the magnitude of the potential energy decreases, which corresponds to the field moving along its potential to progressively less negative values. In this case it is impossible to tell a priori whether a bounce must necessarily occur, since we can always imagine a potential which is sufficiently steep such that the rate at which its magnitude decreases is greater than the rate at which the kinetic term decreases. Nonetheless this seems unlikely, and would probably also require some fine-tuning. We note, however, that based on the arguments given here we cannot be sure that a scalar field with negative potential (in a flat universe) will necessarily give rise to a bounce if the potential is very steep and if the field is moving up the potential to progressively less negative values.

In conclusion, we have succeeded in showing that a collapsing positively-curved, semi-classical LQC universe sourced by a free scalar field, or one interacting through a positive or negative potential must reach a point at which the collapse halts. Generically the universe will then undergo a non-singular bounce. For the case of a flat universe we have shown that a non-singular bounce will also generically occur when the scalar field is self-interacting through a potential of negative-definite form, with the possible exception of a very steep potential up which the field is moving. This of course assumes implicitly

that the semi-classical equations themselves are valid. In particular, we are assuming the energy density bound (3.14) has not been violated during the classical part of the collapse where the energy density is generically increasing (i.e. before the correction term becomes important and the density starts to decrease). We must also assume that the bounce occurs above the minimum length scale consistent with the semi-classical equations, $a_i$. These constraints are important to bear in mind as we develop scenarios within semi-classical LQC which utilise the bouncing mechanism we have just described.

## 5.3 Setting the initial conditions for inflation in a oscillatory universe

Having shown when a bounce occurs by consideration of the semi-classical equations, we now proceed to look in more detail at particular scenarios. In this section we consider a positively-curved universe sourced by a scalar field. In this setting our ultimate aim is to show that if the field is self-interacting through a positive potential, the scalar field can climb the potential monotonically in a series of small steps while the universe undergoes oscillations. We initially consider a massless scalar field in order to understand the dynamics in a simplified setting. As we will see, for the massless case the combined effects of the semi-classical corrections and the spatial curvature mean that the universe undergoes infinite identical oscillations. When a potential is introduced, however, the symmetry of the cycles is broken, and the scalar field moves along its potential monotonically with each cycle. The field can therefore move up its potential during the cycles. We also show that this behaviour ceases when a critical value of the potential is reached, at which point the scalar field will turn around on the potential and a period of inflation will ensue. Assuming that the potential satisfies the slow-roll conditions, this then leads to a prolonged period of slow-roll inflation.

### 5.3.1 Oscillations with a massless scalar field

The case of a massless scalar field simplifies the dynamics greatly. In particular, the field equation (3.9) for a massless scalar field ($V = 0$) admits the first integral:

$$\dot{\phi} = \dot{\phi}_{\text{init}} \left(\frac{a_{\text{init}}}{a}\right)^3 \left(\frac{D}{D_{\text{init}}}\right) \ , \tag{5.7}$$

where $D_{\text{init}} = D(a_{\text{init}}/a_*)$ and a subscript $init$ denotes initial values. This means the effective energy density of the field is completely determined by the scale factor for given initial conditions. In this case we also know that the sign of $\ddot{\phi}$ changes when $A$ passes through three. Moreover, in addition to knowing that the effective energy density behaves

like a phantom energy source below $a_{\rm ph}$, we deduce from Eq. (5.6) that for a massless field the strong energy condition is violated when the universe contracts sufficiently for $A$ to pass through four. This point can be evaluated to be $a_{\rm st} \approx 0.943 a_*$.

To illustrate the oscillatory cosmic dynamics, we choose without loss of generality the initial conditions such that $a_i < a_{\rm init} < a_{\rm ph}$, $\dot{\phi}_{\rm init} > 0$ and $H_{\rm init} = 0$. The subsequent dynamics can then be divided into four phases which can be understood completely from equations (3.8)-(3.10) and (5.1)-(5.6) given our discussion of the semi-classical dynamics given in the previous section. The behaviour has also been followed numerically by integration of Eqs. (3.8)-(3.10). The result of this integration is presented in Fig. 5.1, on which we label the four phases that we now describe in detail.

*Phase I:* Initially $a < a_{\rm ph}$ and the universe is effectively sourced by phantom matter. This drives an epoch of superinflationary expansion ($\dot{H} > 0$). The matter continues to behave like a phantom until $a$ reaches $a_{\rm ph}$ and $A$ passes through six. The scalar field also accelerates during this phase.

*Phase II:* The effective energy density now starts to decrease. The growth of the scale factor continues to accelerate until the strong energy condition becomes satisfied at $a_{\rm st}$, and the scalar field continues to accelerate until $A$ has fallen to $A = 3$. Once the strong energy condition becomes satisfied the energy density starts to decrease more rapidly than the curvature term. Indeed, if the universe reaches the classical regime, $a \gg a_*$, the energy density of the field falls as $\rho_\phi \propto 1/a^6$. At some point, therefore, the energy density is balanced by the curvature and the expansion reaches a turnaround as $H$ reaches zero.

*Phase III:* Eq. (3.9) implies that the scalar field begins to accelerate immediately after the turnaround and continues to do so until the universe has collapsed to the point where $A = 3$ again. The strong energy condition continues to be satisfied until just after the scalar field ceases to accelerate, when $A$ passes through four. At this point the energy density starts to increase less rapidly than the curvature. Shortly afterwards, the universe contracts below the critical scale $a_{\rm ph}$, at which point the energy density begins to decrease.

*Phase IV:* Substituting Eq. (5.7) into Eq. (5.4) implies that the effective energy density varies as $\rho_{\rm eff} = \dot{\phi}^2/(2D) \propto D/a^6$ and it is therefore rapidly decreasing during this phase, since $A > 6$. Hence, a scale is quickly reached where the energy density is again balanced by the growing curvature term and the Hubble parameter vanishes instantaneously. As we have discussed, this then allows the universe to undergo a non-singular bounce into a new phase of super-inflationary expansion (Phase I).

Considering the effective equation of state (5.6) we see that it is independent of the field's kinetic energy when $V = 0$. This implies that identical cycles are repeated in-

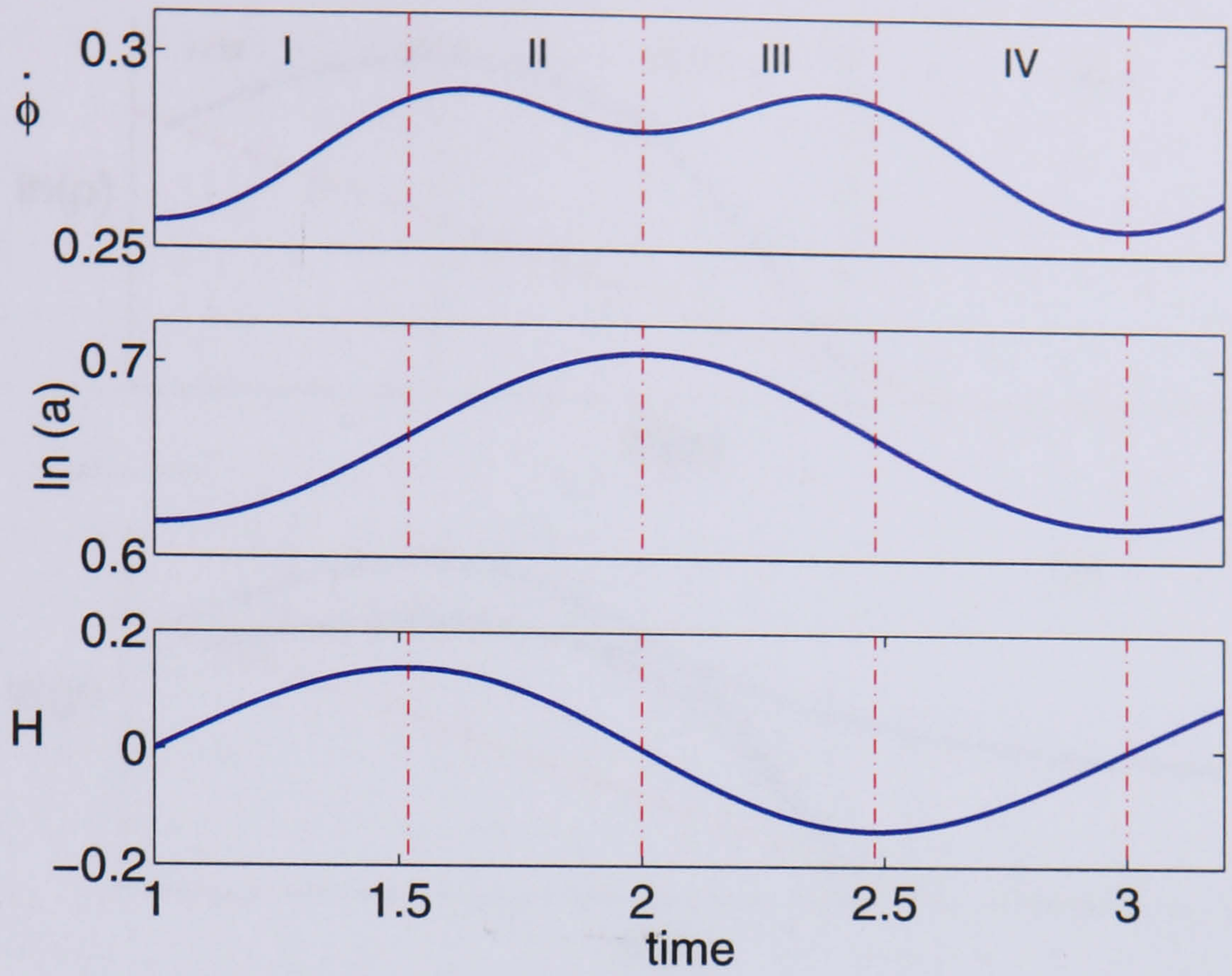


Figure 5.1: Time evolution of the scalar field $\phi$, the logarithmic scale factor and the Hubble parameter when the potential $V = 0$, $j = 100$, $a_{\text{init}}/a_* = 0.9$ and $H_{\text{init}} = 0$. Axes are labeled in Planck units.

definitely into the future (and the past). This is summarised in Fig. 5.2a, which is an illustration of how the energy density evolves as the evolution proceeds. During the collapsing phases, the field retraces the trajectory it mapped out during the expanding phases. The oscillatory behaviour is therefore repeated identically in the absence of an interaction potential. This figure also clearly illustrates the two points at which $H$ vanishes: at the point of recollapse, and at the point where a bounce occurs. Furthermore, Eq. (5.7) implies that the field's kinetic energy never vanishes during the cycle since the scale factor remains finite. This shows that in the absence of a potential the value of the field increases monotonically with time.

Before moving on from the massless case and introducing a self-interaction potential, it is worth pointing out that the initial conditions we chose are not special, and it is clear that any initial conditions lead to oscillations. Moreover, oscillations occur about the point $a_{\text{st}}$, and the initial conditions simply set the size of the oscillations. In particular, it is not necessary for the field to become a phantom, only for the strong energy condition to be successively satisfied and violated as the cycles proceed. However, since $a_{\text{ph}} \approx 0.914a_*$ and $a_{\text{st}} \approx 0.943a_*$ are so close to one another, in practical terms the phantom condition is also successively satisfied and violated.

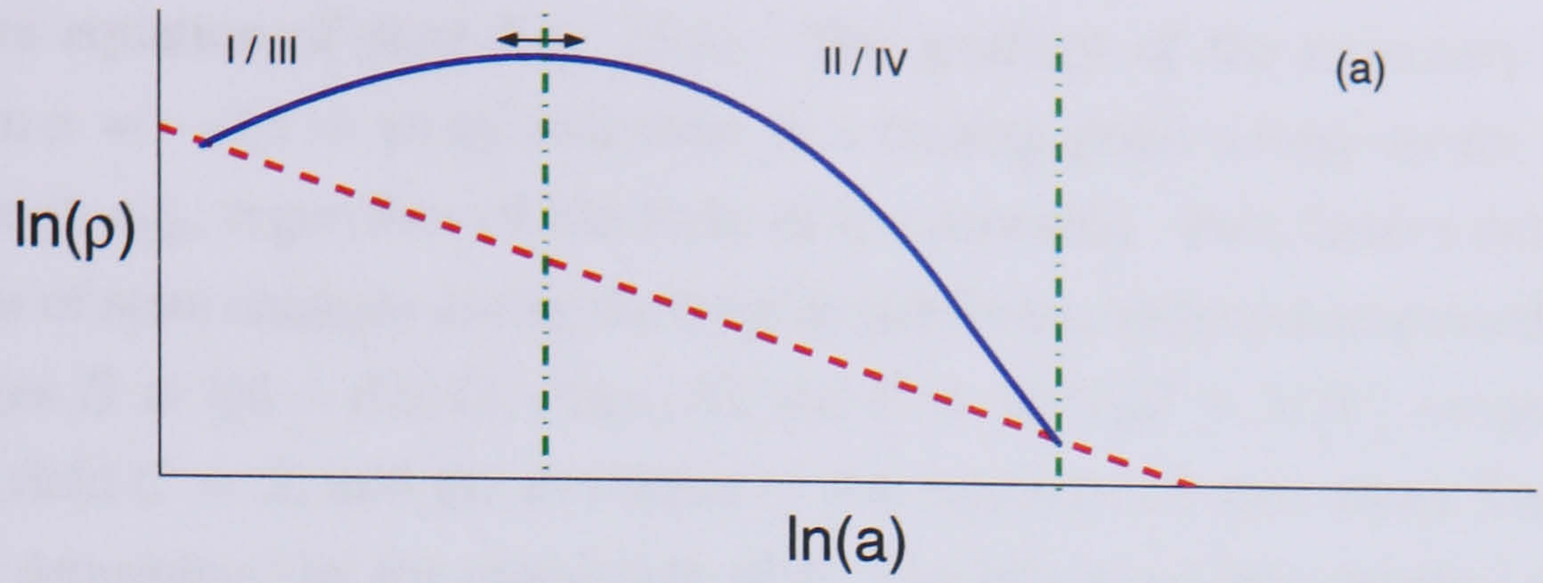


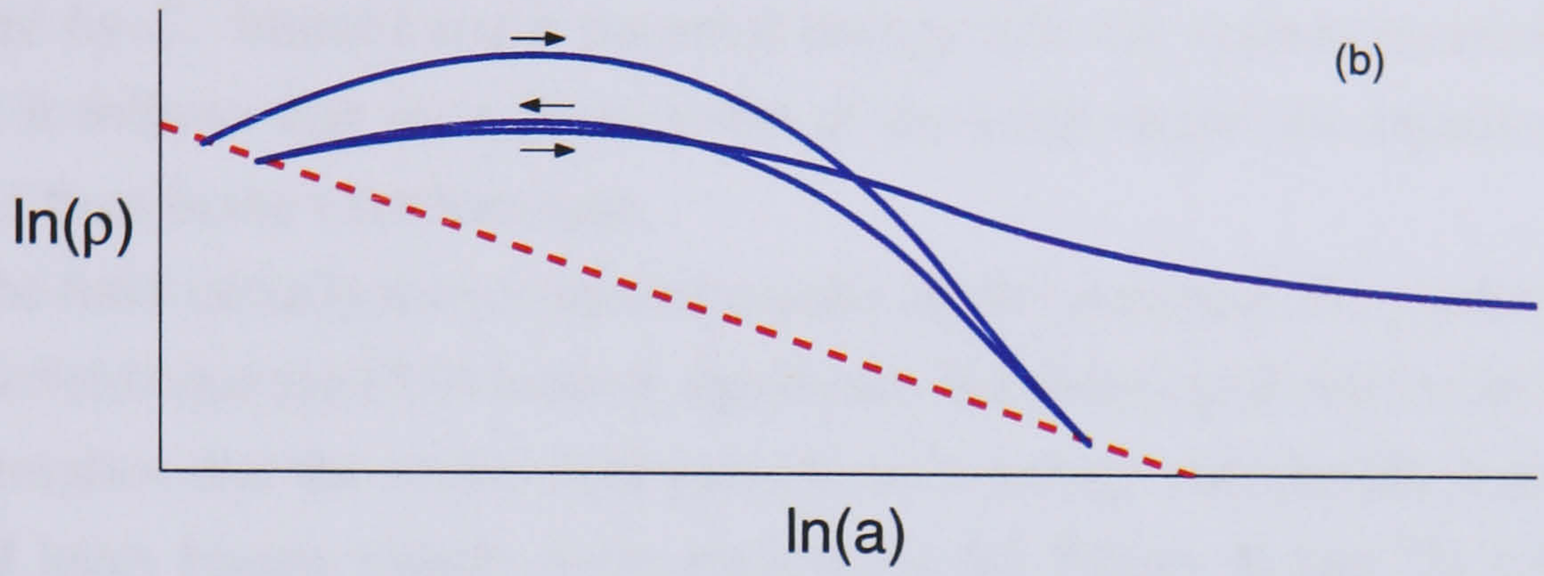


Figure 5.2: (a) Schematically illustrating the logarithmic variation of the effective energy density of a massless scalar field (solid line) and the curvature term in the Friedmann equation (dashed line). The universe oscillates indefinitely between the intersection points of the two lines. (b) Schematically illustrating the effects of introducing a self-interaction potential for the field. The cycles are eventually broken as the potential becomes dynamically significant, thereby resulting in slow-roll inflation. In both figures, the slope of the trajectories is given by $d\ln\rho_{\rm eff}/d\ln a = -3[1+w(a)]$.

### 5.3.2 Self-interacting scalar field

We now consider how self-interactions of the scalar field modify the cyclic dynamics. We make very weak assumptions about the potential, specifying only that it has a global minimum at $V_{\rm min}(0) = 0$ and is a positive-definite and monotonically varying function when $\phi \neq 0$ such that $V'' > 0$. As we did for the investigation in chapter 4 into how the initial conditions for inflation can be established when spatial curvature is neglected, we suppose the field is initially located at the minimum of its potential, with all the same motivations and caveats we discussed there. We further assume that the initial conditions are the same as those for the example we considered in the previous subsection.

Since the potential is negligible initially, the dynamics will be similar to those previously described, but given that the field moves in one direction, the potential gradually increases, and hence so will its influence on the evolution. The deviation of the qualitative dynamics of the universe from the massless case can be understood by considering the evolution of the energy density. This is illustrated in Fig. 5.2b. In general, the path of the field in the $\{\ln\rho_{\rm eff}, \ln a\}$ plane is determined by the variation of

the effective equation of state Eq. (5.6). The gradient of the trajectory is given by $d\ln\rho_{\rm eff}/d\ln a = -3[1+w(a)]$ and there is a turning point whenever the scale factor passes through $a_{\rm ph}$, regardless of the form of the potential. Two factors determine how the equation of state changes during each cycle and these can be parametrised by defining the quantities $\mathcal{B} \equiv [(6 - d\ln D/d\ln a)/6]$ and $\mathcal{C} \equiv 2\dot{\phi}^2/[\dot{\phi}^2 + 2DV]$, respectively. For a massless field $\mathcal{C} = 2$, and the deviation of the equation of state away from the value $w = -1$ is determined by the magnitude of $\mathcal{B}$. The effects of the potential are therefore parametrised by $\mathcal{C}$. Introducing a potential energy into the system necessarily implies $\mathcal{C} < 2$ and it follows that for a given value of the scale factor, the equation of state is closer to $-1$ than in the massless case.

Since the field initially moves monotonically up the potential, the gradient term $DV'$ in the scalar field equation (3.9) is more significant in a given cycle relative to the previous one. This implies that the scalar field gains kinetic energy less rapidly during Phases I and III and loses kinetic energy more rapidly during Phases II and IV. Consequently, the value of $\mathcal{C}$ at the end of Phase I of a given cycle is smaller than the value it had at the corresponding point of the previous cycle. In other words, the rate of change of the trajectory's gradient around $a_{\rm ph}$ becomes progressively smaller with each successive cycle.

A massless field begins accelerating immediately after the turnaround and bounce have been attained. When the field is not massless, however, Eq. (3.9) implies that $\ddot{\phi} = -DV' < 0$ at the instant when the Hubble parameter vanishes, so the field does not accelerate immediately after the bounce. Instead there is a short delay during which $\mathcal{C}$ continues to decrease. The trajectory of the field immediately before the bounce is therefore slightly steeper than the trajectory immediately after, i.e., the trajectory for Phase III (I) lies below that of Phase II (IV). Moreover, because the field does not acquire as much kinetic energy during Phase III as it lost during Phase II, the value of $\mathcal{C}$ (for a given value of the scale factor) is smaller during Phase III than it was during Phase II. Thus, the Phase III part of the trajectory always lies below that of Phase II and, similarly, the trajectory of Phase I lies below that of the Phase IV trajectory of the previous cycle. The potential therefore breaks the symmetric cycles of the massless field and the effective energy density at the end of Phases I and III falls with successive cycles.

So far we have implicitly assumed that the kinetic energy of the field never vanishes during Phase II. However, the potential becomes progressively more important with each completed cycle and this assumption must necessarily break down after a finite number of cycles have been completed. Since the semi-classical effects are negligible once the universe has expanded beyond $a_*$, the energy density of the field during Phase II redshifts more rapidly than the curvature term if $\dot{\phi}^2 > V$ (i.e. if the strong energy condition is

satisfied in the classical regime). As the field moves monotonically up the potential, it becomes progressively harder to maintain this condition. Eventually, therefore, a cycle is reached where this condition is violated during Phase II. This then leads to a period of inflationary expansion as the field slows down, reaches a point of maximum displacement and moves back down the potential. If the potential is of the correct form, slow-roll inflation occurs.

For some initial conditions and choices of parameters, this may arise during the first cycle. In this case, the scenario discussed in chapter 4 is recovered and the field is accelerated up the potential during just one period of super-inflation, during which the curvature term becomes negligible.

The behaviour of the energy density at the transition from oscillatory behaviour to inflation is illustrated in Fig. 5.2b. Full numerical integration of Eqs. (3.8)-(3.10) for an oscillatory universe which subsequently undergoes a transition into a potential-driven, slow-roll inflationary epoch is shown in Fig 5.3, where we have taken an example in which only a small number of cycles occur in order to illustrate the entire evolution. The figure clearly illustrates how the potential energy becomes more important during the cycles, eventually allowing inflation to proceed.

Thus far, we have discussed the general form of the dynamics and implicitly we have fixed the quantisation parameter $j$ (as well as $l$). In spatially flat models, as we showed in chapter 4, the maximum value attained by the field as it moves up the potential increases for larger values of $j$ when the universe begins its evolution at a fixed value of the scale factor, which we took to be $a_i$. Starting the evolution at $a_i$ allowed the field to move the furthest distance possible within this scenario, since the universe then evolved through the entire semi-classical regime. Moreover, the dependence on $j$ arises since the semi-classical regime persists over a larger range of scale factor values when $j$ is larger. The distance the field moved also grew when the initial velocity of the field was increased (with the assumption that the energy density bound was not broken).

For the positively-curved model we have just developed, on the other hand, we will now see that the maximal distance the field can move up the potential before the onset of slow-roll inflation occurs for initial values of $a$ close to $a_*$, and for *smaller* values of $j$. Moreover, this distance increases for smaller values of the field's initial velocity. This result is not obvious since two competing factors are involved. The result follows because the closer the initial value of the scale factor is to $a_*$, and the smaller the field's initial velocity is, the smaller the size of the cycles. Likewise, the distance moved by the field during each cycle is smaller. The number of cycles which can occur is, however, much greater for smaller cycles. Moreover, the classical expansion lasts for a shorter period and hence the kinetic energy of the field decreases by a smaller amount. The potential

$V$, therefore, must be larger in order to become significant compared with the kinetic energy. To illustrate this further let us present an analytic approximation scheme for the maximum value the potential attains for given initial conditions.

### 5.3.3 Analytic approximation

In order to quantitatively understand how the field can move further for smaller values of $j$ we must make a number of simplifying assumptions. First we assume that the total energy which the universe attains before the collapse occurs is conserved through the cycles. We also assume that a very large number of cycles occurs and that the potential is dynamically insignificant during the first cycle.

Considering the first cycle, therefore, we see that the massless case gives us a good estimate of the total energy, and the evolution of this energy is given by Eq. (5.7). Now, assuming the universe to be classical at the point at which the recollapse occurs, we have from Eq. (1.6) that

$$\frac{8\pi\ell_{\rm Pl}^2}{3}\rho_{\rm rc} \approx \frac{1}{a_{\rm rc}^2} \ , \tag{5.8}$$

where 'rc' represents the quantities at the point of recollapse. Using Eq. (5.7) to substitute for $\rho_{\rm rc}$ in terms of $\dot{\phi}_{\rm init}$ and $D_{\rm init}$, we find a relationship between these quantities and the scale factor at the recollapse point $a_{\rm rc}$, given by

$$\frac{8\pi\ell_{\rm Pl}^2}{3}\left(\frac{\dot{\phi}_{\rm init}^2}{2}\frac{a_{\rm init}^6}{a_{\rm rc}^6 D_{\rm init}^2}\right) \approx \frac{1}{a_{\rm rc}^2} \ , \tag{5.9}$$

where we have assumed $D_{\rm rc} = 1$. Finally, we consider the final stages of the evolution, in which the field is rolling up the potential having completed the last cycle. As we discussed above, subsequent cycles cannot occur once $V > \dot{\phi}^2$, so the condition $V \approx \dot{\phi}^2$ gives a good approximation for the onset of inflation. Assuming this condition is just met for $V_{\rm max}$, and using Eq. (5.7) together with conservation of energy, the maximum value of the potential is given by

$$V_{\rm max} \approx \left(\frac{\dot{\phi}_{\rm init}^2}{3}\frac{a_{\rm init}^6}{a_{\rm rc}^6 D_{\rm init}^2}\right) \ . \tag{5.10}$$

Assuming that a recollapse was just avoided so that equations Eqs. (5.9) and (5.10) can be used simultaneously, $a_{\rm rc}$ can be eliminated to give the expression

$$V_{\rm max} \approx \frac{1}{\dot{\phi}_{\rm init}}\left(\frac{8\pi\ell_{\rm Pl}^2}{2}\right)^{-3/2}\frac{D_{\rm init}}{q_{\rm init}^{3/2}}\frac{1}{a_*^3} \ . \tag{5.11}$$

It is also worth pointing out that in deriving this equation we have not used any approximation to the general form of the $D$ term. Consequently, this expression is still

a good estimate of $V_{\max}$ when $a_{\rm init} \ll a_*$ is not satisfied, and even when $a_{\rm init} > a_*$, unlike the analytic approximation developed in chapter 4. We have written the result using $q_{\rm init} = a_{\rm init}^2/a_*^2$. This expression exhibits the dependences we discussed above. For $a_{\rm init} < a_*$, $D_{\rm init}$ becomes progressively smaller, while for $a > a_*$, the factor of $1/q_{\rm init}$ becomes progressively smaller. As a result, when $q_{\rm init}$, and hence $D_{\rm init}$, is close to unity, expression (5.11) leads to the largest values for $V_{\max}$. The expression shows that with a given initial $q_{\rm init}$, the value of $V$ when inflation occurs is inversely proportional to $a_*^3$ and hence inversely proportional to $j^{3/2}$. Finally, the expression also shows an inverse dependence on $\dot{\phi}_{\rm init}$. This inverse dependence on $\dot{\phi}_{\rm init}$ is perhaps the most interesting result, since it strongly suggests that simultaneously satisfying the constraints that the field moves far enough for sufficient inflation to occur and that the energy density does not exceed the Planck scale during the evolution, will not pose the same problem in this scenario as it did for the scenario developed in chapter 4.

### 5.3.4 Comparison with numerics

Let us now compare our approximation function with values for the maximal value of the potential obtained from numerical integration. For this purpose we consider only the quantisation parameter value $l = 3/4$. We also require a concrete form for the potential, and we once again assume the quadratic potential with $m = 10^{-6}\ell_{\rm Pl}^{-1}$. Using this potential the approximation Eq. (5.11) becomes

$$\phi_{\max} = \left( \frac{2}{\dot{\phi}_{\rm init}} \left( \frac{8\pi\ell_{\rm Pl}^2}{2} \right)^{-3/2} \frac{D_{\rm init}}{m^2 q_{\rm init}^{3/2}} \frac{1}{a_*^3} \right)^{\frac{1}{2}} . \tag{5.12}$$

Since we know that under certain initial conditions cycles will not occur and the dynamics will be equivalent to the scenario of chapter 4, we will also employ the approximation Eq. (4.21). Here, however, we alter the expression for the initial conditions so they are given in the form $a_{\rm init}/a_*$. This gives

$$\phi_{\max} \exp\left( \sqrt{12\pi}\ell_{\rm Pl}(\phi_{\max} - \phi_{\rm init}) \right) = \frac{\dot{\phi}_{\rm init}}{m} \frac{\sqrt{2}}{q_{\rm init}^6} \left( \frac{7}{12} \right)^{24/5} . \tag{5.13}$$

The results are presented in Fig. 5.4 where we have used $\dot{\phi}_{\rm init} = 0.01$ and integrated the equations for a wide range of values of $j$ and three different values of $a_{\rm init}$. This figure therefore illustrates the dependence of the maximum value attained by the field on the parameter $j$ and the ratio $a_{\rm init}/a_*$ for a given initial value of the kinetic energy $\dot{\phi}_{\rm init}$. The horizontal lines represent the estimated value of $\phi_{\max}$ extracted from Eq. (5.13) and the lines with negative slope represent the estimate Eq. (5.11). Circles and triangles correspond to the actual values obtained by numerically integrating the equations of motion. When many oscillations occur before the onset of inflation, Eq. (5.11) yields a good

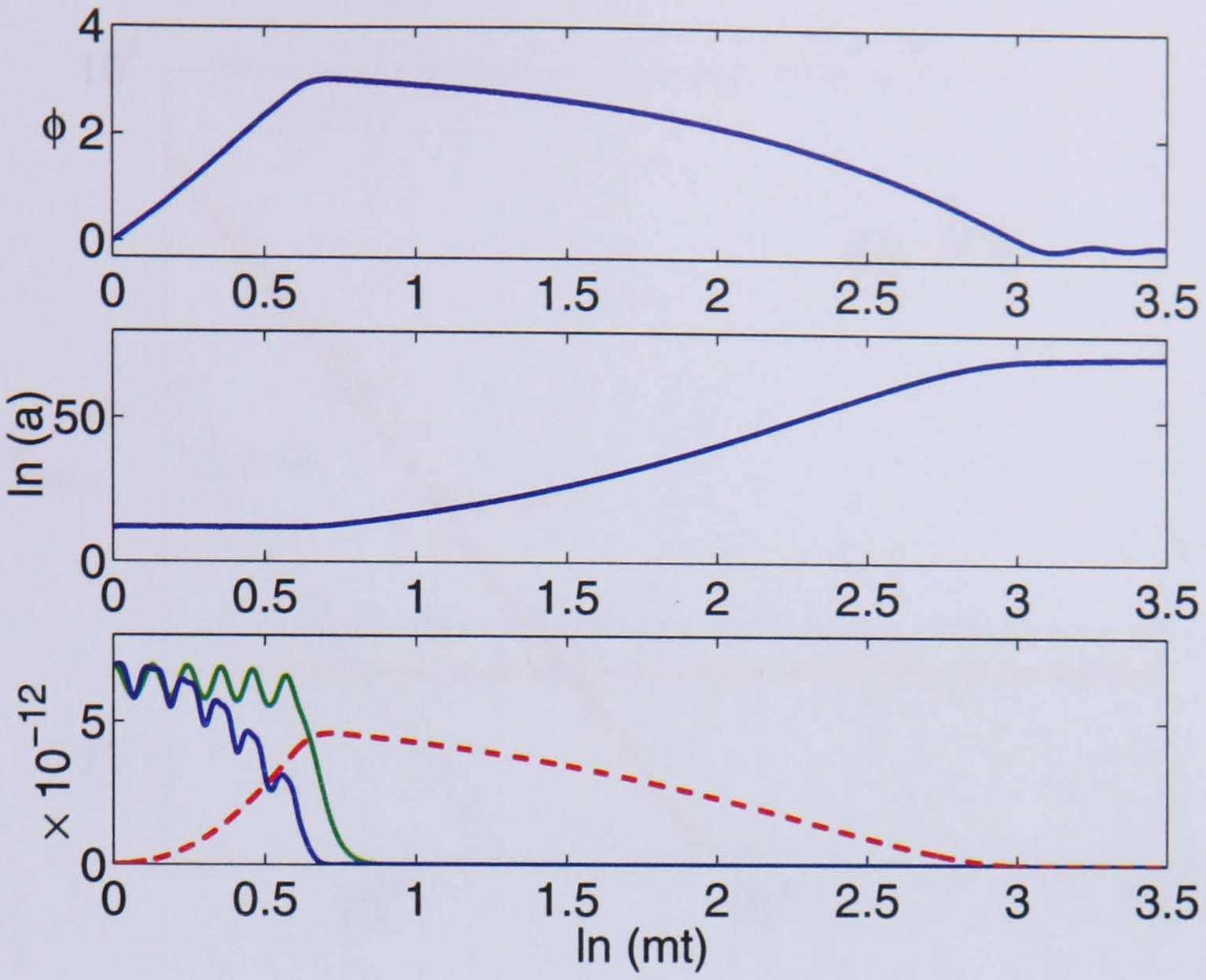


Figure 5.3: Illustrating the time evolution of the scalar field $\phi$ (top panel) and the logarithmic scale factor (middle panel) for a quadratic potential $V = m^2\phi^2/2$. The bottom panel illustrates how the effective kinetic energy $\dot{\phi}^2/2D$ (solid blue line) and potential energy (dashed line) of the field vary compared to the inverse of the curvature term (solid green line). The cycles end and slow-roll inflation commences at the point when the potential begins to dominate the kinetic energy. Initial conditions are chosen such that $\phi_{\rm init} = H_{\rm init} = 0$ and $a_{\rm init}/a_* = 0.9$, with $m = 10^{-6}\ell_{\rm Pl}^{-1}$ and $j = 5 \times 10^{11}$ (see the text for details). The axes are labelled in Planck units.

estimate of $\phi_{\rm max}$. However, if the field is moved far enough in the first period of anti-friction for the strong energy condition to be violated, no oscillations occur. In this case, Eq. (5.13) gives a good estimate of $\phi_{\rm max}$. The points where the lines cross in Fig. 5.4 show the transitions between the two regimes.

The numerical results in Fig. 5.4 show a 'stepping behaviour', with a range of $j$ leading to roughly the same value of $\phi_{\rm max}$, before there is a drop to the next value. This becomes more pronounced at higher $j$. This occurs because our approximation relies on two estimates: firstly, that $V \approx \dot{\phi}^2$ at the onset of inflation, and secondly, that $8\pi\ell_{\rm Pl}^2\rho_{\rm rc}/3 \approx 1/a_{\rm rc}^2$ when the field reaches its maximal value. Clearly, the two approximations cannot be satisfied simultaneously, since the first implies a violation of the strong energy condition, whereas the second represents a turning point in the expansion. In effect, we have invoked the first condition at the end of the evolution and carried over the second condition from the *previous* cycle. Since $8\pi\ell_{\rm Pl}^2\rho_{\rm inf}/3 > 1/a_{\rm rc}^2$ for the cycle in which inflation occurs, the second condition underestimates the amount of energy

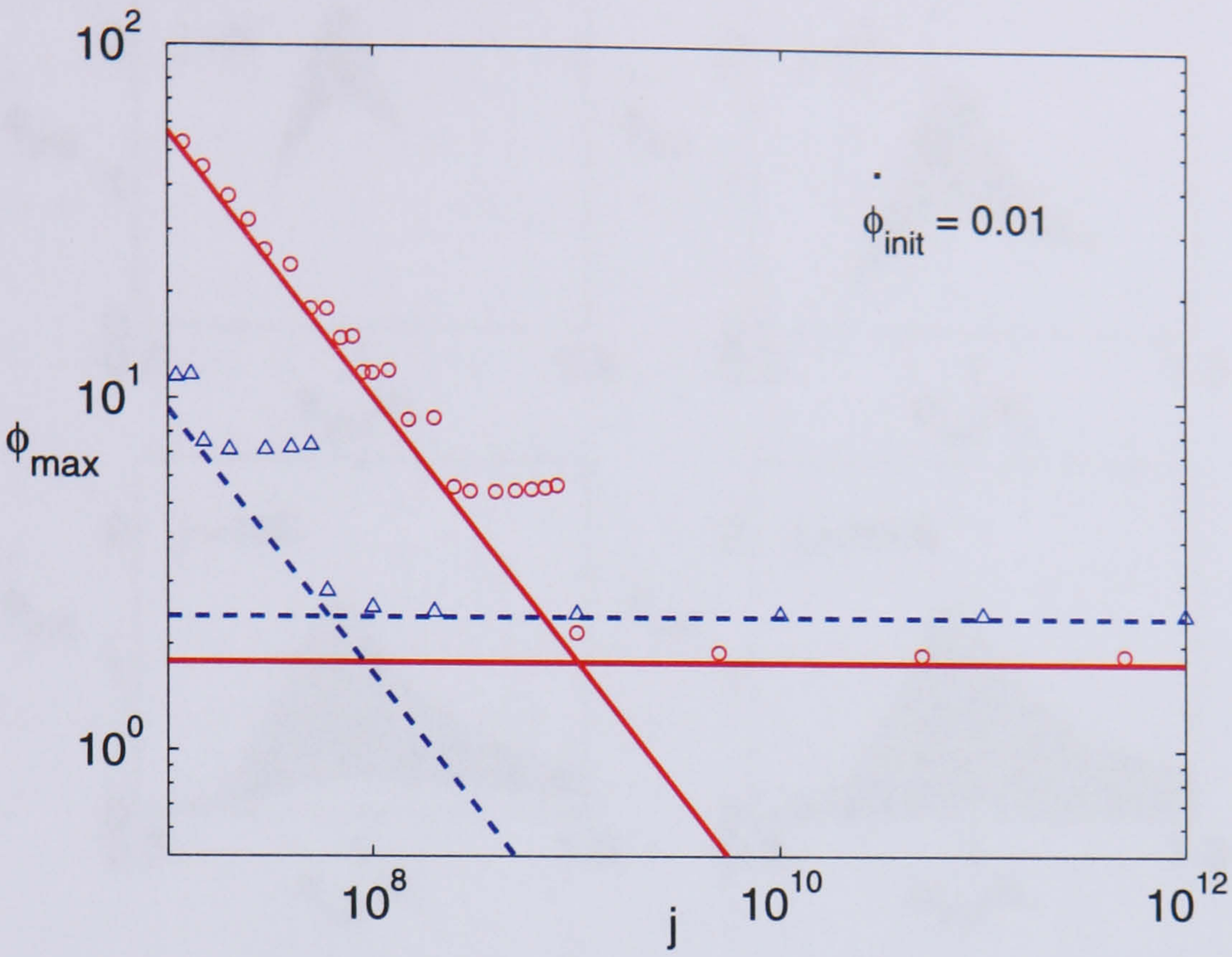


Figure 5.4: Illustrating the dependence of the maximum value of the scalar field, $\phi_{\rm max}$, on the quantisation parameter $j$ for the quadratic potential $V(\phi) = m^2\phi^2/2$ with $m = 10^{-6}\ell_{\rm Pl}^{-1}$. The horizontal lines represent the estimated value of $\phi_{\rm max}$ derived from Eq. (5.13) and the tilted lines represent the estimate (5.12). The solid lines correspond to the initial conditions $a_{\rm init}/a_* = 0.7$ and the dashed lines to $a_{\rm init}/a_* = 0.5$. Circles and triangles represent the actual values obtained by numerically integrating the equations of motion for $a_{\rm init}/a_* = 0.7$ and $a_{\rm init}/a_* = 0.5$.

present and, consequently, underestimates the change in the value of the field before it turns around. A range of values of $j$ will give rise to the same number of cycles: for the lowest value of $j$ in a given range the condition $8\pi\ell_{\rm Pl}^2\rho_{\rm inf}/3 \approx 1/a_{\rm rc}^2$ is a good approximation, since a re-collapse is only just avoided, but for subsequent values the underestimate becomes progressively more severe. This gives rise to the steps which become more evident at larger $j$. This can be understood by recalling from Eq. (5.11) that $\phi_{\rm max} \propto j^{-3/4}$, which implies $\Delta j \propto j^{7/4}\Delta\phi$, thus showing that the steps in $j$ are wider for larger $j$.

### 5.3.5 Parameter space of a viable model

There is one final aspect of the above scenario which requires consideration. This is whether the field can be sufficiently displaced from the minimum of its potential at the end of the oscillatory phase for the horizon problem to be solved, without violating the consistency conditions of the semi-classical phase. These conditions are that the energy density should satisfy the bound (3.14), and that the scale factor at the bounce should exceed $a_i$.

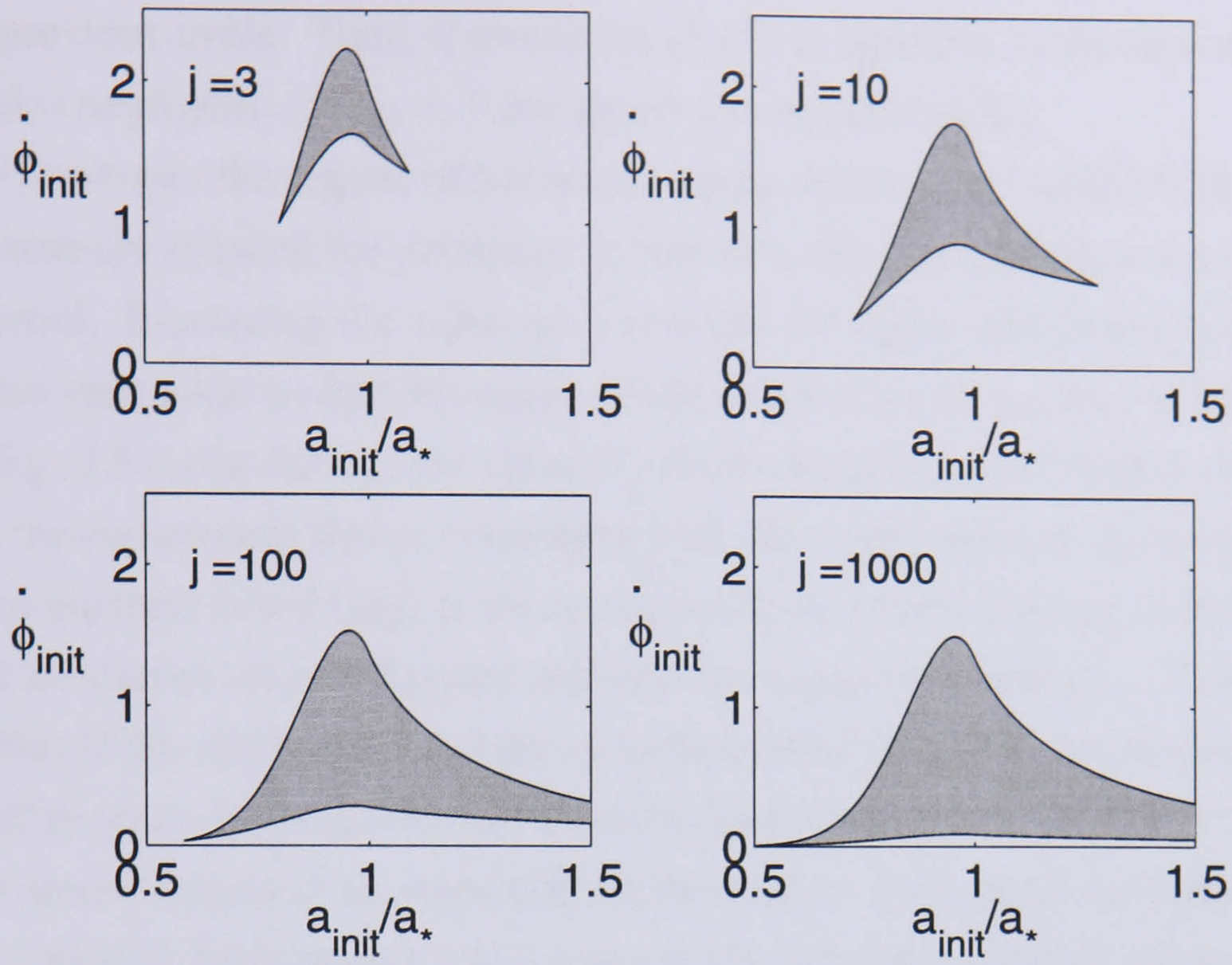


Figure 5.5: Constraints on the initial velocity of the field $|\dot{\phi}|_{\rm init}$ for a given initial value of the scale factor, $a_{\rm init}/a_*$, for different values of the quantisation parameter, $j$. The axes are labelled in Planck units and the shaded areas represent the regions where constraints (5.14) and (5.15) are satisfied. For all values of $j$, the area of the shaded region is finite, and the points of intersection occur further from $a_{\rm init}/a_* \approx 1$ as $j$ is increased. Note that for $a_{\rm init} > a_*$, the universe is initially in a contracting phase and subsequently bounces, after which the behaviour discussed in the text is followed.

We wish to determine the region of parameter space of initial conditions for which sufficient inflation will be realised with the inflaton initially at the minimum of its potential, and with the semi-classical approximation still valid.

In addition to these requirements there is a further physical constraint on the initial conditions, which is that we must have $H^2 > 0$. This necessarily implies that the initial kinetic energy of the field is bounded from below by the Friedmann equation (3.8):

$$\dot{\phi}^2_{\rm init} > \frac{6D_{\rm init}}{8\pi\ell^2_{\rm Pl}a^2_{\rm init}} \ . \tag{5.14}$$

On the other hand, the energy bound results in an upper bound on the field's kinetic energy. The Raychaudhuri equation (3.10) implies that $|H|$ reaches its maximum value during a given cycle when $A \approx 6$ and substituting Eq. (5.7) into the Friedmann equation (3.8) then implies that $|H_{\rm max}|a_i < 1$ when

$$\dot{\phi}^2_{\rm init} < \frac{3}{4\pi\ell^2_{\rm Pl}}\left(\frac{a_{\rm ph}}{a_*}\right)^6\left(\frac{a_*}{a_{\rm init}}\right)^6\frac{D^2_{\rm init}}{D_{\rm ph}}\left(\frac{1}{\gamma\ell^2_{\rm Pl}}+\frac{1}{a^2_{\rm ph}}\right) , \tag{5.15}$$

where $D_{\rm ph} = D(a_{\rm ph}/a_*)$. The discussion leading to Fig. 5.2b has shown that the maximum value of the square of the Hubble parameter during a given cycle is smaller than

that of the previous cycle. Thus, if condition (5.15) is satisfied in the first cycle, where the potential is negligible, $|H|a_i < 1$ during all subsequent cycles.

Fig. 5.5 illustrates the region of parameter space where constraints (5.14) and (5.15) are simultaneously satisfied for particular values of $j$. These constraints are independent of the potential. Increasing the value of $j$ reduces the upper and lower bounds on the initial kinetic energy but widens the range of allowed values of $a_{\rm init}/a_*$. A further consequence of Fig. 5.5 is that for a given value of $j$ there exists an upper limit to the size of the universe at the turnaround that is consistent with the semi-classical dynamics. In other words, if the universe is too large at the turnaround, the kinetic energy of the scalar field will exceed the Planck scale before the universe has contracted below $a_*$. This implies, in particular, that if the inflaton did not decay at the end of inflation, future cycles after the slow-roll inflationary epoch could not be realised within this semi-classical framework.

The constraint imposed by requiring the bounce to have occurred before $a_i$ is not necessarily satisfied if the bounce takes place at progressively smaller values of the scale factor. It is necessary, therefore, to consider this constraint for each specific model. As a particular example we again consider the quadratic potential. We have verified numerically that this constraint remains satisfied for initial values of the parameters contained within the shaded regions of Fig. 5.5 and, furthermore, that the maximum value attained by the field is sufficient to solve the horizon problem, i.e., $\phi_{\rm max} > 3\ell_{\rm Pl}^{-1}$. Indeed, for the initial condition $a_{\rm init} = 0.9a_*$ considered in Fig. 5.3, sufficient inflation is possible for $j \leq 5 \times 10^{11}$. This tells us, as we expected from the analytic approximation, that it is possible to have successful inflation in this framework without violating the validity conditions of the semi-classical regime.

## 5.4 Scalar fields with negative potentials

In the previous section the mechanism of the bounce relied on the universe's positive curvature. This was necessary because we were interested in the initial conditions for inflation, and hence were concerned with a positive inflationary potential. In the spatially flat setting, however, we have seen that a bounce can occur when the universe is sourced by a scalar field self-interacting through a negative potential. In this section, therefore, we discuss whether interesting bouncing cosmological scenarios can be developed using negative potentials.

Let us first consider the cyclic/ekpyrotic scenario which we discussed in section 5.1. We are interested in the possibility that the main aspects of this scenario could be realised within a LQC context. This question has been considered previously by Bojowald *et al* (2004), and the discussion given here is complementary to, and in broad agreement with,

this earlier study.

From the point of view of a four-dimensional observer, the universe in these scenarios is effectively sourced by a negative exponential potential, and this strongly suggests the possibility that the bounce required in this scenario could be described by the bounce which we know can occur within LQC. In the full scenario, the scalar field essentially parametrises the separation of the branes. The steep, negative exponential form of the potential is required for several reasons. First, in the cyclic picture a negative potential is required for a spatially flat universe to undergo a recollapse, thereby facilitating future cycles. Second, the potential must be steep and close to exponential for the perturbations generated during the collapse to be sufficiently close to a scale invariant form. Finally, in a collapsing universe, the steep negative exponential potential leads to stable scaling behaviour for the universe in which the field's kinetic energy grows in proportion to its potential energy. This ensures that the behaviour during the collapse is a dynamical attractor, and hence that generic initial conditions will lead to nearly identical behaviour and to the required perturbation spectra.

We identify three major issues that need to be addressed if a cyclic-type scenario is to be realised within LQC. The first is related to the field's dynamics at the bounce. In the cyclic/ekpyrotic scenario, during the collapse the field moves to progressively more negative values of the potential. At the bounce, however, the field is supposed to change direction and rapidly move to less negative values. From the five-dimensional point of view, this corresponds to the branes rebounding off each other. This behaviour is necessary from a four-dimensional perspective as well, since if the field stayed at large negative values of the potential after the bounce, the subsequent expansionary phase would be very short lived, as the field's kinetic energy would quickly be balanced by the large negative potential. However, as we saw when we described the bouncing mechanism for the negative potential in section 5.1, the balance between the kinetic and potential energies at the bounce is necessarily achieved before the kinetic energy reaches zero. The field therefore continues to move in the same direction during the bounce. This is similar to the dynamics of the positively-curved model with a positive potential. In that case, the monotonic behaviour of the field proved to be very useful, whereas here it is an impediment. This problem might be alleviated by introducing a steep positive section to the potential, which the field could evolve on to after the bounce. This would cause the field to slow down and then reverse its direction of motion, but would probably require fine-tuning.

The second problem is more severe and is directly related to the energy density bound, Eq. (3.14). During a classical collapse, the energy density of the field generically increases due to the anti-friction in the classical field equation (1.16). It starts to fall only when the condition $A > 6$ is attained. Consistency at the semi-classical level requires

that the energy density bound must not be violated before this point is reached. This problem of Planck scale energies in the ekpyrotic scenario has been raised previously by Linde (2002). For a collapse in the ekpyrotic scenario the situation is saved by the scaling solution we mentioned above. In this solution, the increasing kinetic energy is nearly completely cancelled by the negative potential energy and the two grow in proportion to one another. The solution is equivalent to a universe effectively sourced by matter with an equation of state $w \gg 1$. At first sight this seems to be a serious problem since it suggests that the energy density grows very rapidly during the collapse and hence that the energy bound becomes violated very quickly. However, another property of the solution is that $|\dot{a}| \ll 1$, and consequently the collapse also proceeds very slowly. In principle, therefore, the total energy density may remain below the Planck scale for a long period of time, during which the scale factor evolves very slowly. The potential, however, is expected only to have an exponential form over a finite region of parameter space, and once the field evolves through this region, the cosmic dynamics will move away from the scaling solution. This implies that the kinetic energy of the field will no longer be balanced by the negative potential, and that the total energy will rapidly exceed that of the Planck scale. In the context of the semi-classical equations, therefore, we require the universe to collapse to the semi-classical regime soon after the scaling solution breaks down.

A simple example, although not directly related to the ekpyrotic scenario, proves useful in highlighting this problem. We consider a positively-curved, collapsing universe sourced by a massless scalar field. In this case, it is possible to estimate when the bounce must occur in order for the Hubble bound to remain satisfied throughout the evolution. In particular, we can derive a lower limit for the value of the ambiguity parameter, $j$. If the collapse starts well inside the classical regime, it follows that $H_{\rm init} = 0$, $D = 1$, and that the initial kinetic energy of the field is $\dot{\phi}^2_{\rm init} = 6/8\pi\ell^2_{\rm Pl}a^2_{\rm init}$. The subsequent evolution of the field is determined from the relation $\dot{\phi}^2 = \dot{\phi}^2_{\rm init}(a_{\rm init}/a)^6$ and, after substituting this expression into the Friedmann equation (3.8) and imposing the energy bound (3.14), we require that

$$j > \frac{3}{\gamma}\left(\frac{a_{\rm init}}{a_*}\right)^4 \quad , \quad j^3 > \frac{3}{\gamma}\left(\frac{a_{\rm init}}{a_i}\right)^4 \quad , \tag{5.16}$$

where $a_*$ has been employed as the point at which the energy density becomes maximized. Clearly, if the size of the universe is large compared with $a_*$ at the start of the collapse, $j$ must be very large indeed if a bounce is to occur within the semi-classical regime. Although a realistic collapse will involve a self-interacting scalar field, the above estimate highlights the difficulties that arise: even if the field equations generically lead to a bouncing cosmology, the bounce may occur in a regime where the equations are no

longer valid. This was also indicated in subsection 5.3.5, where we noted that bounces were unlikely to be possible after the universe underwent inflationary evolution. In the case of a flat universe, we can set the initial values for the kinetic energy of the scalar field and the size of the universe independently, so we cannot repeat a similar calculation to this example. It is clear, however, that this problem is also likely to occur in that setting.

Finally, a third question that arises in developing a consistent bounce is also related to the size of the universe. For a consistent, semi-classical treatment, it is important that the bounce does not occur after the universe has collapsed beyond the minimal scale consistent with the semi-classical region, $a_i$, since the semi-classical Friedmann equations are no longer valid below this scale. Whether bounces occur above this scale is difficult to answer in general since it will depend on the magnitude of the energy at the point at which the energy density stops increasing and begins to decrease. This occurs at $a_{\rm ph}$, which is again initial-condition dependent. However, this is clearly a constraint that is ameliorated by larger values of $j$, since in this case the semi-classical region is larger and the universe has more time to undergo a bounce before $a_i$ is reached.

To summarise, it appears improbable that realising a scenario with similar properties to the ekpyrotic/cyclic scenario will be possible within the semi-classical regime of LQC. The second and third problems we raised above also mean that it is unlikely that other oscillatory scenarios involving large universes, such as the one in which the maximal size of the universe grows with each bounce, could be realised within semi-classical LQC.

Before concluding this section, it is also worth considering the case where the potential has a global minimum $V_{\rm min}$, such that $V_{\rm min} < 0$, with only a finite region around the minimum that is negative. One example of this class is a potential of the form $V(\phi) = C + m^2\phi^2/2$ for some negative constant $C$. In positively-curved universes, the mechanism described in section 5.3 enables the field to work its way out of the negative region and continue up the potential until the cycles are broken. For spatially flat universes, the picture is similar although the oscillations will come to an end as soon as the field reaches a positive region of the potential. Unfortunately, in the flat case the amount of inflation that results is typically less that 60 e-folds, since we would require the last cycle to move the field roughly $3\ell_{\rm Pl}^{-1}$ for 60 e-folds to occur. This is difficult to achieve because this scenario is essentially the same as that studied in chapter 4. The scenario is therefore subject to the severe constraints that we outlined in that chapter. Furthermore, for such a potential in a flat universe, there is the possibility that the potential becomes positive during the collapsing phase, in which case the universe can undergo no further bounces and ultimately collapses into a big crunch.

## 5.5 Discussion

This chapter has established a number of very interesting results. First, we have shown that a collapsing cosmology can undergo a non-singular bounce into a new expansionary phase when the semi-classical equations of LQC are employed to describe the universe's evolution. In particular, collapsing positively-curved universes sourced by a scalar field, and flat universes sourced by a scalar field with a negative-definite potential, both reach points at which the collapse halts, and this generically results in a bounce. Moreover, we have shown how the dynamics of these models can be understood by reformulating the semi-classical dynamics of LQC in terms of a perfect fluid with a variable equation of state. Crucially, we have shown that this fluid will necessarily become an effective phantom fluid below a specific value of the scale factor $a_{\rm ph}$. These results in themselves are highly interesting, but in this chapter we have gone further and looked at early universe scenarios which exploit these features.

The first such scenario concerned the generation of the initial conditions for slow-roll inflation. In particular, we have shown that LQC corrections to the Friedmann equation in a positively-curved universe enable a scalar field to move up its potential due to a series of contracting and expanding phases in the cosmic dynamics. We were able to understand the complex dynamics remarkably well, and derive quantitative results without the use of numerical integration. When numerical integration was performed, it confirmed our analytic understanding. Our analytic approximation, Eq. (5.11), together with Fig. 5.4 showed that it is very easy for the field to move sufficiently far up its potential to generate a sufficient amount of inflation, without violating the energy bound (3.14) which so constrained the mechanism put forward in chapter 4. This is because in this case the field will actually move further for smaller initial values of its kinetic energy, as shown by the approximation function (5.11). Hence, we can always choose sufficiently small initial values of the field's energy such that its maximum energy remains below the Planck scale.

It is interesting to ask if this phenomenological application can yield insight into the preferred values of the quantisation parameters. In general, however, it suffers in this regard from its success. Considering the $j$ parameter, we have seen that a vast range of values of $j$ will give rise to inflation. Although larger values widen the range of initial conditions which lead to inflation, as seen in Fig. 5.4, smaller values allow the field to move further from the potential minimum. Therefore, this phenomenological application does not appear to place any strong restrictions on $j$. On the other hand, smaller values would appear to be preferable when we only consider the amount of inflation which can occur. This is interesting since we have suggested that smaller values of this parameter can be viewed as more natural from theoretical considerations, though presently all half-

integer values are allowed.

We have hardly mentioned the quantisation parameter $l$ in this chapter. This is because the qualitative nature of the dynamics remains unchanged provided $d\ln D/d\ln a > 6$ is satisfied for sufficiently small values of the scale factor. As we have noted already, this is always the case for values of $l$ in the allowed range $0 < l < 1$, though this condition becomes satisfied over a progressively smaller range of $a$ as $l$ approaches the limit $l \to 0$ (for a given value of $j$). In this sense, phenomenological considerations agree with the theoretical considerations of chapter 3 which already prefer $l$ to be $l > 0.5$ (and also for this parameter to take discrete values). A final point is that even if we allowed the alternative quantisation scheme FRIED, one would naively expect that the dynamics would be qualitatively unchanged, but further investigation is needed to confirm this expectation.

Given the inverse dependence of the maximum value that the field can attain on the parameter $j$, there is a further observation concerning this scenario which deserves attention. This is the possibility that for sufficiently small values of $j$, the field may move far enough up its potential before the cycles are broken for the universe to enter a stage of eternal self-reproduction, called eternal inflation (see Linde, 1986). Eternal inflation means that inflation never ends, because quantum fluctuations continually push the field up the potential in the majority of the volume of the universe. For a particular potential, the value of the field at which this behaviour occurs can be calculated from the inequality $3V'^2 < 128\pi\ell_{\rm Pl}^6 V^3$. For a quadratic potential this implies that $\phi > 1/(2m^{1/2}\ell_{\rm Pl}^{3/2}) \approx 500\ell_{\rm Pl}^{-1}$ (Linde, 1986). Numerical integration indicates, for example, that this condition can be satisfied for $j < 2 \times 10^7$ when $a_{\rm init} = 0.9a_*$.

We conclude, therefore, that even if the field is at the minimum of its potential, a wide range of initial conditions and values of the ambiguity parameters can lead to successful (and eternal) inflation. Moreover, since the assumptions we made regarding the form of the potential in section 5.3 were very weak, this mechanism should be very generic.

Finally, let us review our conclusions regarding the possibility that other bouncing cosmological scenarios can be realised using the semi-classical equations of LQC. Of particular interest are scenarios which utilise a scalar field with a negative potential, since a bounce is possible for a universe sourced by such fields even in the absence of spatial curvature. Moreover, negative potentials are known to arise in string/M-theory compactifications (see for example Emparan and Garriga, 2003), and in particular are utilised in the M-theory motivated ekpyrotic and cyclic scenarios. Unfortunately, the scalar field dynamics of LQC seem unsuited to realising these scenarios. Moreover, we discussed how any scenario which involves large, collapsing classical universes is likely to violate either the energy density bound, or the condition that a bounce must occur above $a_i$. This prob-

lem becomes less severe for larger values of $j$. Given that these values appear less natural from a theoretical perspective, however, we are not optimistic that cyclic-type scenarios involving a classical universe can be realised using the semi-classical LQC framework.

# Chapter 6

# An emergent universe from a loop

The previous chapter was dedicated to the study of bouncing cosmologies within semi-classical LQC. In this chapter we focus on another scenario of the early universe, the 'emergent universe scenario'. In this scenario the universe is positively-curved and sourced by a self-interacting scalar field. The universe begins its evolution as a small Einstein static universe, and after spending an infinite amount of time in this state, subsequently evolves into an inflationary phase. We will find that this scenario can be naturally realised within LQC, and that the dynamics which enables this to occur is closely connected with those studied in section 5.3.

The emergent scenario was first proposed within the context of GR by Ellis and Maartens (2004) and an explicit model was given by Ellis *et al* (2004). A major motivation for the original proposal was the widely accepted view that inflationary spacetimes are generically singular. This is supported by singularity theorems, valid in inflationary cosmologies (see for example Borde *et al*, 2003), which show that such spacetimes cannot be geodesically complete and in that sense are singular. A number of assumptions, however, go into these theorems. In particular, they require either that $H > 0$, or that spatial sections are negatively-curved or flat, as discussed by Ellis and Maartens (2004). The emergent universe is a successful attempt to construct a counter example to singular inflationary scenarios, by allowing at least one of the assumptions mentioned above to be violated. It represents, therefore, an example of a non-singular (geodesically complete) inflationary cosmology.

As well as being an example of a singularity-free cosmology, the emergent universe exhibits a number of other intriguing properties. These properties concern the past-eternal phase of the universe, the Einstein static universe. It has been argued that the Einstein static universe is favoured by entropy considerations as the initial state for our universe (Gibbons, 1987). Moreover, the Jeans length[1] in such a universe can be greater

[1]The Jeans length represents the wavelength above which perturbations are gravitationally unstable.

than the size of the universe, in which case the universe would be neutrally stable to inhomogeneous perturbations (Barrow *et al*, 2003). These intriguing properties, as well as the high symmetry of the Einstein static universe, make it attractive to postulate that the universe originated in this form.

Despite their appeal, however, emergent models within GR suffer from a number of limitations. The most serious of these is that a dynamical analysis reveals the initial Einstein static state to be a saddle equilibrium point in the system's phase space. Such a state is unstable to homogeneous perturbations, and hence cannot be maintained for an infinitely long period of time in the presence of fluctuations, such as quantum fluctuations, which will inevitably occur. Even in the absence of such fluctuations, the assumption that the universe originates and spends an infinite amount of time in such a state represents an extremely severe fine-tuning of the initial conditions. A further drawback of the scenario is the required assumption that the entire history of the universe is governed by classical dynamics. This requires the initial conditions to be set in a regime where quantum effects are negligible.

The purpose of this chapter is to study the existence and stability of such models in the context of LQC. As we shall show, both the limitations discussed above can be partially remedied once semi-classical effects are taken into account. We shall see that an important consequence of these effects is to give rise to an additional static solution (not present in GR), which is dynamically a centre equilibrium point and which is located in the more natural semi-classical regime. That this point might exist was already suggested by the oscillatory dynamics demonstrated in the previous chapter. Here, however, we make a systematic study of all equilibrium points which are present in the semi-classical regime. An understanding of the existence and behaviour of such equilibrium points then allows the construction of emergent models which utilise the centre equilibrium point as the original state of the universe, instead of the classical saddle point. This new scenario is now partially stabilised, in the sense that small perturbations about the centre point simply lead to oscillations of the universe. The scenario, therefore, requires far less fine-tuning than the classical one. Moreover, the semi-classical dynamics allows for considerably more freedom in the class of potentials which realise this new scenario than could be accommodated within the original one.

We shall proceed as follows. First, we recall the properties of the classical Einstein static universe, and review the construction of the classical emergent universe scenario in section 6.1. The semi-classical regime of LQC is then considered in section 6.2. We identify the equilibrium points which occur in this regime and determine their stability. In sections 6.3-6.5 we construct new emergent models based on the dynamics of LQC. These models are stable in the sense discussed above, exhibit all the attractive features of

the emergent scenario, and are consistent with all present-day cosmological observations. We discuss various choices for the inflationary potential, and consider a particularly interesting example in section 6.5 in which the universe possesses both early- and late-time accelerating phases. This case has the intriguing feature that the same region of the potential which supports the pre-inflationary Einstein static phase also acts as the source of dark energy in the present-day universe. Finally, we conclude with a discussion in section 6.6.

## 6.1 Classical Einstein static solution and the emergent universe

Before considering static solutions within the context of LQC, it is instructive to review the corresponding results for classical Einstein gravity, and how they are used to construct the classical emergent universe scenario of Ellis and Maartens (2004).

With this scenario in mind we consider an FRW universe sourced by a scalar field. The equations which govern the evolution of this system are given by Eqs. (1.14)-(1.16). To analyse these equations it proves useful to rewrite them in terms of a three-dimensional autonomous dynamical system using the variables $\{H, a, \phi\}$ thus

$$\dot{H} = 8\pi\ell_{\rm Pl}^2 V(\phi) - 3H^2 - \frac{2k}{a^2} \ , \tag{6.1}$$

$$\dot{a} = Ha \ , \tag{6.2}$$

$$\dot{\phi} = \left(\frac{6H^2}{8\pi\ell_{\rm Pl}^2} - 2V(\phi) + \frac{6k}{8\pi\ell_{\rm Pl}^2 a^2}\right)^{\frac{1}{2}} \ . \tag{6.3}$$

Let us consider the case in which the universe is sourced by a scalar field with constant potential $V$. This is equivalent to considering a free scalar field in the presence of a cosmological constant. In this case Eqs. (6.1)-(6.2) are completely decoupled from Eq. (6.3), and hence the system reduces to a two-dimensional one given by Eqs. (6.1)-(6.2). Static solutions ($\dot{a} = \ddot{a} = 0$) correspond to equilibrium points of this system, and require the conditions $k = 1$, $H_{\rm eq} = 0$ and

$$a_{\rm eq}^2 = \frac{1}{4\pi\ell_{\rm Pl}^2 V} \tag{6.4}$$

to be met, where the subscript eq denotes values evaluated at equilibrium points. Eq. (1.15) implies that the scalar field's kinetic energy is given by

$$\dot{\phi}_{\rm eq}^2 = \frac{1}{4\pi a_{\rm eq}^2 \ell_{\rm Pl}^2} = V \ , \tag{6.5}$$

which is a constant.

This confirms, therefore, that there is a single equilibrium point in this classical setting, which only exists for a positively-curved universe, and represents the Einstein static universe. The stability of this equilibrium point can be determined by linearising about the equilibrium point, and evaluating the eigenvalues of the corresponding Jacobian matrix. In this case the eigenvalues are given by

$$\lambda^2 = \frac{4}{a_{\rm eq}^2} \ , \tag{6.6}$$

and hence there is one real positive eigenvalue and one real negative eigenvalue. The equilibrium point, therefore, is a saddle and is unstable. Furthermore, for the classical emergent universe $a_{\rm eq}$ must lie in a regime where classical dynamics can be applied. This places an upper bound on the value of the potential $V$, since Eq. (6.4) implies that larger values of $V$ cause the position of the equilibrium point to move to progressively smaller values of the scale factor, where we expect quantum effects to become important.

### 6.1.1 Construction of the emergent universe

In the emergent universe scenario it is assumed that the field's self-interaction potential asymptotes to a flat region with a finite, positive value, $V_{-\infty}$, in the limit $\phi \rightarrow -\infty$. For $\phi$ greater than a particular value of the field $\phi_{\rm inf}$, however, the magnitude of the potential is assumed to start to decrease, and the slow-roll conditions are assumed to be satisfied in this region. The initial conditions of the scenario are set such that the universe begins its evolution exactly at the saddle equilibrium point permitted by $V = V_{-\infty}$. This requires that $a = a_{\rm eq}$, $\dot{\phi} = \dot{\phi}_{\rm eq}$ and $\phi = -\infty$. The scalar field's velocity is, however, non-zero and so the field will evolve along its potential. It is further assumed that the field's velocity is positive. The result is that after an infinite period of time the field will evolve from the region of its potential which is flat and positive past $\phi_{\rm inf}$ and onto the region which supports slow-roll inflation. A phase of inflationary expansion will then commence. The Einstein static solution, therefore, represents the past eternal phase of the universe. The universe then evolves from this state into an inflationary epoch.

An example of a potential with the qualitative features required by this scenario is given by the solid line in Fig. 6.5. The motivation for this form of potential is given in section 6.4. From the point of view of the classical emergent universe scenario, the region of the potential corresponding to $\phi > \phi_{\rm min}$, where $\phi_{\rm min}$ represents the position of the potential's minimum, is unconstrained by the requirements of the scenario. A minimum is required for reheating. Beyond the minimum, however, the potential does not have to be monotonically increasing, as in Fig. 6.5, but could take any form.

This section has shown how the classical emergent scenario, in which the universe slowly evolves out of an Einstein static state into an inflationary phase, can be con-

structed. The instability of the saddle equilibrium point, however, ensures that any perturbations – no matter how small – rapidly force the universe away from the static state, thereby aborting the scenario. In the light of this difficulty the following sections address the construction of emergent universes in the semi-classical LQC setting.

## 6.2 Static solutions in semi-classical LQC

In order to determine the equilibrium points which are present in the semi-classical regime of LQC, we follow a similar procedure to the previous section. Here, however, we employ the semi-classical equations (3.8)-(3.10). As in chapter 5, we shall for simplicity focus on just one value of the ambiguity parameter $l$, setting $l = 3/4$, but will allow freedom in the value of $j$.

Eqs. (3.8)-(3.10) can be rewritten in the form of a three-dimensional dynamical system in terms of variables $\{H, a, \phi\}$[2]. Employing the Friedmann equation (3.8) to eliminate the kinetic term of the scalar field allows the complete dynamical system to be described by equations:

$$\dot{H} = \left(8\pi\ell_{\rm Pl}^2 V(\phi) - 3H^2\right)\left(1 - \frac{A}{6}\right) + \frac{k}{a^2}\left(\frac{A}{2} - 2\right) , \tag{6.7}$$

$$\dot{a} = Ha , \tag{6.8}$$

$$\dot{\phi} = \left(\frac{6DH^2}{8\pi\ell_{\rm Pl}^2} - 2DV + \frac{6kD}{8\pi\ell_{\rm Pl}^2 a^2}\right)^{\frac{1}{2}} , \tag{6.9}$$

where again the function $A(a) \equiv d\ln D/d\ln a$. In this section, with the aim of considering emergent universes, we restrict ourselves to the positively-curved ($k = 1$) case, and initially consider constant potentials. In this case, Eqs. (6.7)-(6.8) are decoupled from Eq. (6.9) and, as was the case for the classical system, the equations reduce to a two-dimensional autonomous system.

Static solutions again correspond to the equilibrium points of this system, which are given by

$$H_{\rm eq} = 0 , \qquad a = a_{\rm eq} , \tag{6.10}$$

[2]This system was previously studied numerically by Vereshchagin (2004). However, while this study identified a number of the features we discuss here, our study represents a significant extension of this earlier work. In particular, we give an analytic treatment of the equilibrium points, as well as presenting numerically derived phase portraits. In addition to providing us with a fuller understanding of the dynamics, this confirms the form of the phase portraits and the position and type of equilibrium points. An important result is that an equilibrium point found by Vereshchagin (2004), but not found in this study, does not exist in the phase space of Eqs. (6.7)-(6.8).

where $a_{\rm eq}$ is now given by solutions to the constraint equation

$$A(a_{\rm eq}) = B(a_{\rm eq}) \ , \qquad B(a) \equiv \frac{6(8\pi\ell_{\rm Pl}^2 V a^2 - 2)}{(8\pi\ell_{\rm Pl}^2 V a^2 - 3)} \ . \tag{6.11}$$

It follows from Eq. (3.10) that the field's kinetic energy at the equilibrium points is given by

$$\dot{\phi}_{\rm eq}^2 = \frac{D_{\rm eq}}{4\pi {a_{\rm eq}}^2 \ell_{\rm Pl}^2 (1 - A_{\rm eq}/6)} \ . \tag{6.12}$$

Eq. (6.11) implies that a necessary and sufficient condition for the existence of the equilibrium points is that the functions $A(a)$ and $B(a)$ should intersect.

We wish to understand the position and properties of the equilibrium points, and how these alter as the values of the potential and the quantisation parameter $j$ are changed. This is best seen by considering how the functions $A(a)$ and $B(a)$ (and hence their points of intersection) change with these parameters. The form of the function $A$ is by now familiar. In this discussion, however, the important point is how the $a$ dependence of this function changes with different values of the ambiguity parameter $j$. To give insight, therefore, the form of $A$ as a function of $a$ is plotted in the top panel of Fig. 6.1 for a number of different values of the parameter $j$. The characteristic features of $A$ which remain unaltered for all values of $j$ were discussed in section 3.1.1. For the case of $l = 3/4$, we have that the function asymptotes to the constant value $A = 15$ at $a = 0$, decreases to a minimum value of $A_{\rm min} = -5/2$ at $a = a_*$, and then asymptotes to zero from below as $a \to \infty$ for all values of $j$. Increasing the parameter $j$ increases the value of $a_*$ and this results in moving the turning point of the function $A$ to larger values of the scale factor. The important point to note, however, is that the qualitative form of $A$ remains unaltered for all values of $j$. It also remains unaffected as $V$ is varied.

The qualitative nature of the function $B$, on the other hand, is sensitive to the value of $V$. In particular, its form changes dramatically when the sign of the potential is altered, as can be seen from the bottom panel of Fig. 6.1. We briefly discuss the behaviour of $B$ for each case in turn. For $V = 0$, it is given by the (solid) horizontal line $B = 4$. For $V > 0$ it represents a hyperbola (dot-dashed curve) with a single (since the scale factor $a$ is non-negative) vertical asymptote given by

$$a = \sqrt{\frac{3}{8\pi\ell_{\rm Pl}^2 V}} \ . \tag{6.13}$$

The region to the left of this asymptote defines the region in the $\{A/B, a\}$ plane where the reality condition, $\dot{\phi}^2 > 0$, is satisfied. Thus, the upper-right branch of the hyperbola plays no role in determining the existence of the equilibrium points. In the limit of $a \to 0$, the function $B \to 4$ which coincides with the value of the function in the case of

$V = 0$. As $a$ is increased, the function takes progressively smaller values as the vertical asymptote is approached. As $V$ tends to zero from above, it causes the asymptote to move to progressively larger values of $a$, and we may therefore formally view the $V = 0$ case as the limit where the asymptote moves to infinity. Finally, for negative potentials the qualitative behaviour of the function $B$ is changed to the dashed line in the bottom panel of Fig. 6.1 and there is no vertical asymptote. As in the case of positive potentials, $B \to 4$ as $a \to 0$, but the function $B$ now increases monotonically as $a$ increases, ultimately tending to the value $B = 6$ as $a \to \infty$. As the potential tends to zero from below, the function $B$ still tends to the asymptotic value $B = 6$, but at a larger value of $a$. An important point to note is that for *all* values of $V$, the function $B$ satisfies the condition $B < 6$ (for physically relevant regions of the $\{A/B, a\}$ plane), and hence *equilibrium points can only occur when* $A = B < 6$. This result also follows from Eq. (6.12) by noting that the field's kinetic energy at an equilibrium point must be positive.

Once the positions of the equilibrium points have been determined, their nature can be found by linearising about these points. The eigenvalues of the corresponding Jacobian matrix are given by

$$\lambda^2 = \left[\frac{4-A}{a^2} + \frac{1}{6a(1-A/6)}\frac{dA}{da}\right]_{a_{\rm eq}} . \tag{6.14}$$

When $\lambda^2 < 0$, this leads to imaginary eigenvalues and implies that the equilibrium point is a centre, whereas the point is a saddle when $\lambda^2 > 0$. Although this expression is rather complicated, it can be verified that for $A < 6$ (which is a necessary condition for the existence of equilibrium points), $\lambda^2$ is negative for $a < a_*$ and positive for $a > a_*$. Hence we have the important result that, *equilibrium points occurring in the semi-classical regime are centres and those occurring in the classical regime are saddles.*

Finally we are in a position to determine the existence of equilibrium points and their stability. We shall consider the different signs of the potential separately.

$V = 0$: In the case of a massless scalar field with $V = 0$, the condition (6.11) has a single solution given by $A = 4$, implying a single equilibrium point. The position of this equilibrium point can be seen from the intersection point in the top panel of Fig. 6.2. Since this point occurs at $a < a_*$, it is a centre, with its phase portrait consisting of a continuum of concentric orbits (see the bottom panel of Fig. 6.2).

$V > 0$: As described above, for small positive values of the potential, the vertical asymptote of the function $B$ is far to the right of the origin, which results in two points of intersections between the functions $A$ and $B$ (see the top panel of Fig. 6.3). There are, therefore, *two* equilibrium points in this case: the first occurs at $a < a_*$ and hence is a centre, while the second occurs at $a > a_*$ and is therefore a saddle. As the potential is increased, the asymptote moves towards the origin causing the equilibrium points to

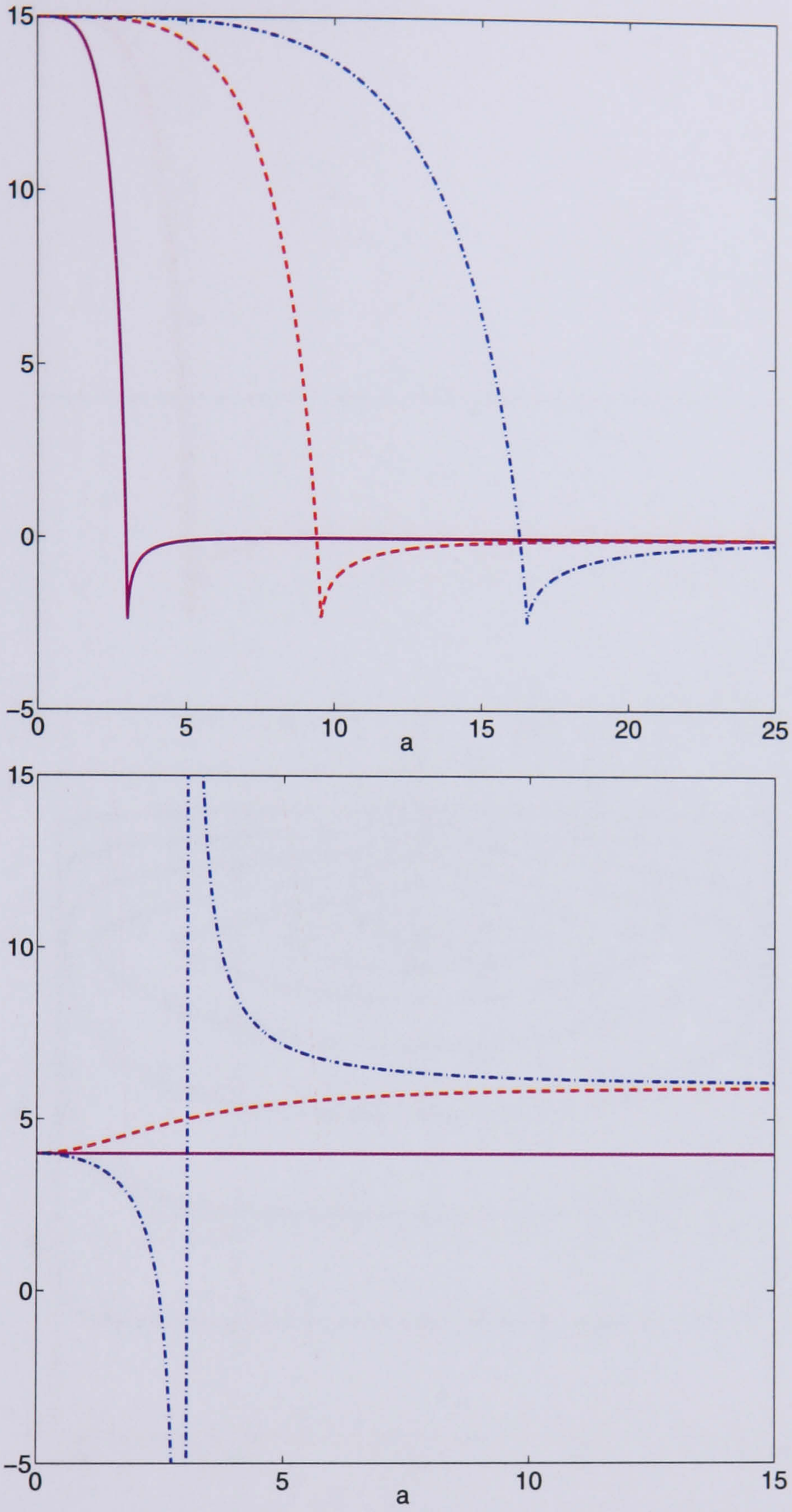


Figure 6.1: The top panel shows the plots for the function $A$ against $a$ for $j = 100$ (solid line), $j = 1000$ (dashed line) and $j = 3000$ (dot-dashed line). The bottom panel shows plots of the function $B$ against $a$ for $V = 0$ (solid line), $V > 0$ (dot-dashed line) and $V < 0$ (dashed line). Note the dramatic change in the shape of the function as the sign of $V$ is altered. Axes are in Planck units.

eventually coalesce when $V = V_*$. This occurs at the point of tangency of the functions $A$ and $B$, i.e. at the minimum (which is a cusp) of the function $A$ located at $a = a_*$.

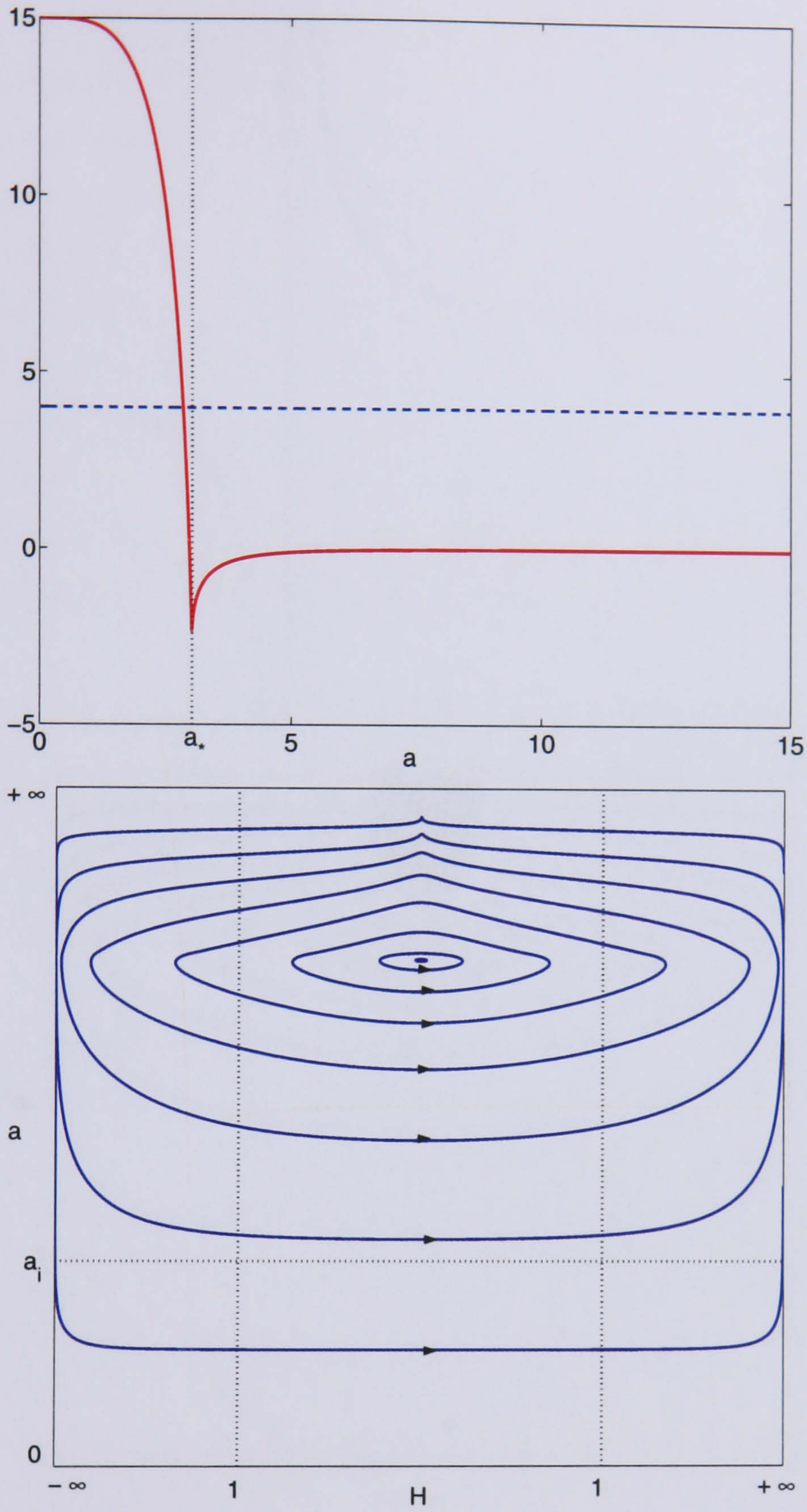


Figure 6.2: The top panel shows the plots of functions $A$ (solid line) and $B$ (dashed line) against $a$ for $V = 0$. The vertical dotted line denotes the position of $a = a_*$. The bottom panel is the corresponding phase portrait demonstrating the centre equilibrium point that occurs in this case. The plot is compactified using $x = \arctan(H)$ and $y = \arctan(\ln a)$, in order to present the entire phase space. The vertical dotted lines in the bottom panel demarcate the region in which the Hubble parameter is less than the Planck scale. The horizontal dotted line marks $a_i$, where the quantum regime begins. All axes are in Planck units, and $j = 100$.

Thus, using $B$ and the fact that $A|_{a_*} = -5/2$, we obtain

$$V_* = \frac{39}{136\pi\ell_{\rm Pl}^2 a_*^2} = \frac{117}{136\pi\gamma j} m_{\rm Pl}^4 \ . \tag{6.15}$$

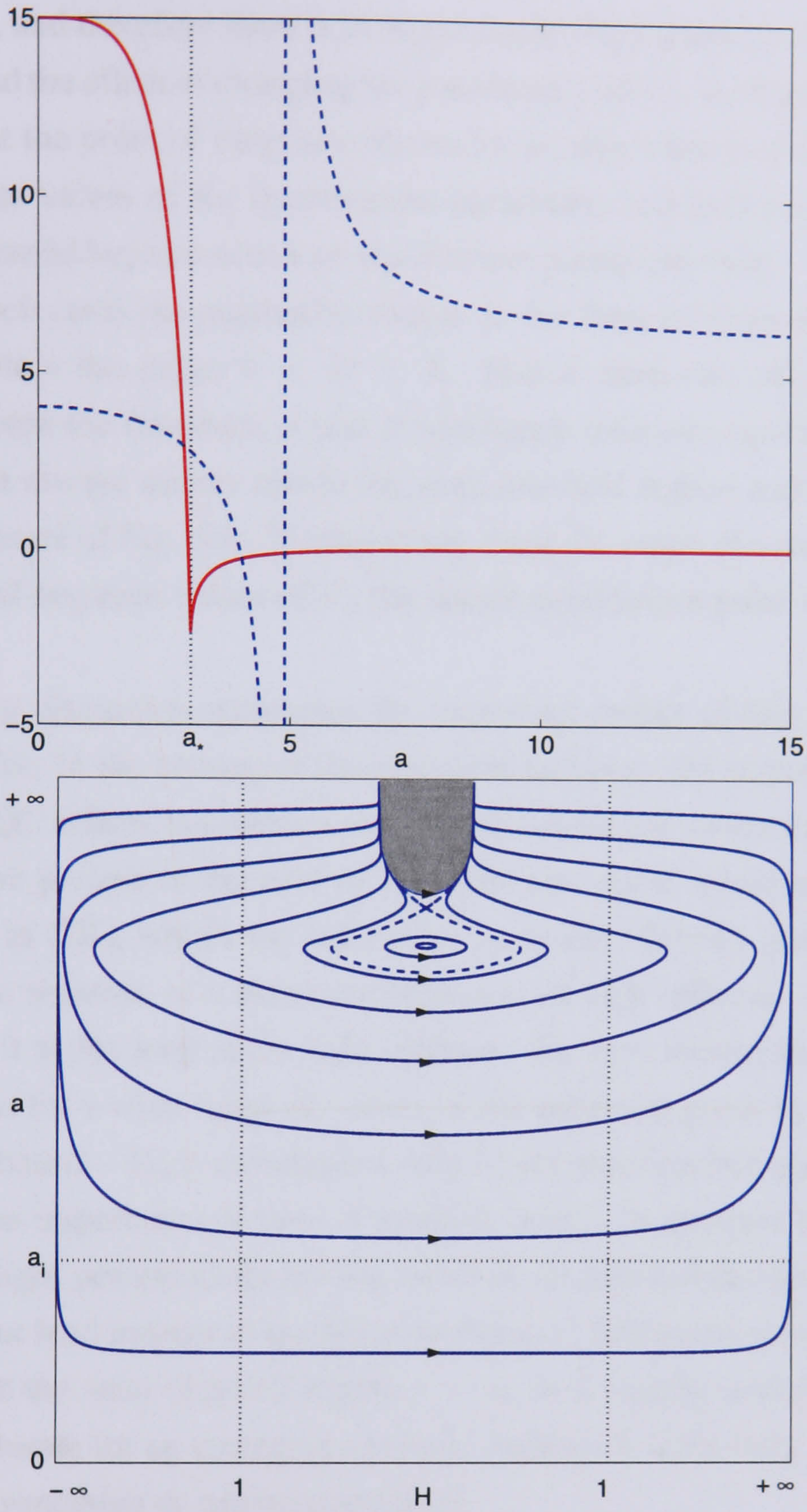


Figure 6.3: The top panel shows the plots of functions $A$ (solid line) and $B$ (dashed line) against $a$ for $V = 0.005$. For this value of $V$, the equilibrium points are close to coalescing. The vertical dotted line denotes the position of $a = a_*$. The bottom panel is the corresponding phase portrait demonstrating the centre equilibrium point and saddle point which occur in this case with the dashed line indicating the separatrix. The shaded area is the unphysical region where $\dot{\phi}^2$ would be negative. The plot is compactified as in Fig. 6.2. The dotted lines in the bottom panel are as described in Fig. 6.2. All axes are in Planck units, and $j = 100$.

For values of $V > V_*$, the asymptote moves further towards the origin. Consequently, the functions $A$ and $B$ will no longer intersect in the part of the plane which satisfies the

reality condition, and therefore there will be no equilibrium points in this case. It is also easy to understand the effect of changing the parameter $j$ on $V_*$. Increasing $j$ increases $a_*$, which means that the point of tangency occurs for smaller values of the potential. This implies that larger values of the quantisation parameter, and hence $a_*$, lead to smaller values of the potential beyond which no equilibrium points can exist.

$V < 0$: In such cases the qualitative change in the form of $B$ results in the function taking values within the range $4 < B < 6$. Hence there can only be one point of intersection between the functions $A$ and $B$ and hence only one equilibrium point. This equilibrium point always occurs inside the semi-classical region and hence is a centre (see the bottom panel of Fig. 6.4). Furthermore, since the range of values which $B$ takes is unaltered for all negative values of $V$, the centre equilibrium point will persist for *all* negative values.

The preceding discussion represents the important results of this chapter, so let us summarise thus far. In the context of the emergent universe, the important consequence of considering LQC effects is to permit two possible static universe solutions, rather than the single solution present in the case of GR. The first static solution corresponds to a saddle point (as in GR), which we shall refer to as the Einstein Static (ES) solution. The second static solution is a direct consequence of LQC effects. It is a centre and we shall refer to it as the loop static (LS) solution. We have shown analytically that the LS solution arises for a wide range of values of the potential given by $V \in (-V_{lb}, V^*)$, where the lower bound $-V_{lb}$ is constrained only by the need for energies to be below the Planck scale. The importance of the LS solution is that, in contrast to the ES solution present in GR, slight perturbations do not result in an exponential divergence from the static universe, but lead instead to oscillations about it. Moreover, since the LS solution always lies within the semi-classical region $a < a_*$, it is ideally suited to act as the past asymptotic initial state for an emerging universe. Indeed, it is the only equilibrium point in models with a vanishing or negative potential.

Finally, we note that if the potential is non-constant, then Eqs. (6.7)-(6.9) admit no equilibrium points at which $\dot{a} = \ddot{a} = 0$. Hence the saddle and centre points for constant potentials discussed above, represent the complete set of equilibrium points possible in semi-classical LQC. This result was referred to in the previous chapter.

### 6.2.1 Equilibrium points and the equation of state

In the previous chapter, we studied oscillatory dynamics within semi-classical LQC. In particular, we described in detail the behaviour of a universe sourced by a massless scalar field. The results of the current chapter give us a complementary understanding of this behaviour as oscillations of the universe about a centre equilibrium point.

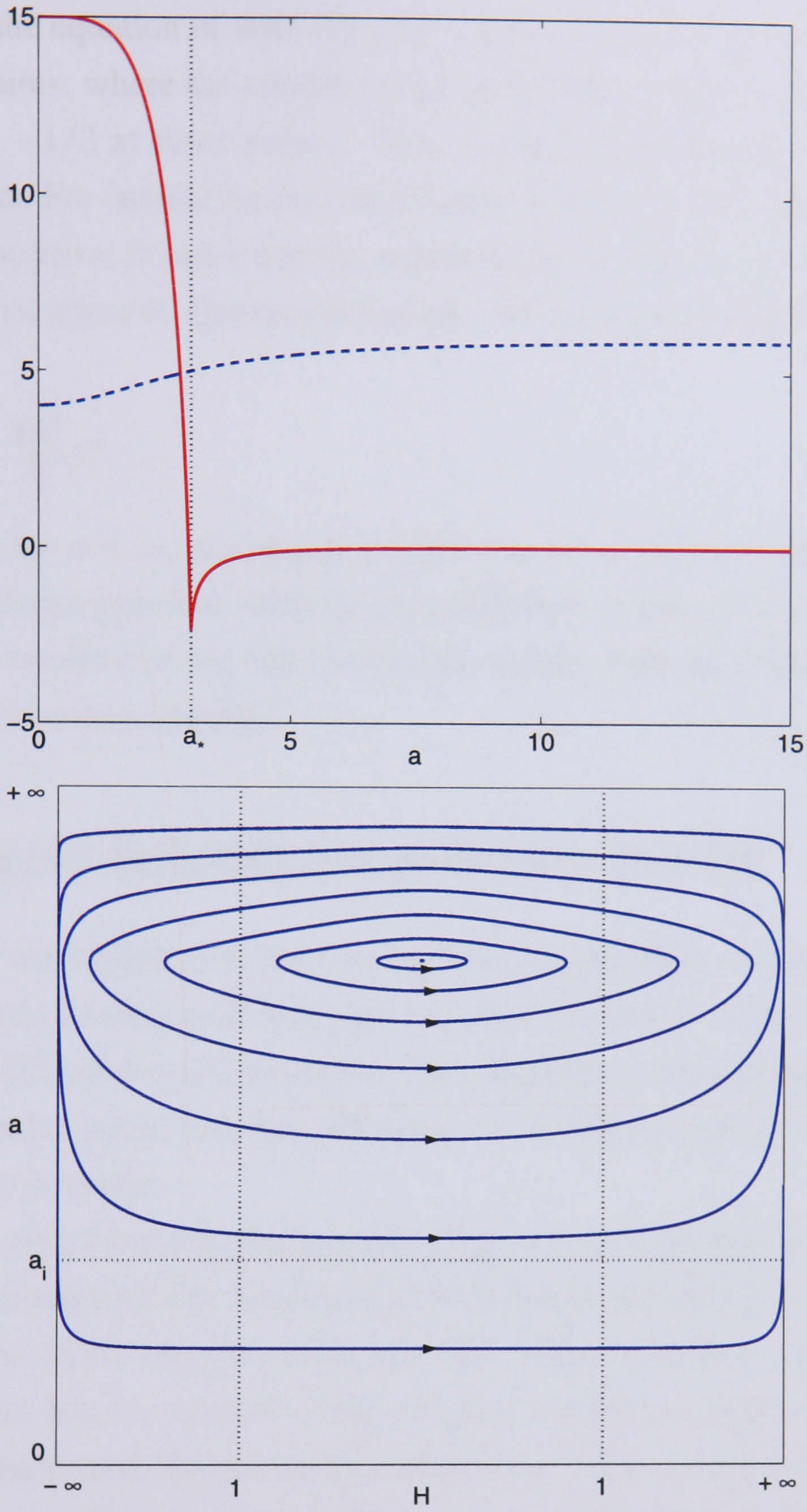


Figure 6.4: The top panel shows the plots of functions $A$ (solid line) and $B$ (dashed line) against $a$ for $V = -0.013$. The vertical dotted line denotes the position of $a = a_*$. The bottom panel is the corresponding phase portrait demonstrating the centre equilibrium point that occurs in this case. The plot is compactified as in Fig. 6.2. The dotted lines in the bottom panel are as described in Fig. 6.2. All axes are in Planck units and $j = 100$.

It is interesting to understand further the correspondence between these alternative ways of describing the dynamics. In particular, the equation of state was central to the description of oscillations in the previous chapter, and we described how the strong energy condition was successively violated and then recovered as the universe evolved.

Considering the equation of state Eq. (5.6), therefore, and evaluating this expression at equilibrium points, where the conditions given in Eqs. (6.10)-(6.12) are satisfied, we find that $w_{\text{eff}} = -1/3$ at these points. This is true for all values of $V$ which permit equilibrium points. For oscillations to occur, however, there is an additional requirement that $dw_{\text{eff}}/da$ is positive, in order that the strong energy can be broken below a particular scale and recovered above it. Differentiating Eq. (5.6) and employing Eqs. (6.10)-(6.12), we find that

$$\frac{dw_{\text{eff}}}{d\ln a} = -\frac{2a^2}{3}\lambda^2 \ , \tag{6.16}$$

which is positive for $a < a_*$ and negative otherwise ($\lambda^2$ is given by Eq. (6.14)). This is in agreement with our previous analysis of equilibrium points, that centre points occur below $a_*$. These results confirm that oscillations occur about the point where the strong energy condition becomes satisfied.

## 6.3 Emergent inflationary universe in LQC

We now wish to understand how the two equilibrium points we have uncovered in the previous section can be used to develop early universe scenarios of the emergent universe type. Clearly the ES point could be used to formulate the emergent scenario described in section 6.1.1. The LS point, however, allows us to develop a qualitatively different 'new emergent universe scenario'.

The scenario postulates that the universe begins in the neighbourhood of this point. This requires an asymptotically flat potential with magnitude below $V_*$, and that the field is initially situated on this region of the potential. The potential is postulated to evolve away from flatness but, in contrast to the classical emergent scenario, it is assumed to evolve such that its magnitude eventually increases to a value greater than $V_*$. The field's velocity is non-zero, and as the field evolves away from the flat region the oscillatory dynamics of chapter 5 allows the field to move up the potential. This behaviour continues until the oscillations are broken and inflation occurs. Then, assuming that the potential satisfies the slow-roll conditions where this occurs, an extended period of slow-roll inflation will ensue.

It is interesting to describe this behaviour in more detail from the dynamical systems point of view. As well as providing a unified description of this new emergent universe scenario – from static initial state to slow-roll inflation – this also provides a complementary description to section 5.3 for how the initial conditions for inflation are set by oscillations.

### 6.3.1 The dynamics of emergence

The phase plane analysis of section 6.2 determined the qualitative LQC dynamics for the case of a constant potential. However, for our emergent inflationary model we require the potential to vary as the scalar field evolves. Nevertheless, the constant potential dynamics (see Figs. 6.2–6.4) provides a good approximation to more general dynamics, if variations in the potential are negligible over a few oscillations. This implies that cosmic dynamics with a variable potential may be studied by treating the potential as a sequence of separate, constant potentials. Here, with the emergent model in mind, we shall consider a general class of potentials that asymptote to a constant $V_{-\infty} < V_*$ as $\phi \to -\infty$ and rise monotonically once the value of the scalar field exceeds a certain value.

As we saw in section 6.2, for any constant potential $V < V_*$, there exists a region of parameter space where the universe undergoes non-singular oscillations about the point LS. For $V > V_*$, the equilibrium points LS and ES merge and the phase plane then contains no equilibrium points. Instead, all trajectories represent a collapsing universe which bounces and asymptotically evolves into a de Sitter (exponential) expanding phase in the infinite future.

Let us consider the universe initially at, or in the neighbourhood of, the static point LS, with the field located on the plateau region of the potential with a positive kinetic energy, $\dot{\phi}_{\rm init} > 0$. The universe will exhibit cyclic behaviour around the LS point for a very wide range of initial values $\dot{\phi}_{\rm init}$ when $V_{-\infty} < 0$. If $0 < V_{-\infty} < V_*$, the range becomes more limited as $V_{-\infty}$ is increased. An important feature to note is that in all cases the field's kinetic energy never vanishes during a given cycle. In the case of a positive potential, the unphysical region of phase space, where the field's kinetic energy would be negative, lies outside the cyclic region that is bounded by the separatrix. Thus, the field will vary monotonically along the potential and eventually reaches the region where the potential begins to rise.

Increasing the magnitude of the potential over a series of cycles has the effect of moving the location of the LS point to progressively higher values of the scale factor, although the shift is moderate. In the case of a positive potential, for example, a necessary condition for the existence of LS is that $4 < A(a_{\rm eq}) < -2.5$, and this corresponds to the range $0.943a_* < a < a_*$. Eq. (6.12) then implies that the field's kinetic energy does not alter significantly, since the universe remains in the vicinity of LS. On the other hand, the saddle point ES occurs at progressively smaller values of the scale factor as the magnitude of the potential increases. As discussed in Section 2.2, this equilibrium point occurs in the range $a_* \leq a \leq \infty$, where the limits are approached as $V \to V_*$ and $V \to 0$, respectively.

The overall effect of increasing the potential, therefore, is to distort the separatrix in

the phase plane, making it narrower in the vertical direction but introducing little change to the position of the LS point. This implies that the dynamics varies only slightly from cycle to cycle for orbits that are close to the LS point. If the magnitude of the potential continues to increase as the field evolves, however, a cycle is eventually reached where the trajectory that represents the universe's evolution now lies *outside* the finite region bounded by the separatrix and this effectively breaks the oscillatory cycles. From a physical point of view, the magnitude of the field's potential energy, relative to its kinetic energy, is now sufficiently large that a recollapse of the universe is prevented, i.e., the strong energy condition of GR remains violated as the universe expands, thereby leading to accelerated expansion. The field decelerates as it moves further up the potential, subsequently reaching a point of maximal displacement and then rolling back down. If the potential has a suitable form in this region, slow-roll inflation will occur.

This description of how the field climbs its potential is in perfect agreement with that given in chapter 5. Here, however, in the spirit of the emergent universe scenario, we have focused on the role of both equilibrium points, and assumed that the universe originates close to the LS point.

### 6.3.2 The energy scale of inflation

An important question to address is the energy scale at the onset of inflation, $V_{\rm inf}$, in our new emergent universe scenario. In the classical scenario inflation begins as soon as the potential evolves away from flatness and hence is set by $V_{-\infty}$. In the new setting, however, the field climbs away from $V_{-\infty}$ before inflation occurs.

In chapter 5, we developed an analytic approximation for the value of the potential at the onset of inflation, Eq. (5.11). This approximation relied on an estimate of the energy of the universe during the first cycle. We can use the same analytic approximation here to estimate the energy scale of inflation in the new emergent universe scenario if we assume that the initial potential energy is negligible compared with the initial kinetic energy. In the spirit of the emergent scenario let us employ this result to approximate the energy scale of inflation when the initial conditions are set close to the equilibrium point LS. The initial scale factor is therefore given by $a_{\rm init} = f a_*$, where $f \approx 1$ and hence $D_{\rm init} = \mathcal{O}(1)$. The field's initial kinetic energy is determined by Eq. (6.12) as $\dot{\phi}^2_{\rm init} \approx 3/(4\pi\ell^2_{\rm Pl} a^2_{\rm eq})$. It follows from Eq. (5.11), therefore, that a universe 'emerging' from the semi-classical LQC phase near to the LS point will begin to inflate when

$$V_{\rm inf} \approx \frac{1}{2jf^2} m^4_{\rm Pl} \ . \tag{6.17}$$

As expected, this is in good agreement with the necessary condition (6.15) for the coalescence of the equilibrium points LS and ES, since if the universe is located near the LS

point initially, we expect that the scale factor will not be able to evolve significantly until $V > V_*$.

Conditions (6.15) and (6.17) both imply that the inflationary energy scale is *higher* for *lower* values of the parameter $j$, which is the behaviour we discussed in chapter 5. Indeed, it is comparable to the Planck scale for $j \leq \mathcal{O}(10)$ and this has implications for the asymptotic form of the potential as the field reaches progressively higher values. Unless the parameter $j$ is sufficiently large, it is unlikely that the oscillatory dynamics will end if the potential asymptotes to a constant value, or reaches a local maximum that is significantly below the Planck scale. In this sense, therefore, the scenario outlined above favours potentials that increase monotonically once the value of the scalar field has exceeded some critical value. As discussed in section 5.5, the possibility of very large values of the potential energy at the onset of inflation mean that eternal inflation is a likely outcome.

While initial conditions very close to the static solution are clearly in the spirit of the emergent scenario, it is also important to ask what range of initial conditions can give rise to a working scenario. To answer this question we can once again employ the results of the previous chapter, if we assume that the initial potential energy is negligible compared with initial kinetic energy. In that case Fig. 5.5 presents typical ranges of valid initial conditions which satisfy the constraints of the semi-classical regime. Eq. (5.11) demonstrates that the further away from the static point the initial conditions are set, the lower the energy scale of inflation. From Fig. 5.5, we can assume a typical initial range of the scale factor, $0.5a_* < a < 1.5a_*$ when $j = 1000$, and a maximum value of the scalar field's velocity of $\mathcal{O}(1)\ell_{\rm Pl}^{-2}$. Employing Eq. (5.11), therefore, we expect the minimum possible value for the potential at the onset of inflation to be $V_{\rm infmin} \approx 10^{-5}\ell_{\rm Pl}^{-4}$ when $j = 1000$. This demonstrates that, while not necessarily in the spirit of the emergent universe, a range of inflationary energy scales can be generated.

## 6.4 A specific model of an emerging universe

We now turn our attention to potentials which have the qualitative form necessary to realise our new emergent universe scenario.

From a dynamical point of view, the scenario can be realised if the potential satisfies a number of rather weak constraints. Asymptotically, it should have a horizontal branch as $\phi \to -\infty$ such that $dV/d\phi \to 0$ and increase monotonically in the region $\phi > \phi_{\rm grow}$, where without loss of generality we may choose $\phi_{\rm grow} = 0$. The reheating of the universe imposes a further constraint that there should be a global minimum in the potential at $V_{\rm min} = 0$ if reheating is to proceed through coherent oscillations of the inflaton. Since

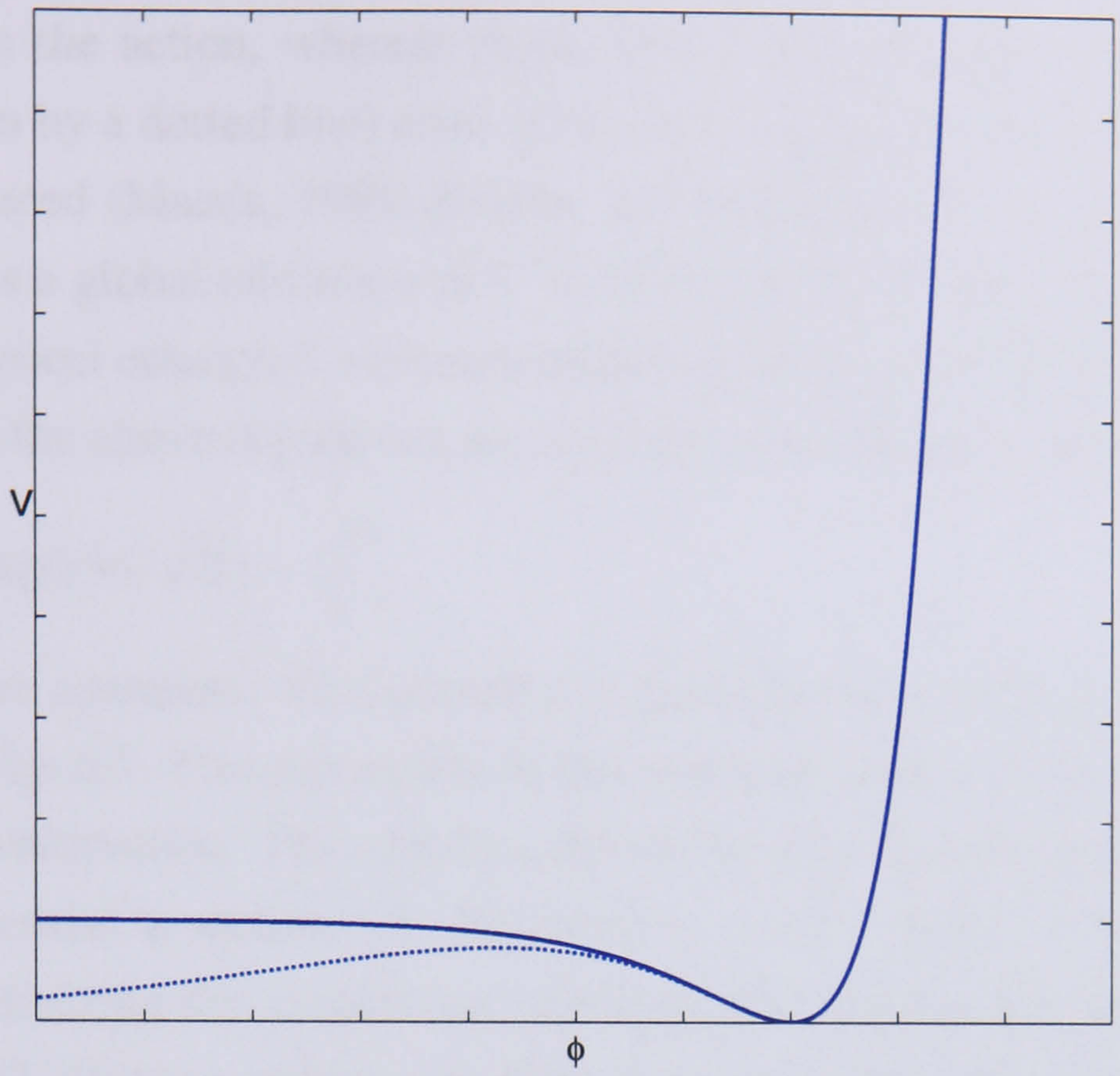


Figure 6.5: The figure depicts two possible forms of emergent potentials that allow for conventional re-heating. The solid line is the form of the potential motivated by the inclusion of a $R^2$ term in the Einstein–Hilbert action, and which is suitable for the classical emergent universe and the LQC emergent universe scenario. The dotted line is the form motivated by the inclusion of higher-order terms, and is suitable only for the LQC emergent universe scenario.

inflation will end after the field has rolled back down the potential, this should occur for $\phi \leq \phi_{\rm grow}$. Finally, the region of the potential that drove the last 60 e-foldings of inflationary expansion is constrained by cosmological observations, as described in section 1.5.

Examples of potentials that exhibit these generic properties are illustrated in Fig. 6.5. It is interesting that potentials of this form have been considered previously in a number of different settings, including cases where higher-order curvature invariants of the form

$$L_N = \frac{1}{16\pi\ell_{\rm Pl}^2}\sum_{i=1}^{N}\epsilon_i\, R^i \ , \tag{6.18}$$

are introduced into the Einstein-Hilbert action, where $R$ is the Ricci scalar, $\epsilon_i$ are coupling constants and $\epsilon_1 = 1$. Such corrections are required when attempting to renormalise theories of quantum gravity (Antoniadis and Tomboulis, 1986) and also arise in low-energy limits of superstring theories (Candelas *et al*, 1985). In general, such theories are conformally equivalent to Einstein gravity sourced by a minimally coupled, self–interacting scalar field. For example, potentials with a nonzero asymptote at $\phi \to -\infty$ (as shown by the solid line in Fig. 6.5) can be obtained from theories that include a

quadratic term in the action, whereas those with a zero asymptotic value and a local maximum (shown by a dotted line) arise when cubic and higher-order terms in the Ricci scalar are introduced (Maeda, 1989; Barrow and Cotsakis, 1991). In general, all these potentials possess a global minimum at $V = 0$. Potentials of this form can also be used to realise the classical emergent universe scenario as shown by Ellis *et al* (2004).

Motivated by the above discussion we consider, as an example, the potential

$$V = \alpha \left[ (\exp(\beta\phi/\sqrt{3}) - 1 \right]^2 \quad , \tag{6.19}$$

where $\alpha$ and $\beta$ are constants. This potential is qualitatively similar to that illustrated by the solid line in Fig. 6.5. The parameters of this potential need to be fixed in order to give agreement with observation. This can be achieved in a similar manner to that shown for the quadratic potential in section 1.5. We chose $\alpha = 10^{-12}$ and $\beta = 0.1$ as representing typical values satisfying the constraints imposed, and numerically integrated the field equations (3.8)–(3.10) for a universe starting from an initial state close to the LS static state. The results of the integration are illustrated in Figs. 6.6 and 6.7. The field starts in the asymptotically flat region of the potential and gradually increases in value, as the scale factor oscillates about the LS point. The field then moves past the minimum and climbs up the potential. The scale factor continues to oscillate until the field reaches the point where the field slows down significantly, thereby bringing the oscillations to an end and initiating the inflationary expansion. This numerical integration confirms that our analysis based on a series of constant potentials is correct.

## 6.5 Emerging quintessential inflation

One drawback of reheating through inflaton decay in the emergent scenario is that the coupling of the scalar field to the standard model degrees of freedom must be strongly suppressed if the field is to survive for a (possibly) infinite time as it emerges from the oscillatory semi-classical phase. It is more natural, therefore, to invoke a 'sterile' inflaton that is not coupled directly to standard model fields, and where reheating proceeds through an alternative mechanism such as gravitational particle production (Ford, 1987; Grishchuk and Sidorov, 1990; Spokoiny, 1993). In this case, the potential need not exhibit a minimum and the field could continue to roll back down the potential towards $\phi \to -\infty$ at late times.

It is notable that the general requirements for a sterile inflaton with a potential exhibiting a decaying tail as $\phi \to -\infty$ are *precisely* those features that are characteristic of the quintessential inflationary scenario, where the field that drove early universe inflation is also identified as the source of dark energy today (Peebles and Vilenkin, 1999). In the

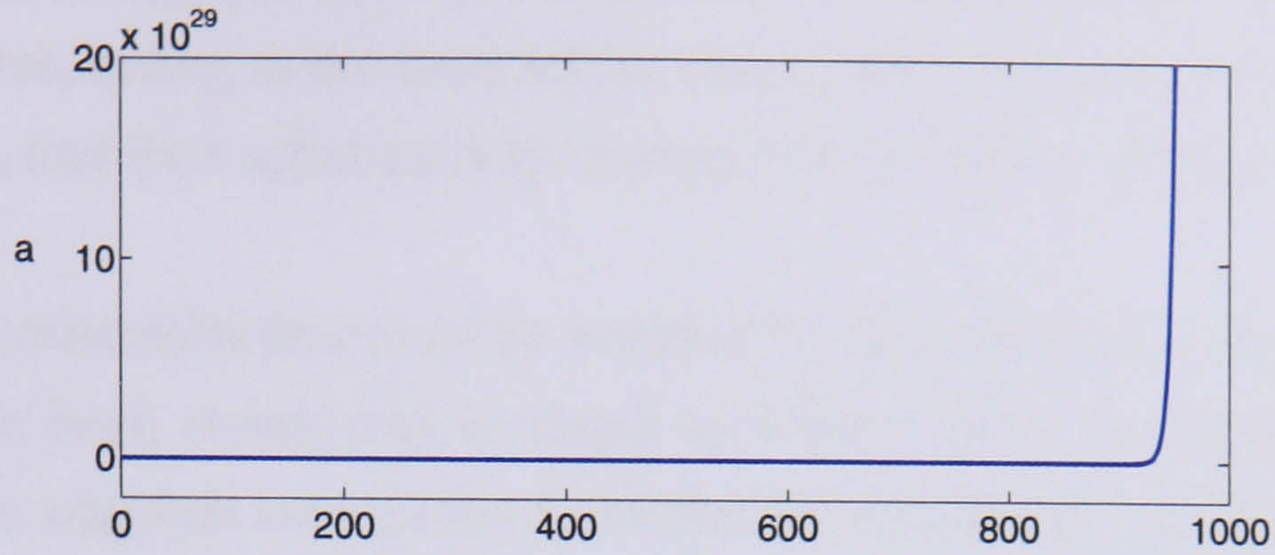


Figure 6.6: Time evolution of the scale factor (top panel) and scalar field (bottom panel) with the field initially on the asymptotically flat region of the potential (6.19) with $\alpha = 10^{-12}$ and $\beta = 0.1$. The field increases in value from initial conditions close to the LS (centre) solution defined by Eq. (6.10). Axes are in Planck units.

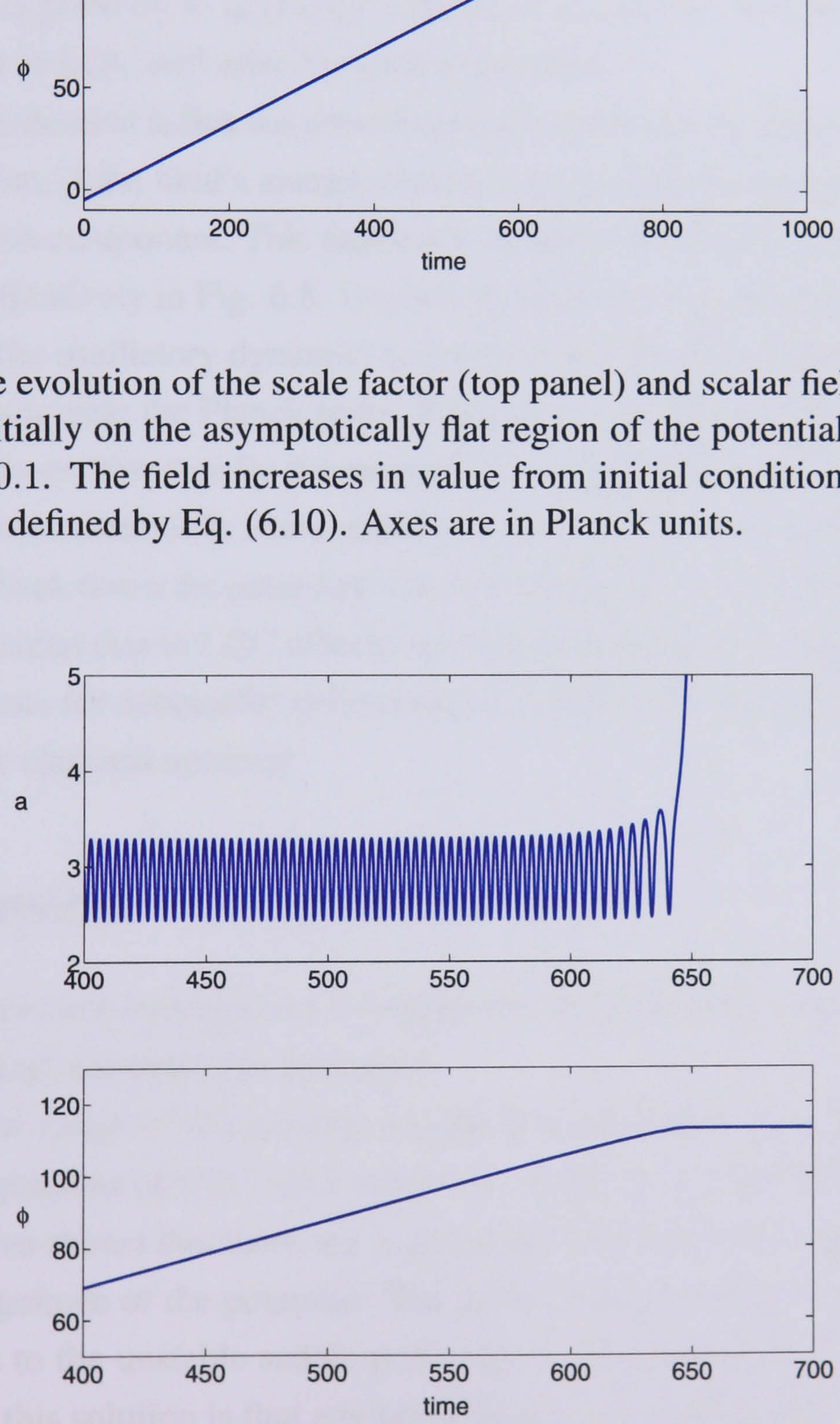


Figure 6.7: Plots illustrating the magnification of Fig. 6.6 around the region where emergence commences, the oscillations cease and inflation begins.

present context, this suggests that the scalar field could play a three-fold role in the history of the universe, acting as the mechanism that enables the universe to emerge into the classical domain, and then subsequently driving both the early- and late-time accelerated expansion.

The specific constraints that must be satisfied by the potential in standard quintessential inflation have been considered in detail by Dimopoulos and Valle (2002). In particular, one of the simplest asymptotic forms for the low-energy tail that simultaneously leads to tracking behaviour (which allows the energy density of the dark energy to be similar to that of the matter) and does not interfere with the predictions of primordial nucleosynthesis is given by $V \propto (m/\phi)^k \exp(\lambda\phi/m_{\rm Pl})$, where $m$, $k$ and $\lambda$ are constants. Cyclic behaviour in LQC will arise for such a potential.

A further requirement is that the potential must be sufficiently steep immediately after the end of inflation, if the field's energy density is to redshift more rapidly than the subdominant radiation component. This requires a second point of inflexion in the potential, as illustrated qualitatively in Fig. 6.8. Beyond this region, the potential must continue to rise in order for the oscillatory dynamics to come to an end and, as discussed above, this is expected to occur near the Planck scale. From a dynamical point of view, there are no further constraints on how rapidly the potential energy need increase in this region. The only remaining consideration is that a phase of successful slow-roll inflation should arise as the field rolls back down the potential. Given the ease with which the inflaton is able to move up the potential due to LQC effects, we anticipate that any potential satisfying the existing constraints for successful quintessential inflation will also lead to a successful emergence of the classical universe.

## 6.6 Discussion

In this chapter, we have extended our investigation of inflationary scenarios within LQC settings to emergent universe type scenarios.

The main new result of this chapter was the determination of static solutions to the semi-classical equations of LQC for a universe sourced by a scalar field with a constant potential. We have shown that there are in principle two such solutions, depending upon the sign and magnitude of the potential. The point ES is always in the classical domain and corresponds to the unstable saddle point that is also present in GR. The important characteristic of this solution is that any perturbations, no matter how small, necessarily force the universe to deviate exponentially from the static state. The second solution LS is always in the semi-classical domain and corresponds to a centre. This is a solution made possible by LQC effects and unlike the ES static point does not exist within the

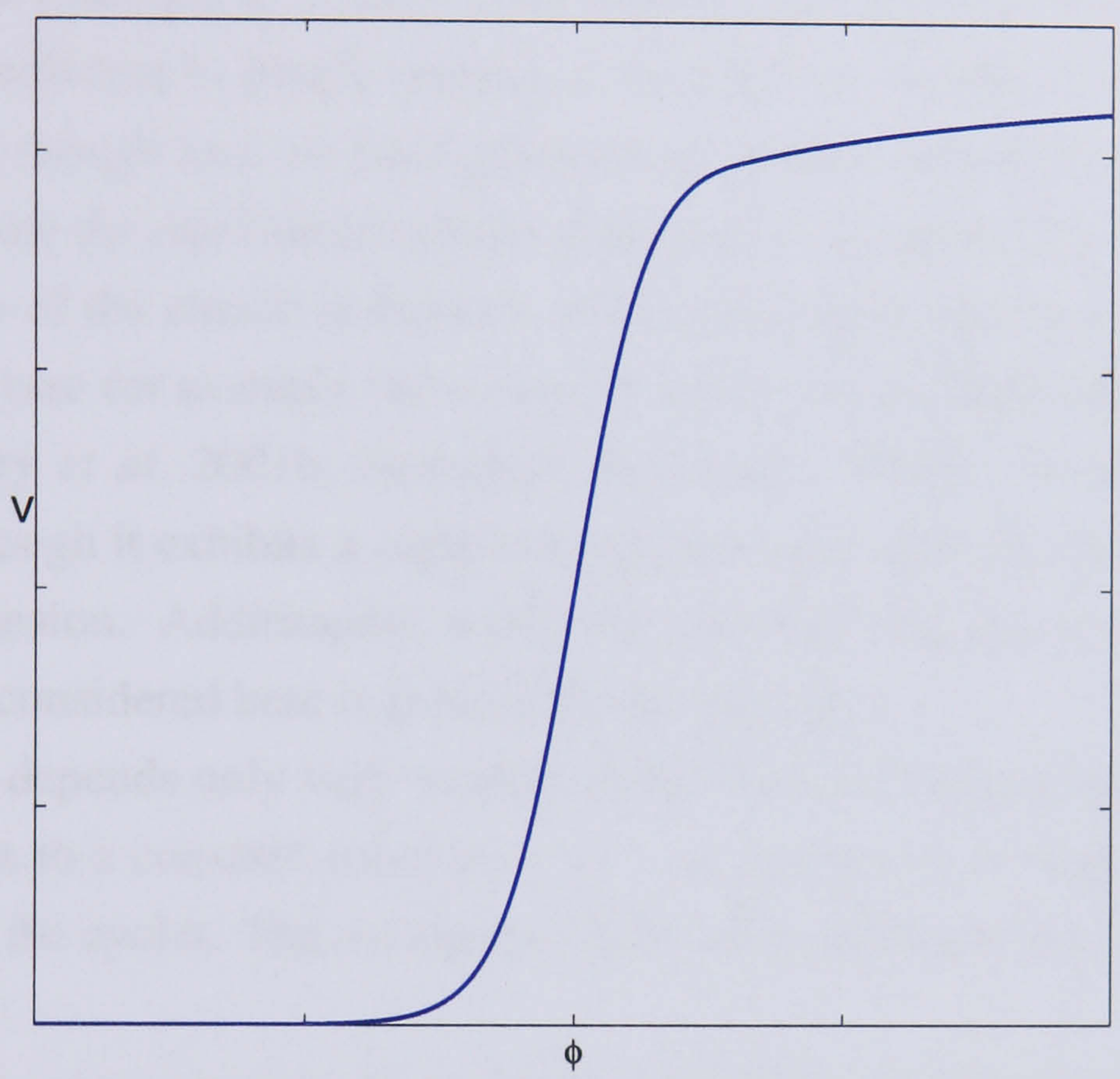


Figure 6.8: Illustrating the generic form of the potential that leads to early- and late-time accelerating phases. The potential exhibits a decaying tail as $\phi \to -\infty$. As the field moves up this tail and increases in value, the universe can oscillate about the LS point. The inflationary regime rises (possibly) towards the Planck scale for large values of $\phi$. As the field turns round, it can drive a phase of inflation and, if the potential exhibits a sufficiently steep middle section around $\phi \approx 0$, reheating may proceed through gravitational particle production. Consequently, the field may survive until the present epoch, where it can act as the source of dark energy by slowly rolling along the tail towards $\phi \to -\infty$.

context of GR. We have shown that it exists for a wide range of values of the potential, including positive, zero and negative values. Its importance lies in the fact that it allows a universe that is slightly displaced from the static state to oscillate in the neighbourhood of the static solution for an arbitrarily long time.

We have exploited these characteristics to develop a working scenario of the emerging inflationary universe in which a past-eternal, oscillating cosmology eventually enters a phase where the symmetry of the oscillations is broken by the scalar field potential, thereby leading in principle to a phase of successful slow-roll inflation. The mechanism that enables the universe to finally emerge is the same as we discussed at length in the previous chapter, though here we have given an alternative description of this behaviour by considering how the equilibrium points change as $V$ is varied. The model developed here shares some of the attractive features of the other early universe scenarios such as the pre-big bang (see for example the review of Lidsey *et al*, 2000) and ekpyrotic/cyclic scenarios (Khoury *et al*, 2001b; Steinhardt and Turok, 2002b), in the sense that it is past eternal, although it exhibits a significant difference in that the cycles are broken by inflationary expansion. Additionally, unlike the pre-big bang and cyclic scenarios, the emergent model considered here is genuinely non-singular.

The scenario depends only very weakly on the form of the potential, requiring only that it asymptotes to a constant value at $\phi \rightarrow -\infty$ and grows in magnitude at larger $\phi$ in order to break the cycles. The asymptotic value of the potential can be either positive, zero or negative.

The above emergent scenario has a further advantage in that the initial state of the universe is set in the more natural semi-classical regime, rather than the classical setting of GR. Nevertheless, an important question that arises is the likelihood of these initial conditions within a more general framework. In particular, there is the issue of why the scalar field should initially be located in the asymptotic low-energy region of the potential. This issue is related to our discussion in section 4.1 where we considered why the minimum of the potential is a natural initial position for the scalar field. In the present context there is a minimum of the potential at $\phi = -\infty$. For potentials which realise quintessential inflation, considered in section 6.5, this is the only minimum, while for the class of potentials considered in section 6.4, there is an additional minimum required for reheating, and we have to assume that this is not the preferred initial position for the field. There is also the related assumption that the field moves from left to right initially. As is discussed in section 4.1, a full understanding of initial conditions will require new developments at a more fundamental level than that of semi-classical equations.

Considering this scenario it does not seem possible to argue that any particular value of the quantisation parameter $j$ is preferable, since the LS point exists for all values of

$j$. However, assuming that the evolution begins close to the initial LS point the onset of slow-roll inflation will occur at higher energy scales for smaller values of $j$. In general, the onset will occur at very high energy scales unless the quantisation parameter $j$ is extremely large, which is considered to be less natural. This indicates that a large amount of slow-roll inflation would arise, at least for a wide class of smoothly varying potentials, and it is expected that the density of the present-day universe should be exponentially close to the critical density, $\Omega_0 = 1 + \epsilon$, where $\epsilon \ll 1$. In principle, therefore, the emergent scenario we have proposed could be ruled out if a significant detection of spatial curvature is ultimately reported by future cosmological observations.

This chapter has also shown an intriguing symmetry in the emerging quintessential scenario between the initial and final states of the universe. Although the size of the universe differs by many orders of magnitude, the field evolves along the tail of the potential at both early and late times, $\phi(t \to -\infty) = \phi(t \to +\infty)$, but with its kinetic energy having changed sign. This implies that a reconstruction of the dark energy equation of state at the present epoch could yield direct observational insight into the nature of the *pre-inflationary* potential in this scenario.

Finally, we should comment on the robustness of this scenario with respect to the ambiguity parameter $l$. The scenario requires the existence of the the LS static point which will always occur for a sufficiently small positive $V$ and when $V$ is negative or zero, provided the function $A$ passes through the value $A = 4$ as $a \to 0$. Eq. (3.12) tells us that this is always true for all allowed values of $l$ ($0 < l < 1$). On the other hand, Eq. (3.13) implies that another major effect of $l$ is to alter the minimum value of $A$. $A_{\rm min}$ varies hugely over the allowed range of $l$, taking values in the range $-\infty > A_{\rm min} > -1.5$. This has an effect on the position at which the equilibrium points merge, which in turn fixes the energy scale of inflation. Indeed, Eq. (6.15) can be generalised for an arbitrary $A|_* = A_{\rm min}$, to give

$$V_* = \frac{4 - A|_*}{\left(16\pi - \frac{8\pi}{3}A|_*\right)\ell_{\rm Pl}^2 a_*^2} \ , \tag{6.20}$$

which takes values in the range $3/(8\pi a_*^2\ell_{\rm Pl}^2) < V* < 11/(40\pi a_*^2\ell_{\rm Pl}^2)$. Despite $A_{\rm min}$ spanning a large range of values, therefore, $V_*$ changes only moderately over the range of allowed values of $l$. This indicates that the scenario is not significantly altered by changing the value of $l$.

# Chapter 7

# The super-inflationary spectrum of perturbations

It has been a long-standing hope that the inflationary paradigm might be connected to theories of quantum gravity, and LQC suggests that this possibility may be realised. Indeed, much of this thesis has focused on connecting LQC to standard slow-roll inflation. In particular, the issue of how the initial conditions for slow-roll inflation can be established by LQC dynamics has been studied in detail. In chapter 4, however, we also noted that in the semi-classical regime the universe naturally evolves through a period of accelerated expansion, quite separately from whether or not a phase of slow-roll inflation subsequently occurs. This is perhaps the most striking feature of semi-classical LQC. In contrast to standard slow-roll inflation, where inflation is driven by the self-interaction potential of the scalar field, this inflationary phase is driven by quantum geometrical effects. It is natural, therefore, to ask whether or not this period of LQC inflation is able either to replace or to supplement standard inflation, and what its observational consequences would be. In order to answer this question one must consider both the number of e-folds of inflation which the LQC phase can give rise to, and the spectrum of perturbations which this phase will produce.

The first of these issues has been addressed previously by Bojowald and Vandersloot (2003) and the conclusion was found to depend both on initial conditions and the value of the ambiguity parameter $j$. In order to generate the 60 e-folds of inflation necessary to solve the problems of the hot big bang model, however, $j$ must be extremely large. In view of this, the possibility that LQC inflation can completely replace standard inflation appears to be strongly disfavoured, given the arguments that smaller values of $j$ are more natural than larger ones.

The issue concerning the spectrum of perturbations produced by the LQC inflationary phase, however, is a more subtle one. If standard inflation were to be replaced by LQC in-

flation, these perturbations would have to account for the origin of cosmic structure, and could therefore leave a signature of the LQC inflationary phase. It is important to recall that during the LQC inflationary phase not only does the expansion of the universe accelerate, but the Hubble parameter also grows, $\dot{H} > 0$ (unlike the case of slow-roll inflation where $H \approx$ constant). Experience from standard inflation, therefore, suggests that we should expect the spectrum of perturbations produced during this super-inflationary phase to be strongly blue tilted ($n > 1$, where $n$ is the spectral index). A recent study, however, has found that the LQC inflationary scenario can produce a nearly scale-invariant spectrum of perturbations (Hossain, 2005). The study also found that a generic prediction is that the spectrum is only slightly blue tilted, in contrast to most slow-roll models which have a small red tilt. Moreover, the study suggests that this result is robust, being independent of ambiguities in the quantisation scheme.

This might lead one to believe that near scale-invariance with a small blue tilt is a generic and observationally falsifiable result of LQC inflation, in contrast to standard inflation where there is a large amount of freedom in the value of the spectral index associated with the form of the potential. The calculation of the power spectrum by Hossain (2005), however, uses the so called direct method of Padmanabhan *et al* (1989). This method is not the standard one which is normally invoked for calculating the power spectrum of slow-roll inflation (reviewed in chapter 1). It is argued by Hossain (2005), however, that the use of the direct method is more natural within LQC because of the minimum natural length scale introduced by LQC, and the lack of a general expression for the stress energy tensor (see Hossain, 2005, for details).

Two further significant aspects of the calculation of Hossain (2005) are important to note. First, it assumes that the effective equation of state, $w = p/\rho$, for the universe as a whole is given by $w \approx -1$ and hence that $H \propto$ constant. This can only be true either at the end of the super-inflationary phase, or under severe fine tuning of the model's parameters. Secondly, it assumes that the background spacetime is unperturbed, and considers only perturbations in the scalar field. At the present time this is a necessary assumption, as the modified semi-classical equations of LQC are only known for an unperturbed background. This assumption is technically invalid as it clearly violates Einstein's field equations. Whether or not it proves to be a useful approximation, however, remains to be seen. Experience from other applications of perturbation theory in the early universe suggests that in some cases this approximation is very useful. For example, for standard slow-roll inflation a calculation of the spectrum of the scalar field perturbations, using this approximation, can be applied to produce an accurate estimate for the spectrum of the comoving curvature perturbations, which is ultimately the important quantity for observations (Liddle and Lyth, 2000; Dodelson, 2003). In other situations it is less useful.

For example in the ekpyrotic scenario the application of a similar procedure to that used for slow-roll inflation yields erroneous predictions (Khoury *et al*, 2001b; Lyth, 2002b). We shall discuss this question further in the discussion section.

The purpose of this chapter is to reconsider the question of the spectrum of primordial perturbations produced during LQC inflation. In chapter 1, we gave a detailed account of the standard method by which the spectrum of scalar perturbations, produced during slow-roll inflation, can be calculated. In contrast to the previous LQC study, our study follows as closely as possible this framework. Moreover, we do not make any assumptions about the universe's expansion rate, rather allowing it to be determined by the LQC dynamics. The focus is on whether or not a scale-invariant spectrum is produced, and under what conditions this can occur. We continue to use the approximation in which the background spacetime is unperturbed and therefore focus on the spectrum of scalar field perturbations produced in this approximation.

We proceed as follows. In section 7.1, we discuss power-law solutions to the LQC equations; these will allow us to calculate the perturbation spectrum in an analytic manner. Sections 7.2 and 7.3 then contain the main body of our calculations. We conclude in section 7.4 with a summary of what we have learned, and a discussion of how the results may be useful in the future.

## 7.1 Power law evolution in LQC

Before moving on to consider perturbations of the scalar field, we require an understanding of the background dynamics. In particular we confine ourselves to the regime $a \ll a_*$, where analytic progress can be made.

In this regime, we use the asymptotic form of the function $D$, given in Eq. (3.1), and write $D = D_* a^n$ where $n = 3(2-l)/(1-l)$ with $0 < l < 1$, and hence $6 < n < \infty$, and where $D_* = (3/(1+l))^{3/(2-2l)} a_*^{3(l-2)/(1-l)}$. From Eq. (3.10) it can be seen that the universe undergoes super-inflationary expansion, $\dot{H} > 0$, for $n > 6$, independently of the form of the self-interaction potential. We will be interested in the cases where the ratio $\sqrt{2D}\, H/\dot{\phi}$ is a constant. There are two such cases for a flat ($k = 0$) universe. First, this is clearly true for a massless scalar field. Secondly, there is a scaling solution derived by Lidsey (2004) in which the ratio of kinetic to potential energy is a constant.

In both these cases, the evolution equations can be solved exactly, and the scale factor undergoes power law growth. When we come to deal with the perturbed equations, we will find it more convenient to work with conformal time $\tau$, where $dt = a\, d\tau$, and so we give the background evolution using this time variable. In this chapter, for convenience we use a prime to denote differentiation with respect to conformal time.

### 7.1.1 Massless scalar field

Considering a massless scalar field, Eqs. (3.8), (3.9) and (3.10) can be solved to yield

$$a^{2-n/2} = a_{\rm init}^{2-n/2} + C^{2-n/2}(\tau_{\rm init} - \tau) \ , \tag{7.1}$$

where

$$C = \left[\left(\frac{n}{2} - 2\right)\left(\frac{4\pi\ell_{\rm Pl}^2}{3} D_* \phi_{\rm init}'^2 \frac{a_{\rm init}^4}{D_{\rm init}^2}\right)^{1/2}\right]^{2/(4-n)} \ , \tag{7.2}$$

which is positive-definite for $n > 4$. It is convenient to rescale time to absorb the constant term into our definition of conformal time such that

$$a = C\,(-\tau)^p \ , \tag{7.3}$$

where

$$p = \frac{2}{4-n} \ , \tag{7.4}$$

and hence $p < 0$. It is important to note that $\tau$ is negative and increasing for an expanding universe and decreasing for a contracting universe.

### 7.1.2 Scaling solution

A second way to achieve power law growth in the regime $a \ll a_*$ is for the field to roll on a self-interaction potential of the form (Lidsey (2004))

$$V(\phi) = V_0\,|\phi|^\beta \ , \tag{7.5}$$

with $\beta > 0$ and $V_0$ a constant.

The analogous potential which gives rise to a scaling solution in the classical regime was given in Eq. (1.41) and, as we saw in section 1.4, it is very useful in understanding the production and evolution of perturbations in the standard single field slow-roll inflationary scenario. We expect, therefore, that the analogous potential and the associated scaling solution have the same degree of importance in the LQC scenario.

Using a rescaled conformal time, the growth of the scale factor and the field are then determined by the expressions

$$a = C\,(-\tau)^p \ , \qquad \phi = F\,(-\tau)^v \ , \tag{7.6}$$

where $v = np/2$, $p = -4/(n\beta + 4) < 0$. We note that $V_0$ is related to the constants $C$ and $F$ and the powers $v$, $n$ and $p$; however, this relation is not important in what follows. Obviously, the constant $C$ does not need to take the same value as in Eq. (7.2). We also note that $p$ is defined differently from our definition of $p$ in section 1.4.

## 7.2 Perturbation theory

As was mentioned above, if we are to fully understand the evolution of cosmological perturbations in LQC, we must perturb both the gravitational and the matter sectors of the theory about the homogeneous background. So far, however, the quantisation procedure in LQC has only been performed for homogeneous spacetimes, and not for the perturbed cases. This means that the full perturbed semi-classical equations have so far not been derived. In their absence, we may adopt a more modest approach. This is to assume that the background spacetime is unperturbed, but to allow perturbations in the scalar field. The assumption is valid for cases in which perturbations of spacetime are much smaller than those of the matter source, or equivalently where the matter perturbations have a negligible effect on the background spacetime. In this case we can calculate the power spectrum of the scalar field's perturbations on super-horizon scales produced from quantum mechanical fluctuations.

Ultimately the quantity which is relevant to observations after the inflationary era is the power spectrum of comoving curvature perturbations. We comment how this might be calculated from the spectrum of the scalar field perturbations in the discussion section.

To follow even this modest approach and allow inhomogeneities in the scalar field, we must include a gradient term in the matter Hamiltonian, $\mathcal{H}_\phi$, given by Eq. (2.6). This term, strictly speaking, violates homogeneity but we will assume that the effect on the background spacetime is sufficiently small such that it can be neglected. Including this extra term, the matter part of the effective semi-classical Hamiltonian (Eq. (3.4)) becomes

$$\begin{aligned}\mathcal{H}_{\phi+\delta\phi} &= \frac{1}{2}D(a)a^{-3}p^2_{\phi+\delta\phi} + \frac{1}{2}\,a\,G(a)\,\delta^{ij}\partial_i(\phi+\delta\phi)\partial_j(\phi+\delta\phi) \\ &\quad + a^3V(\phi+\delta\phi)\ . \end{aligned} \tag{7.7}$$

In this expression we have introduced a correction function $G(a)$, which we expect to arise due to the term $E^a_i E^b_i \partial_a\phi\partial_b\phi/|\det E^c_j|^{-1/2}$ in Eq. (2.6) which involves inverse quantities, and must be regularised in a similar manner to the inverse volume term. This term has so far not been calculated within LQC, and we do not attempt this calculation here. Indeed, in the previous study of perturbations in LQC this term was assumed to be unity. The relevant regularisation procedure for this term is closely connected to that for the inverse volume, and we anticipate it to have a similar form. In particular, we assume that $G = 1$ in the classical regime, but has a region for small values of the scale factor where $G \propto a^r$, where $r$ will depend on a new quantisation parameter. In our study we will again assume, as in previous studies, that $r = 0$. Our method, however, can easily be generalised to take account of a non zero $r$ and in section 7.4 we discuss how this would

affect our results.

Using Eq. (7.7) to derive the equations of motion in the same manner as we detailed in section 3.1, the unperturbed Eqs. (3.8)-(3.10) are unaltered, but we have the additional perturbation equation

$$\delta\phi'' = \left[-2\frac{a'}{a} + \frac{D'}{D}\right]\delta\phi' + D\left[\nabla^2 - a^2\frac{d^2V}{d\phi^2}\right]\delta\phi \ . \tag{7.8}$$

Our use of conformal time proves particularly helpful here, because it allows us to write Eq. (7.8) in the simple form

$$u'' + \left(-D\nabla^2 + m_{\rm eff}^2\right)u = 0 \ , \tag{7.9}$$

where $u$ is defined as $u = aD^{-1/2}\delta\phi$, and

$$m_{\rm eff}^2 = -\frac{(aD^{-1/2})''}{aD^{-1/2}} + a^2 D\frac{\partial^2 V}{\partial\phi^2} \tag{7.10}$$

is the effective mass of the field $u$.

In an equivalent approach, the scalar field equation in the semi-classical LQC regime (in the absence of metric perturbations) can be derived from an effective action. In terms of conformal time, the action can be written as

$$S = \int d\tau d^3\mathbf{x}\mathcal{L} = \int d\tau d^3\mathbf{x} a^4\left(\frac{1}{2}\frac{\phi'^2}{D\,a^2} - V\right) \ . \tag{7.11}$$

Including a gradient term in the above expression, and considering a linear perturbation in the field around its background solution, we find that the perturbed part of $S$ can be written as

$$\delta S = \frac{1}{2}\int d\tau d^3\mathbf{x}\left(u'^2 - D\,\delta^{ij}\partial_i u\,\partial_j u - m_{\rm eff}^2 u^2\right) \ , \tag{7.12}$$

which when varied also leads to Eq. (7.9). We have introduced this action in order to follow the steps of section 1.4 as closely as possible. We could, however, have worked directly with the Hamiltonian, given in Eq. (7.7), and our results would have remained unchanged.

## 7.3 Power spectrum

The action for $u$, given in Eq. (7.12), is now formally equivalent to that of a scalar field with a variable mass term and a $D$ term multiplying the gradient part. In order to calculate the spectrum of perturbations produced during the super-inflation due to quantum fluctuations, we must consider the field theory associated with $u$.

The momentum canonically conjugate to $u$ is given by

$$\pi(\tau, \mathbf{x}) = \frac{\partial \mathcal{L}}{\partial u'} = u'(\tau, \mathbf{x}) \ . \tag{7.13}$$

The theory is then quantised by promoting $u$ and $\pi$ to operators which satisfy the usual commutation relations. We Fourier decompose operator $\hat{u}$ to give

$$\hat{u}(\tau, \mathbf{x}) = \int \frac{d^3\mathbf{k}}{(2\pi)^{3/2}} \left[ w_k(\tau) \hat{a}_\mathbf{k} e^{i\mathbf{k}.\mathbf{x}} + w_k^*(\tau) \hat{a}_\mathbf{k}^\dagger e^{-i\mathbf{k}.\mathbf{x}} \right] \ , \tag{7.14}$$

where $w_k$ are mode functions. Using Eqs. (7.9) and (7.14), we find that $w_k$ satisfy the equation

$$\frac{d^2 w_k}{d\tau^2} + \left( Dk^2 + m_{\text{eff}}^2 \right) w_k = 0 \ . \tag{7.15}$$

In order to have a well defined field theory, we must also ensure that $w_k$ are defined such that the creation and annihilation operators, $\hat{a}_\mathbf{k}^\dagger$ and $\hat{a}_\mathbf{k}$, satisfy the usual commutation relations for bosons given in Eq. (1.35). This means that $w_k$ must satisfy the Wronskian condition given in Eq. (1.36). In general, however, this condition does not give rise to a unique choice for $w_k$. Instead, it allows a set of possible choices corresponding to a set of different Fock representations. In the cosmological context a unique choice is normally determined by considering a limit in which the time-dependence of the scale factor can be neglected, and hence where the physics ought to reduce to that of Minkowski space. In this limit $w_k$ is normalised to select only the advanced solution. Once the initial condition is selected and the Wronskian condition met, a vacuum state is defined which is annihilated by all $\hat{a}_\mathbf{k}$, such that $\hat{a}_\mathbf{k}|0\rangle = 0$.

The power spectrum of fluctuations about this vacuum state is defined by the vacuum expectation value such that

$$\langle u_\mathbf{k} u_\mathbf{l}^* \rangle = \frac{2\pi^2}{k^3} P_u \delta^{(3)}(\mathbf{k} - \mathbf{l}) \ , \tag{7.16}$$

where we have implicitly Fourier decomposed the field perturbation $\delta\phi$, and defined $u_\mathbf{k} = a\delta\phi_\mathbf{k}$. Using Eq. (7.14) we find

$$\langle u_\mathbf{k} u_\mathbf{l}^* \rangle = |w_k|^2 \delta^{(3)}(\mathbf{k} - \mathbf{l}) \ , \tag{7.17}$$

and hence that the power spectrum is given by

$$\mathcal{P}_u = \frac{k^3}{2\pi^2} |w_k|^2 \ . \tag{7.18}$$

We now proceed to derive the form of the power spectra for the two cases under study.

### 7.3.1 Massless field

As we have seen, during the semi-classical phase we have $D = D_* a^n$ and in the massless case we have power law growth with $a = C(-\tau)^p$ and $p = 2/(4-n)$. Using these expressions to substitute for $D$ in Eq. (7.15), therefore, we obtain

$$\frac{d^2 w_k}{d\tau^2} + \left( D_* \, C^n (-\tau)^{np} k^2 + \frac{m_{\rm eff}^2 \tau^2}{\tau^2} \right) w_k = 0 \ . \tag{7.19}$$

Moreover, using these expressions together with Eq. (7.10) we find

$$m_{\rm eff}^2 \, \tau^2 = -p(p-1) \tag{7.20}$$

in the massless case. The general solution admitted by Eq. (7.19) is

$$w_k(\tau) = c_1 \sqrt{-\tau} \, J_{|\nu|}(x) + c_2 \sqrt{-\tau} \, Y_{|\nu|}(x) \ , \tag{7.21}$$

where $J_{|\nu|}(x)$ and $Y_{|\nu|}(x)$ are Bessel functions of the first and second kind respectively and we have defined

$$\nu = -\frac{\sqrt{1 - 4\, m_{\rm eff}^2 \, \tau^2}}{2 + np} \tag{7.22}$$

and

$$x = \alpha \, k \, (-\tau)^{(2+np)/2} = \left| \frac{2p}{2+np} \right| \, \frac{\sqrt{D}\, k}{aH} \ , \tag{7.23}$$

with $\alpha = 2\sqrt{D_* C^n}/|2 + np|$ and $x > 0$. We normalise this solution such that the Wronskian condition (1.36) is satisfied which in general gives

$$w_k(\tau) = \sqrt{\frac{\pi}{2|2+np|}} \left( d_1 \sqrt{-\tau} \, H_{|\nu|}^{(1)}(x) + d_2 \sqrt{-\tau} \, H_{|\nu|}^{(2)}(x) \right) \ , \tag{7.24}$$

where $d_1$ and $d_2$ are constants subject to the condition $|d_1|^2 - |d_2|^2 = 1$ and $H_{|\nu|}^{(1)}(x)$ and $H_{|\nu|}^{(2)}(x)$ are Hankel functions of the first and second kind, respectively. Moreover, the Hankel and Bessel functions are related through the expressions: $H_{|\nu|}^{(1)}(x) = J_{|\nu|}(x) + i \, Y_{|\nu|}(x)$ and $H_{|\nu|}^{(2)}(x) = J_{|\nu|}(x) - i \, Y_{|\nu|}(x)$. We now consider the small wavelength limit in which the wavelength of the mode functions is far inside the cosmological horizon, and where we might expect a Minkowski form for the mode functions. This limit corresponds to $x \gg 1$, and the asymptotic form of Eq. (7.24) is

$$\begin{aligned} w_k(\tau) \ = \ & \frac{(-\tau)^{-np/4}}{\sqrt{|2+np|\,\alpha k}} \left( d_3 \, \exp(i\alpha k (-\tau)^{(2+np)/2}) \right. \\ & \left. + \, d_4 \, \exp(-i\alpha k (-\tau)^{(2+np)/2}) \right) \ , \end{aligned} \tag{7.25}$$

where $d_1$ and $d_3$ are related to each other by a phase factor, as are $d_2$ and $d_4$. In the standard inflationary scenario the analogous solution reduces to two plane waves propagating

in opposite directions in time and, as described in section 1.4, only the advanced solution is selected with $w_k(\tau) = e^{-ik\tau}/\sqrt{2k}$ in this limit. In our case, however, the solution only has the same form as flat spacetime when $n = 0$, i.e. when the universe is classical. The two components to our solution, however, still represent advanced and retarded solutions, and by analogy we select only the advanced solution. This implies that we fix $d_3 = 1$ and $d_4 = 0$. A further justification comes from considering a mode whose wavelength remains well inside the cosmological horizon throughout the super-inflationary evolution. Our normalisation is then consistent with the Minkowski limit once super-inflation has ended. Moreover, we note that ultimately our interest is in the $k$ dependence of the solution in the large wavelength limit, which is unaltered by the normalisation as long as the Wronskian condition is satisfied. That the solution does not reduce to the Minkowski limit, however, already suggests that there are going to be clear differences in the evolution of perturbations with respect to the standard case, whenever a geometric correction to the kinetic term of the field occurs.

We can now look at the long wavelength limit of our properly normalised mode functions. The long wavelength limit is given by $k \ll 1$, and for a specific finite time $\tau$ this corresponds to $x \ll 1$, and hence to wavelengths well outside the effective horizon. In this limit we have

$$J_{|\nu|}(x) \rightarrow \frac{1}{\Gamma(|\nu|+1)}\left(\frac{x}{2}\right)^{|\nu|}, \tag{7.26}$$

$$Y_{|\nu|}(x) \rightarrow -\frac{\Gamma(|\nu|)}{\pi}\left(\frac{x}{2}\right)^{-|\nu|}. \tag{7.27}$$

At this point let us pause and consider the form of the solutions we have just derived. Eq. (7.4) implies that in the massless field case under consideration the growth power $p$ is negative, which means that the quantity $x \propto (-\tau)^{(2+np)/2} \propto (-\tau)^{2p}$ is an increasing function as $\tau \rightarrow 0$. Therefore, although the $Y_{|\nu|}(x)$ solution is the dominant one for a sufficiently large scale ($k \rightarrow 0$), it is decreasing as the evolution proceeds and rapidly becomes sub-dominant with respect to the increasing $J_{|\nu|}(x)$ solution. This is essentially telling us that the late-time limit is not the same as the large wavelength limit. An equivalent way of saying this is that as opposed to the standard inflationary scenario where the modes exit the comoving horizon, $1/aH$, during inflation, here during super-inflation driven by quantum effects, the modes *enter* the effective horizon given by $\sqrt{D}/aH$ [1].

[1] In this context the horizon simply compares the relative size of the the gradient term in equation (7.15) with the mass term which is proportional to $aH$. Consideration of the perturbation equation for other fluids gives rise to a similar equation to Eq. (7.9), but with $D$ replaced by the speed of sound in the fluid, although this speed is generally considered to be a constant unlike $D$. This means the effective horizon $\sqrt{D}/aH$ can be considered to be analogous to the sound horizon of a fluid. For a scalar fluid in classical gravity the sound velocity is unity, so the sound horizon reduces to the usual cosmological horizon we have discussed in section 1.4.

Conversely, in the situation in which the universe is undergoing a collapsing evolution, the modes eventually *exit* the horizon. We will see that this not necessarily the case for the scaling solution.

While this is interesting, it raises a serious interpretational issue. In standard inflation, the short wavelength limit is the same as the $\tau \to -\infty$ limit, so all wavelengths can be considered to be small compared with the cosmological horizon at the earliest times. In this limit it is natural to assume that the small scale perturbations are governed by quantum mechanics and the normalisation is performed in this limit. As the expansion proceeds, however, the physical wavelength of the modes is increased, or equivalently the cosmological horizon size is decreased. The modes are pushed outside the horizon as this behaviour proceeds. The modes effectively become classical, and the spectrum calculated in this limit can also be interpreted as a classical spectrum. In the case at hand, however, this is no longer true and it is not clear whether we can interpret the spectrum calculated on long wavelengths as a classical one.

Taking this caveat on board, let us nevertheless proceed with the calculation. Using only the dominant part of Eq. (7.24) on large scales and employing Eq. (7.27), the power spectrum (7.18) reduces to

$$\begin{aligned}\mathcal{P}_u &= \frac{1}{4\pi}\left|\frac{p}{2+np}\right|^{1-2|\nu|}\left(\frac{\Gamma(|\nu|)}{\pi}\right)^2 \times \\ &\quad \frac{a^2H^2}{D^{3/2}}\left(\frac{\sqrt{D}\,k}{aH}\right)^{3-2|\nu|} \propto k^{3-2|\nu|}\,(-\tau)^{1-|\nu|(np+2)}\,, \end{aligned} \tag{7.28}$$

which for our massless field example (where $\nu = -n/8$ from Eq. (7.22)), yields

$$\mathcal{P}_u \propto k^{3-2|\nu|}\,(-\tau)^{2(n-2)/(n-4)}\,. \tag{7.29}$$

Then using $\mathcal{P}_\phi = D\mathcal{P}_u/a^2$, we find

$$\mathcal{P}_\phi \propto \frac{H^2}{D^{1/2}}\left(\frac{\sqrt{D}\,k}{aH}\right)^{3-2|\nu|} \propto\ k^{3-2|\nu|}\,(-\tau)^{1+p(n-2)-|\nu|(np+2)}\,, \tag{7.30}$$

which for the massless case turns out to be time-independent, telling us that the evolution of the scalar field perturbation is frozen on super horizon scales. From Eq. (7.30), we can clearly see that for scale-invariance we require $|\nu| = 3/2$. In this case, therefore, we conclude that one obtains scale-invariance of the scalar field perturbation only when $n = 12$, and hence $l = 2/3$.

### 7.3.2 Scaling solution

We can follow the same procedure for the scaling solution which arises when the field is self-interacting through the potential given in Eq. (7.5). In this case, using Eq. (7.10) we

obtain

$$m_{\rm eff}^2\tau^2 = -2 + (3-2n)p + \frac{1}{2}(6+2n-n^2)p^2 \ , \tag{7.31}$$

and for the quantity $\nu$ we have from Eq. (7.22)

$$\nu = -\frac{\sqrt{9-12p+8np-12p^2-4p^2n+2n^2p^2}}{2+np} \ , \tag{7.32}$$

where we recall that in this case $p = -4/(n\beta+4)$. In this case we do not necessarily encounter the same behaviour found in the massless case where the modes enter the horizon during the super inflationary phase. In fact, for $\beta > 2-4/n$ we have that $x$ is now decreasing as $\tau \to 0$. Hence, for these values of $\beta$, the dominant solution is always the $Y_{|\nu|}(x)$ function and the modes exit the effective horizon during the evolution.

In the limit of large $\beta$ we have that $p$ approaches zero and hence we have $\nu \to -3/2$ which gives scale-invariance. It is interesting to note that in the limit of large $\beta$, the power spectrum is scale-invariant regardless of $n$ (and hence the quantisation parameter $l$). This is easy to understand because in this limit Eq. (7.15) approaches

$$w_k'' + \tilde{k}^2 w_k - \frac{2}{\tau^2}\, w_k = 0 \, , \tag{7.33}$$

with $k^2 = D_* C^n k^2$, which is of similar form to the analogous equation in the case of slow-roll inflation (Eq. (1.44)). Because the equation takes this form, the $x \ll 1$ limit is identical to that for standard slow-roll inflation and the Minkowski space limit is recovered, removing another conceptual problem. The multiplicative factor in $\tilde{k}^2$ affects the normalisation of the power spectrum but not the scale-dependence, which is independent of $n$. It is also interesting that no fine tuning of the $n$ (or $l$) parameter is required and that the solution is stable in the sense that $\beta \gg 1$ corresponds to background solutions which are stable to linear homogeneous perturbations (Lidsey, 2004). This stability is important as it implies that the solution is an attractor and that generic initial conditions will evolve towards it. From the results of Lidsey (2004), we can determine that this stability requires $\beta > 2(n-6)/n$ which implies $p > 2/(4-n)$. The $\beta \gg 1$ limit corresponds to the condition of a very steep potential and means that $a$, and hence $D$, are nearly constant despite $H$ varying. From Eq. (7.10) we can see that this means that in this case the potential term is the most significant part of $m_{\rm eff}^2$.

Using Eqs. (7.28) and (7.30) we see that in the limit of large $\beta$ the power spectrum is given by

$$P_\phi = \left(D_* C^{n+4}\right)^{-1/2} (2\pi\tau)^{-2} \ , \tag{7.34}$$

which is independent of $k$ regardless of the value of $n$.

We conclude that nearly scale-invariance is a natural prediction of the LQC universe sourced by a steep potential of the form given by Eq. (7.5). As will be discussed below, we must not over-emphasise this result as it may change if metric perturbations are significant.

There is also an additional solution for a particular fine-tuned value of $\beta$ which gives $\nu = 3/2$ and hence also scale-invariance. Indeed, as we decrease the value of $\beta$, we see that at $np = -2$ which implies $\beta = (2n-4)/n$, the value of $\nu$ blows up to $-\infty$ and switches sign. As $\beta$ approaches zero, $p$ approaches $-1$. Consequently $\nu \to \sqrt{9-12n+2n^2}/(n-2)$ which is always between $\sqrt{2} < \nu < 3/2$. Therefore, $\nu$ must cross the value $\nu = 3/2$ at small $\beta$. This implies that a scale-invariant power spectrum is possible for small $\beta$, but is subject to a severe fine-tuning.

## 7.4 Discussion

In this chapter we have computed the power spectrum of the scalar field perturbations for two distinct situations. First, we considered the dynamics of a massless scalar field. We found the interesting behaviour that the modes of the scalar field perturbations enter the effective horizon during the super-inflationary phase. This is in clear contrast with the evolution in standard slow-roll inflation, and leads to a serious conceptual difficulty concerning the interpretation of the calculated spectrum. Scale-invariance is possible in this case, but at the cost of fine-tuning the quantisation parameter $l$. We note, however, that the required value of $n = 12$ implies that $l = 2/3$ and that this is not one of the favoured values, which are motivated by consideration of the full theory.

An interesting question is whether allowing the function $G$ to vary from unity would modify the phenomenology. It is easy to see that the effect of the function $G$ on the $k$ dependence is to change Eq. (7.22) such that $\nu = -(1-4m_{\rm eff}^2\tau^2)^{1/2}/(2+np+rp)$, while $m_{\rm eff}$ remains unaltered. Hence, there is an extra degree of freedom in this case, and it would be interesting to investigate whether scale-invariance can be achieved without moving away from the preferred values of quantisation parameters by using this freedom. Changing $G(a)$ from unity, however, will clearly not affect the problem of modes evolving into the effective horizon.

Before leaving the massless case, it is also worth noting that even in the limit $l = 0$, which represents exponential expansion (de Sitter-like evolution with $\dot{H} = 0$), we do not find a scale-invariant spectrum and we still have the problem of modes entering the effective horizon. This is in stark contrast with earlier work of Hossain (2005) which, at least in part, motivated the investigation of this chapter. Indeed, within the calculation presented here, even if we had imposed by hand that the background evolution was expo-

nential (i.e. fixing $p = -1$ but leaving $n$ free), we would have obtained scale-invariance only provided that $n = 0$, which corresponds to a classical universe and is equivalent to the limiting slow-roll case, or in the case where $n = 12/5$. However, neither of these values of $n$ are permitted in the $a \ll a_*$ regime. Again this result is in contrast with the previous study.

The fine tuning displayed in the massless case is avoided in the second situation we investigated, that of the scaling solution. By including a self-interaction potential we gain a degree of freedom that can be used to recover the desired features of the inflationary scenario (i.e. modes exiting the horizon and near scale-invariant power spectrum of perturbations). Moreover, it is clear that allowing the $G$ function to vary will not affect this limiting behaviour since the $p \longrightarrow 0$ limit ensures $G$ will be close to a constant.

At this point in the discussion it is useful to say something about when we might expect our calculation to be accurate, and how it could be applied to derive the spectrum of comoving curvature perturbations. The comoving curvature perturbation is a useful quantity to consider since under very general circumstances it is conserved on super-horizon scales. Hence its spectrum, calculated as modes leave the horizon during inflation, is equal to the spectrum as these modes re-enter at a later time, when they account for the formation of cosmic structure. In our calculation we have simply calculated the scalar field spectrum during super-inflation; however, we would like to convert this result into the comoving curvature spectrum. To make this conversion we must pick a gauge in which we assume that the metric perturbations in the scalar field equation are sub-dominant to the scalar field perturbations, as in this gauge our calculation will be accurate. If this is the spatially flat gauge then the conversion to the curvature perturbation would simply be given by $P_{\mathcal{R}} = (\mathcal{H}/\phi')^2 P_\phi$. To convert the spectrum in this way is the procedure used, for example, in Liddle and Lyth (2000) for standard inflation, to where the reader can turn for details of the origin of this formula. Until the full equations of gravitational and matter perturbations are known, however, we will not know in what gauges, if any, the metric perturbations can be ignored, and hence how to convert our spectrum to the spectrum of curvature perturbations.

In addition to the inclusion of the background perturbations into our calculation, a further way to improve its accuracy consists of relaxing the assumption that $a \ll a_*$, and hence using the full form of the function $D(a)$, rather than its asymptotic approximation. This would require the mode functions to be solved numerically, and it would be interesting to compare this approach with the analytic results derived here.

Nonetheless, the aim of this chapter was not to establish a robust prediction for the spectral index from LQC inflation, since the potential hazard of not including background perturbations was known from the start. Rather the ultimate purpose was to highlight the

potential freedom in the spectrum of perturbations produced in LQC once the universe's evolution is allowed to be consistently determined by the semi-classical equations of LQC. Moreover, this calculation has highlighted three important points, likely to carry over to a full analysis. First, that subject to the approximations we have to make, a scale-invariant spectrum is possible for LQC inflation even when the equation of state differs from $w \approx -1$. This is a great surprise considering our experience from standard slow-roll inflation. Secondly, that even when the universe is super-inflating the Fourier space modes of the scalar field perturbation are not necessarily pushed outside a suitably defined horizon. We encountered this type of behaviour in the massless case. This again is unexpected considering standard inflation. And thirdly, that just like in slow-roll inflation, when calculated with the standard techniques there is considerable freedom in the value of the spectral index from LQC inflation. This freedom is related to the form of the potential and, uniquely to LQC, it is also dependent on the choice of quantisation ambiguities. In particular, we expect that if we considered steep potentials other than those that generate a scaling solution, close to scale-invariance could be achieved and that the spectral index could be greater or less than unity.

The dependence of the spectral index on the quantisation parameter $l$ is potentially very interesting. If perturbations observed on the CMB were identified with a LQC origin, it might be possible to put constraints on $l$ from these observations. This is particularly so for the massless case, where only $l$ determines the scale-dependence of the spectrum. Moreover, it is expected that if the scalar field's potential is shallow, the semi-classical dynamics will approximate those of a massless field for generic initial conditions. Indeed, we saw this in chapter 4, where the analytic approximation, which agreed well with the full numerical analysis, neglected the quadratic potential until the universe exited from the semi-classical regime. In this sense the massless case is rather generic and it is therefore disappointing that we encountered so many problems for realising a scale-invariant spectrum in that setting. In any case, it is probably too soon to say anything definite regarding constraining quantisation parameters in this way. The possibility, however, remains an intriguing one.

To summarise, our calculation, while not yet a complete answer, is a step towards understanding the phenomenology of inflation in LQC. In particular it highlights the three features we have discussed above, which deserve considerable attention and are likely to carry over to a full analysis including metric perturbations. The calculation is also important given the likely complexity of the full perturbed equations. Once the full equations are known we will be able to determine when our calculation ought to provide an accurate answer, and in these cases it will provide a useful check on any spectrum of perturbations calculated using the full equations. As we have seen there are

many subtleties in any calculation of a perturbation spectrum. In particular, the standard method relies on a single variable (like the $u$ variable in this chapter, or the Mukhanov variable of section 1.4) being identified, which can be quantised in a similar manner to a scalar field in Minkowski space. We may even find that this is not possible with the full equations for LQC. In that case, the approach of using the full equations to determine when background perturbations can be ignored, and performing the calculation given here, could be the only way in which the spectrum of perturbations from LQC inflation can be determined using the standard techniques.

# Part II

# Braneworlds

# Chapter 8

# Background

In this second part of the thesis we consider cosmological scenarios inspired by another theory of quantum gravity: string theory. In particular, we will be concerned with so called braneworld models and specifically braneworld models which allow a collapsing universe to undergo a bounce into an expanding phase.

String theory is perhaps the most promising candidate for a theory of quantum gravity and is certainly the most widely studied at the present time. In contrast to LQC, string theory is not only a theory of quantum gravity, but also a candidate for a unified theory of all fundamental interactions including gravity. String theory is a vastly complicated and rapidly growing area of research and we will not attempt to review it here, instead referring the reader to the excellent standard texts of Green *et al* (1987a,b) and Polchinski (1998a,b). Our interest here lies in braneworld scenarios of the early universe which, while finding their inspiration in string theory, can be studied as models in their own right within the context of purely classical gravity. That said, it is important to briefly describe the important elements of string theory and particularly those aspects of the theory which motivate braneworld cosmology.

## 8.1 Motivation for considering braneworlds

There are five distinct superstring theories and each of these provides a theory of perturbative quantum gravity. These theories, however, are consistent only in $1+9$ dimensions, and even at this level it is clear that extra dimensions may play an important role in any cosmology derived from, or inspired by, string theory. A discovery of great importance was the realisation in the mid 1990s that these theories were in fact related to one another, and this in turn raised the possibility that they were actually just different aspects of the same underlying theory. More specifically, duality transformations were found which relate all the superstring theories to one another and there is reason to believe that

they in turn are particular limits of a single theory, which exists in $1 + 10$ dimensions and has become known as M-theory. Moreover, the low energy limit of M-theory is eleven-dimensional supergravity.

Within the context of string/M-theory another extremely important realisation has been that extended objects of more than one dimension also play a crucial role. In particular, there exist D-branes on which open strings end. Open strings mediate the non-gravitational forces of nature and, since they end on branes, the gauge groups associated with these forces are confined to the brane. On the other hand closed strings, which propagate freely, mediate the gravitational interaction. This behaviour can be interpreted classically as matter fields being confined to a brane, while gravity can propagate in an unconfined manner. Moreover, a particular low energy solution of M-theory, the Horava-Witten solution (Horava and Witten, 1996b), represents eleven-dimensional supergravity with the eleventh dimension compactified on an orbifold with $Z_2$ symmetry. This is then effectively a one-dimensional interval with two boundaries each of $1 + 9$ dimensions. It was also later shown by Horava and Witten (1996a) that six of the eleven dimensions can be consistently compactified on a scale smaller than the dimension representing the interval between the two boundaries, essentially at the Planck scale. This leads to a picture of two boundaries of $1 + 3$ dimensions separated by a large extra dimension, where by 'large' we mean orders of magnitude larger than the fundamental Planck scale, but much smaller than the three spatial dimensions which make up the boundary.

These considerations have led to the idea of modelling our universe as a $1 + 3$ dimensional hypersurface embedded within a higher-dimensional bulk spacetime, where matter is confined to the brane, but gravity can propagate into the bulk dimensions. This is the premise on which braneworld scenarios are built. For excellent and complementary reviews of the braneworld scenario, see Maartens (2004) and Brax *et al* (2004).

Throughout this thesis we have emphasised how studies of cosmological models motivated by fundamental physics may help resolve long-standing problems of cosmology and of physics as a whole. Let us mention one particular problem that has motivated the consideration of extra dimensions and, in particular, the braneworld paradigm. This is the hierarchy problem.

The hierarchy problem is simply the question of why the weak force is so much stronger than the gravitational force. An equivalent question is why the Planck mass is so large. The way in which the braneworld scenario ameliorates the hierarchy problem can be seen by considering Newtonian gravity and braneworld models in which the brane is embedded into a flat geometry in $1 + (3 + d)$ dimensions (with $d$ dimensions compactified on a scale much smaller than the three spatial dimensions which make up the boundary). Models of this type are know as ADD models, named after their proposers

Arkani-Hamed, Dimopoulos and Dvali (see Arkani-Hamed *et al*, 1998; Antoniadis, 1990; Antoniadis *et al*, 1998).

The Newtonian potential between two masses in such a flat spacetime is given by the expression

$$V(r) \approx \frac{m_1 m_2}{r^{d+1} m_{\text{fund}}^{2+d}} \ , \tag{8.1}$$

where masses $m_1$ and $m_2$ are separated by a distance $r$, and $m_{\text{fund}}$ is the fundamental Planck mass. Considering the braneworld scenario, however, it is clear that for $r > R$, where $R$ is the size of the extra dimensions,

$$V(r) \approx \frac{m_1 m_2}{R^d r m_{\text{fund}}^{2+d}} \ . \tag{8.2}$$

Hence, for any observations made over scales larger than $R$, we would observe an effective four-dimensional Planck mass $m_{Pl}^2 = R^d m_{\text{fund}}^{2+d}$. If the extra dimensions are sufficiently large, therefore, the four-dimensional Planck mass can be considerably larger than the fundamental Planck mass. On the other hand, Eq. (8.1) would become relevant for tests of gravity on scales significantly smaller than $R$ and Newton's law would appear to be modified. Such tests can constrain the size of the extra dimensions. To date, table-top experiments indicate that Newton's law is valid on sub-millimetre scales ($10^{-1}$mm), implying that the extra dimensions must be smaller than this scale (Long *et al*, 2003).

## 8.2 Braneworlds and cosmology

The ADD type braneworld models are the simplest possible examples of braneworld scenarios. More careful investigation, however, reveals that such models can be consistent with observations only if there is more than one extra dimension. Alternatives which allow consistent cosmologies to be constructed with only one extra dimension include the famous models of Randall and Sundrum (1999a,b), referred to as the RS models. These models draw their inspiration more directly from the M-theory solution of Horava and Witten. In the first RS model (RS1) there are two boundary branes each with $Z_2$ symmetry, and the bulk spacetime between these branes is a portion of anti-de Sitter space (ADS). The feature of this model, which distinguishes it from ADD type models, is that at low energies gravity appears to be four-dimensional, not because of the compactification of the extra dimension, but because of the curvature of the bulk spacetime. In the second RS model (RS2), one of the boundary branes is assumed to be displaced to infinity. In both models the brane universe is assumed to have a positive tension, which, as we will see, is required to counter the negative cosmological constant in the bulk. In the following subsection we will study the simplest method of constructing the RS2 model with a

FRW brane. This serves both as an instructive example as well as providing further motivation for studying braneworld cosmologies. This motivation, which will be discussed further in subsection 8.2.2, is that the cosmological dynamics for a brane universe become significantly modified when compared with standard relativistic cosmology. This is interesting because it may be that the modified dynamics will allow solutions of existing cosmological problems to be found, or allow the construction of new scenarios of the early universe. A final motivation for studying the construction of the RS2 model is that a similar derivation gives rise to a model first suggested by Shtanov and Sahni (2003), and which we refer to as the S-S model. This model is an example of a braneworld which permits a collapsing universe to undergo a bounce into an expanding phase, and we study it further in chapter 9.

### 8.2.1 Construction of a RS2 braneworld

There is a straightforward way of arriving at the cosmological evolution equations of the RS2 braneworld, which we now demonstrate.

The line element of the $1+4$ dimensional bulk space-time can be written as

$$\begin{aligned} ds^2 &= g_{AB}dx^A dx^B \\ &= N^2(t,y)d\nu^2 - a(t,y)^2\gamma_{ab}dx^a dx^b - dy^2 \ , \end{aligned} \tag{8.3}$$

where $A, B = 0, 1, 2, 3, 4$ and $a, b = 1, 2, 3$, and $\gamma_{ab}$ represents the usual isotropic and homogeneous spatial three metric given by

$$\gamma_{ab} = \mathrm{diag}\left(\frac{1}{1-kr^2},\ r^2,\ r^2\sin^2(\theta)\right) \ . \tag{8.4}$$

It can clearly be seen that spatial sections representing hypersurfaces of constant $y$ represent isotropic and homogeneous spaces.

The field equations for this five-dimensional model, with a matter source confined to a $1+3$ dimensional brane located at $y=0$, can be derived from the action

$$S = -\frac{1}{16\pi l_{\mathrm{fund}}^3}\int d^4x dy\sqrt{-g}(R+2\Lambda_5) + \int d^4x dy\sqrt{-g}\delta(y)\mathcal{L}_m \ , \tag{8.5}$$

where $l_{\mathrm{fund}}$ represents the fundamental Planck length, and $\mathcal{L}_m$ represents the Lagrangian for the matter source. Varying this action with respect to the metric leads to the Einstein equations in five dimensions (cf Eq. (1.3)) with a bulk cosmological constant and stress energy tensor confined to the brane:

$$G_{AB} = \Lambda_5 g_{AB} + 8\pi l_{\mathrm{fund}}^3 T_{AB}\delta(y) \ . \tag{8.6}$$

For a perfect fluid matter source on the brane, $T^A_B = \mathrm{diag}(\rho, -p, -p, -p, 0)$ (cf Eq. (1.5)). This matter source can also represent a scalar field on the brane using the identifications given in Eq. (1.17). We have assumed that matter is only present on the brane with no matter fields (just the cosmological constant) present in the bulk. Inserting the metric (8.3) into Eq. (8.6), we arrive at the five-dimensional Einstein equations

$$G^0{}_0 \equiv \frac{-3a'^2}{a^2} - \frac{3a''}{a} + \frac{3k}{a^2} + \frac{3\dot{a}^2}{a^2N^2} = \Lambda_5 + 8\pi l^3_{\mathrm{fund}}\delta(y)\rho \ , \tag{8.7}$$

$$\begin{aligned} G^a{}_b &\equiv \delta^a_b\left(\frac{2\ddot{a}}{aN^2} - \frac{2N'a'}{Na} - \frac{2\dot{N}\dot{a}}{aN^3} + \frac{\dot{a}^2}{a^2N^2} + \frac{k}{a^2} - \frac{a'^2}{a^2} - \frac{2a''}{a} - \frac{N''}{N}\right) \\ &= \delta^a_b\left(\Lambda_5 - 8\pi l^3_{\mathrm{fund}}\delta(y)p\right) \ , \end{aligned} \tag{8.8}$$

$$G^5{}_5 \equiv \frac{3\dot{a}^2}{a^2N^2} - \frac{3\dot{N}\dot{a}}{N^3a} + \frac{3\ddot{a}}{aN^2} - \frac{3N'a'}{aN} + \frac{3k}{a^2} - \frac{3a'^2}{a^2} = \Lambda_5 \ , \tag{8.9}$$

$$G^0{}_5 \equiv \frac{-3\dot{a}'}{N^2a} + \frac{3N'\dot{a}}{N^3a} = 0 \ , \tag{8.10}$$

where a dot represents a derivative with respect to $\nu$ and a prime (in this section only) a derivative with respect to $y$.

Ultimately, we are interested in the evolution equations for an observer confined to the brane and these can be determined by restricting Eqs. (8.7)-(8.10) to $y = 0$ and eliminating $N$ from the resulting equations. An important element of this calculation is that the presence of the brane causes a 'jump' in the first derivative of the metric at $y = 0$ in the direction perpendicular to the brane. Another important point is that by imposing a $Z_2$ symmetry at the brane we have the additional constraints $N(y) = N(-y)$, $a(y) = a(-y)$, $N'(y) = -N'(-y)$ and $a'(y) = -a'(-y)$, which must also be satisfied. Integrating Eq. (8.7) over $y$ from $-\epsilon$ to $+\epsilon$, and taking the limit $\epsilon \to 0$ one arrives at the equation

$$\left[\frac{a'}{a}\right]_0 = \left[-\frac{8\pi l^3_{\mathrm{fund}}}{6}\rho\right]_0 \ . \tag{8.11}$$

Considering the $ab$ equation (8.8) in a similar manner and using Eq. (8.11) then gives

$$\left[\frac{N'}{N}\right]_0 = \left[\frac{8\pi l^3_{\mathrm{fund}}}{2}\left(\frac{2}{3}\rho + p\right)\right]_0 \ . \tag{8.12}$$

We are now in a position to derive the evolution equations restricted to the brane. Considering the 05 equation (8.10) with $y = 0$ and using Eqs. (8.11)-(8.12) leads to

$$\dot{\rho} + 3\frac{\dot{a}}{a}(\rho + p) = 0 \ , \tag{8.13}$$

which is clearly the continuity equation on the brane and takes the same form as the classical expression Eq. (1.8). This is due to the fact that the fluid is confined to the brane and there is no flow in the $y$ direction.

Let us now consider the 55 equation (8.9). Considering again $y = 0$ and using Eqs. (8.11)-(8.12) we find

$$\frac{3\dot{a}^2}{a^2N^2} - \frac{3\dot{N}\dot{a}}{N^3a} + \frac{\ddot{a}}{aN^2} + \frac{(8\pi l_{\rm fund}^3)^2}{4}\rho\left(\frac{1}{3}\rho + p\right) + \frac{3k}{a^2} = \Lambda_5 \ . \tag{8.14}$$

At this point it is convenient to change the time variable to cosmic time on the brane such that $dt = Nd\nu$. Using this change of variables, and from this point on using a dot to refer to a derivative with respect to cosmic time, Eq. (8.13) remains unchanged and Eq. (8.14) becomes

$$\frac{3\dot{a}^2}{a^2} + \frac{3\ddot{a}}{a} + \frac{(8\pi l_{\rm fund}^3)^2}{4}\rho\left(\frac{1}{3}\rho + p\right) + \frac{3k}{a^2} = \Lambda_5 \ . \tag{8.15}$$

One can easily verify that Eqs. (8.13) and (8.15) admit the first integral

$$\left(\frac{\dot{a}}{a}\right)^2 = H^2 = \frac{(8\pi l_{\rm fund}^3)^2}{36}\left(\rho^2\right) + \frac{\Lambda_5}{6} - \frac{k}{a^2} + \frac{m}{a^4} \ , \tag{8.16}$$

where $m$ is a constant of integration.

Let us consider Eq. (8.16) in more detail. In particular, let us assume the total energy density and pressure are comprised of two components, one arising from standard matter on the brane and the other from a brane tension. We therefore rename $\rho$ above to be $\rho_{\rm tot}$, and set $\rho_{\rm tot} = \rho + \sigma$ and $p_{\rm tot} = p - \sigma$, where $\sigma$ is the brane tension. Then, using Eq. (8.16) we arrive at the Friedmann equation for a brane universe

$$H^2 = \frac{8\pi\ell_{\rm Pl}^2}{3}\rho\left(1 + \frac{\rho}{2\sigma}\right) + \frac{\Lambda_4}{3} - \frac{k}{a^2} + \frac{m}{a^4} \ , \tag{8.17}$$

where we have defined

$$\frac{8\pi\ell_{\rm Pl}^2}{3} = \frac{(8\pi l_{\rm fund}^3)^2\sigma}{18} \ , \tag{8.18}$$

$$\frac{\Lambda_4}{3} = \frac{(8\pi l_{\rm fund}^3\sigma)^2}{36} + \frac{\Lambda_5}{6} \ . \tag{8.19}$$

An immediate result is that the four-dimensional Planck mass is related to the five-dimensional Planck mass via the relationship

$$m_{Pl} = \sqrt{\frac{3}{4\pi}}\frac{m_{\rm fund}^3}{\sqrt{\sigma}} \ . \tag{8.20}$$

This implies that if the brane tension is much lower than the fundamental Planck scale, the four-dimensional Planck mass can appear much larger than the five-dimensional fundamental Planck mass. At this point we can also impose the fine-tuning relationship

$$\frac{(8\pi l_{\rm fund}^3\sigma)^2}{6} = -\Lambda_5 \tag{8.21}$$

between the five-dimensional cosmological constant and the brane tension in order to set the overall four-dimensional cosmological constant to zero. This clearly requires the five-dimensional cosmological constant to be negative.

The Raychaudhuri equation on the brane can also be derived using the Friedmann equation (8.17) together with either Eq. (8.15) or Eq. (8.13). The result is

$$\dot{H} = -4\pi\ell_{\rm Pl}^2\left(\rho + p\right)\left(1 + \frac{\rho}{\sigma}\right) + \frac{k}{a^2} - \frac{2m}{a^4} \ . \tag{8.22}$$

The term $m/a^4$ in the Friedmann equation is often referred to as the dark radiation term. In the derivation we have just presented $m$ is a constant of integration. An analysis of the form of the five-dimensional metric we have employed to derive this system of equations can be used to gain insight into the meaning of this dark radiation term. A version of Birkhoff's theorem in five dimensions can be used to show that if the bulk spacetime is ADS, and therefore conformally flat, $m$ is zero. If, however, the bulk is ADS-Schwarzschild, $m$ is non-zero and provides a measure of the mass of the bulk black hole. In this case the bulk is not conformally flat and the dark radiation term is the projection of the five-dimensional Weyl tensor on the brane (see Mukohyama *et al*, 2000; Mukohyama, 2000; Ida, 2000; Bowcock *et al*, 2000, for the global properties of the bulk spacetimes and the relation to dark radiation).

Moreover, it can be shown that ADS-Schwarzschild is the most general bulk metric which is a solution of the five-dimensional vacuum Einstein equations (with a cosmological constant) and which admits hypersurfaces of the FRW form. In this sense the model we have derived above is the most general FRW model possible in five dimensions if the bulk is an Einstein space. It is of course possible to generalise the bulk, such that it contains scalar or form fields. These possibilities have also been extensively studied (see Brax *et al*, 2004, and references therein).

### 8.2.2 Modified dynamics and cosmological scenarios

The major result of the previous subsection, from a cosmological perspective, is that the equations which govern the evolution of the four-dimensional braneworld can be significantly modified when compared to the standard field equations (1.6)-(1.8) arising from GR. The immediate hope, therefore, is that the new properties of these equations could offer resolutions to existing cosmological problems or inspire new scenarios of the early universe. Indeed, even in this simplest of models which we have just studied, the departure from standard cosmology is extremely interesting.

The first major modification in the Friedmann equation (8.17) is the presence of the dark radiation term. This term acts like an additional matter source on the brane but is a purely geometrical effect, arising because of the embedding of the universe into a

higher-dimensional bulk. That such additional terms can exist is very interesting since they offer the possibility of matter sources, such as dark energy and dark matter, being explained in terms of purely geometrical effects. This particular term takes the form equivalent to a radiation source, and primordial nucleosynthesis constraints imply that it can provide at most 10% of the energy density of radiation present in the universe today (Ichiki *et al*, 2002). The RS scenario, therefore, does not address the question of the origin of dark energy or dark matter. The general paradigm that the universe is embedded in a higher-dimensional spacetime, however, does offer the possibility that more complicated models, for example those with more general bulk spacetimes, may lead to different additional terms which exhibit properties similar to dark energy or matter.

The most important difference for the early universe, however, is the presence of the additional $\rho^2$ term in the Fiedmann equation (8.17). This suggests that at high energy densities the Friedmann equation is significantly altered from the relativistic form. On the other hand, at low energies the standard Friedmann equation and other evolution equations are recovered. The energy scale at which the $\rho^2$ term becomes important is set by the brane tension $\sigma$. If, therefore, $\sigma$ is significantly greater than the energy density at nucleosynthesis ($(1MeV)^4$), all the quantitative predictions of the highly successful hot big bang model of cosmology are unaltered in the braneworld context. In the early universe, however, the $\rho^2$ term will become important and eventually dominate the dynamics. In fact the strongest restrictions on $\sigma$ come from table top experiments of Newton's law of gravity and provide the constraint $\sigma > (10^5 MeV)^4$.

The $\rho^2$ term has a particularly important effect on the single field inflationary scenario of the early universe. The result of the modified braneworld equations is that a period of inflation becomes significantly more generic compared to the standard case. More quantitatively, the slow-roll parameters Eqs. (1.21)-(1.22) become altered in such a way that at energies above the brane tension the slow-roll conditions $\epsilon \ll 1$ and $\eta \ll 1$ are satisfied by a wider class of potentials, including those too steep to satisfy the conventional slow-roll conditions. Consequently, potentials previously thought too steep to drive slow-roll inflation become viable inflationary potentials (Maartens *et al*, 2000; Copeland *et al*, 2001).

The results of this section are interesting in their own right. However, for the purposes of this thesis the key point is that additional degrees of freedom which necessarily arise within braneworld scenarios can have important consequences for the dynamics of the early universe. In the subsequent subsection we will discuss a further example of modified dynamics which forms the basis for chapter 9.

### 8.2.3 Bouncing braneworlds

In chapter 5 it was shown how the modified equations of LQC allow a collapsing universe to undergo a bounce into an expanding phase. This property of the modified equations was then used to formulate interesting scenarios of the pre-inflationary universe. In particular, we studied the setting of the initial conditions for inflation through oscillations and the emergent universe scenario in chapters 5 and 6. Given that we have just seen that the dynamics of the early universe are also modified in braneworld settings, it is interesting to ask whether there are any braneworld scenarios which permit bouncing universes, and whether these can also be used to develop similar cosmological scenarios. A number of bouncing braneworld models have been developed to date (see Shtanov and Sahni, 2003; Brax and Steer, 2002; Mukherji and Peloso, 2002; Burgess *et al*, 2004; Kanti and Tamvakis, 2003; Foffa, 2003; Piao and Zhang, 2005). All these realisations of a bouncing braneworld cosmology involve a more complicated bulk spacetime than that of the RS2 model, and can lead to modifications in the braneworld evolution equations that induce a bounce under certain conditions.

A simple example of a bouncing braneworld comes from generalising the ADS-Schwarzschild bulk spacetime to the case of a charged bulk black hole (Mukherji and Peloso, 2002). (See also Hovdebo and Myers, 2003, for criticisms concerning the model's stability). The resulting Friedmann equation can be shown to contain a term proportional to $-1/a^6$. This term acts like a negative energy density matter source, which violates the weak energy condition. During cosmic collapse the magnitude of this term increases more rapidly than matter sources corresponding to dust, radiation or a scalar field self-interacting though a positive potential (until the $\rho^2$ term becomes important). Therefore, $H$ can go to zero during a collapse and a bounce proceed. Burgess *et al* (2004) consider further generalisations of this model and new models containing various bulk scalar fields and additional form-fields.

In chapter 9 we determine the essential conditions a given set of braneworld scenarios must satisfy in order that they can set the initial conditions for inflation and realise the emergent universe model. As an example we choose one model to study in detail. The model chosen is the model of Shtanov and Sahni (2003) (the S-S model). Let us therefore present an overview of this model and its equations of motion.

The set-up of the S-S model is nearly identical to the RS2 model we studied in subsection 8.2.1. The fundamental difference, however, is that in the case of the S-S model the extra dimension is assumed to be time-like. The result of this difference for the five-dimensional Einstein equations (8.7)-(8.10) is simply that terms containing one or more derivatives with respect to $y$ are multiplied by a factor of $-1$. Following the method and equations laid out in subsection 8.2.1 it is therefore straightforward to verify that the

continuity equation (8.13) is unmodified, while Eq. (8.16) becomes

$$H^2 = -\frac{(8\pi l_{\rm fund}^3)^2}{36}\left(\rho^2\right) + \frac{\Lambda_5}{6} - \frac{k}{a^2} + \frac{m}{a^4} \ . \tag{8.23}$$

Once again, considering the matter on the brane to consist of a fluid and a brane tension such that $\rho_{\rm tot} = \rho + \tilde{\sigma}$ and $p_{\rm tot} = p - \tilde{\sigma}$, and using similar definitions to those in Eq. (8.18) such that

$$\frac{8\pi\ell_{\rm Pl}^2}{3} = -\frac{(8\pi l_{\rm fund}^2)^2\tilde{\sigma}}{18} \ , \tag{8.24}$$

$$\frac{\Lambda_4}{3} = -\frac{(8\pi l_{\rm fund}^3\tilde{\sigma})^2}{36} + \frac{\Lambda_5}{6} \ , \tag{8.25}$$

we arrive at the Friedmann equation in the S-S braneworld:

$$H^2 = \frac{8\pi\ell_{\rm Pl}^2}{3}\rho\left(1 - \frac{\rho}{2|\tilde{\sigma}|}\right) + \frac{\Lambda_4}{3} - \frac{k}{a^2} + \frac{m}{a^4} \ , \tag{8.26}$$

where we have assumed the brane tension $\tilde{\sigma}$ is negative. A fine-tuning relation can be imposed to set the four-dimensional cosmological constant to zero, which requires that the five-dimensional cosmological constant is positive in this case. Differentiating Eq. (8.26) and using Eq. (8.13) we can also derive the Raychaudhuri equation for this model:

$$\dot{H} = -4\pi\ell_{\rm Pl}^2\left(\rho + p\right)\left(1 - \frac{\rho}{\sigma}\right) + \frac{k}{a^2} - \frac{2m}{a^4} \ . \tag{8.27}$$

Considering the form of Eq. (8.26), it is clear that a collapsing universe sourced by any matter satisfying the weak energy condition will undergo a bounce. This occurs because during a collapse the energy density of such a matter source will increase. Once it becomes of the order of the brane tension, however, the $-\rho^2$ term becomes important. Since this negative term grows more rapidly than the $\rho$ term, a point is necessarily reached at which $H$ goes to zero and a bounce then occurs.

As an aside, it is important to realise that the extra time-like dimension in this model is accessible only to the gravitational field, just like the extra space dimension in the RS2 model. Matter itself, therefore, is prevented from acting in an acausal manner. The Kaluza-Klein gravitational modes could in principle lead to a violation of causality, and the severity of this behaviour may put restrictions on the parameters of this model. This has not been studied in detail, though a related discussion of models with more than one extra time dimension can be found in Dvali *et al* (1999) and Chaichian and Kobakhidze (2000).

Having discussed how the modified dynamics of braneworld scenarios arises, and shown that this can lead to bouncing braneworld models, we now proceed to analyse and construct cosmological scenarios in this context in the next chapter.

# Chapter 9

# A graceful entrance to braneworld inflation

In chapters 5 and 6, positively-curved, oscillatory universes were shown to have important consequences for the pre-inflationary dynamics of the early universe. In particular, it was shown that the modified dynamics of semi-classical LQC may allow a self-interacting scalar field to climb up its potential during a very large number of these cycles. Moreover, we showed that for a massless scalar field the oscillations occur about a centre equilibrium point, and that this point can be utilised to develop a 'stable' version of the emergent universe scenario. The general dynamics encompassing both these scenarios may be described as a 'graceful entrance' to early universe inflation[1]. As we discuss below, the key conditions required for the dynamics of a graceful entrance are in fact rather weak, and it is therefore important to investigate whether similar effects are possible in other cosmological scenarios such as the braneworld paradigm. This chapter is dedicated to studying the graceful entrance dynamics in the context of braneworld cosmology. In particular, the aim is to determine whether braneworld models which exhibit a bounce from a collapsing to an expanding phase can also exhibit a graceful entrance into inflation.

In chapter 6 we saw that the dynamics of the scalar field climbing its self-interaction potential in LQC could be understood by studying the case of a universe sourced by a scalar field with a constant potential. Consideration of the equilibrium points of this system, together with phase portraits, offered a powerful way of understanding the dynamics, complementing the alternative description of chapter 5. At the same time such an approach also showed how the emergent universe scenario can be realised within LQC. Chapter 5 demonstrated the usefulness of considering an effective equation of state in understanding the dynamics. In this chapter, therefore, we combine these approaches

[1]The term 'graceful entrance' was first coined in the LQC setting by Nunes (2005).

and use the resulting method to consider a general class of braneworld models.

We proceed as follows. Sections 9.1 and 9.2 review the importance of the equation of state and a phase portrait analysis in understanding the graceful entrance mechanism. Section 9.3 then combines these approaches and determines the conditions a given model must satisfy for a graceful entrance to be possible in principle. Finally, in sections 9.4-9.5, we consider the bouncing braneworld model proposed by Shtanov and Sahni (2003) (the S-S model) as an explicit example. We show that it satisfies our required conditions and exhibits the features needed to realise a graceful entrance to inflation for a wide region of parameter space. We conclude with a discussion in section 9.6.

## 9.1 A graceful entrance and the equation of state

Let us briefly recall the dynamics of a graceful entrance, uncovered in the context of semi-classical LQC, and the role played by the equation of state. In this chapter we denote for later convenience the equation of state by $\gamma$, where

$$\gamma = w + 1 \ . \tag{9.1}$$

The graceful entrance dynamics rely on oscillations of the universe, which in turn require a bounce from a contracting phase into an expanding one, as well as a recollapse of the subsequent expanding phase. For a positively-curved universe, this requires that the strong energy condition is violated below a particular critical value of the scale factor ($a_*$ in the case of LQC) and is satisfied above it. In terms of a standard FRW cosmology this requires the equation of state, $\gamma$, to satisfy $\gamma < 2/3$ for $a < a_*$ and $\gamma > 2/3$ for $a > a_*$. In the case of LQC, it was shown that oscillations can occur by expressing the equations of motion in terms of the standard equations with a modified equation of state. This equation of state was shown to necessarily violate the strong energy condition below $a_*$, while above $a_*$ the classical form for the equation of state was recovered. If the condition $\dot{\phi}^2 > V$ is satisfied in the classical regime (i.e. the field's kinetic energy dominates its potential energy), the strong energy condition is satisfied and a recollapse occurs.

If the kinetic energy of the scalar field is initially dominant, it is a good approximation to assume that it behaves as a massless field with its value either increasing or decreasing monotonically with time. In principle, therefore, the field may gradually roll *up* its potential (assuming implicitly that it is evolving along a region of the potential that is increasing in magnitude). As a result, the potential energy will gradually increase during each successive cycle with the net result that it becomes progressively harder to satisfy the strong energy condition on scales above $a_*$. Eventually, therefore, a cycle will be

reached when the strong energy condition becomes violated during the classical, expansionary phase of the cycle ($a > a_*$). Since the condition for the strong energy condition to be violated in an expanding universe is also that for inflation to occur, a phase of inflation then proceeds. This implies that slow-roll inflation may be possible even if the field is initially located in a region of the potential that would not generate accelerated expansion, such as a minimum.

This requirement – that the strong energy condition is violated below a particular scale and satisfied above it – is a rather weak constraint. In fact any model which exhibits a bounce on small scales, and approximates to standard cosmology on large scales, is expected to exhibit this behaviour.

## 9.2 The phase space description of a graceful entrance to inflation

In addition to considering the effective equation of state, a phase space analysis of the LQC dynamics for isotropic universes sourced by a scalar field with a constant potential also proved very useful for understanding the graceful entrance dynamics. As we will show, this approach is also fruitful in more general contexts for determining the necessary conditions a given cosmological model must satisfy for a graceful entrance to be possible.

In general, the dynamics of any homogeneous and isotropic model sourced by a scalar field with constant potential are determined by three evolution equations for the scale factor, the Hubble parameter, and the velocity of the scalar field, respectively. In addition, there is the Friedmann equation, which represents a constraint. This implies that the dynamics can be expressed as a two-dimensional system of equations and presented on a two-dimensional phase space. In the LQC scenarios considered previously, it proved convenient to parametrise the phase space in terms of the scale factor and the Hubble parameter. However, these may not be the most convenient variables in other models.

Using our experience with the dynamics of LQC, we can understand the qualitative nature of the phase space of a general model which can result in a graceful entrance to inflation. This is illustrated in Fig. 9.1. For a positive potential, taking values in the range $0 < V < V_{\rm crit}$, where $V_{\rm crit}$ is some critical value that is determined by the parameters of the model, the phase space contains a centre and a saddle equilibrium point. Two types of behaviour are therefore possible. Trajectories that are sufficiently close to the centre encircle it and represent solutions that undergo eternal oscillations. On the other hand, universes which pass above the saddle point represent initially collapsing models which evolve through a bounce into an eternal (de Sitter) inflationary era. This is illustrated qualitatively in the top panel of Fig. 9.1.

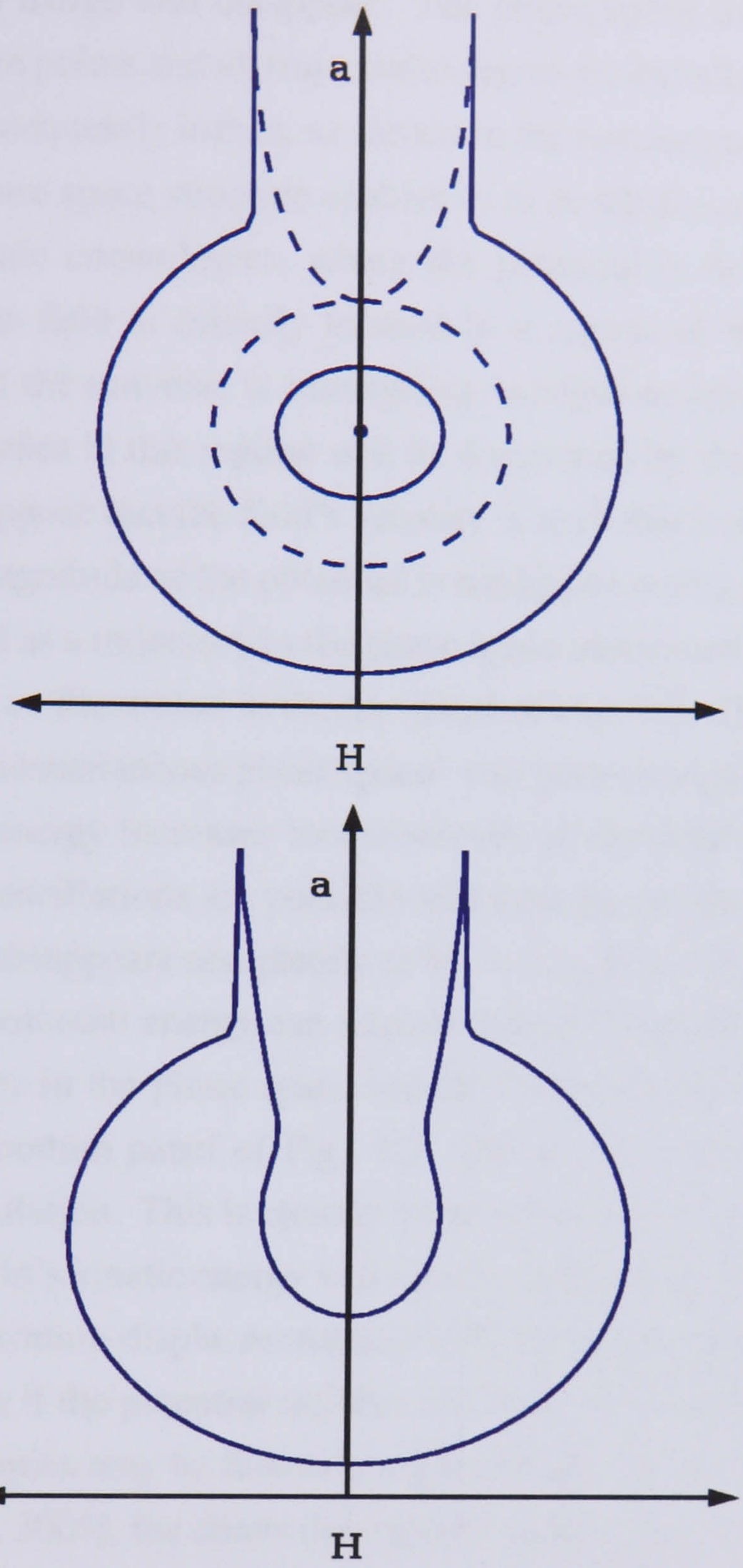


Figure 9.1: The top panel is a sketch of the phase space in the variables $\{H, a\}$, for $0 < V < V_{\rm crit}$. Present are the important features for a graceful entrance: an area in which oscillations take place indicated by the region enclosed by the dotted line, and trajectories which evolve into an inflationary phase. The centre equilibrium point about which oscillations occur is marked with a circle, the separatrix with a dotted line and the saddle equilibrium point by the self-intersection of the separatrix. The bottom panel is a sketch of the same phase space for $V > V_{\rm crit}$. In this case there are no centre or saddle points present and all trajectories evolve into inflation. Trajectories in both panels evolve contra-clockwise.

If the value of the potential is increased, the effect on the phase space is such that the centre and saddle points are positioned closer to each other. At the critical value

$V = V_{\rm crit}$, the points merge and disappear. The phase space for $V > V_{\rm crit}$ therefore contains no equilibrium points and all trajectories represent initially contracting universes which bounce and subsequently inflate, as shown in the bottom panel of Fig. 9.1.

This simplified phase space structure enables us to develop a graceful entrance mechanism for more realistic cosmologies, where the potential is field-dependent. Let us assume that the scalar field is initially located in a region of the potential such that $V(\phi) < V_{\rm crit}$ and that the universe is undergoing oscillations about the centre equilibrium point. The dynamics in this regime will be dominated by the field's kinetic energy and we will further suppose that the field's velocity is such that it moves up the potential. If the change in the magnitude of the potential is negligible over a given cycle, this cycle can still be represented as a trajectory in the phase space associated with an instantaneous value of the potential, as illustrated in the top panel of Fig. 9.1. Over a large number of cycles, however, this 'instantaneous phase space' will become significantly modified. Indeed, if the potential energy increases monotonically as the field evolves, the region of phase space in which oscillations are possible will become progressively smaller. Since the oscillatory region disappears completely at $V = V_{\rm crit}$, this corresponds to the largest value that the field's potential energy can acquire before the oscillations are broken. At this point the trajectory in the phase space rapidly evolves into the inflationary regime corresponding to the bottom panel of Fig. 9.1. Hence, the value $V_{\rm crit}$ sets the energy scale at the onset of inflation. This is exactly what was seen in the LQC scenario. Once inflation begins, the field's kinetic energy will rapidly tend to zero as the field slows down, reaches a point of maximum displacement and rolls back down the potential. Slow-roll inflation will then arise if the potential satisfies the usual slow-roll constraints.

Although the dynamics may be further complicated by the introduction of additional matter sources (Nunes, 2005), the above description outlines how a field can evolve up its self-interaction potential while the universe undergoes oscillations. This forms the basis for a graceful entrance mechanism that generates the conditions for slow-roll inflation. A phase plane analysis is important since it highlights the relevance of the centre and saddle equilibrium points. In particular, a sufficient but not necessary condition for cyclic behaviour is the existence of a centre equilibrium point, while a saddle point is required to separate those regions of phase space where cyclic and non-cyclic behaviour takes place. Furthermore, the disappearance of the saddle point at a critical value of the potential is central to the graceful entrance mechanism.

In the following section, therefore, we will consider the conditions for the existence of saddle and centre equilibrium points in cosmologies described by a set of generalised Friedmann equations.

## 9.3 General conditions for a centre and saddle equilibrium points

### 9.3.1 Relativistic cosmology

We wish to study classes of cosmological models that are motivated by the braneworld paradigm and to determine whether such models display the general characteristics required for a graceful entrance to inflation. In section 9.1 we discussed the usefulness of the approach of considering a standard cosmology with an effective equation of state. We will therefore first consider the relativistic cosmology based on classical Einstein gravity. This system provides a suitable framework for considering more general models and allows us to simultaneously consider an effective equation of state and determine the equilibrium points of a given model. Specifically, we will consider a positively-curved FRW cosmology sourced by an effective perfect fluid with an energy density and pressure related by an arbitrary equation of state, $p_{\rm eff} = [\gamma_{\rm eff} - 1]\rho_{\rm eff}$, where it is assumed implicitly that the equation of state parameter is a known function of the scale factor, $\gamma_{\rm eff} = \gamma_{\rm eff}(a)$.

The Friedmann and fluid equations for this model are given by

$$H^2 = \frac{8\pi\ell_{\rm Pl}^2}{3}\rho_{\rm eff} - \frac{1}{a^2} \ , \tag{9.2}$$

$$\dot{\rho}_{\rm eff} = -3H\gamma_{\rm eff}\rho_{\rm eff} \ , \tag{9.3}$$

where

$$\dot{a} = Ha \ , \tag{9.4}$$

and Eqs. (9.2) and (9.3) fully determine the cosmic dynamics. Differentiating Eq. (9.2) with respect to cosmic time implies that

$$\dot{H} = -\frac{3\gamma_{\rm eff}}{2}H^2 + \left(1 - \frac{3\gamma_{\rm eff}}{2}\right)\frac{1}{a^2} \ , \tag{9.5}$$

and Eqs. (9.4) and (9.5) then describe a closed dynamical system, where the Friedmann equation (9.2) represents a constraint. The equilibrium points of this system arise whenever $\dot{a} = \ddot{a} = 0$, which implies that

$$\gamma_{\rm eff}(a_{\rm eq}) = \frac{2}{3} \ , \qquad H(a_{\rm eq}) = 0 \ . \tag{9.6}$$

The stability of the system (9.4)-(9.5) can be determined by linearising about the equilibrium points and evaluating the corresponding eigenvalues. It is straightforward to show that the eigenvalues are given by

$$\lambda^2 = -\frac{3}{2}\left[\frac{1}{a^2}\frac{d\gamma_{\rm eff}}{d\ln a}\right]_{\rm eq} \ . \tag{9.7}$$

In general, therefore, a necessary and sufficient condition for the equilibrium point to be a centre is

$$\lambda^2 < 0 \ , \qquad H = 0 \ , \qquad \gamma_{\text{eff}} = \frac{2}{3} \ , \qquad \frac{d\gamma_{\text{eff}}}{d\ln a} > 0 \ , \tag{9.8}$$

whereas the corresponding condition to be a saddle is

$$\lambda^2 > 0 \ , \qquad H = 0 \ , \qquad \gamma_{\text{eff}} = \frac{2}{3} \ , \qquad \frac{d\gamma_{\text{eff}}}{d\ln a} < 0 \ . \tag{9.9}$$

It is interesting to note that under the assumptions we have made, centre and saddle points are the only types of equilibrium points permitted. This was also found in the LQC context.

These results also show that the behaviour of the effective equation of state described in section 9.1 is equivalent to the presence of a centre equilibrium point. This is in complete agreement with Eq. (6.16), and generalises that result.

### 9.3.2 Braneworld scenarios

The four-dimensional cosmological dynamics for a wide class of positively-curved FRW braneworld scenarios can be modelled in terms of a generalised Friedmann equation of the form (Copeland *et al*, 2006)

$$H^2 = \frac{8\pi\ell_{\text{Pl}}^2}{3}\rho L^2(\rho) + f(a) - \frac{1}{a^2} \ , \tag{9.10}$$

where $\rho$ is the total energy density of the matter confined to the brane. The function $L(\rho)$ is assumed to be positive-definite and parametrises the departure of the model from the standard relativistic behaviour, $H^2 \propto \rho$. The function $f(a)$ is a function of the scale factor and, in a braneworld context, usually parametrises the effects of a bulk black hole on the four-dimensional dynamics and represents the dark radiation terms discussed in subsection 8.2.1.

If the matter fields are confined to the brane, they satisfy the standard conservation equation

$$\dot{\rho} = -3H\gamma\rho \ , \tag{9.11}$$

where the equation of state parameter is defined by $p = (\gamma - 1)\rho$ and is once more to be viewed implicitly as a known function of the scale factor. This was explicitly shown for the RS2 model and the S-S model in the previous chapter.

The system (9.10)-(9.11) can be expressed in the standard form of Eqs. (9.2)-(9.3) by defining an effective energy density

$$\rho_{\text{eff}} = \rho L^2 + \frac{3}{8\pi\ell_{\text{Pl}}^2} f(a) \ . \tag{9.12}$$

Differentiating Eq. (9.12) and comparing with Eq. (9.3) then implies that the effective equation of state parameter has the form

$$\gamma_{\rm eff} = \left[\gamma\left(\rho L^2 + \rho^2\frac{d(L^2)}{d\rho}\right) - \frac{1}{8\pi\ell_{\rm Pl}^2}\frac{df}{d\ln a}\right]\left(\rho L^2 + \frac{3}{8\pi\ell_{\rm Pl}^2}f\right)^{-1} \ . \tag{9.13}$$

In principle, therefore, if the conservation equation (9.11) can be solved for a given equation of state, $\gamma(a)$, the effective equation of state (9.13) will be a known function of the scale factor once the functional forms of $L(\rho)$ and $f(a)$ have been specified for a particular braneworld model. Differentiation will then yield the necessary information to determine the existence (or not) of the centre and saddle equilibrium points, as summarised in Eqs. (9.8) and (9.9).

In the following section, we employ these results within the context of a specific braneworld model.

## 9.4 Shtanov-Sahni braneworld

The Shtanov-Sahni (S-S) braneworld scenario was described in subsection 8.2.3. It embeds a co-dimension one brane with a negative tension $\tilde{\sigma}$ in a five-dimensional Einstein space, sourced by a positive cosmological constant, where the fifth dimension is time-like. The effective Friedmann equation on the brane is given by Eq. (8.26) which we present once more for convenience:

$$H^2 = \frac{8\pi\ell_{\rm Pl}^2}{3}\left[\rho - \frac{\rho^2}{2\sigma}\right] + \frac{m}{a^4} - \frac{1}{a^2} \ , \tag{9.14}$$

where we have defined $\sigma \equiv -\tilde{\sigma}$, and taken $k = 1$.

Comparison of the Friedmann equations (9.10) and (9.14) implies immediately that

$$L^2 = \left(1 - \frac{\rho}{2\sigma}\right) \ , \ f(a) = \frac{m}{a^4} \ , \tag{9.15}$$

and substituting Eq. (9.15) into Eq. (9.13) implies that the effective equation of state parameter is given by

$$\gamma_{\rm eff} = \frac{\gamma\rho(1-\rho/\sigma)a^4 + m/2\pi\ell_{\rm Pl}^2}{\rho(1-\rho/2\sigma)a^4 + 3m/8\pi\ell_{\rm Pl}^2} \ . \tag{9.16}$$

Since we are interested in whether a graceful entrance to inflation can occur in this model, we will determine the equilibrium points that arise when the matter confined to the brane corresponds to a scalar field that is rolling along a constant potential, $V$. The equation of state for the field is given by

$$\gamma = 2\left(1 - \frac{V}{\rho}\right) \ . \tag{9.17}$$

In general, the equilibrium points for this system will arise whenever Eqs. (9.8) or (9.9) are satisfied. It follows from Eqs. (9.14) and (9.16) that such points occur when

$$\frac{8\pi\ell_{\rm Pl}^2}{3}\left(\rho-\frac{\rho^2}{2\sigma}\right)+\frac{m}{a^4}=\frac{1}{a^2}\ , \tag{9.18}$$

$$\gamma\left(\rho-\frac{\rho^2}{\sigma}\right)-\frac{2}{3}\left(\rho-\frac{\rho^2}{2\sigma}\right)=-\frac{m}{4\pi\ell_{\rm Pl}^2}\frac{1}{a^4}\ . \tag{9.19}$$

For finite values of the scale factor, Eq. (9.18) may be simplified after substitution of Eq. (9.19):

$$\frac{1}{a^2}=4\pi\ell_{\rm Pl}^2\rho\left[\frac{4}{3}-\frac{2\rho}{3\sigma}+\gamma\left(\frac{\rho}{\sigma}-1\right)\right]\ , \tag{9.20}$$

and Eq. (9.20) may then be employed to express Eq. (9.18) in the form of a quartic equation in the energy density:

$$8\pi\ell_{\rm Pl}^2 m\left[\frac{2\rho_{\rm eq}^2}{3\sigma}-\left(\frac{1}{3}+\frac{V}{\sigma}\right)\rho_{\rm eq}+V\right]^2 -\frac{5\rho_{\rm eq}^2}{6\sigma}+\left(\frac{2}{3}+\frac{V}{\sigma}\right)\rho_{\rm eq}-V=0\ . \tag{9.21}$$

The solutions to Eq. (9.21) yield the values of the energy density at the equilibrium points and the corresponding value of the scale factor can then be deduced directly from Eq. (9.20). For physical solutions, one must ensure that the energy density and scale factor are positive and real at each point.

The dark radiation on the brane can significantly influence the dynamics of the system. In view of this, we consider separately the cases where this radiation is present or absent in the following sections.

## 9.5 No dark radiation

If no dark radiation is present ($m = 0$), the quartic equation (9.21) reduces to the quadratic constraint

$$\frac{10\rho_{\rm eq}^2}{3\sigma}-\left(\frac{8}{3}+\frac{4V}{\sigma}\right)\rho_{\rm eq}+4V=0\ , \tag{9.22}$$

and this equation can be solved in terms of the field's kinetic energy:

$$\dot{\phi}_{\rm eq}^2=\frac{4\sigma-4V\pm2\left[9V^2-18V\sigma+4\sigma^2\right]^{1/2}}{5}\ . \tag{9.23}$$

It follows that there can be at most two static (physical) solutions to Eqs. (9.10) and (9.11), depending on the magnitude of the potential. If $V < 0$, there is only one solution

to Eq. (9.22) where the field's kinetic energy is positive, implying there is only one equilibrium point in the phase space. For $V = 0$, there is one solution with $\dot{\phi}^2 > 0$ and a second, but physically uninteresting, point where the field's kinetic energy vanishes and the scale factor diverges. For a positive potential, on the other hand, there are two real roots to Eq. (9.22) if $V$ satisfies the condition

$$9V^2 - 18V\sigma + 4\sigma^2 > 0 \ . \tag{9.24}$$

The values of the potential which bound the region of parameter space in which there are no real solutions are therefore given by

$$V = \left(1 \pm \frac{\sqrt{5}}{3}\right)\sigma \ . \tag{9.25}$$

We find that for $0 < V < V_{\rm crit}$, where

$$V_{\rm crit} \equiv \left(1 - \frac{\sqrt{5}}{3}\right)\sigma \ , \tag{9.26}$$

there are two real solutions to Eq. (9.22). Moreover the roots are physical, since they are positive and lead to real values of the scale factor. The roots merge and disappear at $V_{\rm crit}$. While there are other solutions to Eq. (9.22) for $V$ greater than the upper branch of Eq. (9.25), they do not correspond to physical equilibrium points, either because the solution requires $\dot{\phi}^2$ to be negative or the value of the scale factor to be imaginary.

Hence, there are two static equilibrium points for $0 < V < V_{\rm crit}$. The nature of these points can be determined from condition (9.7) after substituting Eqs. (9.16), (9.18) and (9.22) and we find that the eigenvalues are given by

$$\lambda^2 = 4\pi\ell_{\rm Pl}^2\dot{\phi}^2\left[4 - \frac{1}{\sigma}\left(5\dot{\phi}^2 + 4V\right)\right] \ . \tag{9.27}$$

This implies that a given point will correspond to a centre if $\dot{\phi}^2 > \frac{4}{5}(\sigma - V)$, otherwise it will represent a saddle. Consequently, for physical roots to Eq. (9.22), the field's kinetic energy at the centre equilibrium point has a value

$$\dot{\phi}^2_{\rm eq} = \frac{-4V + 4\sigma + 2\sqrt{9V^2 - 18V\sigma + 4\sigma^2}}{5} \ , \tag{9.28}$$

whereas at the saddle it takes the value

$$\dot{\phi}^2_{\rm eq} = \frac{-4V + 4\sigma - 2\sqrt{9V^2 - 18V\sigma + \sigma^2}}{5} \ . \tag{9.29}$$

It follows from Eqs. (9.28) and (9.29) that the centre and saddle equilibrium points move towards each other as the value of the potential is increased, eventually merging and disappearing at $V = V_{\rm crit}$. These are precisely the requirements for a graceful entrance to inflation that were outlined in section 9.2.

We now proceed to illustrate the cosmic dynamics in the phase space. The dynamics is clearly two-dimensional due to the Friedmann constraint equation (9.14). As we discussed in section 9.2, the phase space could therefore in principle be represented in two dimensions by introducing appropriate variables. However, this may be non-trivial in practice, since more than one set of variables may be required. (This would then imply that more than one phase plane diagram would be needed in order to present the full dynamics). In the context of the present discussion, it proves convenient to numerically integrate the field equations and then view the evolution of the universe in the three-dimensional space spanned by $\{a, H, \dot{\phi}\}$. Since the Friedmann constraint defines a surface in this phase space, the evolution of the universe can then be parametrised in terms of a trajectory on this surface. In the following, we will refer to such a surface as the Friedmann surface. Identifying a coordinate system that covers the Friedmann surface is then equivalent to finding variables in which the dynamical system becomes explicitly two-dimensional, and the need for more than one coordinate patch to cover the surface is then equivalent to requiring more than one set of variables to complete the phase space.

We focus on the case of a positive potential since we are interested in establishing the conditions for inflation via the graceful entrance mechanism. Fig. 9.2 illustrates the Friedmann surface and the integrated trajectories on this surface when $V < V_{\rm crit}$. The lower part of the figure represents the projection of these trajectories onto the two-dimensional plane spanned by the variables $\{\dot{\phi}, H\}$. The two equilibrium points representing the centre and saddle are shown. Fig. 9.3 illustrates the corresponding dynamics for $V > V_{\rm crit}$, where the equilibrium points have effectively merged. *All* trajectories now evolve through a bounce into an ever-expanding inflationary period of de Sitter expansion with $H \to$ constant, $\dot{\phi} \to 0$ and $a \to \infty$.

Comparison between the phase spaces of Fig. 9.1 and those of Figs. 9.2 and 9.3 confirms that a graceful entrance to inflation, as outlined in section 9.2, can occur in this model.

## 9.6 Effects of dark radiation

In the case where dark radiation plays a dynamical role in the Friedmann equation (9.14), the full quartic expression given by Eq. (9.21) must be solved to determine the nature of the equilibrium points. One must also ensure that the scale factor and kinetic energy of the field take positive and real values at these points. The constraint (9.21) can be solved analytically using the standard techniques for quartic equations (see for example Abramowitz and Stegun, 1964). The resulting expressions are not directly useful in

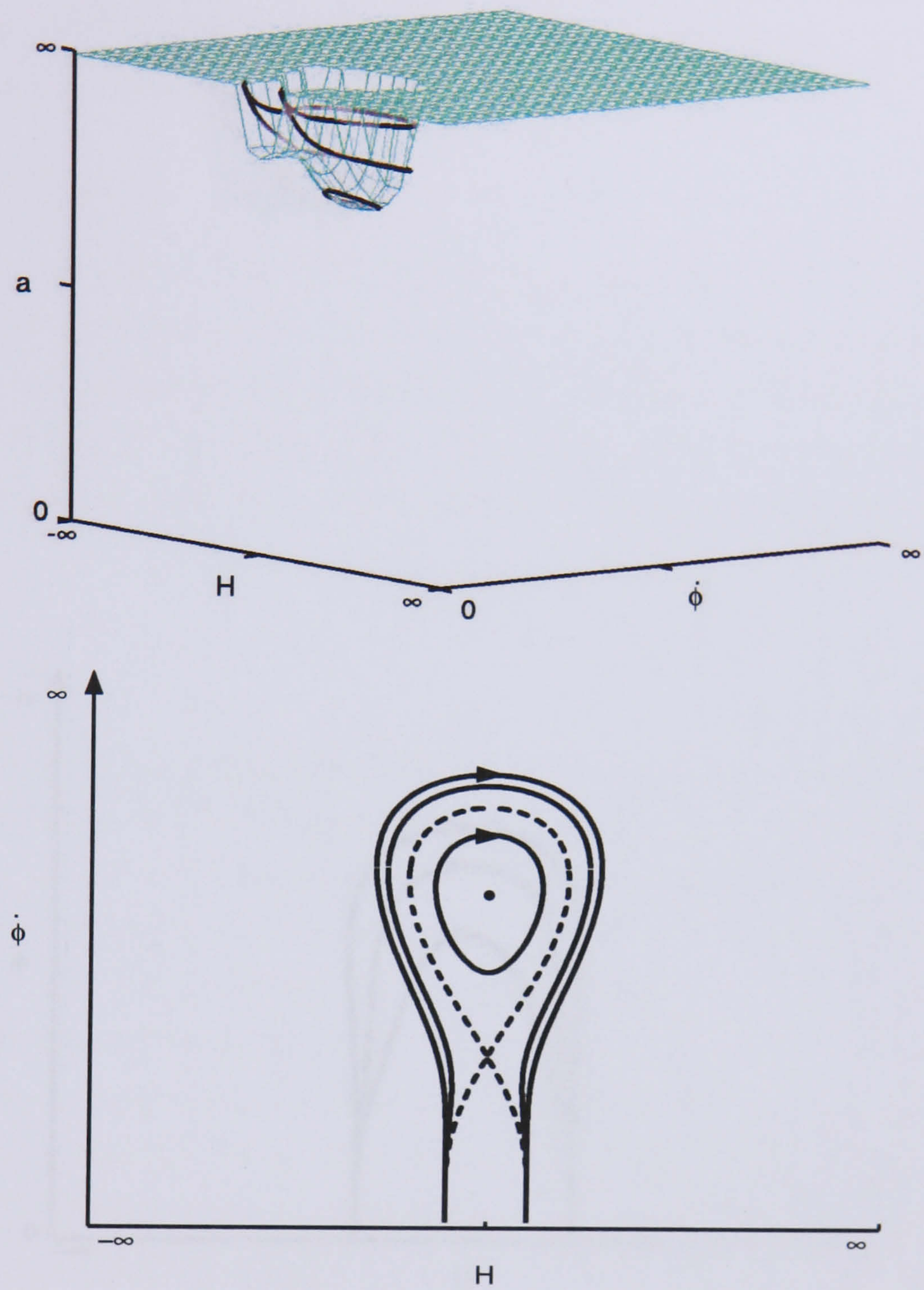


Figure 9.2: The top panel represents the phase space in the variables $\{H, \dot{\phi}, a\}$, when $m = 0$, $\sigma = 0.05$ and $0 < V < V_{\rm crit}$, where $V_{\rm crit}$ is defined in Eq. (9.26). Numerical values are given in Planck units. The surface defined by the Friedmann equation (9.14), with $\rho = \dot{\phi}^2/2 + V$, is also shown and all phase space trajectories lie on this surface. The compactified coordinates $x \equiv \arctan(H)$, $y \equiv \arctan(\ln \phi)$ and $z \equiv \arctan(\ln a)$ have been employed in order to show the entire phase space. The lower panel represents the two-dimensional projection of this space onto the plane spanned by the variables $\{H, \dot{\phi}\}$. The centre equilibrium point is denoted by the solid circle and the separatrix is represented by the dotted line. The saddle point occurs at the point where the separatrix self-intersects. The axes have been compactified using the coordinate change $x = \arctan(H)$ and $y = \arctan(\ln \dot{\phi})$.

themselves since they are very lengthy and provide no insight in their general form. We will therefore not present them here. In what follows, however, we will use the ana-

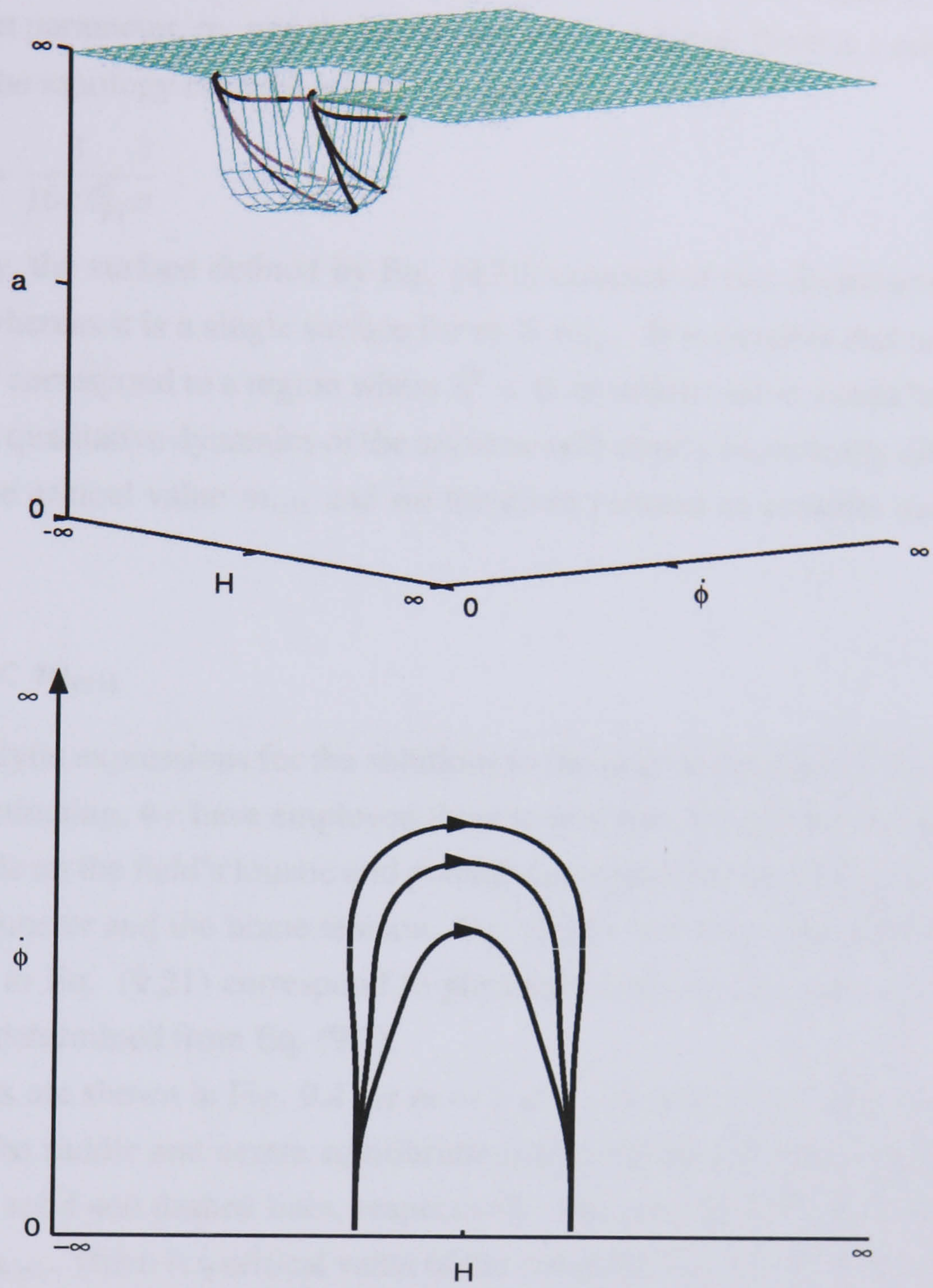


Figure 9.3: As for Fig. 9.2, but now for a potential $V > V_{\rm crit}$. There are no finite equilibrium points in the phase space in this region of parameter space.

lytic expressions to plot the behaviour of solutions in specific illustrative cases. On the other hand, some analytical progress can first be made by considering the topology of the Friedmann surface. This plays an important role in understanding the dynamics, as may be deduced by writing the Friedmann constraint equation (9.14) in the form of a hyperboloid:

$$H^2 + \frac{8\pi\ell_{\rm Pl}^2}{3}\left(\frac{\dot\phi^2}{2\sqrt{2\sigma}} - \left(\frac{\sqrt{2\sigma}}{2} - \frac{V}{\sqrt{2\sigma}}\right)\right)^2 - \left(\frac{\sqrt{m}}{a^2} - \frac{1}{2\sqrt{m}}\right)^2 = \frac{4\pi\ell_{\rm Pl}^2\sigma}{3} - \frac{1}{4m}\,. \tag{9.30}$$

Provided $V < \sigma$, the hyperboloid's topology depends only on the relative values of the dark radiation parameter, $m$, and the brane tension, $\sigma$. Indeed, there is a critical value of $m$ at which the topology changes and this is given by

$$m_{\rm crit} = \frac{3}{16\pi\ell_{\rm Pl}^2}\frac{1}{\sigma} \ . \tag{9.31}$$

Consequently, the surface defined by Eq. (9.30) consists of two disconnected pieces if $m < m_{\rm crit}$, whereas it is a single surface for $m > m_{\rm crit}$. It is possible that one of the two surfaces may correspond to a region where $\dot{\phi}^2 < 0$, in which case it would be unphysical. However, the qualitative dynamics of the universe will clearly be radically different above and below the critical value $m_{\rm crit}$ and we therefore proceed to consider each regime in turn.

### 9.6.1 $m < m_{\rm crit}$

Since the analytic expressions for the solutions to the quartic equation (9.21) are not particularly illuminating, we have employed them to plot how the nature of the equilibrium points depends on the field's kinetic and potential energies for specific values of the dark radiation parameter and the brane tension. Eq. (9.20) was also employed to verify that the solutions to Eq. (9.21) correspond to physical values of the scale factor, and their stability was determined from Eq. (9.7).

The results are shown in Fig. 9.4 for $m = 1$ and $\sigma = 0.05$ in Planck units, where the locations of the saddle and centre equilibrium points for given field energies are represented by the solid and dashed lines, respectively. The qualitative behaviour is the same for all $m < m_{\rm crit}$. There is a critical value of the potential, $V_{\rm crit2}$, such that there are three real roots to the quartic equation (9.21) when $0 < V < V_{\rm crit2}$. These correspond to three distinct equilibrium points, two of which are centres whereas the third is a saddle point. At $V = V_{\rm crit2}$, however, the saddle and one of the centre points merge and, for $V > V_{\rm crit2}$, these points correspond to unphysical roots. Consequently, there is only one equilibrium point for $V > V_{\rm crit2}$ and this is a centre.

The qualitative evolution of the universe in the regimes $V < V_{\rm crit2}$ and $V > V_{\rm crit2}$ is shown in Figs. 9.5 and 9.6, respectively, where the trajectories have been calculated by numerically integrating the field equations for the specific choices $m = 1$ and $\sigma = 0.05$. The topology of the Friedmann surface in the upper panels of these figures, together with Eq. (9.30), implies that the entire phase space can be represented as a single two-dimensional plot by employing cylindrical polar coordinates. These are shown in the lower panels of the figures.

The dynamics in the upper sectors of the Friedmann surface in Figs. 9.5 and 9.6 are qualitatively similar to the case where no dark radiation is present ($m = 0$). The

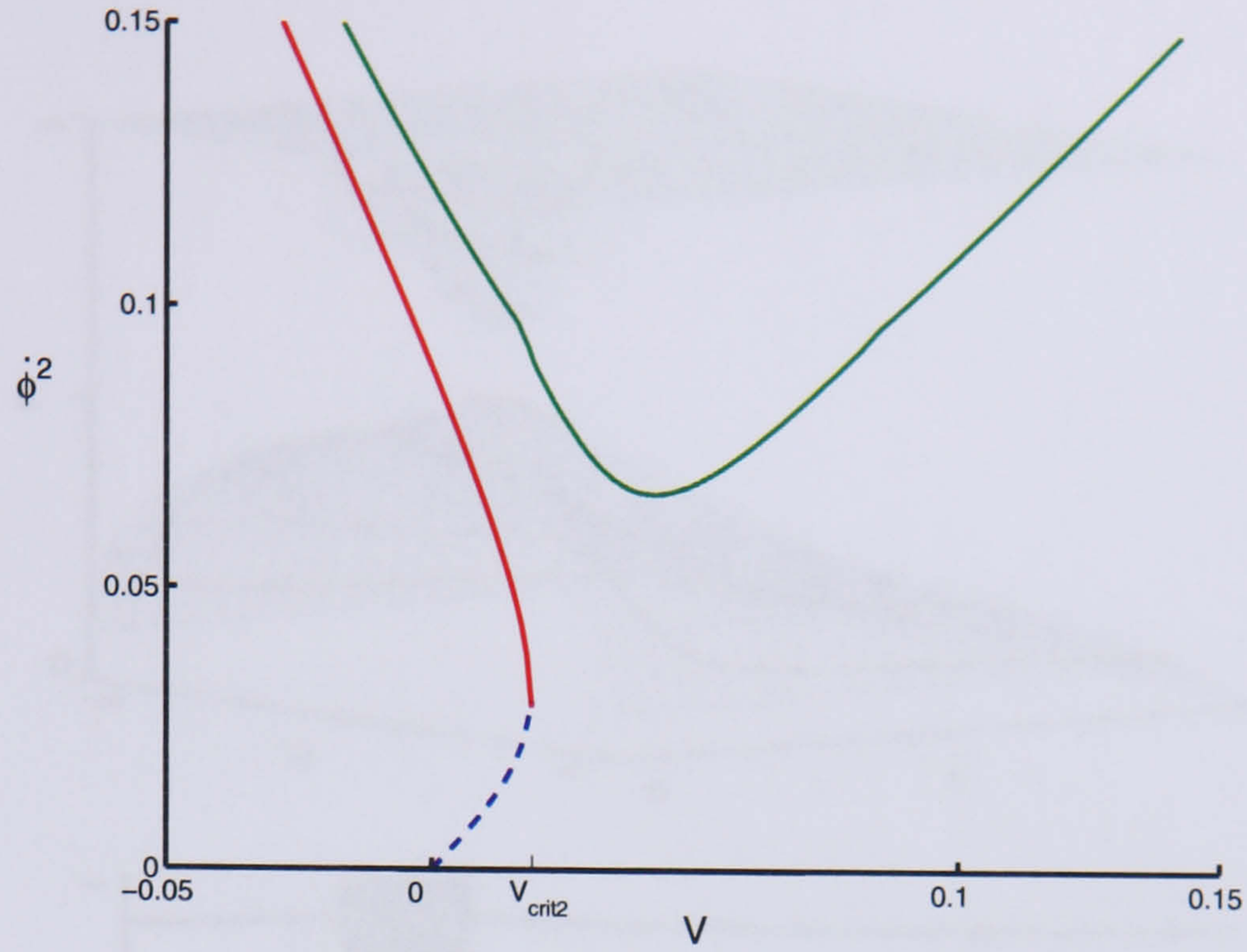


Figure 9.4: Illustrating the position and nature of the equilibrium points as a function of the field's kinetic and potential energies when $0 < m < m_{\text{crit}}$. A dashed line corresponds to a saddle point and a solid line to a centre point. The critical value $V_{\text{crit2}}$ represents the magnitude of the potetnial when one of the centre points and the saddle disappear from the phase space. The numerical values chosen for the plot are $\sigma = 0.05$ and $m = 1.0$ and the axes are measured in Planck units.

lower sector of the Friedmann surface contains the new centre equilibrium point that arises when $m \neq 0$. This point is real for all values of the potential. Hence, as shown in Figs. 9.5 and 9.6, the universe remains trapped in an indefinite cycle of expansion and contraction if it is initially located in the lower half of the Friedmann surface. This behaviour can be understood since a sufficiently large (positive) cosmological constant introduces a large negative *effective* cosmological constant in the Friedmann equation (9.14) as a consequence of the quadratic term in the energy density. This will prevent the universe from entering a phase of accelerated inflationary expansion. Indeed, although it is not relevant for the graceful entrance mechanism, it can be shown that if $V$ exceeds yet another critical value, the upper region of the Friedmann surface is no longer physical since the field's kinetic energy becomes negative. In effect, therefore, the size of the universe is bounded from above.

By comparing the qualitative dynamics of the universe when no dark radiation is present (Figs. 9.2 and 9.3) to that illustrated in the upper sectors of the Friedmann surfaces in Figs. 9.5 and 9.6, we may infer that a graceful entrance to inflation, as outlined in section 9.2, may in principle occur for suitable choices of initial conditions.

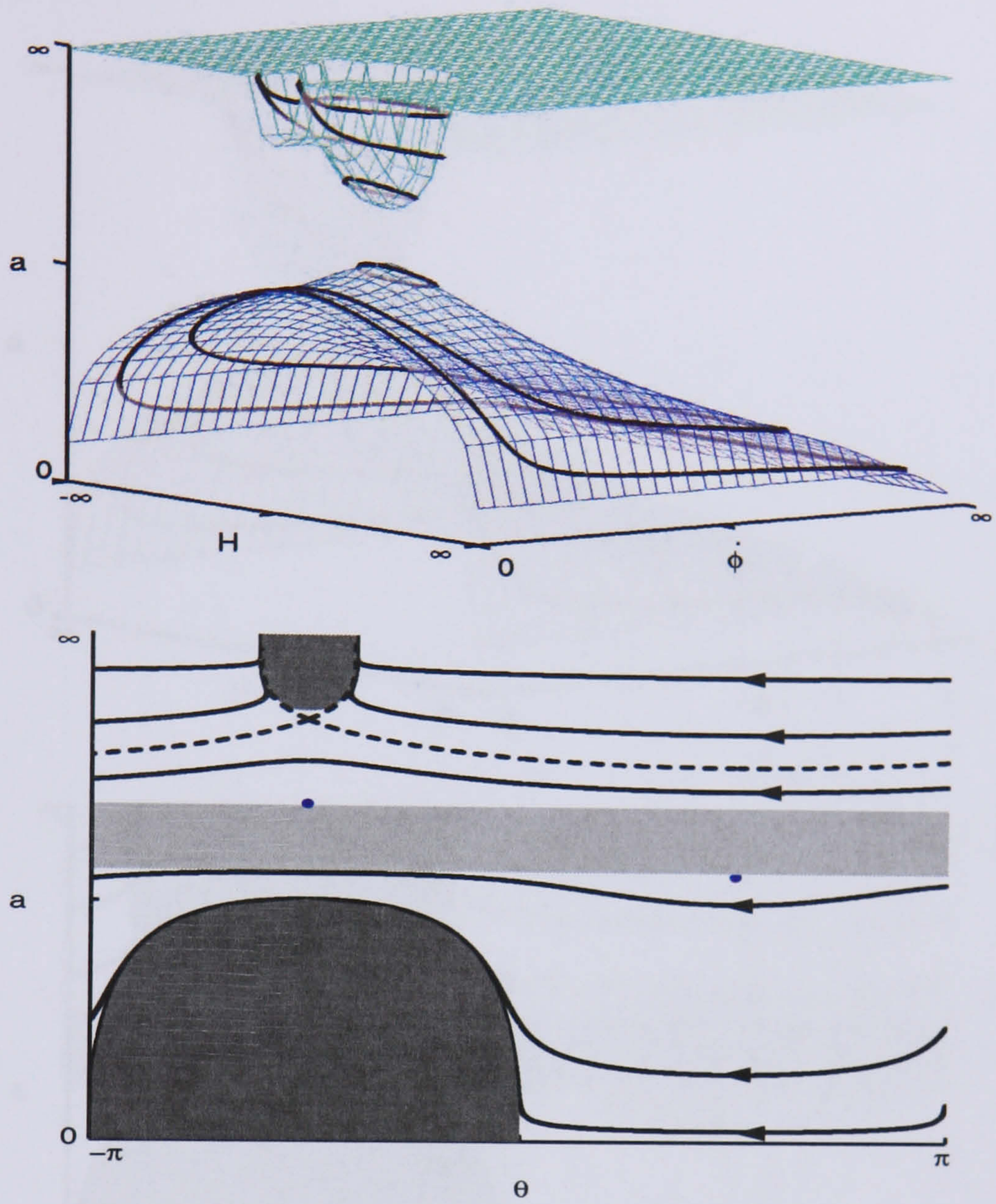


Figure 9.5: The top panel represents the phase space in the variables $\{H, \dot{\phi}, a\}$, when $m = 1.0$, $\sigma = 0.05$ and $0 < V < V_{\text{crit2}}$. The surface defined by the Friedmann equation (9.14), with $\rho = \dot{\phi}^2/2 + V$, is also plotted. The phase space trajectories lie on this surface. The axes have been compactified using the rescalings $x = \arctan(H)$, $y = \arctan(\ln \dot{\phi})$ and $z = \arctan(\ln a)$. The lower panel illustrates a corresponding two-dimensional phase space. It follows from Eq. (9.30) that there exists an axis of symmetry parallel to the $a$-axis through the point $H = 0$, $\dot{\phi}^2 = 2\sigma - 2V$. Cylindrical polar coordinates can then be defined by using this axis. Specifically, we define $a = a$, $\mathrm{X} = \mathrm{R}\cos\theta$ and $\mathrm{Y} = \mathrm{R}\sin\theta$, where $\mathrm{X} = \frac{\sqrt{8\pi\ell_{\text{Pl}}^2}}{\sqrt{3}}\left(\frac{\dot{\phi}^2}{2\sqrt{2\sigma}} - \left(\frac{\sqrt{2\sigma}}{2} - \frac{V}{\sqrt{2\sigma}}\right)\right)$, $\mathrm{Y} = H$, and $\mathrm{R} = \left(\left(\frac{\sqrt{m}}{a^2} - \frac{1}{2\sqrt{m}}\right)^2 + \frac{4\pi\ell_{\text{Pl}}^2\sigma}{3} - \frac{1}{4m}\right)^{\frac{1}{2}}$. The two-dimensional plot is then presented in the $\{\theta, a\}$ plane, where we have once more compactified the $a$-axis using $y = \arctan(\ln a)$. This diagram is essentially a projection of the top panel about the axis defined above, with the points at $\theta = \pi$ identified with those at $\theta = -\pi$. The shaded areas mark the unphysical regions in this coordinate system. The centre equilibrium points are identified by a solid circle and the separatrix is represented by a dotted line. The saddle point occurs at the point where the separatrix intersects with itself.

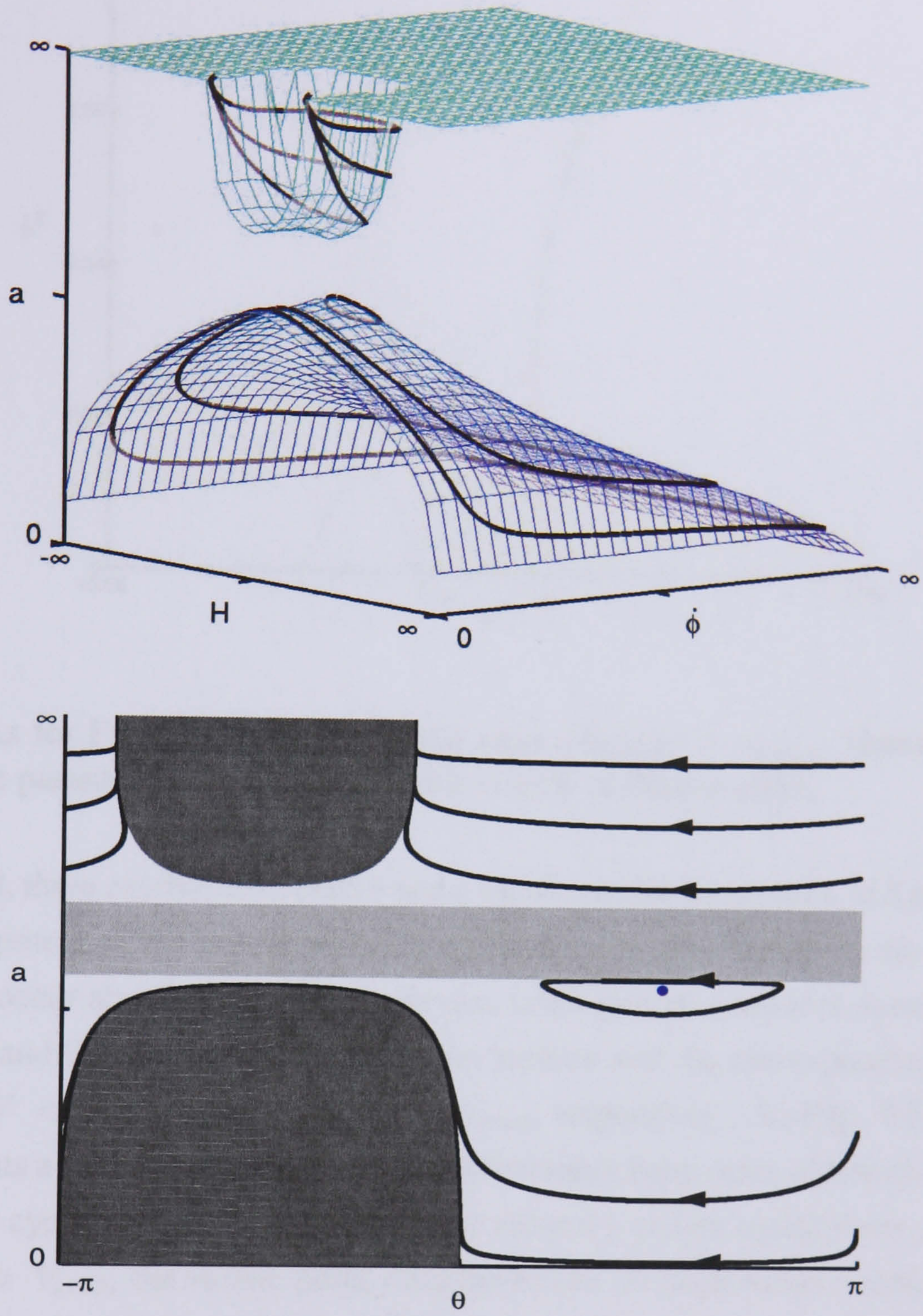


Figure 9.6: As in Fig. 9.5, but now for a potential $V > V_{\rm crit2}$. There are no saddle points and only one centre equilibrium point in the phase plane.

### 9.6.2 $m > m_{\rm crit}$

We may adopt a similar approach for $m > m_{\rm crit}$. Fig. 9.7 illustrates the position and nature of the physically relevant equilibrium points as a function of the field's kinetic and potential energies for the specific choices $m = 1.4$ and $\sigma = 0.05$ in Planck units. The qualitative nature of this plot remains unaltered for all $m > m_{\rm crit}$. It follows from Fig. 9.7 that there is only a single saddle equilibrium point when the magnitude of the potential falls below a critical value $V_{\rm crit3}$. There is then a finite range of values of the potential, $V_{\rm crit3} \leq V \leq V_{\rm crit4}$, for which there are *no* physical equilibrium points. For $V > V_{\rm crit4}$, on

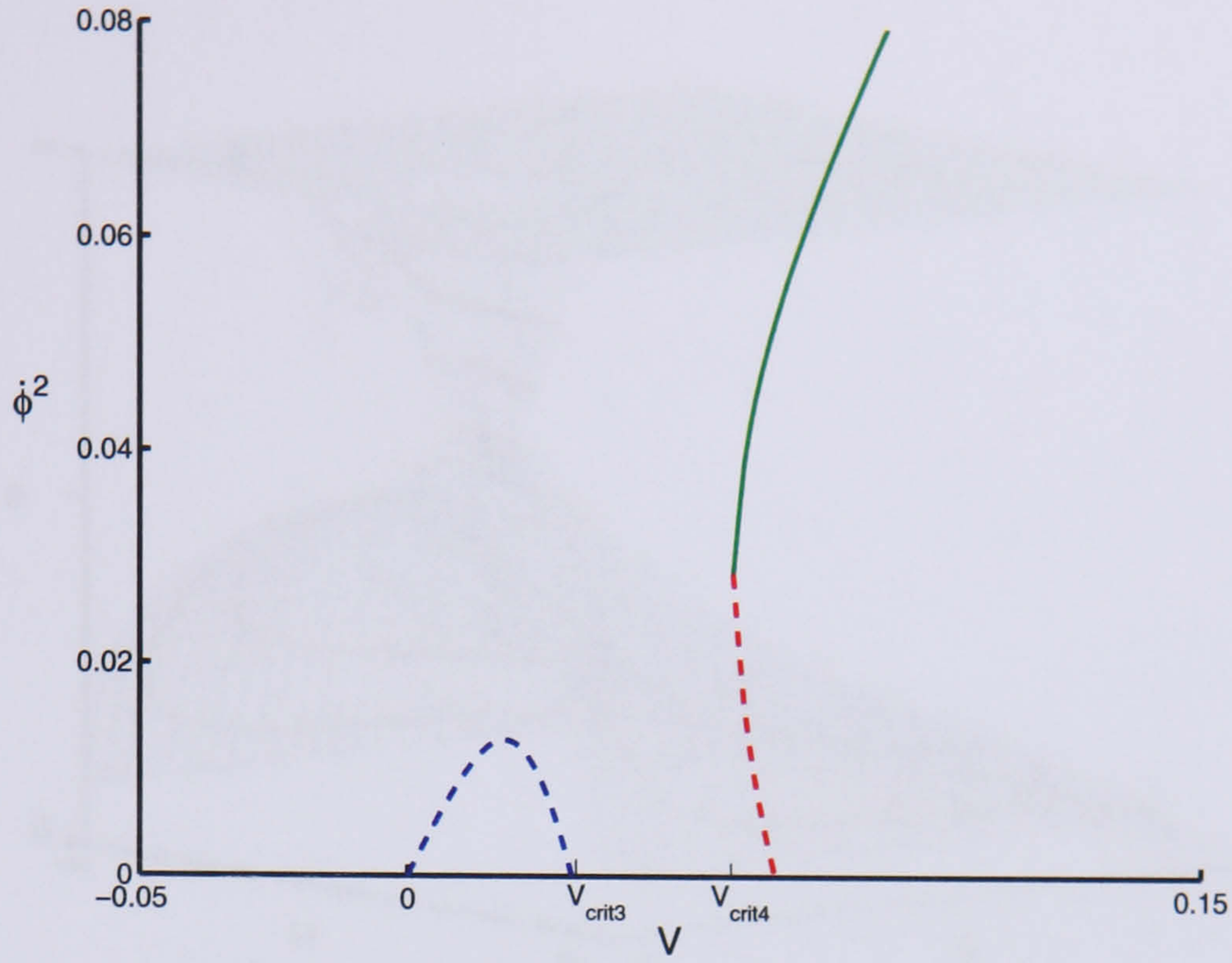


Figure 9.7: As for Fig. 9.4, but now for the case where $m > m_{crit}$. Numerical values chosen for the parameters are $m = 1.4$ and $\sigma = 0.05$ in Planck units.

the other hand, there exists both a centre and a saddle equilibrium point, and at still higher values of the potential, the saddle point disappears once more. However, the equilibrium points which occur above $V_{\rm crit4}$ are not relevant to the graceful entrance scenario.

Figs. 9.8 and 9.9 illustrate the Friedmann surface and the corresponding phase trajectories for $V < V_{\rm crit3}$ and $V_{\rm crit3} < V < V_{\rm crit4}$, respectively. In Fig. 9.8, the saddle point represents a divide between cyclic and inflationary behaviour, although it should be noted that the cyclic dynamics does not occur around a centre equilibrium point in this case. For $V > V_{\rm crit3}$, the saddle point disappears and all trajectories eventually evolve into an inflationary region, as shown in Fig. 9.9. As was the case in the previous subsection, it can be shown that for a sufficiently large value of the potential, the Friedmann surface becomes modified in such a way that the surface is bounded to always lie below a critical value of the scale factor. This implies that the size of the universe is bounded from above and such behaviour follows once more due to the presence of an effective negative cosmological constant in the Friedmann equation.

The question of whether a graceful entrance to inflation is possible if $m > m_{\rm crit}$ is more difficult to answer. The key features of a cyclic region and a saddle point in the phase space, which disappear at a critical value of the potential, are indeed present. However, there is a further complication. For $m < m_{\rm crit}$, the cyclic dynamics is always dominated by the field's kinetic energy, but this is no longer the case when $m > m_{\rm crit}$.

Further insight may be gained from Figs. 9.8 and 9.9. The shaded gray areas represent the regions of phase space where the field's kinetic energy is negative, with the

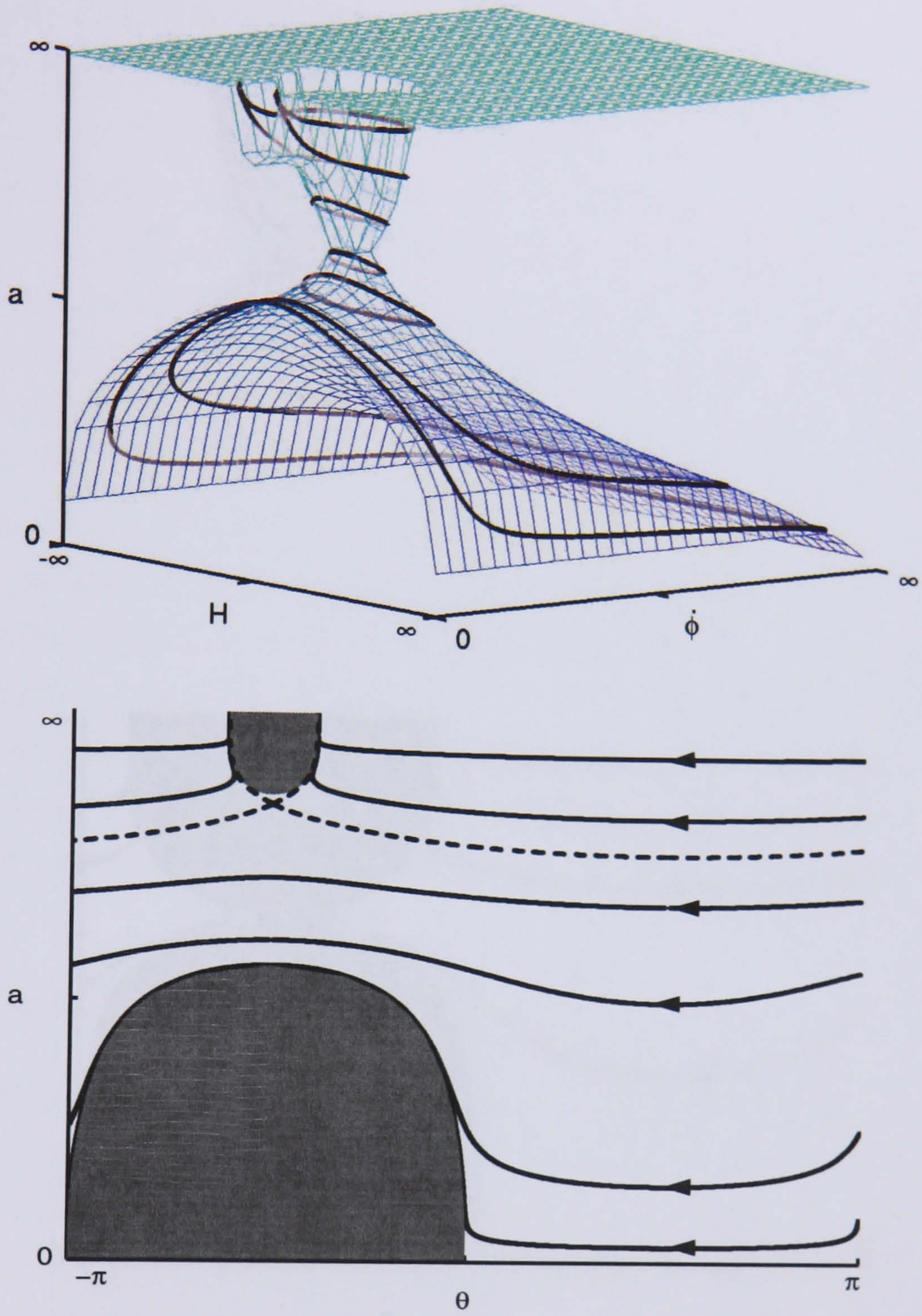


Figure 9.8: The top and bottom panels are as described for Fig. 9.5, but now for $m > m_{\rm crit}$ and $0 < V < V_{\rm crit3}$. Numerical values for the parameters are $m = 1.4$ and $\sigma = 0.05$ in Planck units. Trajectories representing cyclic behaviour are present in this case but there are no centre equilibrium points, just a single saddle point is present.

boundaries corresponding to the limit $\dot{\phi}^2 = 0$. For a realistic (i.e. sufficiently flat but field-dependent) potential, this implies that on a trajectory which passes sufficiently close to these boundaries in the 'instantaneous phase space', the field's kinetic energy will be so small that the gradient of the potential will become significant. This will result in the kinetic energy of the field falling to zero and the field turning around on the potential before it has climbed sufficiently far up the potential to drive a successful phase of slow-roll inflation. In the previous cases, the kinetic energy could only fall to zero in the region

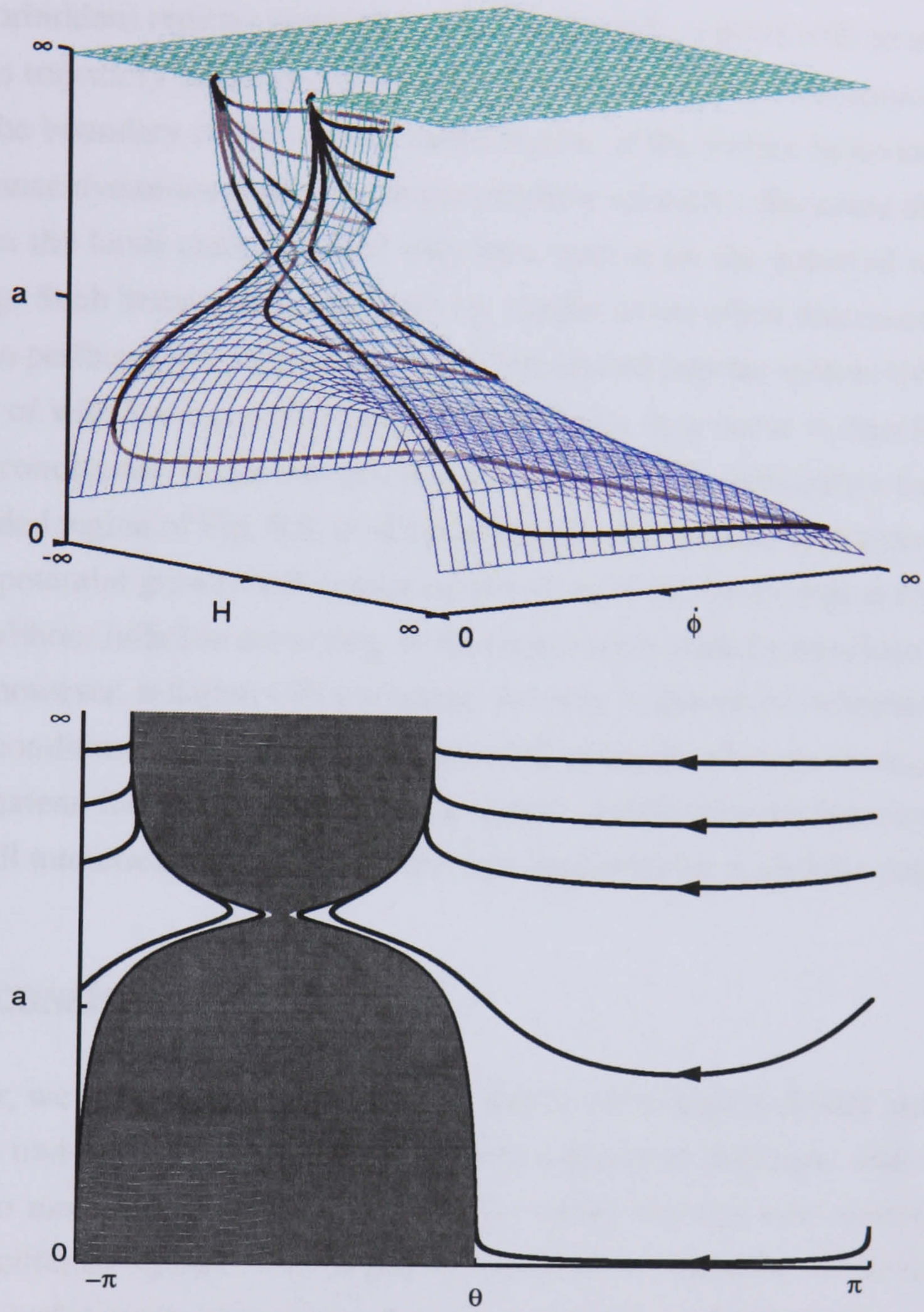


Figure 9.9: The top and bottom panels are as described for Fig. 9.5, but now for $m > m_{\rm crit}$ and $V_{\rm crit3} < V < V_{\rm crit4}$. Numerical values of the parameters are specified as $m = 1.4$ and $\sigma = 0.05$ in Planck units. There are no equilibrium points for this case.

of parameter space relevant to inflation, or in a region disconnected from it, such as the lower section of the Friedmann surface. In the present case, however, the two regions of the previously disjointed Friedmann surface are connected. In effect, therefore, the turn-around in the field may occur too soon for inflation to occur if $m > m_{\rm crit}$.

More specifically, let us assume as before that we have a realistic inflationary potential, with a magnitude initially in the range $0 < V < V_{\rm crit3}$, and that the universe begins in the oscillatory region of the phase space. As the universe oscillates, the field climbs its potential. In terms of Fig. 9.8, the instantaneous phase space is therefore altered, with

the saddle point moving to successively smaller values of the scale factor, and the shaded (physically forbidden) regions growing in size. Ultimately, a point will be attained when the universe's trajectory either moves outside the region of the oscillations or it passes too close to the boundary of the lower, shaded region. If the former behaviour arises, the graceful entrance dynamics applies as in the previous scenarios discussed above. On the other hand, in the latter case, the field may turn around on the potential *without* inflation occurring. Such behaviour is qualitatively similar to the effect discussed in the LQC scenario when perfect fluid matter sources are introduced into the system (Nunes, 2005).

The issue of whether a graceful entrance to inflation may occur is therefore sensitive to the initial conditions. If the universe's initial trajectory is sufficiently far away from the lower shaded region of Fig. 9.8, it will pass outside the oscillatory region (as the magnitude of the potential grows) before passing too close to the lower region for the field to turn around without inflation occurring. If the trajectory is initially too close to the lower shaded area, however, inflation will not occur. In order to determine whether a particular set of initial conditions will give rise to a graceful entrance when $m > m_{\rm crit}$, it will be necessary to extend the 'instantaneous phase space' analysis that we have employed and complete a full numerical integration of the field equations for a realistic potential.

## 9.7 Discussion

In this chapter, we have examined the criteria that a cosmological model must satisfy in order for it to undergo a 'graceful entrance' into a phase of inflation, whereby a scalar field is able to move up its interaction potential whilst the universe undergoes a large number of oscillatory cycles. Our approach has been to consider an idealised model, which proved useful in the context of semi-classical LQC, where the matter is composed of a scalar field evolving along a constant potential. This system provides a good approximation to more realistic scenarios where the potential is field-dependent if the change in the potential is sufficiently small over a large number of cycles. It therefore provides us with a methodology for identifying whether a particular cosmological scenario will meet the necessary requirements for a graceful entrance.

The mechanism we have outlined is very generic. The important ingredients are that the phase space should exhibit both a centre and saddle equilibrium point when the magnitude of the potential $V$ falls below a critical value $V_{\rm crit}$. These points gradually move towards each other as $V$ increases and eventually merge when $V = V_{\rm crit}$. Above this scale, the points should disappear from the phase space. From the physical viewpoint, this behaviour arises becasue the potential now dominates the field's kinetic energy, $V > \dot{\phi}^2$, and consequently drives a phase of inflationary expansion. It follows that the critical

value $V_{\rm crit}$ sets the energy scale for the onset of inflation.

We have developed a framework for investigating a general class of braneworld models in this context that are characterised by a Friedmann equation with an arbitrary dependence on the energy density. Such a class of models can be represented as a standard, relativistic Friedmann universe by reinterpreting the effective equation of state of the matter on the brane. This approach has highlighted the role played by the equation of state in this mechanism and the importance of the successive violation and recovery of the strong energy condition. Moreover, it combined this understanding of the dynamics with the phase space description.

As a concrete example, we focused on the Shtanov-Sahni braneworld, where the extra bulk dimension is timelike. We found that the question of whether the braneworld oscillates or expands indefinitely is dependent on the field's kinetic and potential energies, as well as the dark radiation term and the brane tension, $\sigma$. If the dark radiation is negligible, the phase space has a similar structure to that outlined above and a graceful entrance to inflation can therefore be realised, where the energy scale at the onset of inflation is given by $V_{\rm crit} \approx \sigma$. The dark radiation can have a significant effect on the dynamics, however, and the question of whether a graceful entrance is possible in this case is sensitive to the initial conditions.

In conclusion, therefore, we have presented a non-singular, oscillating braneworld that can in principle exhibit a graceful entrance to inflation. We anticipate that such behaviour will apply for a wide range of collapsing braneworld scenarios that are able to undergo non-singular bounces and, moreover, will not be strongly dependent on the precise form of the inflaton potential. It is very interesting that this behaviour first discovered in the LQC setting is also possible in braneworld models motivated by string/M-theory.

Finally, it is important to realise that our analysis also provides the basis for realising the recently proposed emergent universe scenario in a braneworld context. Such a scenario could be constructed in exactly the same manner as in chapter 6, but now assuming that the initial state of the universe is close to the centre equilibrium point which we have shown occurs in the S-S braneworld setting. In this example, the universe would correspond initially to a braneworld Einstein static universe or to one that is oscillating about such a solution in the infinite past. The potential has an asymptotically flat section, where $V < V_{\rm crit}$ as $\phi \to -\infty$, but subsequently increases above $V_{\rm crit}$ once the value of the field has increased beyond a certain value. If the field is initially located in the plateau region of the potential and moving in the appropriate direction, it will eventually reach the section of the potential which rises above $V_{\rm crit}$, thus initiating inflation. This braneworld realisation of the emergent universe scenario solves the severe fine-tuning problem which the classical scenario suffered from, and allows for a greater freedom in

the choice of inflationary potential in exactly the same manner as the LQC model. It is again interesting that both these scenarios, motivated by different theories of quantum gravity, can realise this attractive model of the very early universe.

# Chapter 10

# Concluding summary

In this concluding chapter, we summarise the most important results contained within this thesis, and highlight areas where future investigation is necessary.

The work described in the thesis can be separated into three major topics. First, there was the issue of the initial conditions required for slow-roll inflation, and we considered how these conditions could be established in a pre-inflationary universe. Secondly, we considered the non-singular emergent universe scenario, and discussed how the problems of the classical scenario could be resolved in settings inspired by quantum gravity such as LQC and braneworlds. Finally, we investigated the super-inflationary scenario of LQC and considered whether it could replace the standard inflationary scenario, by calculating a first approximation to the spectrum of perturbations produced during this phase.

Regarding the initial conditions for inflation, we considered two separate mechanisms. The first was the anti-frictional effect which occurred in the semi-classical regime of LQC, and which was studied in chapter 4. The ability of this mechanism to accelerate a scalar field up its self-interaction potential was studied. The main conclusion was that for the theoretically preferred HAM quantisation scheme, this mechanism cannot move the field by the required $3\ell_{\mathrm{Pl}}^{-1}$ before the framework of the semi-classical regime breaks down. It is therefore unlikely to succeed on its own in setting the initial conditions for inflation. This conclusion was largely independent of the quantisation parameters $j$ and $l$, though we noted that if the energy condition of the semi-classical regime were to be relaxed, this mechanism would favour larger values of the parameter $j$, since the field moves further as $j$ is increased. On the other hand, since the field can only be moved by a moderate amount (when the energy condition is imposed), there is the real possibility of observable effects arising at the point when the field turns around on its potential roughly 60 e-folds before the end of inflation. This is assuming, of course, that this mechanism did play a role in establishing the initial conditions for inflation. Future work in this scenario is needed to compare the results obtained within the semi-classical framework to

those generated by utilising the full quantum equations.

The second mechanism for generating the initial conditions for inflation was studied in chapters 5 and 9. This mechanism utilised oscillatory dynamics to move the field up its self-interaction potential during a very large number of cycles. In contrast to the mechanism of chapter 4, this oscillatory mechanism was able to move the field to very high energy scales, and even to energies approaching the Planck scale. The discovery of this mechanism was perhaps the most notable result of this thesis. More remarkable still was that this mechanism could be realised in two very different early universe settings: that of positively-curved bouncing braneworld models and of positively-curved LQC. In fact, the discussion of this mechanism culminated in chapter 9 with the derivation of the (very weak) necessary conditions required by any bouncing model to realise this behaviour. Due to the success of the mechanism and the weakness of the requirements needed to realise it, it is hard to draw concrete conclusions as to favoured parameters and models. In particular, in both settings much more than 60 e-folds of inflation is typically generated, and hence all observable signatures of this scenario would be washed away. On the other hand, considering the LQC setting, we found that smaller values of the parameter $j$ lead to a longer period of inflation. This was in stark contrast to the mechanism discussed in chapter 4, and particularly interesting since smaller values of this parameter are considered to be more natural. An obvious extension of this work is to consider more general bouncing cosmological models, and to test them against the criteria established in chapter 9. It would be interesting to see just how common the behaviour we have studied is.

Another highlight of the thesis was the discovery in chapter 6 that the positively-curved semi-classical LQC universe sourced by a scalar field admits two static equilibrium solutions, in contrast to classical cosmology which admits only one – the Einstein static model. We utilised this discovery, together with the oscillatory dynamics which establish the initial conditions for inflation, to develop a new version of the emergent universe scenario. In this scenario the universe begins its evolution as an Einstein static universe, but subsequently evolves into an inflationary expansion. Unlike the classical scenario, however, this new model used the additional equilibrium point, which was found to be a centre, in contrast to the classical unstable saddle point. In the braneworld model of Shtanov and Sahni, discussed in chapter 9, we also found additional centre equilibrium points for various parameter choices. Although we did not demonstrate it explicitly, we noted that some of these points could also be used to develop a 'stable' emergent braneworld scenario. It is very interesting, therefore, that the emergent scenario can also be realised in such different settings. A key question for future work regarding our new emergent universe scenario is the stability of the equilibrium configuration to

inhomogeneous perturbations. We discussed in chapter 6 that the classical Einstein static universe is surprisingly stable to such perturbations. It is crucial, therefore, to determine whether this property is also true of the new static solutions that we have identified. The technology in LQC has not been developed to deal with perturbative inhomogeneities, and this is a key challenge for future studies. Perturbations are also difficult to deal with in the braneworld context due to the gravitational modes which propagate into the bulk. It will be necessary, therefore, to develop approximations which allow perturbations to be considered in order to extend the emergent universe scenario further.

Finally, this thesis considered the super-inflationary regime of semi-classical LQC. Despite the absence of a framework that can rigorously deal with perturbations in this regime, we derived a first approximation to the spectrum of perturbations by considering perturbations to the scalar field. We found two notable results. First, that subject to our approximation, scale-invariance was possible in this regime if specific parameter choices were made. In particular, a steep potential naturally leads to a scale-invariant spectrum. Secondly, for a massless scalar field, the modes in this regime behaved in a rather different manner to those produced during slow-roll inflation. Indeed they exhibited the disturbing behaviour of evolving into the cosmological horizon, rather than out of it. It was difficult to draw any conclusions regarding preferred parameter values because of our approximations, and because in the case of the steep potential the results became largely independent of the parameter $l$. Concerning the parameter $j$, we noted that very large and unnatural values would be required if this inflationary regime were to replace standard inflation, but the fact that scale-invariance is possible in this regime means that it may still have a role to play, perhaps supplementing standard inflation. The immediate extension of this work is to introduce perturbations to the background spacetime into this calculation. As we mentioned above, however, this is at present not possible within LQC.

In conclusion, we have presented three novel cosmological scenarios in this thesis which are ultimately inspired by two leading theories of quantum gravity: LQG and string theory. These models provide us with examples of how the consequences of fundamental theories can be concretely investigated within the context of the very early universe.

# References


Abramowitz M and Stegun I A (1964). *Handbook of Mathematical Functions with Formulas, Graphs, and Mathematical Tables*. Dover, New York, USA.

Albrecht A and Steinhardt P J (1982). Cosmology for grand unified theories with radiatively induced symmetry breaking. *Phys. Rev. Lett.*, **48**, 1220–1223.

Alfaro J, Morales-Tecotl H A, and Urrutia L F (2002). Loop quantum gravity and light propagation. *Phys. Rev.*, **D65**, 103509.

Alfaro J, Reyes M, Morales-Tecotl H A, and Urrutia L F (2004). On alternative approaches to Lorentz violation in loop quantum gravity inspired models. *Phys. Rev.*, **D70**, 084002.

Amelino-Camelia G and Piran T (2001). Planck-scale deformation of Lorentz symmetry as a solution to the UHECR and the TeV-$\gamma$ paradoxes. *Phys. Rev.*, **D64**, 036005.

Antoniadis I (1990). A possible new dimension at a few TeV. *Phys. Lett.*, **B246**, 377–384.

Antoniadis I, Arkani-Hamed N, Dimopoulos S, and Dvali G R (1998). New dimensions at a millimeter to a Fermi and superstrings at a TeV. *Phys. Lett.*, **B436**, 257–263.

Antoniadis I and Tomboulis E T (1986). Gauge invariance and unitarity in higher derivative quantum gravity. *Phys. Rev.*, **D33**, 2756.

Arkani-Hamed N, Dimopoulos S, and Dvali G R (1998). The hierarchy problem and new dimensions at a millimeter. *Phys. Lett.*, **B429**, 263–272.

Ashtekar A, Baez J, Corichi A, and Krasnov K (1998). Quantum geometry and black hole entropy. *Phys. Rev. Lett.*, **80**, 904–907.

Ashtekar A, Bojowald M, and Lewandowski J (2003). Mathematical structure of loop quantum cosmology. *Adv. Theor. Math. Phys.*, **7**, 233–268.

Ashtekar A and Lewandowski J (1997). Quantum theory of geometry I: Area operators. *Class. Quant. Grav.*, **14**, A55–A82.

Ashtekar A and Lewandowski J (1998). Quantum theory of geometry II: Volume operators. *Adv. Theor. Math. Phys.*, **1**, 388.

Ashtekar A and Lewandowski J (2004). Background independent quantum gravity: A status report. *Class. Quant. Grav.*, **21**, R53.

Barrow J D and Cotsakis S (1991). Selfregenerating inflationary universe in higher order gravity in arbitrary dimension. *Phys. Lett.*, **B258**, 299–304.

Barrow J D, Ellis G F R, Maartens R, and Tsagas C G (2003). On the stability of the Einstein static universe. *Class. Quant. Grav.*, **20**, L155–L164.

Bojowald M (2001a). Absence of singularity in loop quantum cosmology. *Phys. Rev. Lett.*, **86**, 5227–5230.

Bojowald M (2001b). Dynamical initial conditions in quantum cosmology. *Phys. Rev. Lett.*, **87**, 121301.

Bojowald M (2001c). Loop quantum cosmology IV: Discrete time evolution. *Class. Quant. Grav.*, **18**, 1071–1088.

Bojowald M (2002a). Inflation from quantum geometry. *Phys. Rev. Lett.*, **89**, 261301.

Bojowald M (2002b). Quantization ambiguities in isotropic quantum geometry. *Class. Quant. Grav.*, **19**, 5113–5230.

Bojowald M (2004). Loop quantum cosmology: Recent progress. *Pramana*, **63**, 765–776.

Bojowald M (2005a). The early universe in loop quantum cosmology. *J. Phys. Conf. Ser.*, **24**, 77–86.

Bojowald M (2005b). Elements of loop quantum cosmology. In *100 Years of relativity - space-time structure: Einstein and beyond*. Ed. A Ashtekar. World Scientific, Singapore.

Bojowald M (2005c). Loop quantum cosmology. *Living Rev. Rel.*, **8**, 11.

Bojowald M and Date G (2004). A non-chaotic quantum Bianchi IX universe and the quantum structure of classical singularities. *Phys. Rev. Lett.*, **92**, 071302.

Bojowald M, Maartens R, and Singh P (2004). Loop quantum gravity and the cyclic universe. *Phys. Rev.*, **D70**, 083517.

Bojowald M and Morales-Tecotl H A (2004). Cosmological applications of loop quantum gravity. *Lect. Notes Phys.*, **646**, 421–462.

Bojowald M, Singh P, and Skirzewski A (2004). Time dependence in quantum gravity. *Phys. Rev.*, **D70**, 124022.

Bojowald M and Vandersloot K (2003). Loop quantum cosmology, boundary proposals, and inflation. *Phys. Rev.*, **D67**, 124023.

Borde A, Guth A H, and Vilenkin A (2003). Inflationary space-times are incomplete in past directions. *Phys. Rev. Lett.*, **90**, 151301.

Bowcock P, Charmousis C, and Gregory R (2000). General brane cosmologies and their global spacetime structure. *Class. Quant. Grav.*, **17**, 4745–4764.

Brax P and Steer D A (2002). Remark on bouncing and cyclic branes in more than one extra dimension. *Phys. Rev.*, **D66**, 061501.

Brax P, van de Bruck C, and Davis A C (2004). Brane world cosmology. *Rept. Prog. Phys.*, **67**, 2183–2232.

Burgess C P, Quevedo F, Rabadan R, Tasinato G, and Zavala I (2004). Bouncing branes. *JCAP*, **0402**, 008.

Candelas P, Horowitz G T, Strominger A, and Witten E (1985). Vacuum configurations for superstrings. *Nucl. Phys.*, **B258**, 46–74.

Chaichian M and Kobakhidze A B (2000). Mass hierarchy and localization of gravity in extra time. *Phys. Lett.*, **B488**, 117–122.

Copeland E J, Liddle A R, and Lidsey J E (2001). Steep inflation: Ending braneworld inflation by gravitational particle production. *Phys. Rev.*, **D64**, 023509.

Copeland E J, Lidsey J E, and Mizuno S (2006). Correspondence between loop-inspired and braneworld cosmology. *Phys. Rev.*, **D73**, 043503.

Corichi A and Hauser A (2005). Bibliography of publications related to classical self-dual variables and loop quantum gravity. *gr-qc/0509039*.

Date G and Hossain G M (2004). Effective Hamiltonian for isotropic loop quantum cosmology. *Class. Quant. Grav.*, **21**, 4941–4953.

Date G and Hossain G M (2005). Genericity of big bounce in isotropic loop quantum cosmology. *Phys. Rev. Lett.*, **94**, 011302.

DeWitt B S (1967). Quantum theory of gravity. 1: The canonical theory. *Phys. Rev.*, **160**, 1113–1148.

Dimopoulos K and Valle J W F (2002). Modeling quintessential inflation. *Astropart. Phys.*, **18**, 287–306.

Dodelson S (2003). *Modern cosmology*. Academic Press, Amsterdam, Netherlands.

Domagala M and Lewandowski J (2004). Black hole entropy from quantum geometry. *Class. Quant. Grav.*, **21**, 5233–5244.

Durrer R and Laukenmann J (1996). The oscillating universe: an alternative to inflation. *Class. Quant. Grav.*, **13**, 1069–1088.

Dvali G R, Gabadadze G, and Senjanovic G (1999). Constraints on extra time dimensions. In *The Yu. A. Golfand memorial volume*. Ed. M A Shifman. World Scientific, Singapore.

Ellis G F R and Maartens R (2004). The emergent universe: Inflationary cosmology with no singularity. *Class. Quant. Grav.*, **21**, 223–232.

Ellis G F R, Murugan J, and Tsagas C G (2004). The emergent universe: An explicit construction. *Class. Quant. Grav.*, **21**, 233–250.

Emparan R and Garriga J (2003). A note on accelerating cosmologies from compactifications and s-branes. *JHEP*, **05**, 028.

Foffa S (2003). Bouncing pre-big bang on the brane. *Phys. Rev.*, **D68**, 043511.

Ford L H (1987). Gravitational particle creation and inflation. *Phys. Rev.*, **D35**, 2955.

Gambini R and Pullin J (1999). Nonstandard optics from quantum spacetime. *Phys. Rev.*, **D59**, 124021.

Gibbons G W (1987). The entropy and stability of the universe. *Nucl. Phys.*, **B292**, 784.

Gratton S, Khoury J, Steinhardt P J, and Turok N (2004). Conditions for generating scale-invariant density perturbations. *Phys. Rev.*, **D69**, 103505.

Green M B, Schwarz J H, and Witten E (1987a). *Superstring Theory. Vol. 1: Introduction*. Cambridge University Press, Cambridge, UK.

Green M B, Schwarz J H, and Witten E (1987b). *Superstring Theory. Vol. 2: Loop Amplitudes, Anomalies and Phenomenology*. Cambridge University Press, Cambridge, UK.

Grishchuk L P and Sidorov Y V (1990). Squeezed quantum states of relic gravitons and primordial density fluctuations. *Phys. Rev.*, **D42**, 3413–3421.

Guth A H (1981). The inflationary universe: A possible solution to the horizon and flatness problems. *Phys. Rev.*, **D23**, 347–356.

Hartle J B and Hawking S W (1983). Wave function of the universe. *Phys. Rev.*, **D28**, 2960–2975.

Hawking S W and Moss I G (1982). Supercooled phase transitions in the very early universe. *Phys. Lett.*, **B110**, 35.

Horava P and Witten E (1996a). Eleven-dimensional supergravity on a manifold with boundary. *Nucl. Phys.*, **B475**, 94–114.

Horava P and Witten E (1996b). Heterotic and type i string dynamics from eleven dimensions. *Nucl. Phys.*, **B460**, 506–524.

Hossain G M (2004). Hubble operator in isotropic loop quantum cosmology. *Class. Quant. Grav.*, **21**, 179–196.

Hossain G M (2005). Primordial density perturbation in effective loop quantum cosmology. *Class. Quant. Grav.*, **22**, 2511.

Hovdebo J L and Myers R C (2003). Bouncing braneworlds go crunch! *JCAP*, **0311**, 012.

Ichiki K, Yahiro M, Kajino T, Orito M, and Mathews G J (2002). Observational constraints on dark radiation in brane cosmology. *Phys. Rev.*, **D66**, 043521.

Ida D (2000). Brane-world cosmology. *JHEP*, **09**, 014.

Kallosh R, Kofman L, and Linde A D (2001). Pyrotechnic universe. *Phys. Rev.*, **D64**, 123523.

Kanekar N, Sahni V, and Shtanov Y (2001). Recycling the universe using scalar fields. *Phys. Rev.*, **D63**, 083520.

Kanti P and Tamvakis K (2003). Challenges and obstacles for a bouncing universe in brane models. *Phys. Rev.*, **D68**, 024014.

Khoury J, Ovrut B A, Seiberg N, Steinhardt P J, and Turok N (2002). From big crunch to big bang. *Phys. Rev.*, **D65**, 086007.

Khoury J, Ovrut B A, Steinhardt P J, and Turok N (2001a). A brief comment on 'the pyrotechnic universe'. *hep-th/0105212*.

Khoury J, Ovrut B A, Steinhardt P J, and Turok N (2001b). The ekpyrotic universe: Colliding branes and the origin of the hot big bang. *Phys. Rev.*, **D64**, 123522.

Khoury J, Ovrut B A, Steinhardt P J, and Turok N (2002). Density perturbations in the ekpyrotic scenario. *Phys. Rev.*, **D66**, 046005.

Kolb E W and Turner M S (1990). The early universe. *Front. Phys.*, **69**, 1–547.

Krasnov K V (1998). On statistical mechanics of gravitational systems. *Gen. Rel. Grav.*, **30**, 53–68.

Liddle A R (1994). The inflationary energy scale. *Phys. Rev.*, **D49**, 739–747.

Liddle A R and Lyth D H (1992). COBE, gravitational waves, inflation and extended inflation. *Phys. Lett.*, **B291**, 391–398.

Liddle A R and Lyth D H (1993). The cold dark matter density perturbation. *Phys. Rept.*, **231**, 1–105.

Liddle A R and Lyth D H (2000). *Cosmological inflation and large-scale structure*. Cambridge University Press, Cambridge, UK.

Lidsey J E (2004). Early universe dynamics in semi-classical loop quantum cosmology. *JCAP*, **0412**, 007.

Lidsey J E, Wands D, and Copeland E J (2000). Superstring cosmology. *Phys. Rept.*, **337**, 343–492.

Lidsey J E *et al* (1997). Reconstructing the inflaton potential: An overview. *Rev. Mod. Phys.*, **69**, 373–410.

Linde A (2002). Inflationary theory versus ekpyrotic / cyclic scenario. *hep-th/0205259*.

Linde A D (1982). A new inflationary universe scenario: A possible solution of the horizon, flatness, homogeneity, isotropy and primordial monopole problems. *Phys. Lett.*, **B108**, 389–393.

Linde A D (1983). Chaotic inflation. *Phys. Lett.*, **B129**, 177–181.

Linde A D (1984). Quantum creation of the inflationary universe. *Nuovo Cim. Lett.*, **39**, 401–405.

Linde A D (1986). Eternal Chaotic Inflation. *Modern Physics Letters A*, **1**, 81–85.

Long J C *et al* (2003). Upper limits to submillimeter-range forces from extra space-time dimensions. *Nature*, **421**, 922–925.

Lucchin F and Matarrese S (1985a). Kinematical properties of generalized inflation. *Phys. Lett.*, **B164**, 282.

Lucchin F and Matarrese S (1985b). Power law inflation. *Phys. Rev.*, **D32**, 1316.

Lyth D H (2002a). The failure of cosmological perturbation theory in the new ekpyrotic scenario. *Phys. Lett.*, **B526**, 173–178.

Lyth D H (2002b). The primordial curvature perturbation in the ekpyrotic universe. *Phys. Lett.*, **B524**, 1–4.

Lyth D H, Malik K A, and Sasaki M (2005). A general proof of the conservation of the curvature perturbation. *JCAP*, **0505**, 004.

Lyth D H and Riotto A (1999). Particle physics models of inflation and the cosmological density perturbation. *Phys. Rept.*, **314**, 1–146.

Maartens R (2004). Brane-world gravity. *Living Rev. Rel.*, **7**, 7.

Maartens R, Wands D, Bassett B A, and Heard I (2000). Chaotic inflation on the brane. *Phys. Rev.*, **D62**, 041301.

Madsen M S and Coles P (1988). Chaotic inflation. *Nucl. Phys.*, **B298**, 701–725.

Maeda K i (1989). Towards the Einstein-Hilbert action via conformal transformation. *Phys. Rev.*, **D39**, 3159.

McFadden P L, Turok N, and Steinhardt P J (2005). Solution of a braneworld big crunch / big bang cosmology. *hep-th/0512123*.

Meissner K A (2004). Black hole entropy in loop quantum gravity. *Class. Quant. Grav.*, **21**, 5245–5252.

Mukhanov V F (1985). Gravitational instability of the universe filled with a scalar field. *JETP Lett.*, **41**, 493–496.

Mukhanov V F (1988). Quantum theory of gauge invariant cosmological perturbations. *Sov. Phys. JETP*, **67**, 1297–1302.

Mukhanov V F, Feldman H A, and Brandenberger R H (1992). Theory of cosmological perturbations. Part 1: Classical perturbations. Part 2: Quantum theory of perturbations. Part 3: Extensions. *Phys. Rept.*, **215**, 203–333.

Mukherji S and Peloso M (2002). Bouncing and cyclic universes from brane models. *Phys. Lett.*, **B547**, 297–305.

Mukohyama S (2000). Brane-world solutions, standard cosmology, and dark radiation. *Phys. Lett.*, **B473**, 241–245.

Mukohyama S, Shiromizu T, and Maeda K i (2000). Global structure of exact cosmological solutions in the brane world. *Phys. Rev.*, **D62**, 024028.

Nicolai H and Peeters K (2006). Loop and spin foam quantum gravity: A brief guide for beginners. In *An assessment of current paradigms in the physics of fundamental interactions*. Ed. I Stamatescu. Springer, USA.

Niz G and Turok N (2006). Classical propagation of strings across a big crunch / big bang singularity. *hep-th/0601007*.

Nunes N J (2005). Inflation: A graceful entrance from loop quantum cosmology. *Phys. Rev.*, **D72**, 103510.

Padmanabhan T, Seshadri T R, and Singh T P (1989). Making inflation work: Damping of density perturbations due to Planck energy cutoff. *Phys. Rev.*, **D39**, 2100.

Peacock J A (1999). *Cosmological physics*. Cambridge University Press, Cambridge, UK.

Peebles P J E and Vilenkin A (1999). Quintessential inflation. *Phys. Rev.*, **D59**, 063505.

Perlmutter S *et al* (1999). Measurements of Omega and Lambda from 42 high-redshift supernovae. *Astrophys. J.*, **517**, 565–586.

Piao Y S and Zhang Y Z (2005). Inflation in oscillating universe. *Nucl. Phys.*, **B725**, 265–274.

Polchinski J (1998a). *String theory. Vol. 1: An introduction to the bosonic string*. Cambridge University Press, Cambridge, UK.

Polchinski J (1998b). *String theory. Vol. 2: Superstring theory and beyond*. Cambridge University Press, Cambridge UK.

Randall L and Sundrum R (1999a). An alternative to compactification. *Phys. Rev. Lett.*, **83**, 4690–4693.

Randall L and Sundrum R (1999b). A large mass hierarchy from a small extra dimension. *Phys. Rev. Lett.*, **83**, 3370–3373.

Riess A G *et al* (1998). Observational evidence from supernovae for an accelerating universe and a cosmological constant. *Astron. J.*, **116**, 1009–1038.

Rovelli C (1996). Black hole entropy from loop quantum gravity. *Phys. Rev. Lett.*, **77**, 3288–3291.

Rovelli C (1998). Loop quantum gravity. *Living Rev. Rel.*, **1**, 1.

Rovelli C (2004). *Quantum gravity*. Cambridge University Press, Cambridge, UK.

Rovelli C and Smolin L (1995). Discreteness of area and volume in quantum gravity. *Nucl. Phys.*, **B442**, 593–622.

Salopek D S and Bond J R (1990). Nonlinear evolution of long wavelength metric fluctuations in inflationary models. *Phys. Rev.*, **D42**, 3936–3962.

Shtanov Y and Sahni V (2003). Bouncing braneworlds. *Phys. Lett.*, **B557**, 1–6.

Singh P and Toporensky A (2004). Big crunch avoidance in k = 1 loop quantum cosmology. *Phys. Rev.*, **D69**, 104008.

Singh P and Vandersloot K (2005). Semi-classical states, effective dynamics and classical emergence in loop quantum cosmology. *Phys. Rev.*, **D72**, 084004.

Smith M S, Kawano L H, and Malaney R A (1993). Experimental, computational, and observational analysis of primordial nucleosynthesis. *Astrophys. J. Suppl.*, **85**, 219–247.

Spergel D N *et al* (2003). First year Wilkinson microwave anisotropy probe (WMAP) observations: Determination of cosmological parameters. *Astrophys. J. Suppl.*, **148**, 175.

Spergel D N *et al* (2006). Wilkinson microwave anisotropy probe (WMAP) three year results: Implications for cosmology. *astro-ph/0603449*.

Spokoiny B (1993). Deflationary universe scenario. *Phys. Lett.*, **B315**, 40–45.

Starobinsky A A (1980). A new type of isotropic cosmological models without singularity. *Phys. Lett.*, **B91**, 99–102.

Steinhardt P J and Turok N (2002a). Cosmic evolution in a cyclic universe. *Phys. Rev.*, **D65**, 126003.

Steinhardt P J and Turok N (2002b). A cyclic model of the universe. *Science*, **296**, 1436–1439.

Stewart E D and Lyth D H (1993). A more accurate analytic calculation of the spectrum of cosmological perturbations produced during inflation. *Phys. Lett.*, **B302**, 171–175.

Tegmark M *et al* (2004). The 3d power spectrum of galaxies from the SDSS. *Astrophys. J.*, **606**, 702–740.

Thiemann T (1998a). Closed formula for the matrix elements of the volume operator in canonical quantum gravity. *J. Math. Phys.*, **39**, 3347–3371.

Thiemann T (1998b). QSD V: Quantum gravity as the natural regulator of matter quantum field theories. *Class. Quant. Grav.*, **15**, 1281–1314.

Thiemann T (1998c). Quantum spin dynamics (QSD). *Class. Quant. Grav.*, **15**, 839–873.

Thiemann T (2001). Introduction to modern canonical quantum general relativity. *gr-qc/0110034*.

Thiemann T (2003). Lectures on loop quantum gravity. *Lect. Notes Phys.*, **631**, 41–135.

Tolley A J, Turok N, and Steinhardt P J (2004). Cosmological perturbations in a big crunch / big bang space-time. *Phys. Rev.*, **D69**, 106005.

Tolman R C (1934). *Relativity, Thermodynamics, and Cosmology*. Oxford University Press, Oxford, UK.

Tsujikawa S, Singh P, and Maartens R (2004). Loop quantum gravity effects on inflation and the CMB. *Class. Quant. Grav.*, **21**, 5767–5775.

Turok N, Perry M, and Steinhardt P J (2004). M theory model of a big crunch / big bang transition. *Phys. Rev.*, **D70**, 106004.

Vandersloot K (2005). On the Hamiltonian constraint of loop quantum cosmology. *Phys. Rev.*, **D71**, 103506.

Vereshchagin G V (2004). Qualitative approach to semi-classical loop quantum cosmology. *JCAP*, **0407**, 013.

Vilenkin A (1984). Quantum creation of universes. *Phys. Rev.*, **D30**, 509–511.

Walker T P, Steigman G, Schramm D N, Olive K A, and Kang H S (1991). Primordial nucleosynthesis redux. *Astrophys. J.*, **376**, 51–69.

White S D M, Navarro J F, Evrard A E, and Frenk C S (1993). The baryon content of galaxy clusters: A challenge to cosmological orthodoxy. *Nature*, **366**, 429–433.